Universidade do Minho
Escola de Engenharia

Hélio Rui Caldeira da Silva Jorge

Compounding and Processing of a Water Soluble Binder for Powder Injection Moulding

Tese de Doutoramento
Ciência e Engenharia de Polímeros

Trabalho efectuado sob orientação do
Professor Doutor António M. Cunha

Maio 2008

The sponsorship and the availability of the PIM process facilities for this PhD project by CTCV - Technological Centre for Ceramics and Glass Industries are gratefully acknowledged.

À memória do meu Pai

Para a Lena, a minha Mãe e os meus Irmãos

"O caminho da sabedoria é não ter medo de errar"

"The path of wisdom is not to be afraid of making mistakes"

Paulo Coelho

Acknowledgements

Professor António Cunha	pela orientação no desenvolvimento deste trabalho, valorizando a interrogação, a irreverência e o rigor científico. Pela disponibilidade, abertura, honestidade e clareza com que me apoiou e ensinou, o meu muito obrigado;
Eng. Vaz Serra Eng. Sousa Correia Eng. Alcântara Gonçalves	da Administração e Direcção do CTCV, por me terem lançado neste novo domínio científico e tecnológico e pelas condições que proporcionaram para a realização deste trabalho;
Ana Rita Campos Susana Faria	pela ajuda nos trabalhos experimentais e na logística no DEP, pela sua amizade e carinho com que me acolheram;
Luc Hennetier Luís Rodrigues	pelo apoio nos procedimentos experimentais, discussões, vivências e desabafos, e pelo exemplo de companheirismo e amizade demonstrados;
Maria Carlos Figueiredo Rui Lucas	pela disponibilidade e conhecimentos laboratoriais na caracterização de materiais;
DURIT Lda.	pela valiosa colaboração prestada ao longo destes anos na área da sinterização;
Dr. Joaquim Sacramento Carlos Araújo	pelos conhecimentos e disponibilidade nos ensaios de sinterização;
Sr. Manuel Maurício Malheiro Dr. Filipe Samuel Silva Sr. Araújo Miguel Abreu	pelo auxílio, disponibilidade e suporte técnico e científico nos laboratórios do DEP e do DEM;
	A todas as pessoas envolvidas noutros projectos que, embora não mencionadas, possam de alguma forma ter contribuído para a minha formação e prossecução deste trabalho.
	Um agradecimento muito especial à minha família, aos meus amigos e, especialmente, à minha mulher pelo constante incentivo, confiança e compreensão dedicados ao longo destes anos.

Compounding and Processing of a Water Soluble Binder for Powder Injection Moulding

Abstract

The present work was focused on the development of new polymeric binder compounds for eco-sustainable powder injection moulding (PIM) process. Consequently, water debinding was a requirement once it is a lower environmental impact technology, economically attractive and less hazardous than the conventional catalytic, thermal or solvent debinding. Furthermore, the understanding of the influence of the binder composition on the overall process, from feedstock compounding to final sintered parts, and the development of a structured engineering methodology for new PIM binders was also aimed.

The research program was carried out with AISI 316L stainless steel powder and developed in two main parts: i) characterisation of feedstock formulations and consequent discrimination; and ii) study of the influence of the developed binders in a pilot-scale process. The binder compositions followed a classic design based on a thermoplastic blend, using polyethylene glycol as selected as the water soluble main constituent. The influence of the other binder components, such as back-bone polymers, lubricants and surfactants, was assessed and a reference framework to relate binder formulation and PIM processing was developed. Moreover, promising binder compositions, to produce dimensional stable and precision sintered parts in a high densified and low contaminated sintered stainless steel, are proposed. As a result, a metallocene polyethylene base formulation is proposed as the ultimate binder to produce sintered parts with higher mechanical properties and minimum part defects.

The results confirm the importance of the binder and demonstrate the influence of its composition in PIM process and support an innovative methodology to develop or optimise eco-friendly binders in an industrial environment.

Composição e Processamento de um Ligante Hidrossolúvel para Moldação por Injecção de Pós

Resumo

O objectivo principal deste trabalho é o desenvolvimento de sistemas de ligantes poliméricos eco-sustentáveis para moldação por injecção de pós (PIM). Consequentemente, extracção aquosa foi considerada como um requisito, uma vez que é um processo com menor impacto ambiental, economicamente atractivo e menos nocivo para a saúde no trabalho, comparativamente com as soluções correntes de degradação catalítica, térmica ou por extracção com solventes. Adicionalmente, o trabalho teve como objectivos complementares, o aprofundamento do conhecimento sobre o processo PIM, em particular a compreensão da influência da formulação do ligante, desde a preparação do feedstock até à sinterização, e o desenvolvimento de uma metodologia de engenharia para a produção de novos ligantes.

O programa de investigação assentou na utilização de um pó de aço inoxidável AISI 316L e foi implementado em duas partes principais: i) caracterização das formulações e consequente discriminação; ii) estudo da influência da composição dos ligantes num processo à escala-piloto. As formulações dos ligantes seguiram o conceito mais usual, baseado numa mistura termoplástica, usando polietilenoglicol como constituinte principal hidrossolúvel. O plano de trabalho permitiu o estudo da influência dos componentes minoritários, como os polímeros de estrutura, os lubrificantes e os agentes de superfície, bem como o desenvolvimento de um quadro de referência capaz de relacionar formulação e processamento em PIM. Foram identificadas algumas composições capazes de produzirem peças sinterizadas com elevada precisão dimensional e baixa variabilidade, num material com elevada densificação e baixa contaminação. O ligante com polietileno metalocénico, como polímero de estrutura, permitiu a obtenção de peças sinterizados com propriedades mecânicas satisfatórias e incidência de defeitos miníma.

Os resultados confirmam a importância do ligante e a sua influência no processo de moldação por injecção de pós, e permitem propor uma metodologia inovadora para o desenvolvimento ou optimização de ligantes capaz de ser utilizada em ambientes industriais.

Table of Contents

List of Tables

List of Figures

Symbols and Abbreviations

Symbols

A	Hamaker's constant, J
b	specimen width in bending test, m
d	particle size, m
d	specimen thickness in bending test, m
D	deflection at the centre of the beam in bending test, m
D_{10}	particle size with cumulative undersize 10 %, m
D_{50}	particle size with cumulative undersize 50 %, m
D_{90}	particle size with cumulative undersize 90 %, m
e	strain
E_a	activation energy, J mol^{-1}
E_B	flexural modulus, Pa
E_T	tensile modulus, Pa
E_m	the elastic modulus, Pa
F	load or force in bending test, N
k	thermal conductivity, W m^{-1} K^{-1}
k_0	power law constant
k_D	reciprocal Debye thickness, m^{-1}
L	length, m
l	length, m
L	span of specimen between supports in bending test, m
m	weight, kg
M	molar mass, kg mol^{-1}
n	power law exponent
N	particle coordination number
P	porosity
Q	volume flow rate, m^3 s^{-1}
R	gas constant (R = 8,314 J mol^{-1} K^{-1})

r	cappilary radius, m
R	barrel radius, m
R	fitting correlation coefficient
R_L	linear shrinkage
S_W	distribution slope parameter
T	temperature, K
t	thickness, m
T_c	crystallisation temperature
T_{cp}	crystallisation peak temperature, K
T_{efg}	extrapolated end temperature, K
T_{eig}	extrapolated onset temperature, K
T^e_m	equilibrium melting temperatures of the polymer blend, K
T_g	glass transition temperature, K
T_{id}	initial degradation temperature, K
T_m^{e0}	equilibrium melting temperatures of the pure polymer, K
T_{mg}	midpoint glass transition temperature, K
T_{mp}	melting peak temperature, K
V	specific vapour volume, m^3 kg^{-1}
v	piston speed, $m.s^{-1}$
V_m	molar volumes, $m^3.mol^{-1}$
w	weight fraction
w	width, m

Greek symbols

$\dot{\gamma}$	shear rate, s^{-1}
$\dot{\gamma}_{ap}$	apparent shear rate, s^{-1}
δ	miscibility parameter
ψ_0	surface potential of the particles, V
ΔS_{mix}	entropy variation, J kg^{-1} K^{-1}
ΔE	activation energy for vaporization, J kg^{-1}
ΔG_{mix}	free energy of mixing, J kg^{-1}

ΔP	pressure drop, Pa
ΔH	enthalpy variation, J kg^{-1}
ΔH_{f0}	enthalpy of fusion of the perfect crystal, J mol^{-1}
α	thermal expansion coefficient, K^{-1}
χ	Flory-Huggins interaction parameter
ε	electric permittivity, C^2 J^{-1} m^{-1}
ϕ	solids volume fraction
ϕ_c	critical solids volume fraction
ϕ_m	maximum solids volume fraction
η	viscosity
η_{ap}	apparent viscosity, Pa.s
ρ	density, kg m^{-3}
ρ_a	apparent density, kg m^{-3}
σ	stress, Pa
τ	shear stress, Pa
τ_y	yield stress, Pa

Subscripts

f	filler
m	matrix
p	powder
b	binder
mix	mixture

Abbreviations

AISI	American Iron and Steel Institute
CAB	cellulose acetate butyrate
CIM	ceramic Injection Moulding
CPVC	critical powder volume concentration
DBP	dibutyl phthalate

DSC	differential scanning calorimetry
EO	ethylene oxide
EVA	ethylene-vinyl acetate copolymer
HDPE	high density polyethylene
ISO	International Organisation for Standard
LDPE	low density polyethylene
MIM	metal Injection Moulding
mpd	melting point depression
MPE	metallocene polyethylene
OA	oleic acid
OAG	organic alcohol glyceryl
OPEW	oxidized polyethylene wax
PEG	polyethylene glycol
PEW1	polyethylene wax 1
PEW2	polyethylene wax 2
PIM	powder injection moulding
PMMA	poly(methyl methacrylate)
PP	polypropylene
PS	polystyrene
PVA	poly(vinyl alcohol)
PVB	poly(vinyl butyral)
SA	stearic acid
s.d.	standard deviation
SEM	scanning electron microscopy
SS	stainless steel
STA	simultaneous thermal analysis
TGA	thermogravimetric analysis
UTS	ultimate tensile strength, Pa

1. INTRODUCTION

1.1. Motivation and strategy

Powder injection moulding (PIM) is a productive and mature technology to form complex shape metals and ceramics [1, 2]. This technology has presented a sustainable growing since its industrialization in 1980s, reaching worldwide sales in 2007 of about 1065 million US dollars and an average growth rate in this decade of 8 % (Figure 1.1). Despite of the success, the process is not intensively understood, especially the behaviour of the binder, which has been recognised as one of the most critical issues, and the overall process [3]. The present work aims to contribute to the improvement of the process knowledge, specifically the effect of the binder formulation on the global process, from feedstock compounding to final sintered parts. The ultimate goal is to develop a binder, designed for a lower environmental impact, unlocking PIM manufacturers out from the dependence of feedstock and binders suppliers.

PIM is a shaping technology for the production of dense metallic and ceramic parts from powder raw material. A binder is added to the powder obtaining a plastic material ready for a hot injection moulding step. Shaped parts are submitted to two more steps to remove the binder and

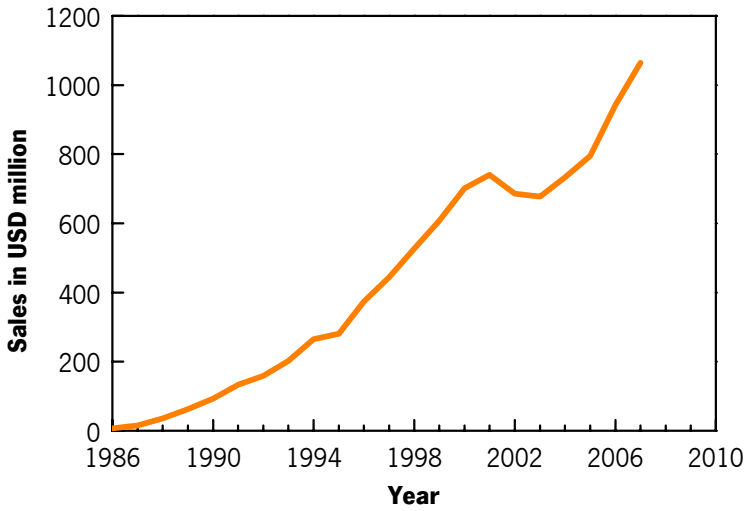

Figure 1.1 Worldwide PIM sales [4].

to densify the material by sintering. The mouldable powder and a binder mixture, usually denominated as feedstock, can be purchased or can be in-house compounded the parts manufacturers. The choice will depend on economic and knowledge criteria [5]. Binder has been considered to have a major role in the process, as it can influence all parts production stages, from quality of the mixture of the feedstock, trough the stability of the injection moulding [6-8], the occurrence of defected debinding parts [9, 10] and the properties of sintered parts [11-13]. The interest in binders topic has galloped in the industrial context since it was realised a lack of understanding of the binder science combined with an overprotection of binder formulations and a restrictive ready-to-mould feedstock market, causing a high value added of the commercial feedstocks [3, 14]. Therefore, the knowledge improvement about binders and compounding and their effect of the process is an opportunity of research.

Among the debinding methods, thermal debinding is widely used as the major mean to remove organics before sintering. However, the release of degradation vapours can cause pressure buildup within the moulded body and create voids at its center, bloating and cracks at its surface if thermal debinding is carried out hastily [15, 16]. In order to overcome these problems in thermal debinding, solvent debinding has been widely adopted [17-19]. In the solvent debinding process, a portion of the binder can be removed by using solvents like acetone, trichloroethane, heptane or hexane [20-22]. A large amount of open porosities, after solvent debinding, allows the thermal degraded products to diffuse to the surface easily. Therefore, the subsequent thermal removal of insoluble binder components can be finished shortly, possibly included as a first stage in the sintering phase. Although solvent extraction would be considered the fastest debinding route, a problem remains with solvent debinding concerning the nature of common solvents; most of the organic solvents adopted in solvent debinding are flammable, carcinogenic and not environmentally acceptable [1]. In order to eliminate the use of unsound solvents, application of water-soluble binder to powder injection moulding is being developed [23-26].

The present work attempts to develop a new binder composition, using a science-based methodology, by improving the use and the understanding of a sequence of experimental procedures. Considered an important step for the development, semi-industrial processing is also tested. Water soluble binder philosophy was chosen, as a very attractive system in terms of low debinding cost and environmental impact. The binder removal without thermal degradation is

also important for the reduction of contamination by organic elements in the sintered material. This is an important feature in metals, specially in high reactive metals.

The proposed methodology to address the binder study and development, is illustrated in the Figure 1.2. The first stage starts by a binder formulation plan. The use of multicomponent thermoplastic binder systems is fundamental. The respective formulation should include: i) a base polymer, in major content, which is removed in water debinding; ii), a back-bone polymer, responsible for shape preservation when parts are subject bear loading during process operations; and iii) a surfactant additive to improve adhesion of binder and powder. In some formulations a wax was also added attempting to improve the feedstock flowability. Polyethylene glycol (PEG) was used as base component as it is water soluble, thermoplastic, non-hazardous and is used quite extensively in food industry [27]. Low density polyethylene (LDPE), metallocene polyethylene (MPE), poly(methyl metahcrylate) (PMMA) and poly(vinyl butyral) (PVB) were tested as back-bone candidates. The effect of two of the most referenced surfactants, stearic and oleic acid, was also studied. An AISI 316 L stainless steel metal powder was used as a case-study, as it is the most processed material by powder injection moulding, accepted for a lot of high demanding applications.

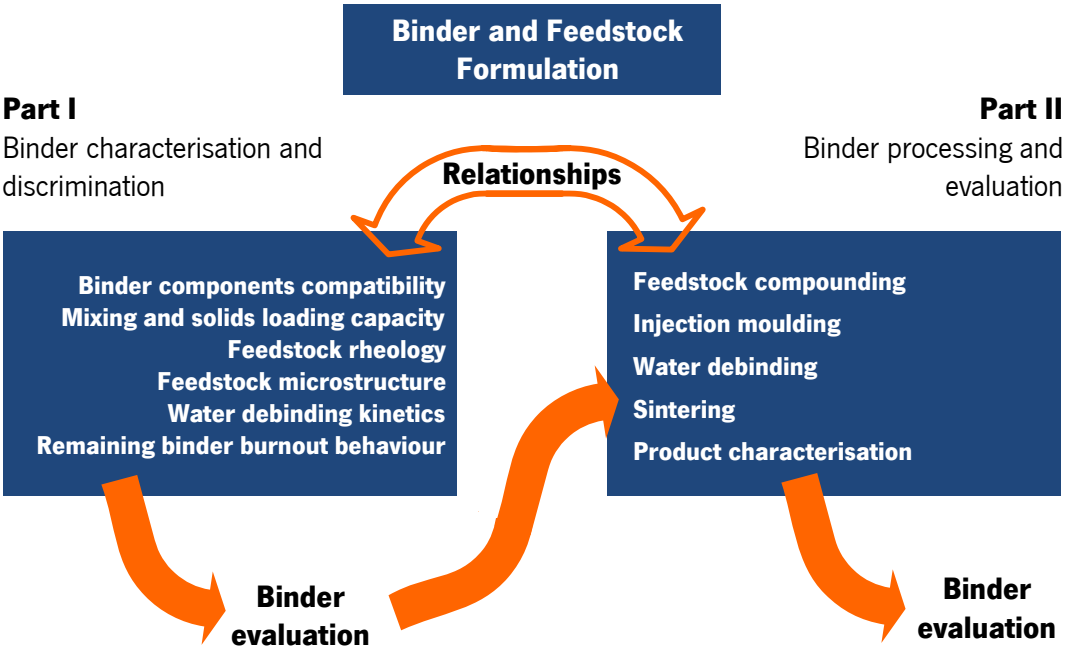

Figure 1.2 Methodology for the approach to binders study and development.

Binder formulation candidates were characterised in six relevant aspects: compatibility, mixing behaviour and solids loading capacity, feedstock rheology, feedstock microstructure, water debinding performance and binder burnout behaviour. It was expected to be possible to predict binder and feedstock behaviour in processing or to eliminate some inadequate binders. Therefore, an evaluation and a selection were carried to enter in process testing (Figure 1.2 – Part I). Processing of 316L stainless steel using the water soluble binders were characterised to evaluate their adequacy and eventually decide the best binder (Figure 1.2 – Part II).

1.2. Research significance and industrial impact

Research activities were steered to improve knowledge about the influence of the binder in PIM process, by relating binder, the process and the manufactured parts characteristics. In order to comply its role, many requirements have been pointed out for the binder system, but effectively none have been capable to match all points [1]. The key has been to balance the binder characteristics to obtain equilibrium of some good characteristics and to work with processing conditions to suppress the worse characteristics. This work intends to explore this balance paradigm in binder design for PIM and to establish a structured binder design procedure.

Increase of binder and feedstock knowledge can have impact in manufacturing chain. European PIM companies are more dependent on ready-to-use feedstock. It assures a high quality raw material, reflected in the final product, but it carries higher cost and less flexibility. This work also intends to have impact in the increase and spreading of binder and feedstock knowledge providing new approaches and methods, helping an emancipation of PIM producers from feedstock market. Control of binders and feedstocks enables cost reduction, offers new materials, allows formulating feedstocks precisely to customer's properties specifications and innovating in new application sectors [28]. Some technology benefits for PIM manufactures are the freedom to choose the debinding method, powder suppliers or to tailor feedstock composition and so the process and parts characteristics. In fact, this has been a natural trend in western world to resist against low cost competitors in Asian countries.

The greenhouse effect caused by burning gases and the human health in industrial environments are important contemporaneous issues. Legislation has been created to control these risks and

become crucial to industries competition. Solvent debinding can be called as green technology because the non gaseous emissions and the solvent recycling. However, the human health has been in risk by leading with such hazardous liquids. Water debinding is seen as a relatively new improvement of an eco-friendly debinding process with much less risk to health. This research contributes to the implantation of this process in industry and to become PIM industry less pollutant and risky.

Last but not least, from a regionalist point of view, the ultimate expected impact of this work is boosting the PIM technology in Portugal. This country has a limited community and scientific work in powder injection moulding and none industry. Yet, it can be considered to have strong factors to be a base for the implantation of PIM companies. Portugal has a strong tradition in ceramic processing, which is technological based in powder processing, having the same conceptual processing phases (moulding, drying and sintering) as PIM. Experience with thermal processing, shrinkage and warping effects are common. On the other hand, portuguese suppliers of injection moulding tooling are international respected and experienced to respond to the very demanding technical applications markets. There is a relevant plastics injection moulding industry producing high tech applications, as automotive and electronics sectors. In fact, it has been reported that the major part of the European PIM companies came from traditional ceramics (38%) and thermoplastics moulding (27%) fields [29]. Therefore, joining this already implanted knowledge and experience and increasing the scientific support from the research centres can be a relevant push for the introduction of PIM parts manufacturing in Portugal.

2. STATE OF THE ART

2.1. Powder injection moulding process

Until recent times, injection moulding was only applied to polymers, especially to those with thermoplastic behaviour. Metals and ceramics can have property advantages over polymers – higher strength, higher stiffness, higher operating temperature and they exhibit electrical, magnetic, and thermal properties not possible with common and cost-competitive polymers. However, conventional metals and ceramics processing and manufacturing technologies can't compete with injection moulding in cost-effectiveness. Powder injection moulding (PIM) enables the use of shaping advantage of injection moulding but is applicable to metals and ceramics. It is commonly called Metal Injection Moulding (MIM) or Ceramic Injection Moulding (CIM) in case of producing components from metallic or ceramic powder, respectively. This process combines a small quantity of a polymer with an inorganic powder to form a feedstock that can be moulded into complex shapes. After moulding, the polymeric binder is extracted and the powder is sintered. PIM delivers structural materials in a shaping technology previously restricted to polymers.

PIM technology was developed at the beginning of the twenty century, but only became wide commercialized in the 1980s. Early demonstrations of PIM followed closely behind the first developments in plastic injection moulding in the 1920s. Its first use was to form ceramic spark plug bodies in 1940s. By the late 1950s, many carbide and ceramic components were being moulded using epoxy, wax, or cellulose binders, but the production volumes were small. Major attention was given to the process in 1979 when two design awards were given to metal products. One component was a screw seal used on a commercial jetliner. The second award was for a niobium alloy thrust-chamber and injector for a liquid-propellant rocket engine. In the 1980s major progress was made in forming ceramic heat engine components by PIM technology. Today, the number of companies using PIM is large and it is regarded as a leading net-shaping technique [30].

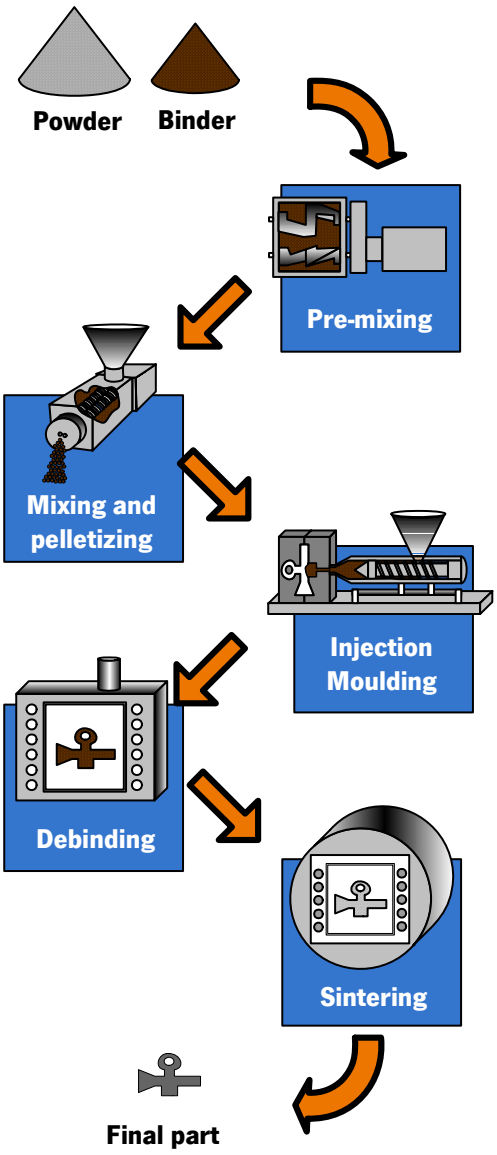

Figure 2.1 Schematic diagram of PIM process, showing the basic flow from powder and binder to sintered part.

Process description

A schematic flow chart of the powder injection moulding process is shown in Figure 2.1. The process begins by mixing a selected powder and the binder. Usually, binders are based on a common thermoplastic polymer of low molecular weight, such as wax or polyethylene, cellulose, gels, silanes, water, and several inorganic substances are also in use. A typical binder content is about 40 % by volume of the mixture; for steel corresponds to about 6 wt.% of binder and for

alumina to about 15 wt.%. The particles are small to aid sintering, usually ranging from 0.1 to 20 μm with near spherical shapes.

a) Feedstock

The term feedstock designates a mixture of powder and binder. The composition of a suitable feedstock balances several considerations. Sufficient binder is needed to fill all voids between particles and to lubricate particle sliding during moulding. Flowability is crucial for the moulding step, which depends on several rheological and physical factors. A high powder-binder ratio leads to a high viscosity and to consequent difficulties to fill adequately the mould cavity. In opposite, too much binder is undesirable since component shape will be lost during debinding. A non-homogeneous feedstock leads to defects in moulding, so a high shear mixing if required to disperse the powder among the binder phase. Therefore, special mixing practice is needed to compound feedstock. The final step in feedstock preparation is to form pellets that are easily fed into the moulding machine.

b) Moulding

For the common thermoplastic binder systems, the pelletized feedstock is injection moulded into the desired shape (the green part) by the combined action of the heat and the pressure developed by the injection moulding machine and the geometry of the tool cavity. Here the role of the binder is evidenced giving to the feedstock a viscosity low enough to flow into the moulding cavity in result of a pressure driven flow. Cooling channels enable the temperature control of the tool assuring the efficient heat removal, the quality of the material solidification process and competitive production rates. The injection moulding machine is the same as used for plastics moulding, but functional components should have improved wear resistance.

c) Debinding

These green parts are already useful for certain applications, including bonded magnets and fragile bullets. However, in a complete PIM process the binder is removed from the

component by debinding, producing the commonly designated brown parts. A wide range of options exists for binder removal. Thermal debinding is the first way to envision, as in general polymers undergo to a chain scission mechanics above the respective degradation temperature [31]. To achieve this, the component is slowly heated to decompose the binder. Among the other alternatives, the most popular is to immerse the component in a solvent to dissolve partially the binder [19, 32]. In this method, some polymer is left to hold the powder particles in place for subsequent handling. The remaining binder is thermally extracted as part of the sintering process. Newer binders are water soluble, so they can be extracted by water immersion [26, 33, 34]. Another popular technique involves catalytic thermal degradation of the binder, where most of the binder is attacked by a catalytic acid vapour [35, 36].

d) Sintering

The following step is sintering, which can be incorporated into a thermal debinding cycle. Sintering is a heating process up to a temperature somewhat below the melting temperature of the powder material in order to bond the particles together, leading to part densification. Often, sintering serves not only for densification but also for chemical homogenisation. In the latter process, sintering a moulding of chemically different mixed powders leads to the formation of homogeneous alloys by long-range atomic motion [37].

Component shrinkage is a known physical phenomenon associated to sintering, so the moulded component should be criteriously oversized to reach the desired final dimension. The process atmosphere is dependent of the chemistry of the powders. For example, for steels and stainless steels, the sintering is often at 1120 to 1350 °C in a protective atmosphere or vacuum. The oxide ceramics, such as silica, alumina, zirconia and yttria, can be sintered in air at temperatures in the 1200 to 2000 °C range [37].

After sintering, the parts have high strength, with properties often superior to those available from other processing routes. In cases where the densification is not high enough, both hot and cold deformation based additional processes can be used, including hot isostatic pressing. Other post-sintering steps include coining, drilling, reaming,

machining, plating, passivation and heat treatment. Options in heat treatment include tempering, precipitation hardening, nitriding and carburization [1].

Technology attributes and products

Primary advantages of PIM technology are components shape complexity, competitive cost and high performance, derived from the outstanding properties obtained with the wide materials range (Figure 2.2). The low porosity and microstructure homogeneity of PIM materials gives a high strength, toughness, ductility and reliable electric and magnetic response. It is also possible to produce both internal and external threads in the moulded component, avoiding post sintering machining, as well as waffle patterns and insignias directly on the component. Furthermore, the surface finish is typically good.

For the producer, PIM is a desirable option because of manufacturing is reliable, flexible and with a relatively easy process control and automation. Inherently, injection moulding is associated with large production volumes. Various components are produced at rates approaching 100,000 per day. On the other hand, small production runs are possible, with as few as 5000 parts per year being economical. This flexibility fits well with the current demand for quick response in manufacturing.

On the key economic issue, PIM is cost advantageous for the more complex shapes and high

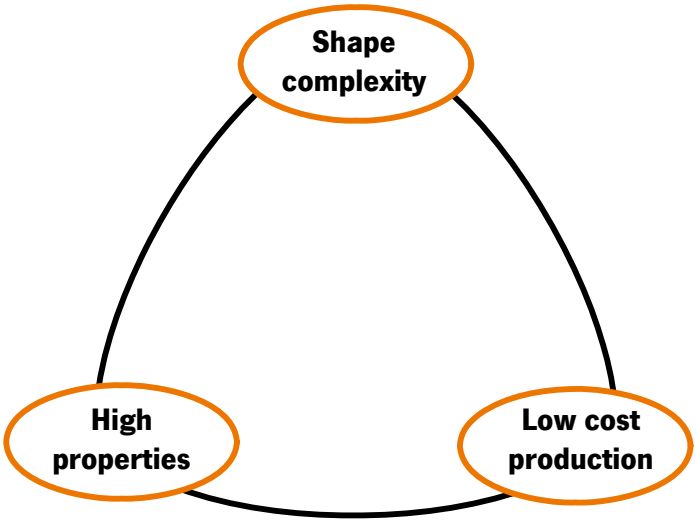

Figure 2.2 Major attributes of PIM technology.

demanding parts. The largest advantages are:

i) the elimination of secondary operations, like grinding, machining, drilling or boring, typically required for precision components;

ii) efficient material use (nearly 100%), since the feedstock used in runners, sprues, and failed mouldings can be recycled. This is particularly important for costly raw materials such as refractory metals, speciality ceramics and precious metals.

Figure 2.3 shows examples of components produced by PIM. Generally, PIM is viable for all shapes that can be formed by plastic injection moulding. However, for shapes with simple or axial-symmetric geometries, it is not competitive with standard machining, compaction and sintering or casting techniques. Another limitation is the component size. Large components require more powder, which is a large expense, and large moulding and sintering devices, which are more expensive and difficult to control. Parts shrinkage in sintering can be also admitted as a factor for the size limit. Typically, the large dimension is below 100 mm with a total part volume below 100 cm^3 [1].

Debinding is a key problem because the time for binder removal depends on the wall thickness.

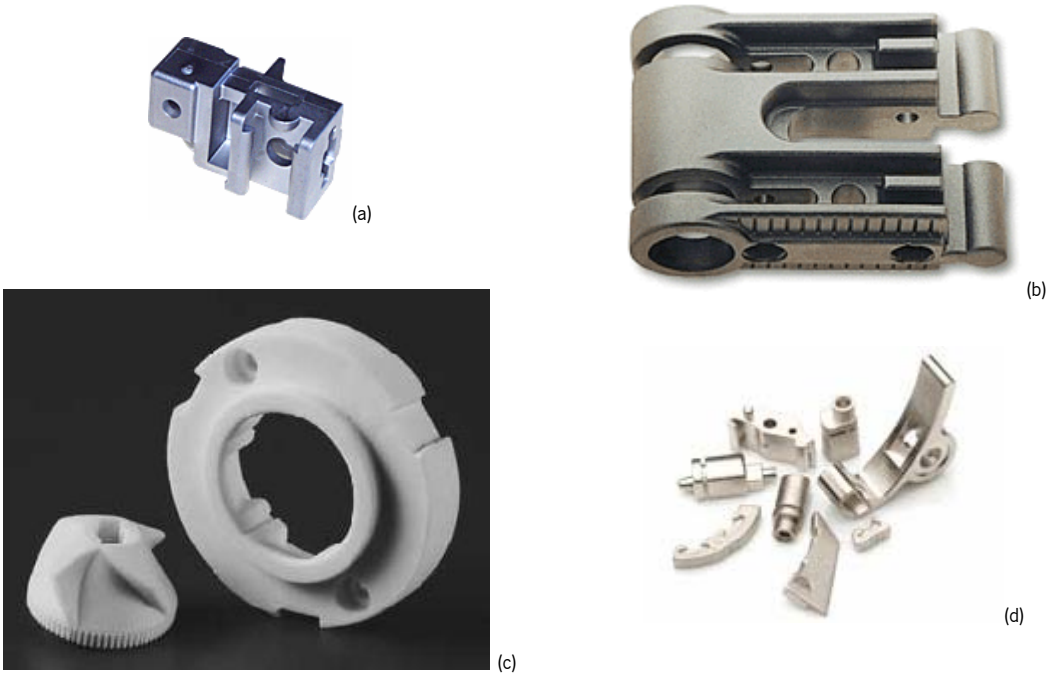

Source: (a) [38], (b) [39], (c) [40], (d) [41]

Figure 2.3 Components produced by PIM.

So, manufacturers use to set upper limits on wall thickness ranging 10 to 50 mm. On the other hand, PIM has been used to mould wall thickness less than 0.5 mm. In practice, dimensional tolerances are typically within 0.3%, although holding tighter tolerances is possible with very tuned feedstock and equipments [30].

Materials processed by PIM include most common ceramics and alloys – steel stainless steel, tool steel, silicon nitride, cemented carbide, silicon carbide, copper, tungsten heavy alloys, nickel-base alloys, alumina, cobalt-base alloys, and composites. Besides traditional materials, PIM can also produce speciality materials such as silicon carbide, nickel superalloys, intermetallics, precious metals and ceramic-fibre reinforced ceramic composites [1]. Co-injection moulding is another possibility, where two materials are combined to make sandwich-like structure. This option is useful for creating corrosion barriers, wear surfaces, electrical interconnections or high toughness structures.

2.1.1. Feedstock

The pelletised mixture of powder and binder used in injection moulding is called feedstock (Figure 2.4). Five main factors determine the attributes of the feedstock: powder characteristics, binder composition, powder/binder ratio, mixing process and pelletization technique. Many manufacturing sites are producing from precompounded feedstock. In such cases, knowledge about powder characteristics and optimization of the binder is not a critical issue. The precompounded feedstocks contain the defined proportion of powder concentration. Therefore, attention to moulding and the further processes are possible without digressions into the compounding stage. Compounding sites need high knowledge of powder and binder technology, but they are free for customise the formulations, such as powder chemistry and powder to binder ratio. Consequently, they can tailor the feedstock characteristics and thus the final components properties [5, 28].

Ideally, the feedstock formulation results from a balance between mouldability and the need to attain control over the final dimensions and specified properties. To achieve this equilibrium, binders often include low molecular weight polymers to reduce viscosity and enable easy flow inside the mould. A minimum amount of binder is required to fill the interparticle spaces and

Figure 2.4 An example of PIM feedstock in pellet form, ready to feed into the injection moulding machine.

provide sliding of particles. When possible, the powder is chosen for a high particle density. This might require adjustments of the particle size distribution or particle shape. Alternatively, differing particle sizes can be mixed to form bimodal size distribution. An excess of binder lowers the feedstock viscosity but fails to provide sufficient particle to particle contact to ensure shape prevention during debinding and sintering. Thus, determination of the ratio of powder and binder is crucial to success of injection moulding. A typical binder content is near 40 vol.% of the mixture [1]. For steel, it corresponds to about 6 wt.%; alumina it will be 15 wt.% and for tungsten it will be less than 3 wt.%.

At mixing and moulding temperature, the PIM feedstock is a viscous liquid. On cooling, the behaviour turns to a solid with elastic response. Depending on cooling rate, residual stresses can develop within a moulded part leading to distortion in debinding. Feedstock is injected at high pressure to ensure cavity filling, immediately is cooled by the heat transfer to the moulding walls. The differential cooling rates along the part thickness and the pressure field within the moulding under cooling causes local thermo-mechanical gradients and subsequent shrinkage gradients. Further, to reduce part distortion, the feedstock must have a low and stable viscosity during moulding but a large viscosity increase on cooling.

The green part strength is very important to maintain the desired shape, especially during debinding, where the materials can slump under the influence of the gravity force. Typically, the need for strength dictates the use of small particles with high interparticle friction. For feedstock the elastic modulus depends in the binder composition and solids fraction. Polymers can store

deformation energy as molecular orientations and volume dilations. The module decreases as temperature increases, but the relaxation of stresses due to the difference in thermal expansion coefficients between the powder and binder complicates the behaviour. Consequently, the modulus will depend on the stress-temperature history of the feedstock [1].

Binder composition influences strength, but high binder strengths can not produce high green strengths. Adhesion between the powder and binder is important in determining the resistance to handling defects [3], in such a way that a paraffin-wax-based feedstock can exhibit higher strength than a polyethylene-based. Further, proper surfactants can improve adhesion and strength and rheology of feedstocks [8, 11, 42-45].

2.1.2. Powders

The powder is the feedstock constituent present in the all process stages and correspond to the final material. Thus, it should be considered a key constituent. Several powder characteristics influence the PIM process, namely: particle size and its distribution, particle shape, surface area, interparticle friction as measured by packing and flow, internal particle structure and chemical gradients, surface films and admixed materials. Studies attempted to designate the most appropriate requirements of powders for PIM [1]. For any single attribute, certain particle features dominate. However, requirements can be contradictory. Easier moulding and high solids fractions are favoured by spherical particles, but reduced distortions in debinding is favoured by irregular particles. Thus a balance is needed in selecting a PIM powder.

Powder chemistry and production methods

Often, the chemical compositions are adapted from existing applications produced by other technologies. The main adaptation is to turn the particles finer and roughly there are no particular limitations. Table 2.1 shows the materials in use for injection moulding.

For alloys compositions, there are three process: mixing elemental powder and the alloys is formed during sintering, pre-alloying powders or mixing of pre-alloy and elemental powders. Sintered components produced from alloy powders compared with powders mixtures of pure

metals have a more uniform structure, giving higher mechanical properties. However, the latter gives better green strength and less moulding defects [46, 47].

A wide range of powder chemistries demand a large variety of powder production techniques. These techniques influence the size, shape, microstructure, chemistry and cost of the powder. Ceramic powders are produced usually by comminution techniques. Grinding and milling are common ways for generating small powders from brittle materials. Most powder materials can be fabricated by one form of chemical precipitation or reaction. The particle size and shape can be adjusted over a wide range. Very small ceramic particles are produced by the decomposition of oxides, alkoxides, carbonates, acetates or oxalates. Precipitation techniques are useful for

Table 2.1 Chemistries available in fine powders [1].

alumina (Al_2O_3), alumina-silica (Al_2O_3-SiO_2), alumina-chromia (Al_2O_3-Cr_2O_3),
aluminium nitride (AlN)
bronze (Cu-Sn)
cemented carbide (WC-Co)
cobalt-chromium (Co-Cr-W-C or Co-Cr-Mo)
copper (Cu)
ferrite (Fe_3O_4)
iron (Fe), iron-silicon (Fe-Si), iron-phosphorus (Fe-P), iron-nickel-cobalt (Fe-Ni-Co)
molybdenium (Mo), molybdedium-copper (Mo-Cu)
nickel (Ni), nickel aluminide (NiAl and Ni_3Al), nickel-iron (Ni-Fe)
nickel-base (Ni-Cr-Mo)
sílica (SiO_2)
silicon carbide (SiC)
silicon nitride (Si_3N_4), sialon (Si_3N_4-Al_2O_3)
spinel (MgO-Al_2O_3)
steel (Fe-C), copper-steel (Fe-Cu-C), nickel-steel (Fe-Ni-C)
stainless steel (Fe-Cr-Ni)
superalloy (Ni-Co-Cr-Ti-Al-Mo)
titanium (Ti), titanium alloy (Ti-Al-V), titanium aluminide (TiAl, Ti_3Al)
tool steel (Fe-Co-Cr-W-V-C)
tungsten (W), tungsten-copper (W-Cu), tungsten heavy alloy (W-Ni-Fe, W-Ni-Cu)
yttria (Y_2O_3)
zirconia (ZrO_2), zirconia alloys (ZrO_2-MgO, ZrO_2-Y_2O_3, ZrO_2-CaO)

forming refractory, reactive metal, ceramic and composite powders. Atomisation is a common process involving the formation of powder from a liquid using a spray of droplets, which solidify forming the powder [48].

Powder characteristics

Three powder characteristics dominate in PIM process: particle size, packing density and particle shape. Fine powders, i.e. with a particle diameter less than 20-30 μm (average diameter preferably about 4 to10 μm), are mainly used in production [1]. As the green density is low, about 60 % of the full, small particles, having consequently high surface area, are needed to aid sintering. There is no definitive ideal particle size distribution. Narrow distribution provides less likely to powder segregation, faster debinding and higher homogeneous microstructure. Wide particle size distribution creates higher packing density, less sintering shrinkage and thus eases dimensional control. Fine powder, as it is regularly used, are expensive and the search of blending techniques are incrementing [49]. For example, concerning stainless steel powders, if there are mainly specifications concerning the mechanical and corrosion properties, coarser powders may be an alternative to the ordinary MIM powder that reduces production cost. If there are stringent specifications for the surface quality, the use of fine powder is obligatory [50]. Also, bimodal powder mixtures with two distinctly different particle sizes, having a high concentration of large particles, the tap density improves as the small particles fill the interstices between large particles [37, 51].

Regarding shape, spherical particles are ideal for an easy flow during injection moulding, but they do not provide higher final geometry retention as the irregular shape particles. As an example, gas atomised steel powder produce less dimensional variability than the water atomised powder from lot to lot, however, the water atomised powders produce less in lot dimensional variability and are generally less susceptible to distortion of cantilevered members during sintering [52]. Balancing shape is crucial, and an aspect ratio slightly over the unity, typically near 1.2, is generally considered to be adequate [1].

High packing density powders are desirable leading to less dimensional change in sintering and better strength. Higher packing is attainable by the used of finer powders. Despite of these

powder are more expensive, as the particle size decreases, friction in a powder mass increase which interferes with mixing and moulding. Alternatively, a low interparticle friction creates problems with component slumping and shape retention during debinding. Tap density is a example of a simple way to evaluate the packing capacity of the powder, and know how far the feedstock solids fraction can go. Tap density of over 50% of theoretical density is satisfactory.

Table 2.2 presents examples of powders for PIM and some of their characteristics. SEM micrographs of those powders are shown in Figure 2.5. They are a short example of the long variety of powder used in injection moulding.

2.1.3. Binders

The binder is a temporary vehicle for the injection moulding, serving to promote the homogeneous packing of the powder into the desired shape and holding the particles in that

Table 2.2 Examples of powders used in PIM.

Material	Particle size	Specific surface area	Particle shape	Production process	Photo in Figure 2.5	Ref.
Titanium alloy (Ti-6Al-4V)	7.7 μm (mean)	0.23 m^2/g	angular	HDH		[53]
M2 high speed steel	9 μm (mean)	0.662 m^2/g	spherical	gas atomisation	(a)	[54]
Niobium	7.4 μm (median)	-	irregular	-	(b)	[55]
Stainless steel (17-4PH)	10 μm (median)	-	spherical	gas atomisation		[24]
zirconia (ZrO2-3%Y2O3)	0.25 μm (mean)	6.9 m^2/g	relatively spherical	-	(c)	[56]
Cemented carbide (WC-8%Co)	3.2 μm (mean)	0.397 m^2/g	angular	-	(d)	[57]
Stainless steel (316L)	11 μm (median)	-	irregular	-		[47]
Alumina	1 μm (mean)	9.3 m^2/g	irregular	-		[23]

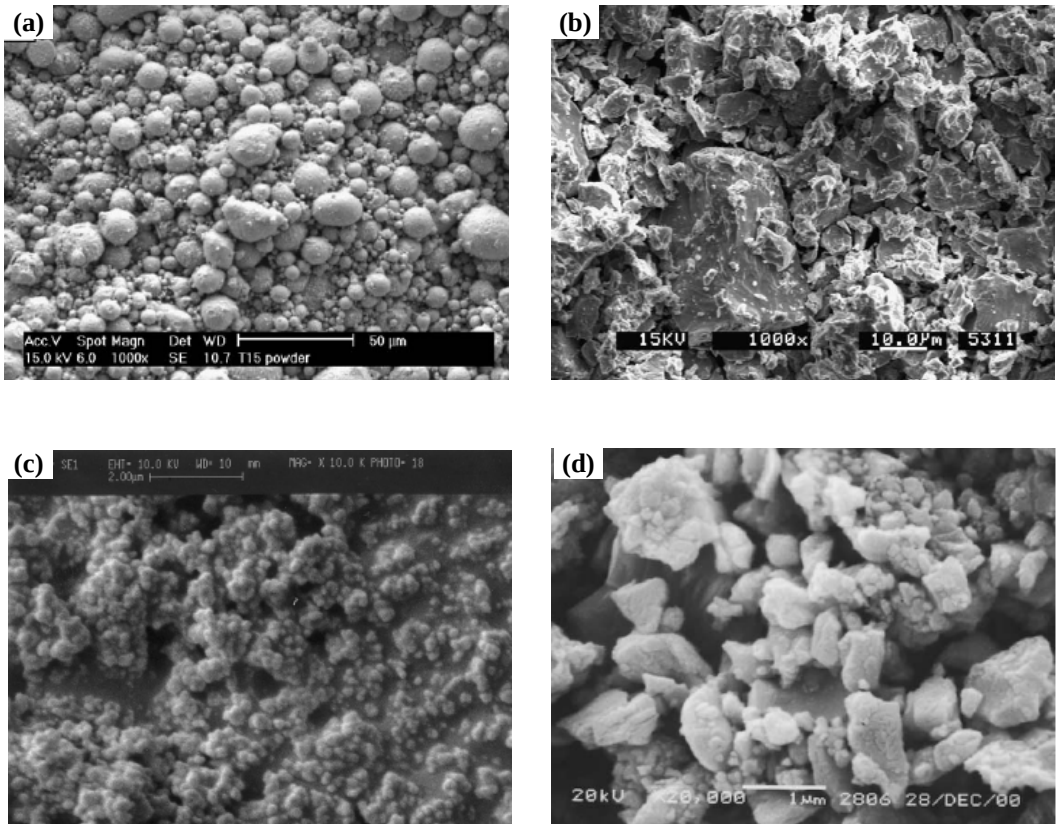

Figure 2.5 SEM micrograph of some PIM powder, according to Table 2.2: (a) M2 high speed steel, (b) niobium, (c) zirconia-yttria and (d) cemented carbide.

shape until the beginning of sintering. Although the binder is not a raw material for the composition of the sintered component, it has a major influence on the success of PIM processing.

Most binders are multiple-component systems that contain a major component which gives the basic properties, blended with several other materials in order to be adjusted for a suitable application. Its main role is to provide the flow needed to fill the mould cavity. After moulding, the binder holds the powder particles and is removed from the part. A remaining quantity is let in the parts in order to avoid cracking and parts failure during the transport for the sintering equipment.

Finally, in sintering, the remaining binder is burned out and the particles are heated to the sintering temperature. The binder is eliminated leaving a minimum or none residue.

Binder requirements

Table 2.3 lists the requirements of a binder system, classified under different process considerations: mixing and moulding, debinding and general manufacturing issues**.** The binder strongly influences the process operations and the final properties of the products, leading to numerous material requirements. However, some of these attributes are contradictory to one another. Thus there is no ideal binder and the selection is dependent on the particular situation. Binders represent a compromise between various desired attributes [1].

Powder fillers increase dramatically the viscosity of the feedstock. In fact, the powder fraction in PIM compounds is near the limit for feedstock flowing, where a hypothetic binder fully based on a regular grade of thermoplastic will not be able to be injection moulded. The need for a binder with extremely high flowability dictates the use of low molecular weight binders, typically waxes. The small molecules fit between particles and avoid orientation during the flowing process. Beside the low viscosity at high solids fraction, the binder must inhibit powder separation or agglomeration [7]. Waxes are inadequate at this respect, so they are blended with polymeric materials.

It is fundamental that the binder wets the powder surface in order to aid mixing, easing the particles deagglomeration, and moulding [58]. So, several substances are widely used to modify the wetting behaviour, namely titanates, silanes and stearates. These surface active additives reduce mixture viscosity and increase the solids content by playing a role of bridge between the powder and the binder [44, 45, 59-61]. This link must be strong enough to maintain the homogeneity of feedstock mixture and moulding process, but the binder must be chemically passive with respect to powders.

Recyclability of the binder and thus the feedstock is a key factor for the economic viability of the process, as the moulding process produce an appreciable quantity of scrap from the moulding gates, runners and sprues. This is an important factor which contributes for the competitivity of this process when compared to other forming technologies. The thermo-mechanical actions of repeated moulding cycles causes feedstock degradation in level dependent on the chemical nature of the materials used and on the adjusted processing conditions. So, to minimise

Table 2.3 Binder requirements [1, 62].

Process consideration	Requirement of binder
Mixing and moulding	Extremely low viscosity (<10 Pa.s at moulding temperature)
	Small molecules to fit between particles and avoid orientation during flow
	Thermally stable
	High thermal conductivity
	Low thermal expansion coefficient
	Good mechanical properties after cooling
	Good wetting on powder surface
	Chemically passive with respect to powders
	Recyclable / reusable
Debinding	Very low viscosity for wicking
	Good solubility for solvent extraction
	Easy pyrolysis for thermal debinding
	No distortion, slumping or blow-out
	Non-corrosive and non-toxic decomposition product
	Decomposition before sintering temperature and low ash content
	Some remaining in presintering to retain shape after debinding
Manufacturing	Reasonable cost and availability
	Long shelf life
	Minimized process variability
	Safe and environmentally acceptable

property losses, recycled material is often mixed with fresh feedstock, order to maintain green parts quality.

The binder and the debinding process are selected to reduce defects and allow rapid binder removal. The major part of the binder is removed by several techniques, namely solvent extraction, wicking, evaporation, sublimation, catalytic reaction or thermal degradation. On the early stages of the sintering, the remaining binder is removed by thermal degradation. The gaseous products are released through the open pores in a quite controlled process without generating internal vapour pressure that can cause component failure [63, 64]. They must not be corrosive to the sintering furnace and leave a lower as possible residue on the particle. This

remaining material is added to the powder material and, usually is detrimental for the sintered parts properties [9, 13, 53].

Manufacturing attributes associated with the binder include a reasonable cost, high availability, minimized variability and long shelf life [52]. To prevent property changes over time, the binder cannot interact with the ambient environment. Accordingly, it cannot absorb moisture or contain volatile components.

Binder composition

Many binder systems and debinding techniques are used in industry and research. Part of these variations reflects the little differences in powder characteristics and debinding techniques. Table 2.4 shows some examples of binders claimed in patents and used in research publications. Generally, the most representative binders can be classified as: thermoplastic based, thermosetting based and gelation [62].

Thermoplastics yield solid materials by cooling a polymer melt and soften upon heating and can be reshaped. Thermoplastic based binders are the most widely used. They usually consist of a wax as major component and a thermoplastic as backbone polymer. Additives are added for lubrication, viscosity control and wetting. Debinding of such binders is normally made by thermal degradation, solvent extraction, wicking or, in minor cases, by photo-degradation [1].

Thermoplastics used are frequently polyethylene, polystyrene, polypropylene and ethylene vinyl acetate. In spite of the fact there are many types of thermoplastic based binders being formulated, only a few binders are used in commercial production. The most popular are the waxbased binders. Wax is chosen as the major component because of its low viscosity, low melting point, good wetting behaviour and low decomposition temperature [13]. This is advantageous for mixing, moulding and decreases debinding time.

Thermosetting resins harden by chemical crosslinking, leading to a physically irreversible three-dimensional network whose properties and shape are set by the process. Resins, such as phenolic and epoxies, usually cured at elevated temperatures between 110 and 180 °C or upon

Table 2.4 Examples of binders for PIM.

Binder formulation	Ref.
Thermoplastic based	
72 % polyethylene glycol, 24 % polyethylene, 4 % tritolyl phosphate	[65]
94 % polycaprolactone resin, 6 % stearic acid	[66]
58 % polystyrene, 29 % oil, 12 % stearic acid	[67]
45 % polyamide, 25 % ethylene-bis-laurylamide, 30 % N,N-diacetylpiperazine	[68]
58 % polystyrene, 30 % mineral oil, 12 % vegetable oil	[69]
44 % polystyrene, 44 % oil, 6 % polyethylene, 6 % stearic acid	[70]
62 % paraffin wax, 33 % polypropylene, 5 % stearic acid	[71]
80 % microcrystalline wax, 20 % stearic acid	[72]
74 % polystyrene, 26 % butyloleate	[73]
40 % paraffin wax, 37 % ethylene vinylacetate copolymer	[44]
79 % paraffin wax, 10 % ethylene vinylacetate copolymer, 10 % high density polyethylene, 1 % stearic acid	[74]
65 % poly(ethylene glycol), 35 % cellulose acetate butyrate	[34]
60 % paraffin wax, 10 % high density polyethylene, 10 % polypropylene, 5 % liquid paraffin, 5 % dioctylphthalate, 5 % ethylene propylene diene monomer, 5 % stearic acid	[75]
53 % low density polyethylene, 26 % ethylene-acrylic acid block copolymer, 21 % paraffin wax, 5 % stearic acid	[76]
93 % naphthalene, 6 % ethylene vinyl acetate, 1 % stearic acid	[77]
Thermosetting based	
thermosetting methacrylate resin (Loctite)	[78]
65% epoxy resin, 25 % paraffin wax, 10 % butyl stearate	[1]
polycarbosilane, 0.5 % p-benzoquinone, paraffin wax, oleic acid	[79]
Gelation	
98.4 % water, 1.2 % agar, 0.4 % Darvan C dispersant	[80]
56.5 % water, 25 % methyl cellulose, 12.5 % glycerine, 6 % boric acid	[80]

mixing with a hardener. Debinding is also accomplished by thermal degradation or solvent extraction. The alternatively condensation crosslinking (typically of polyurethanes) usually involves vapour formation as a by-product which is a source of moulding defects. Therefore, only the addition crosslinking reactions are of interest for PIM. The hardening process is generally slow, so that the time needed to mould a part is longer than using a thermoplastics binder. The fundamental advantage of using thermosetting based binder is that it provides higher green strength due to crosslinked structure [1].

Gelation approach is a result of the acknowledgment of the limitation that the binders placed in the PIM process. The polymeric binder system, which allows the forming of complex shapes with particles, is also the cause of many technical and economical problems. This approach lowers the processing temperature and pressure, leading to the use of lower capacity equipment and hence more economical. Fastening debinding is the most popular advantageous. Gels are chemically lightly crosslinked polymers formed by swelling upon addition of solvent, like water and alcohol. The gel involves only a small portion of the binder, since the solvent can be trapped in the large network molecule. The liquid, once evaporated due to elevated temperature, would result in a highly viscous structure that would result in a highly viscous structure that binds the powder particles together. Debinding is carried via evaporation followed by thermal degradation [3].

2.1.4. Mixing

Mixing involves the transport of material in the mixture to produce the desired spatial arrangement of the individual components. Although mixing is a critical process step for reliable production of quality injection moulded parts, it generally is regarded as a somewhat simple operation. The best mixing is achieved with high shear, but not so high where the work of mixing can damage the particles or overheats the binder [2].

The mixer design is important to ensure uniform mixing, once PIM feedstock is sensitive to shear rate. The shear level has a space variation in a mixing chamber, and good mixing requires all regions be equally sheared. Several high shear mixer designs are used for PIM feedstock, which include double planetary, single and twin screw extruders, shear roll compounder and sigma or z-

blade mixers. The twin screw extruder is the most successful, since it combines high shear with short residence time at elevated temperatures [71, 81] (Figure 2.6). It consists of two intermeshing counter-rotating screws that move the mixture along the heated cylinder to extrude a noodle. Unfortunately, this design is expensive, but it has the fewest problems with scale-up. On the other hand, sigma blade and double planetary mixers are more economical, but they produce lower homogeneity. In each case of equipment, there are regions at which there is the highest shear to provide the needed mixture homogeneity. Feedstocks are high filled composites in such a way that are very abrasive, therefore these same regions experience the greatest wear, releasing some contamination. Generally, a continuous mixer gives higher homogeneity and the lowest contamination level. To reduce contamination, the mixer construction materials need to de smooth and very hard [1].

Heating is performed using internal heaters or double-walled vessels with externally heated oil or steam around the chamber. On exit, the mixed feedstock is cooled and formed into granules or pellets. There are two goals in granulating or pelletising feedstock. The first is to prepare clusters

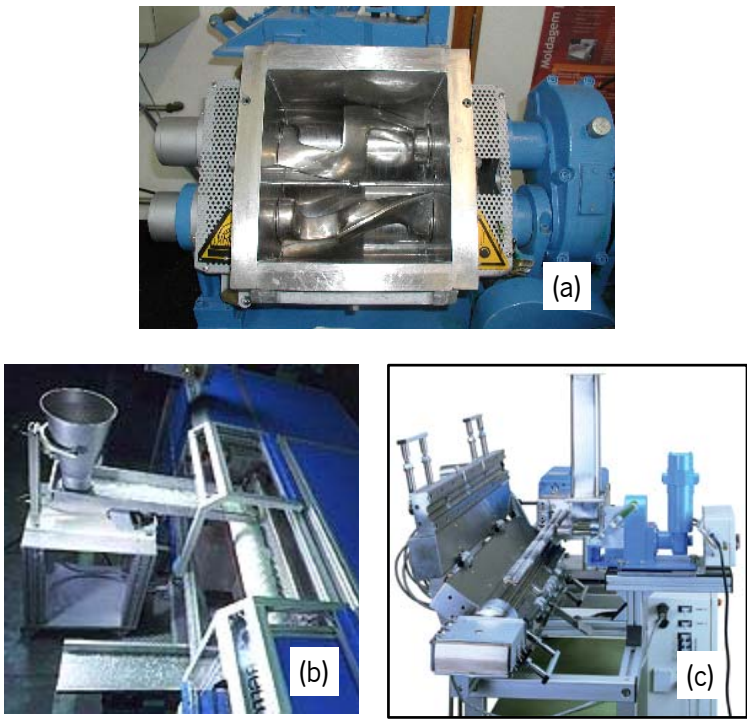

Figure 2.6 Typical feedstock compounding equipments: (a) z-blade mixer, (b) shear roll compounder and (c) twin screw extruder.

of mixture weighed sufficient for the automatic feed of the moulding machine. The second is to incorporate recycled material back into the process. The recycled material proceeds from sprues, runners and improper green parts.

An adequate mixed compound consists of a homogeneous powder dispersion among the binder with no internal porosity or agglomerates [58]. Inhomogeneities result in non-uniform viscosities, inconsistent moulding and non-quality sintered parts. These problems occur in two main forms, separation of binder from the powder and segregation. This phenomenon leads to distortion of the final product. Small and irregular-shaped particles require longer mixing times to achieve homogeneity. Problems with agglomeration are magnified at particle sizes below 1 μm, especially if the particle shape is irregular. Examples are fine ceramic powders produced by milling, such as alumina and zirconia. Here, it is best to premill the powder with a surfactant that causes the agglomerates to break down [82]. Then, during mixing the surface-treated powder is added to molten binder and the liquid is wicked into particle clusters by capillary action [2].

Feedstock quality control should be in industrial environments is desired to be rapid and reliable. A first level of homogeneity assessment is density, which is dependent on the powder and binder densities and proportion. The magnitude of the deviation between the theoretical and actual densities can indicate improper mixing. However the feedstock homogeneity can be better assessed by the viscosity measurements, that can detect instabilities and poorly mixed systems [1, 71, 83].

2.1.5. Injection moulding

Thermoplastics are the most used binders in PIM technology. Therefore, this section will focus the moulding step for a thermoplastic binder. In the moulding cycle, temperature and pressure are applied to drive the feedstock into the mould cavity. For this purpose a plastics injection moulding machine is used. High volume PIM productions use a horizontal moulding machine with a reciprocating screw inside a heated cylinder.

Process

The production runs with repeated injection moulding cycles, in each one the feedstock is melted through a plasticizing process and injected into a mould cavity, due to pressure action of the screw that acts as a piston with axial movement. The material cools down and consolidates into its shape inside the mould, which relatively cold walls assure the necessary heat removal.

The injection cycle includes the main following stages (Figure 2.7):

- Closing – closing of the mould and application of the clamping force;
- Filling – filling of the mould cavity by the melted feedstock driven by the advance of the reciprocating screw;
- Packing – the screw remain pressing the melt into the cavity to compensate material shrinkage and to prevent counterflow from the mould before material cooling;
- Cooling and Plasticizing – the part remains in the mould until cools down and recovers the adequate stiffness to assure shape stability. During this stage, the screw rotates and plasticize the material for the next cycle;

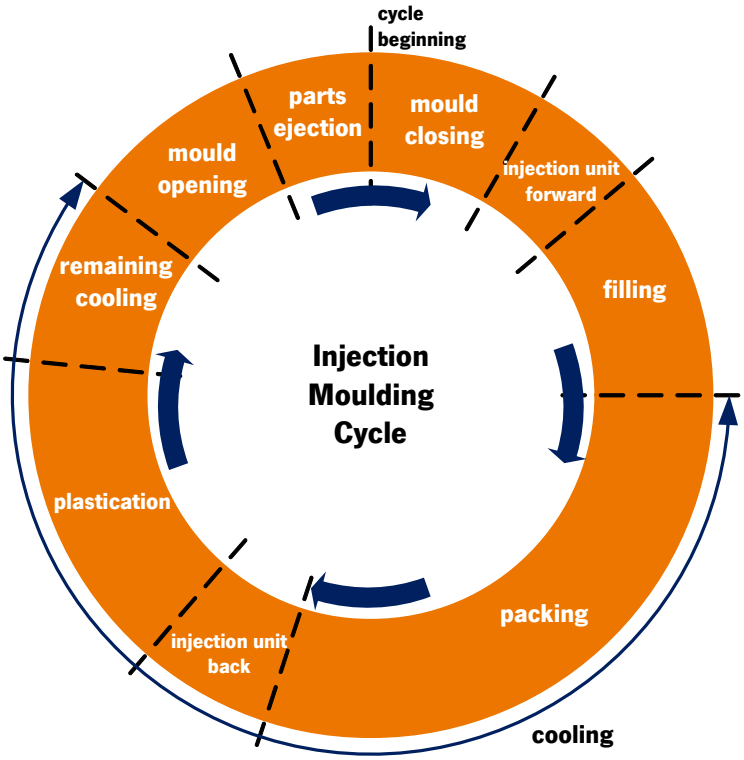

Figure 2.7 The injection moulding cycle.

- Opening – the mould opens;
- Ejection – the parts are ejected by the mechanical action of the ejector pins.

Filling flow rates are relatively high to prevent the melt flow to solidificate before full filling of mould cavity. Comparing to plastics injection moulding, the flow rates are higher because the concentration of metallic or ceramic particles in the feedstock increases dramatically the thermal diffusivity [84] and the viscosity.

Once an appropriate moulding machine is selected, the moulding conditions must be determined based on the material and the part being moulded. The size and the shape of the mould cavity are determined by the part geometry, the number of parts to be moulded and the filling capacity of the machine. The mould design – the number of cavities per mould, their size and their shape – plays a role in the fabrication of cost-effective powder injection moulded parts.

Equipment

Considerable variability of injection moulding machines is encountered, because of the larger number of companies offering to adapt plastic moulding machines into custom PIM machines [1]. Figure 2.8 shows schematically a typical machine, with cross-section details of the cylinder, the screw and the tool, identifying the major components.

A very important part is the design of the screw; which geometry defines functional zones. The

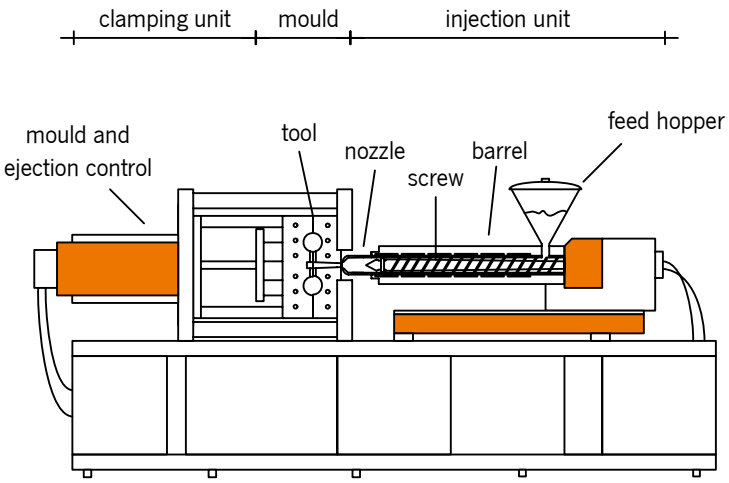

Figure 2.8 Schematic drawing of a typical horizontal injection moulding machine.

screw is a typical three zone screw as used for thermoplastics, but it has a lower compression ratio and a zone splitting as shown in the picture Figure 2.9. The cold feedstock enters in the feeding zone, where the screw has a large flight depth. The flight depth progressively decreases to compresses the feedstock, along the compressing zone, as it is heated and moved forward in the cylinder. During plasticizing, the screw acts as a mixer to ensure uniform heating. The screw has a check ring behind the tip that acts as a non-return valve that allows feedstock flow into the front of the cylinder during plasticizing and seals against a seat ring on the screw during mould filling and force flow trough the cylinder nozzle [85].

The cylinder holds the screw and is surrounded by heaters that control the mixture temperature. The materials used in constructing the wear components (screw, cylinder, check ring, nozzle and screw tip) are critical to long service without contamination. PIM feedstock is abrasive to motion components, especially ceramic feedstocks. Accordingly, hard materials and close tolerances are required to reduce wear. The vanadium carbide containing tools steels and boride clad steels prove to be the most durable in PIM [1].

The clamping unit is the section of the machine in which the mould is mounted. It supplies the motion and the force to open and close the mould and to hold the mould closed tightly during the injection cycle [86].

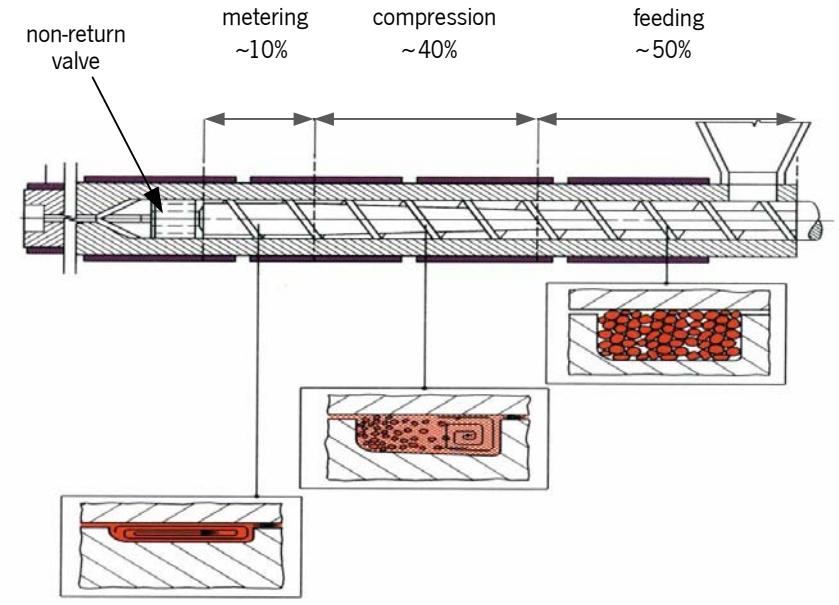

Figure 2.9 Screw functional sections for a powder injection moulding machine (courtesy of Arburg).

Process variables and common defects

Defects in the PIM parts are widely generated in moulding, although they may not be evident until the subsequent processing steps [87-89]. To avoid them, the moulding process should be optimised, since the plasticizing of feedstock to cooling and ejection. The most complex steps, and the main defects source, are the filling and packing stages. Figure 2.10 provides a conceptual guide to drive a right moulding process by tuning the screw speed (equivalent to the flow rate) and pressure. Moulding process is composed by two steps: filling, where the injection flow rate is controlled until the cavity is full, and a packing, where a pressure control is employed. During both cooling takes place, although it is almost negligible in filling due to the very short times. Changeover occurs when the cavity is almost filled (about 95%) and begins pressurisation to the holding pressure. In such cycle, the defects can be originated by the deviations from the ideal screw injection speed or cavity pressure pathway. Consequently, there is a limited operating window for a given feedstock and cavity geometry for the production of free defect parts.

Short shots occur at lower pressures and temperatures. At higher pressures and temperatures, the parts stick to the cavity walls or separate the cavity along the parting line, called flash. Jetting occurs with a quick fill rate and a low viscosity. Intermediate temperatures and pressures provide

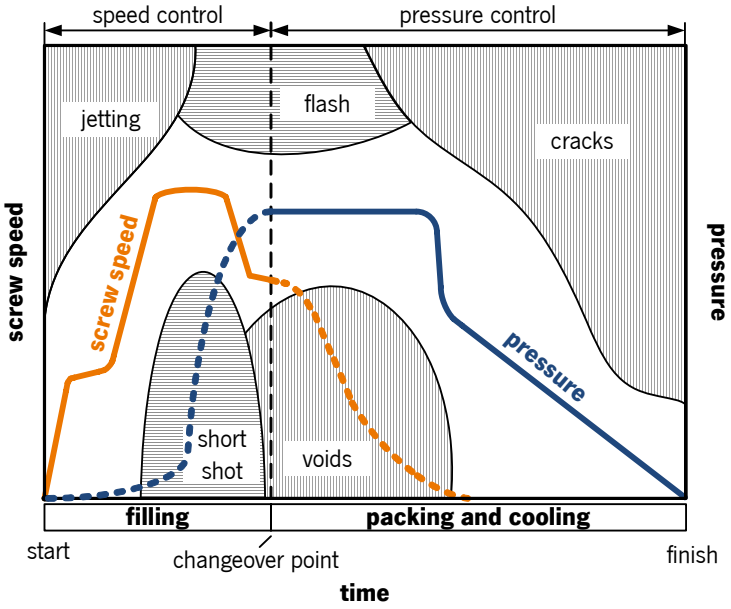

Figure 2.10 Diagram of the defects in injection moulding of PIM parts and typical occurrence conditions relating to the speed profile, during the filling phase, and the pressure, during the packing phase (adapted from [1]).

good mouldings. Pressurisation is employed to compensate the volume shrinkage of the part during cooling, so that voids can be avoided. Higher pressure can lead to residual stresses and consequently cracks. Therefore, a set of melt temperature, injection flow rate and a packing pressure must be optimised [86, 90-92].

Feedstock characteristics as well as reproducibility are very important to a well succeeded moulding process. It is imperative that in order to obtain a well optimised set of well tuned machine parameters, the feed material must have high and regular quality [7, 52, 86, 93, 94].

New processes

New developments imported from plastics injection moulding have been applied in order to increase the range of applications of PIM process. An example is the gas-assisted injection moulding. In this technique, a gas is fed into the melt flow to produce hollow parts. The consumption of raw material can be cut while the stiffness of the part remains on a high level. It is possible as well to increase part volume while keeping the consumption of material constant. For these reasons gas-assisted injection moulding has been popular by conducting to a more cost effective production of plastics. Altogether the use of gas-assisted injection moulding in powder injection moulding provides the same advantages as in the processing of thermoplastics [95, 96]. Figure 2.11 shows a ceramic laboratory spoon produce by this technique.

Bi-material injection moulding is also a plastics-imported technique under development for PIM applications. It has two variants - over-moulding and co-injection moulding. In over-moulding, a

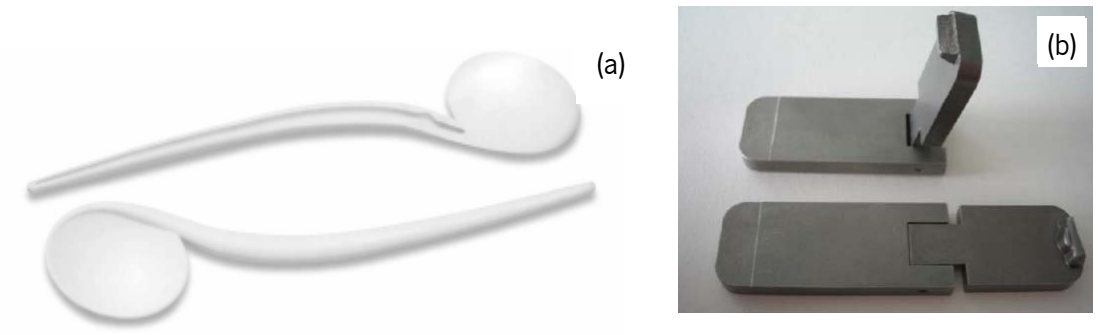

Figure 2.11 Examples of PIM parts moulded by gas-assisted ceramic injection moulding (a) and metal injection assembly-moulding (b) [97].

moulding machine equipped with two injection units is used to inject two different polymer-powder mixtures into the desired shape. The method involves moulding one part in a cavity and then rotating the tooling to form another cavity and moulding around the previously moulded part. When ejected, the part is composed of two interlocked materials. The moulded part is then thermally processed to remove the polymer and sintered to produce a single, integrated component. It also possible to produce assembled components with this technique, as the example shown in Figure 2.11. In co-injection moulding, a functionally graded structure is produced using the flow behaviour of the materials, through the same runner system, to produce a structured component that has a core and skin of two different materials. This is a well-established technology for plastics and has been examined for two metal and ceramic powders [98, 99].

2.1.6. Tooling

The tooling for powder injection moulding is similar to that used in plastics injection moulding. The major difference is that PIM tools are oversized to account for sintering parts shrinkage. A tool set has cavities and further consists of pathways for filling those cavities with ejectors for extracting the part. Considering the diversity of injection moulding and wide range of binder characteristics, in this chapter it is assumed a typical combination of a thermoplastics binder and a reciprocating screw moulding machine.

Before designing a mould one should consider the design of the desired parts. The possibility of producing a given part by injection moulding must be based on factors such as its size and weight, radius, thickness of sections, shrinkage, tolerances, draft angles and the presence, number, size and location of threads and holes. After a deep review of all information about the part that will be moulded, the design of mould can be started [2].

Figure 2.12 shows a moulding tool set represented in a simple way to introduce the main components.

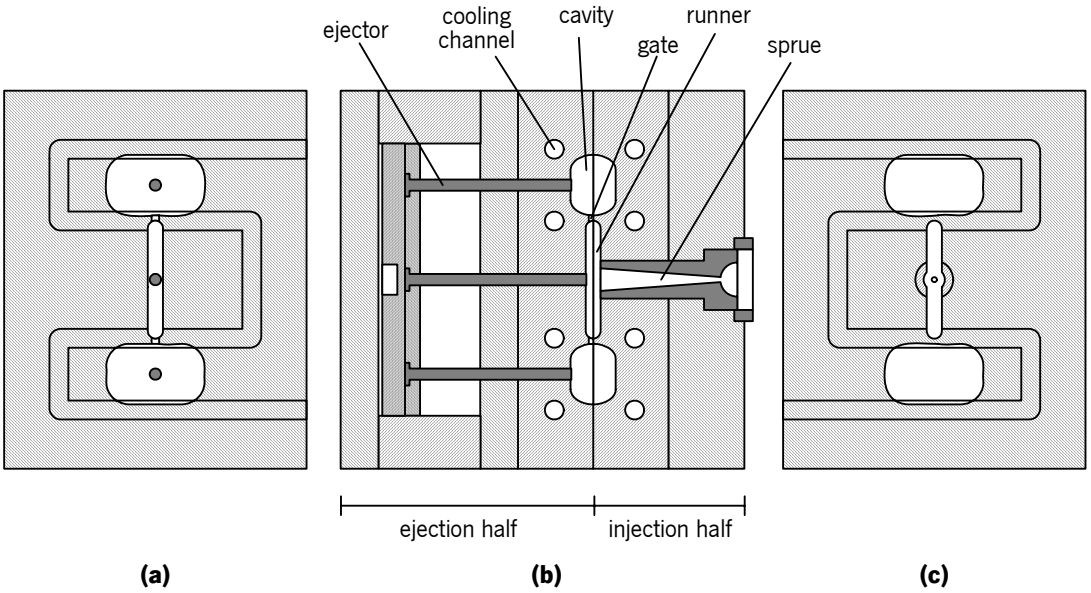

Figure 2.12 Two-plates tool set with two part cavities, showing the main components in both halves (b) and the surface of the ejection (a) and injection plates (c).

Cavity

The oversized cavity is the heart of the tool. In spite of being a small percentage of the sintering shrinkage, the size of the cavity must be also oversize in account of the part cooling shrinkage during the moulding cycle.

Sintering shrinkage depends on several factors regarding to process parameters and feedstock characteristics. The major factor is solids fraction. For example, parts moulded from typical feedstock containing 60 % by volume of solids will shrink in each linear dimension about 15 %. This value is supposed to be known exactly when the tool is designed to assure right sintered dimensions. Especially for complex parts, shrinkage is dependent in filling conditions which are also dependent on cavity design, in such way that an iterative process must be performed. In practice, a first tool cavity is created with under sized dimensions. A batch of testing parts are produced and, according to the real shrinkage obtained, the tool cavity is finished with the dimensions now calculated. This process can be repeated until final adjustments drive to a final sintered dimensions and tolerances. The number of cavities in the tool set depends on the number of parts to be fabricated, the shot capacity of the moulding machine, the fabrication

costs and the available clamping force. Most PIM parts are shaped in tool sets with one to eight cavities [1].

Feeding system

The sprue provides the path for the flow of plasticized feedstock from the cylinder nozzle to the runner network. The component of mould that forms this path is called the sprue bushing. Sprues are tapered with about 5°. The runners direct the injection material into the mould cavities through the gates. Large runners are desirable since it eases the filling; typical diameter is in the 3 to 10 mm range [2]. Other advantages of large runners are that the parts shrink less, and because the mould fills quickly, there are fewer flows or knit lines produces in the parts. It takes longer for the material to solidify in a larger runner, so the pressure must be maintained longer. This aids minimizing the production of knit lines and voids. A circular runner design is most common since this reduces heat loss and stresses during filling. Other cross-sectional designs are used, such as rectangular and trapezoidal. These systems lowers the tool costs since they are only milled in one mould half [100]. In a multicavity mould, each cavity usually is fed by a separate runner. The total area of the main runner should equal the sum of all branches stemming from it. Because of the pressure drop in the runner is approximately proportional to the square of the increase in its length, the shortest runner network is the optimal choice [1].

Gating

The gate is the geometrical interface between the runner system and the cavity. The objective of the gate is to allow enough material flow for both cavity filling and thermal shrinkage compensation. The moulding process and the properties of the green part are directly affected by the type of the gate used, the location within the overall moulding and the size [101]. There are a number of gate designs available, e.g. rectangular, circular, fan or film. Circular gates have approximately diameters in the 1 to 4 mm range and cross-sectional areas of 4 to 12 mm^2 [1].

The location of the gate requires a careful evaluation, as it defines the flow pattern and the maintenance of the pressure field. If the gate is located in a thin section, then filling is more difficult to go to the adjacent thick sections because of the quick feedstock cooling and thus the increase of viscosity. A small gate combined with high flow rates can cause jetting. Jetting is feedstock shooting across the cavity and flowing back toward de gate [92]. This forms internal voids and weld lines. Most desirable is progressive cavity filling with the feedstock wetting the cavity walls, pushing air trough the vent at the end of the cavity. Gating in thermoplastics moulding is easier in respect to the wetting of the cavity walls, because thermoplastics have higher swelling than molten feedstocks. The elastic response of the stressed thermoplastics after passing the gate allows to rich and sticks material to the wall and leads to a front flow. When possible, gating for feedstock moulding usually is based in some particular strategies. To avoid jetting, gate can be located close to a side wall that keeps contact with molten feedstock. Also, it can be considered in a direct position to flow against an obstacle inside the cavity. For instance, a wall in the opposite side or an inside pin [102].

Conditions where the feedstock splits and joins within the mould cavity must be avoided when possible, since feedstocks usually forms weld line defects. These weld line defects grow into cracks during sintering. The weld line problem is another reason for a fast cavity filling because hot feedstock better seal weld lines. Therefore, multiple gates on one cavity are used only in special cases.

Venting

When the feedstock is filling the cavity, the air inside is forced to escape trough a vent at the end of the cavity opposite to the gate. Vents are very thin relieves in the tooling sized to allow the escape of air, but preventing the feedstock progression. A typical vent locate in the tool parting line is 0.015 mm deep with a width up to 12 mm in large parts [1]. It is also recommend vents at the junction points of the melt fronts resulting in welds lines. Venting can be considered a problem in PIM rather than plastics moulding because shot speed is higher and air escape does not compensate the cavity filling rate. It is expected that vacuum moulds must be used to prevent venting problems [2].

Ejection system

In the last moulding cycle step, the cooled parts are ejected from the tool cavities. Ejectors are integrated in the tool body and they move forward with the ejector plate and push the parts from the cavities. In Figure 2.12, the mould has three ejectors, one to each one of the cavities and one located in central position to push the runners and sprue. The force required for ejection depends on the elastic modulus of the feedstock, contact area between the tooling and part, coefficient of friction and thermal contraction in the cavity. Green parts have low strength and limited elastic properties, so any tensile, torsional or shear stress can cause distortion, cracking, and residual stress. To prevent these problems, tools should include the following characteristics: uniform ejection (using a large number of ejector pins or blades) will ensure the entire part is ejected without exposure to tensile, shear or torsional stresses; excellent mould polishing will minimizes the coefficient of friction; powder filler is incompressible and closely packed, so moulded parts typically exhibit very little shrinkage as they solidify. Usually, as this operation is not enough, it is recommended to use a maximum amount of draft wherever component geometry permits [102].

Temperature control system

The control of the mould temperature is assured by a channel system inside the tool. Water or oil can be pumped trough these channels to control the tool temperature. For systems that requires very low temperatures, it is possible to use refrigerants or even liquid nitrogen for cooling [1]. The thermal liquid is pumped out from an external tempering unit. For most PIM materials, cooling is the slowest step of the moulding cycle. For a set of molten feedstock and mould temperatures, minimised cooling times require thin walls and higher thermal conductivity for the tooling material.

Tool construction material

Durability of the PIM tool set is a primary concern for the choice of the construction materials. Because the feedstock is more abrasive than most plastics, wear resistance is a great concern. After machining, the tooling is heat treated or subjected to surface hardening in order to be obtained a hard surface. Such a procedures is widely used in ceramic injection moulding [2].

Various surface enhancements reduce wear and improve surface finish, including tungsten disulfide coatings, electroplating chromium or nickel phosphide, ion nitriding, salt bath nitriding and even boron carbide coating. The desired tool hardness is typically more than 30 HRC. Many heat-treated stainless steels or tool steel are used with a final hardness between 40 and 60 HRC [1].

2.1.7. Debinding

Binders major role is played during moulding, after what it becomes a disposal. The goal of debinding is to remove the binder in the shortest time with the last impact on the part. Failure to remove most of the binder before sintering can result in component distortion, cracking and contamination. Removing the binder without disrupting the particles is a delicate process that is best achieved in multiple steps [1]. When the most part of the binder is removed, in the first stage of removal, the part becomes fragile until sintered, thus it must be strong enough to retain the shape. A remaining quantity of binder is present at starting of sintering. Final debinding occurs as part of the heating cycle before the sintering temperature e reached.

There are several debinding techniques that can be classified as thermal and solvent processes (Table 2.5). Thermal debinding is performed by heating the parts so that binder is removed by thermal degradation, evaporation or liquid wicking using a wick medium.

Thermal degradation

In thermal degradation (commonly referred as thermal debinding) the parts are slowly heated in

Table 2.5 Classification of the most common debinding techniques based on either thermal or solvent approaches.

Thermal	Solvent
degradation	extraction
evaporation	supercritical
wicking	condensation vapour
catalytic	

an oven to give progressive degradation of binder. A flowing gas over the parts is used to help the removal of gaseous degradation products, as well as cleaning the chamber and send those harmful gases to a flame burning upstream the chimney. The binder is removed in an oxidizing, reducing or inert atmosphere or in a vacuum with soaking for up to 35 h or more. Heating rate, atmosphere, and the content and type of binder can affect part characteristics [31, 74, 103-105]. This technique is used more often because of its simplicity, requires low investment and no solid or liquid waste is need to be treated. However, it suffers from long process time and a tendency to parts slump or distort. This has been a major obstacle for the economic process for powder injection moulding [106, 107]. More, some burning residues, mainly carbon, can be detrimental for the final sintered parts [9].

Catalytic degradation

Thermal debinding temperature can be decreased using a vapour catalyst dissolved in an inert gas stream. This technique is so called catalytic debinding. The catalyst initiates the polymer cracking reaction at low temperatures, below softening point of the binder, which is advantageous in avoid a wide range of thermal defects.

The reaction occurs at the contact zones between the polymer and the catalytic atmosphere, so a nearly planar debinding front moves trough the part. This process was developed for polyoxymethylene based binders and it is depolymerised in acidic medium [35]. This process is rapid and works finely on both thick and thin sections with excellent shape retention. However, possible hazards can be pointed with high concentrated acid catalysts. The process has an appreciate consumables cost of catalyst and inert gas [36].

Evaporation

Evaporation is typically used for the removal of water or other solvents from the parts moulded with gellation binders. Gels which are formed by a great amount of solvent (60 to 95 %) can be dried in a warmed flowing air oven or in air at room conditions. This process is relatively quick and cheap [1]. Similar technique is the sublimation debinding, which is applied to aromatics based binders. The advantage of these substances, such as naphthalene, anthracene, and

pyrene is that they melt at relatively low temperatures and can be completely removed by sublimation under reduced pressure at temperatures well below their melting point. One verified that sintered parts had very low contamination when using these kinds of binder and debinding approach [53].

Wicking

Wicking is used when using very low viscosity binders. The parts are putted in a packed powder bed or on a porous substrate. Binder is melted by heat and it is absorbed out the parts by capillary forces of the wicking medium [108]. This technique is similar to thermal debinding, but the early times are less critical and defects are avoided because binder is removed by liquid flowing instead of gaseous flowing. The debound part must have higher strength than in other debinding technique, since the part has to de separated from the wick.

Solvent debinding

Solvent liquid extraction involves immersing the compact in a liquid that dissolves at least on binder component. Quite similar is condensed vapour solvent extraction, when the parts are subject to a heated vapour of solvent and it is condensed on the parts surface. The condensate absorbs selectively the binder and is dripped off to replenish surface solvent [75]. Water and organic solvents are used. Among the used organic solvents there are hexane, toluene, pentane, heptane, methylene chloride and acetone [19, 32]. With these processes, the parts remain rigid without chemical reactions and it leaves an open pore structure for subsequent binder burnout in sintering [22, 106]. On the other hand, generally it is used hazard solvents, with handling and environmental concerns. Process time of solvent debinding is typically smaller than thermal debinding but parts need drying prior to sintering. An additional potential advantage is that the process can be automated by continuously conveying the parts trough a solvent bath and dryer [18]. The solvent can be purified by distillation and recycled.

Supercritical debinding

Supercritical fluids, which are intermediate between gases and liquids, can also be used for solvent extraction. Substances, such as carbon dioxide, become supercritical fluids above but near their critical temperature and above their critical pressure. Supercritical fluids are better solvents than ordinary liquids at relatively low temperatures. Carbon dioxide is the preferred solvent for supercritical extraction. It becomes supercritical at 31 °C and 7.38 MPa of pressure. With supercritical extraction it has been reported a minimized defect formation, but it requires a precise temperature and pressure control in high expensive equipment [109, 110].

Plasma debinding

New technologies are recently under development to apply in debinding, always aiming the decreasing the process time and minimizing the part defects. Plasma is an alternative attempting to be industrialised, which consists in the use of high kinetic energy of the electrons to dissociate the hydrocarbon molecules of binder components, resulting in an activated debinding. The parts are constantly exposed to a gas flow and light radicals or molecules produced by the dissociation of the binder are pumped out of the furnace. In addition, the reactive species generated in the glow discharge resulted in an efficient cleaning of the supports and walls of the plasma reactor. As a consequence of the activated debinding cycle, the total processing time is significantly reduced [111].

2.1.8. Sintering

Sintering was first used to form bricks and pottery by heating a green ceramic body to a high temperature. Nowadays, it is applied in powder metal, ceramic, cemented carbide and some polymer production [30]. PIM parts get their structural integrity in the sintering process, which is a thermal treatment for bonding the particles into a solid mass. The most acceptable model describing the structural changes of the sintering materials is sketched in Figure 2.13. The final stage of sintering has a few small pores sitting on grain boundaries.

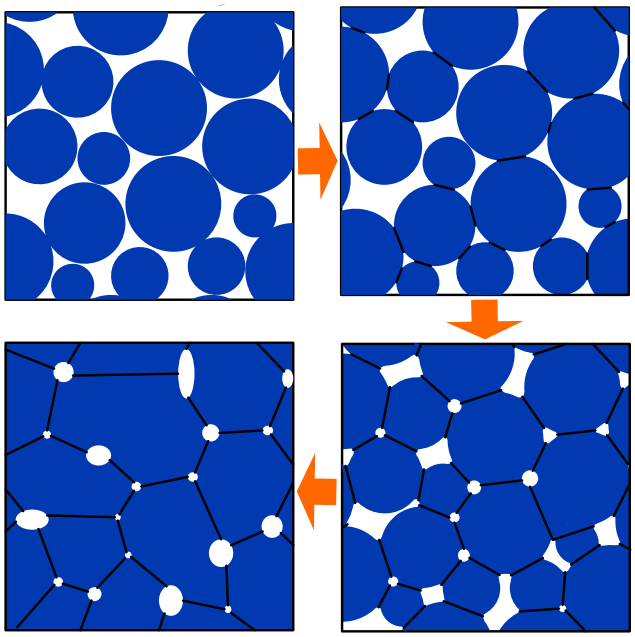

Figure 2.13 Microstructure evolution in PIM sintering, from the initial bonding of the particles, followed by pore rounding and grain growth in the final stage (adapted from [1]).

The particulate system (injection moulded brown part), which contains large amounts of surface free energy, is converted into more stable state and a less porous body. Consequently, the part shrinks to a smaller dimension. The driving force for this thermal-induced process is the difference in free energy between the initial and final conditions. In single-phase systems (homogeneous powders), this difference is levelled out by reducing the all outer (powder particle boundaries, internal surfaces of surface-connected pores) and inner surfaces (walls of encapsulated pores, grain boundaries).

Temperature program and microstructure evolution

The sintering temperature program (temperature, soaking, heating and cooling rate) are established in relation to material composition, shape and size of an article, and the type of furnace equipment. The most general sintering process consists of the following stages: non-isothermal heating to sintering temperature; isothermal stage at sintering temperature; relatively slow cooling to room temperature. During the heating stage, the moulded part is held at one or more isothermal stages in order to eliminate the remaining binder, thus allowing adjacent powder

particles to come into direct contact. Special care is taken to control the heating and cooling stages to prevent defects in densification and chemical composition. Sintering temperatures of single-phase powders is 2/3 to 4/5 of the melting or solidus temperature. Multiple-phase powders (powder mixtures) are normally sintered near or above the melting or solidus point of the lowest melting phase. In this case the process is so called liquid-phase sintering, since one liquid phase is present whose transport cause material densification [112]. The sintering temperature varies between materials. As an example, steels are often sintered near 1250 °C, alumina near 1600 °C and copper near 1045 °C.

At the same time particle bonding happens during sintering a significant increase of the properties of the part material is occurring, like hardness, strength, ductility, conductivity, magnetic permeability, wear resistance and corrosion resistance. These properties are generally the objective of a lot of applications. For this reason, the sintering cycles are design in function of those property requirements. To understand property evolution, understanding the microstructure changes is important.

Brown parts, which come from debinding, have a density of about 60 % of the desired final density and so ca. 40 % porosity. After sintering, the final density usually approaches 95 to 100 % of theoretical. Thus, sintering involves substantial shrinkage, i.e. the pores are eliminated and the final dimensions are smaller. Linear shrinkage, dependent in many factors, as particle packing, shape and powder chemistry, is about 14 to 16 %. Close final tolerances requires reproducible and homogeneous sintering shrinkage, however this dimensional change can be a source of distortion. Maintaining a high uniform powder packing density in the feedstock lowers shrinkage and eliminates one source of distortion. Sintering is improved by a high initial packing density, in part because there are more particle contacts involved in the bonding process [1].

Sintering atmosphere

Many sintering atmospheres are used in PIM, including air, inert gas, hydrogen, hydrogen-nitrogen mixtures, hydrogen-argon mixtures and vacuum. The chose of the atmosphere chemistry is mainly concerned in the concentration of the reactive species. Air is used in the sintering of oxide ceramics while nitrogen is chosen for nitride ceramics. An inert gas atmosphere (typically argon) gives a little chemical interaction with the parts. Blends of hydrogen and nitrogen are used

Table 2.6 Examples of PIM sintered materials.

Material	Powder size	Sintering temp. (°C) / time (h)	Sintering atmosphere	Density (g/cm^3)	Porosity	Ref.
Titanium alloy (Ti-6Al-4V)	7.7 μm (mean)	1100 / 4	Vacuum (10^{-4} Pa)	4.36	3 %	[53]
M2 high speed steel	9 μm (mean)	1240 / 0.5	N_2 – 10% H_2	-	≈ 1 %	[54]
Stainless steel (17-4PH)	10 μm (median)	1350 / 1	H_2	7.51	< 1 %	[24]
zirconia (ZrO2-5%Y2O3)	0.1 μm (mean)	1450 / 1	Air	6.02	0.5 %	[113]
Cemented carbide (WC-8%Co)	3.2 μm (mean)	1400 / -	Vacuum (20 Pa)	14.72	< 0.02 %	[57]
Stainless steel (316L)	11 μm (median)	1340 / 1	H_2	7.81	≈ 1.5 %	[47]
Alumina (Al_2O_3)	0.4 μm (median)	1580 / 1	Air	-	2 -3 %	[90]

to sinter ferrous alloys. Dissociated ammonia, forming under heat a mixture of 75 % hydrogen and 25 % nitrogen, is often used and it is a cheap way to obtain such a kind of atmosphere. Nitrogen is a neutral gas, but hydrogen has a reducing character, able to reduce oxides on the metal powder surfaces. Sintering in vacuum provides a clean, reproducible and non-reactive environment. Most materials can be sintered in vacuum, for example titanium, too steels and stainless steels.

Table 2.6 shows some examples of sintered PIM materials. Typically they a porosity lower than 5 %, which provide identical properties to those of the wrought material.

2.2. Commercial feedstocks and binders

2.2.1. Available products and binder design

A primary strategic choice of PIM companies relies in use of in-house compounded or ready-to-mould feedstock. Some good reasons to compound the feedstock are the possibility to adjust the feedstock rather than modifying the mould cavities, the flexibility to produce low volume non-conventional materials at a reasonable price and the freedom to change from one feedstock system to another with a pre-existing tool sets. To produce a consistent and homogeneous feedstock for the production of high quality articles is a complex task. The characterisation and quality control of feedstock need a lot of practical experience and the availability of mixing equipment and analytical devices. Advantageous of pre-formulated feedstocks are: quality control at the feedstock supplier, repeatable shrinkage factor from batch to batch, no need for an investment into mixing machinery and for specialized expertise in mixing. Also, price of feedstock is an issue, but there are no costs for labour and equipment for mixing, pelletising and quality control [5, 114] .

Some PIM part producers make own feedstock or use both, pre-formulated and in-house mixed feedstock. This depends on the technical background of the PIM company and the material to be processed. Often some costumers are specifying parts in the name-brand feestocks, because ready-to-use feedstock has a greater degree of standardisation and it is a warranty that parts made from two PIM suppliers can be similar by the use of the same brand feedstock [5].

This chapter introduces an updated list of ready-to-use commercial feedstocks and binders and their characteristics, in terms of process conditions and chemical formulation. The collected data is based on commercial information claimed by vendors, review papers, patents and scientific articles.

Table 2.7 lists the commercially available feedstock and binders. The products are produced in two the most developed countries in PIM technology, United States of America and Germany. Asian products have not been found in technical papers or in the World Wide Web. A wide range of binder types are available. However, this can be disadvantageous to part manufacturers since there are many choices and can be difficult of selecting the feedstock for a particular application

Table 2.7 Commercially available feedstock and binder systems.

Trade name	Binder type	Powders	Supplier	Website
Advamet	wax-polymer	metals	Advanced Metal Working Practices Inc. (IN, USA)	www.advancedmetalworking.com
Aquamim	water soluble	metals	Ryer, Inc. (CA, USA)	www.ryerinc.com
Catamold	poliacetal based	metals and ceramics	BASF AG (Germany)	www.catamold.com
Elutec	water soluble	metals and oxide ceramics	Hagedorn-NC (Germany)	www.hagedorn-nc.de
Inmafeed	wax-polymer	oxide ceramics	Inmatec GmbH (Germany)	www.inmatec-gmbh.com
Metasol/ Cerasol	solvent soluble	metals and ceramics	Imeta GmbH (Germany)	www.imeta-dresden.de
Powderflo	water based gel	metals	Latitude Manufacturing Technologies (NJ, USA)	www.latitude manufacturing.com
Licomont EK-583	wax-based	-	Clariant GmbH (Germany)	www.pa.clariant.com
Siliplast	water soluble	-	Zschimmer & Schwarz GmbH (Germany)	www.zschimmer-schwarz.de

[115]. The planning of a PIM industrial facility is of the binder type once the equipment to be selected is depending on the debinding solution. As examples, ovens are used for thermal debinding, leaching bath are used for solvent extraction, sealed and low temperature oven are used for catalytic debinding and moisture control in feeding system of the injection moulding machine is need for water-based systems.

Feedstock or binder suppliers are used to provide technical consultancy in start-up operation in new facilities to whom acquires their products. So, if a costumer wants to make use of such technology transfer or licensing without incurring high cost, experience in technology and resources of a supplier must taken in account for a correct the choice.

Table 2.8 is an overview of the process conditions of the different feedstocks and binders. They are mostly based in thermal and solvent extraction debinding, these latter using organic solvents or water. Catamold and Powderflo heighten by its original debinding method. The variety of process conditions is an example of the different behaviour of such systems. These aspects constrains the change in feedstock or binder system industrial operations, once it requires significant training and the process optimisation.

In order to understand the differences between the feedstoks and binders, information about the binders chemical formulation and the debinding characteristics is given below. It was not found this kind of details about Advamet and Metasol/Cerasol binder systems.

a) Aquamim

Aquamim by Ryer is a ready-to-mould feedstock using a water soluble polymer binder. The binder system was patented by Planet Polymer Technologies Inc. for the use with metal and ceramic powders [124]. In 2004, Ryer Inc. was established with technologies and intellectual property purchased from some companies, including Planet Polymer, and become a manufacturer, developer and supplier of custom and standard MIM feedstocks [125, 126].

Table 2.8 Process conditions of the commercial feedstocks and binder systems.

Trade name	Injection temperature (°C)	Mould temperature (°C)	Debinding method	Source
Advamet	177	43	solvent or/and thermal	[116]
Aquamim	120 - 205	20 - 40	water extraction	[117]
Catamold	160 - 190	125 - 140	catalytic degradation	
Elutec	140 - 160	55	water extraction	[118]
Inmafeed	150 - 160	50 - 65	water or/and thermal	[119]
Metasol/ Cerasol	120 - 140	30 - 40	acetone extraction	[120]
Powderflo	71 - 93	10 - 24	evaporation	[121]
Licomont EK-583	160	50 - 60	water or/and thermal	[122]
Siliplast	160	50	water extraction	[123]

The binder of the Aquamim products is based on a partially hydrolysed poly(vinyl alcohol) (PVOH) with a concentration up to 67 %. It includes a back-bone polymer of polypropylene or polyethylene and some processing aids. These are preferable constituted of water, glycerine or other adequate lubricant, a release agent and debinding aid. PVOH is preferable 87 % hydrolyzed, in such a way that it is soluble in water at room temperature. Therefore, an unique debinding stage is possible by water leaching without temperature controlling [124]. This technique is more environmentally friendly since it does not use hazardous solvents or acids.

b) Catamold

BASF has protected a binder formulation and the process for the production of feedstock for metal injection moulded [127]. The binder base component is a poliacetal (polyoxymethylene), homopolymer or copolymer, in a concentration at least 70 % by weight. A secondary component with up to 30 % by weight is composed by polybutanediol formal, polyethylene or polypropylene or a mixture of at least two of these polymers. They are also added some additives in order to improve powder dispersion and surface modification. The binder mixture has a softening temperature of about 165 °C. It is relatively high viscous which has benefits during feedstock mixing. High viscosity binders lead to high shear forces in mixture, so that agglomerates of particles of powder are dispersed or cannot be formed. As an example, a metallic feedstock is moulded at 170 – 200 °C under pressure up to 200 MPa.

The method of removal of binder is specific for this binder chemistry and for Catamold feedstocks. Polyacetals are vulnerable to an acidic atmosphere. This vulnerability of polyacetals is used in the BASF system for PIM in order to debind injection moulded parts [128]. Green parts are put into a nitrogen purged oven into which an amount of an acid is dosed. The vaporized acid decomposes the polyacetal binder starting from the outer surface. The decomposition takes place at temperatures below the melting point of the binder so that this reaction can be regarded as a direct transition from the solid binder into its decomposition product, the gaseous monomer formaldehyde. As a catalyst, nitric acid is the preferred substance [129].

c) Licomont

Licomont binder system is commercialised by Clariant GmbH. This company supplies the binder as well as some technology knowledge transfer for the optimisation of the formulation, by adding any necessary additives, and for the mixing process. Depending on the specific application of that binder, Clariant recommends the addition of some thermoplastics (particulary polyolefins) to the formulation in order to improve its performance [130]. When the binder was development and was first sold, the company was called Hoechst AG. This company made some patents about a binder formulation for injection moulding of ceramics and metals, with thermosetting characteristics designed for higher shape resistance during the thermal debinding. The formulation includes a semisynthetic wax (base on crude montan wax), a polyolefin wax, an ethylene-vinyl acetate copolymer (EVA), an alcohol and, with in a short concentration, organic peroxide and an azo ester [131, 132]. This binder has also protected for the processing of sinterable polymers [133].

The binder is removed in two steps. First the moulded parts are kept in an organic solvent or water at a temperature of about 50 °C; this extracts the alcohol component. Then, the parts are subjected to thermal debinding in an oven, where they are firstly heated to about 190 °C and maintained for a period up to 1 hour. This creates a three-dimensional network by free-radical crosslinking of the EVA as a result of the cleavage of the organic peroxide to such extent that deformation of the moulding as a result of the reduction in viscosity, caused by further temperature increase, does not occur. This binder design enables to shape maintenance over of the subsequent debinding and sintering processes. The temperature is then increased up to 400 °C in an oxygen-enriched atmosphere. At a temperature above 220 °C, the wax components, in particular those containing polypropylene, are degraded by free radical as a result of the cleavage of the organic peroxide. Inside the parts, in areas with lack of oxygen, the components of the binder which contain polymerized ethylene (including EVA) are degraded by free radicals formed by the cleavage of the azo ester in a temperature range of between 300 and 350 °C. The degradation product flows out the parts trough the porosity created in the extraction stage. After this, the oven atmosphere is changed to protective gas in those cases where the powder requires this treatment.

d) Inmatec

In 2000, Clariant announced the cooperation with the german feedstock supplier Inmatec GmbH. They started to develop metallic and ceramic feedstock using Licomont, but nowadays Inmatec product catalogue only includes alumina and zirconia, complemented with consultancy in the entire CIM process. Therefore, process conditions of Inmatec feedstocks are similar to those used for Licomont binder based mixtures [119, 134].

e) Siliplast

Siliplast binder, developed by Zschimmer & Schwarz, is based on a polyalcohol. This company has proposed a non-pollutant PIM process, based on a water extraction debinding, where the residual water can be recycle or a biological treated disposal. The polyalcohol is obtained by the modification of sugars, i.e. mono and oligosaccharides. These short molecular chain carbohydrates are characteristic sweet and water solubles. The binder formulation also includes thermoplastic polymer, such as polyolefin and EVA copolymers, and wetting agents [135]. Overall composition of the binder is 65 % water-soluble and 35 % water-insoluble, therefore it allows debinding by water immersion. If water is heated, for example at 50 to 70 °C temperature, practically all of the soluble part of the binder can be extracted [18, 123, 136].

f) Elutec

Zschimmer and Schawrz not only has being supplying the Siliplast binder but also the feedstock with the brand name Elutec. Since 2006, Zschimmer and Schawrz has provided license for the production of ready-to-use feedstock of metals and ceramics to Hagedorn-NC, but remained the business of the binder. Elutec ranges the most common metals (carbonyl irons, iron-nickel, tool steel and stainless steels) and ceramics feedstock (alumina, stabilised zirconia and steatite) [137].

g) Powderflo

Powderflo products are plasticised by a water-gel binder, consisting of less than 2 % by weight of binder of organic material. This binder was initially developed by AlliedSignal, then after some business operations the Powderflo feedstock is now supplied by Latitude [138, 139], both from U.S.A.. According to AlliedSignal's patents, the binder can be used for many materials, ceramics, metals or cemented carbides. The binder is a hydrogel which gelling agent is agar, a polysaccharide derived from seaweed used as a common food additive. The agar can be present preferably at 0.5 to 6 wt% based on the mixture powder. Water is the main component, in a concentration between about 45% and 55% by volume. The binder contains several additives: dispersants, to ensure a more homogenous mixture, lubricants, such as glycerine, to assist mixture flow, and vapour pressure modifiers to reduce water escape during moulding. The gel point of the binder is about between 30 to 45°C [80, 140-143]. The feedstock is moulded at a temperature above the gel point of the hydrogel and under 100 °C. Primary differences from other commercial systems are lower moulding temperature and pressures. Upon cooling in the mould to near room temperature, the moulded feedstock drops below its gelation temperature, setting into a green part [144, 145].

Debinding could be the most popular characteristic of this feedstock. Because of its low boiling point, water is easily removed from the moulded part by drying in ambient air, during approximately 1 hour (for PIM usual wall thickness). Therefore, the process almost can be considered without the debinding step. Dry can also be extended to the initial phase of the sintering stage.

2.2.2. Strengths and weaknesses

Table 2.9 summarises the most important characteristics of the analysed feedstocks and binders, in terms of strengths and weaknesses.

Table 2.9 Summary of the strengths and weaknesses of feedstocks and binder systems.

Aquamim
Strengths
Debinding process is economical and with a minimum impact for the environment. The removed substances, dissolved in water, can be separated by evaporation or water can be treated by the traditional methods.
Weaknesses
The binder, based on poly(vinyl alcohol), is high hydrophilic and very sensitive to atmosphere humidity. It is recommended to take some measures to avoid humidity absorption of the feedstock; otherwise its characteristics were modified. More, it is recommend to dry the feedstock before the injection moulding, so one more unit operation is added to the process.
Catamold
Strengths
The injection moulded parts have a high green strength, because of the use of a high strength thermoplastic, providing easier parts ejection and manipulation with minimum breaks and distortions. This makes possible to use a fully automatic injection moulding.
Comparing to the other debinding techniques, catalytic debinding is claimed to be the faster process. The elimination is spatially controlled, happening at the interface of the binder, and under the softening temperature of the binder. Reject rates claimed to be less than 1 % in the manufacture of components [114, 146]
Weaknesses
Despite of the announced low formaldehyde and NO_x concentration (less than 1 ppm and 500 ppm, respectively) in the gaseous effluent after a two-stage flare combustion of the exhaustion of the debinding, there is emission of CO_2 [146]. This is a harmful gas contributor for the greenhouse effect.
The consumption of acid catalyst used in debinding is an extra cost comparing to other debinding techniques. Nitrogen is also a surplus cost in the production of oxide ceramic parts, when with other techniques it is not necessary the use of a protective atmosphere.

Table 2.10 Summary of the strengths and weaknesses of feedstocks and binder systems (cont.).

Inmafeed and Licomont EK 583

Strengths

Two debinding technique can be used: two-stage water and thermal debinding or one-stage thermal debinding. The water extraction is advantageous for diminish the likely of defect appearance during the thermal debinding, and it is recommend for thicker wall parts.

During the thermal debinding stage, some binder components are thermosetted providing an extra mechanical strength minimizing debinding and sintering defects.

Weaknesses

Thermal debinding is a typical long process, not economically attractive.

Elutec and Siliplast

Strengths

Water debinding process used in this binder system has lower environment impact comparing to thermal and catalytic debinding. The output binder water solution can be recycled or treated by the conventional waste water treatment methods.

Weaknesses

The collected information is not enough to take conclusion about claimed weaknesses of this product. However, the water soluble part of the binder can thus be able to absorb moisture from atmosphere, so some actions must be taken to avoid that.

PowderFlo

Strengths

The debinding process, water drying, is very simple and quick and it is not presumed to have impact in the environment. Drying time is typically between 1 and 3 hours. It is announced to enable the production of the thicker parts, and in this case the parts are dried at air.

Weaknesses

Feedstock is mostly constituted by water. So, change in water content by exposing to the room atmosphere, can modify the feedstock characteristics. It is recommend to take special precautions in material storage and to install sealed feeding system in moulding machines, to prevent any moisture loss from the feedstock. So, some investments are needed to maintain moisture level of the feedstock [121].

Table 2.11 Summary of the strengths and weaknesses of feedstocks and binder systems (cont.).

Metasol/ Cerasol
Strengths
Debinding technique is solvent debinding, using acetone. Acetone has a high vapour pressure, making possible to be separated from the extracted binder by vacuum distillation, a cost effective way to regenerate it and make possible the reuse of such liquid back in the process. Accordingly, the solvent consumption is low.
Weaknesses
Acetone is a high risk substance. It is toxic, extremely inflammable and, in some conditions, explosive. Rigours design and expensive equipment must be accounted in order to be explosion proof, to avoid man exposure and to have emergency measures is the manufacturing room. This has been the particular weakness of solvent debinding systems [1].
Advamet
Strengths
Binder can be removed by thermal debinding only, or with a first solvent extraction stage. The first solvent stage is particularly interesting when producing ticker parts, allowing to a controlled removal of the binder.
Weaknesses
Thermal debinding is a typical long process, thus a economically not attractive

2.3. Feedstock characteristics

2.3.1. Rheology

The feedstock is essentially a highly concentrated suspension (in the range of 45 to 75 % by volume), which is subjected to several thermal, pressure and shear rate conditions along the PIM process [1]. Hence, it is important to understand and describe the rheology of the feedstock under these conditions and search for the optimised rheological characteristics. The most important property is the viscosity, a measure of the opposition to the flow motion.

The level of shear rates imposed in different stages of the PIM process is in Figure 2.14. Slumping and sinking of the green parts during thermal debinding is identified in the low shear rate regime. Intermediate shear rate are found in injection flow in the mould cavity and the highest rate can be present in mixing and injection flow in runners, gates and in the thin cavity sections. The techniques commonly used in the rheological analysis of feedstocks include the cone-plate or parallel plate rheometry and the capillary rheometry. The first is normally used for the low to intermediate shear rate regions while the latter is used for the higher shear rate range [147].

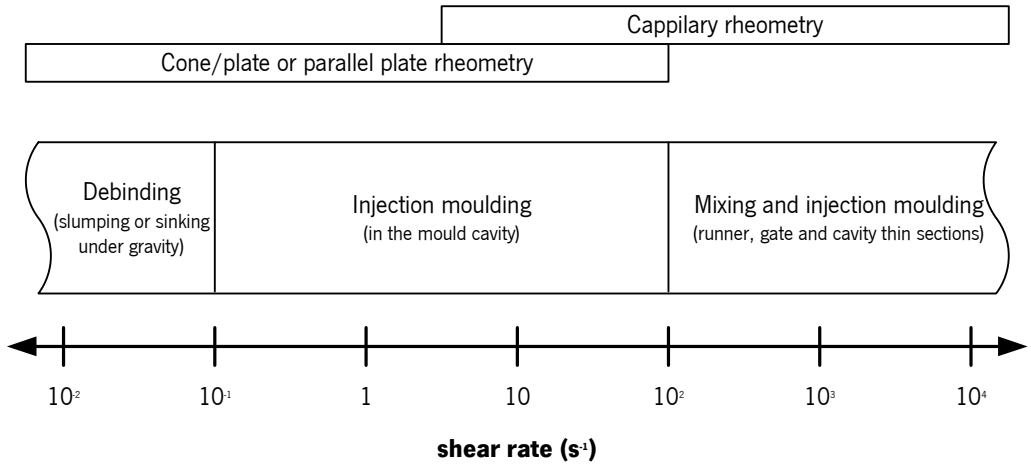

Figure 2.14 Range of shear rate experienced by a feedstock during the PIM process and the used rheology characterisation techniques (adapted from [3]).

Effect of shear rate

Most PIM suspensions exhibit first a Newtonian behaviour, followed by a pseudoplastic region and finally, at high shear rates, a Newtonian region or a dilatant flow [3, 148] (Figure 2.15). The shear thining behaviour is attributed to particle orientation and ordering with flow, breakage of particle agglomerates with increasing shear stresses, binder molecular orientation and can also means a higher homogeneity. Pseudoplastic binders are a further contribution for the pseudoplasticity of feedstock [1, 26, 149, 150].

In processing conditions, at intermediate-higher shear rate range, the feedstock viscosity decrease due to shear thinning phenomenon. One of the most simple and popular expression to describe the viscosity dependence on shear rate is generally expressed by the Ostwal-de-Waele or power law equation,

$$\tau = k_0 \, \dot{\gamma}^n \qquad (2.1)$$

where τ is the shear stress (Pa), $\dot{\gamma}$ is the shear rate (s^{-1}), k_o is the consistency coefficient and n is the power law exponent. The exponent has been defined as the flow behaviour index of a fluid, and, like the consistency coefficient, can be considered a property of the fluid. When n is unity, the flow is termed Newtonian; when n is less than unity, the flow is pseudoplastic or shear thinning and, when n is higher than unity, the flow is considered dilatant or shear thickening.

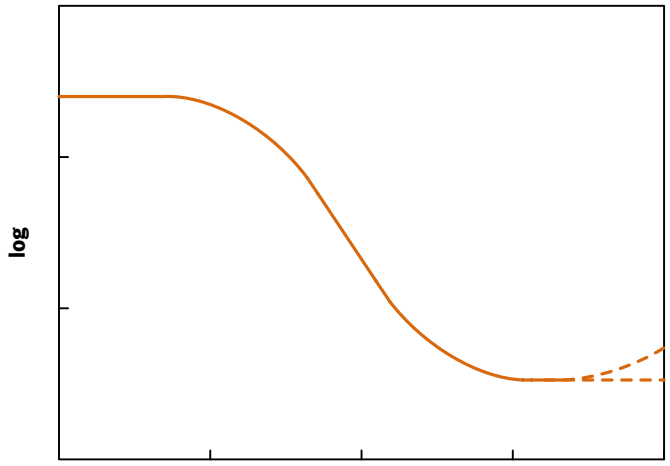

Figure 2.15 Typical viscosity behaviour of PIM feedstock suspensions in function of shear rate.

According to this model, the viscosity, η (Pa.s), of a shear thinning fluid is given by

$$\eta = \frac{\tau}{\dot{\gamma}} = k_0 \, \dot{\gamma}^{n-1} \qquad (2.2)$$

Figure 2.16 shows plots of viscosity and shear stress versus shear rate for two feedstocks of zirconia and a 316L stainless steel composite at various temperatures. It can be observed that within the range of shear rate analysed, the feedstock exhibited shear thinning behaviour. The lower the value of *n*, the higher the shear sensitivity, and therefore the viscosity decreases faster

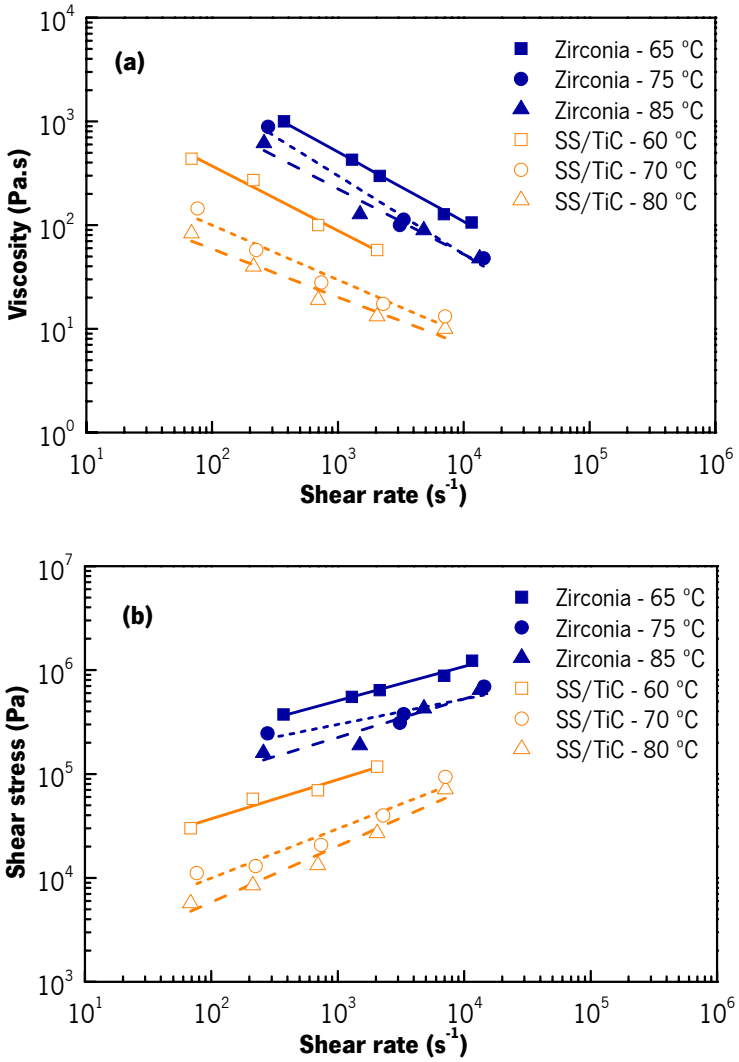

Figure 2.16 Viscosity (a) and shear stress (b) versus shear rate at various temperatures for two feedstocks: zirconia at 55 vol% with wax binder [151] and a composite of 316L stainless steel with 3 wt% titanium carbide (TiC) with EVA/wax binder [152].

with increasing shear rate. It is recommended that viscosity has high shear sensitivity during injection, because this yields the production of complex and delicate parts [1, 153]. The shear rate encountered during the injection moulding is at the range 10^{2}-10^{5} s^{-1} [1, 6, 7].

However, it is commonly accepted that the maximum recommended viscosity of feedstock in those ranges must be 1000 Pa.s. Dilatant behaviour is generally encountered in suspensions at high shear rates. It has been found that exists

a critical shear rate which marks the onset of this behaviour [154]. Dilatancy in concentrated suspensions has been attributed to lost of powder-binder adhesion and further rearrangement and collision of the particles. Such effects increase inhomogenity with increasing shear rates and, hence, higher viscosity. Dilatant behaviour must be avoided and it is restriction in the optimisation of the process.

Yield stress / Bingham fluid

A Bingham behaviour has been observed in PIM feedstocks [82, 151, 155, 156], presenting an yield stress that has to be exceeded to initiate a shear flow [147]. When it is applied a stress less than the yield stress, the fluid will not flow. When the stress exceeds the yield stress, the fluid will flow like a viscous fluid with a finite viscosity [157]. This concept is shown by the plot of shear stress versus shear rate, as shown in Figure 2.17. The flow behaviour of a normal viscous fluid, for example, a polymer melt, would follow curve (b), and the curve begins at the origin, indicating zero shear rate at zero shear stress. A viscoelastic fluid, curve (a), would start to flow after the shear stress has exceeded a defined amount, the yield stress.

In a concentrated suspension, the particles are close with one another. Interparticle interactions are present and it is then form a three dimension network. The yield stress can be viewed as the force per unit are necessary to overcome such interparticle interactions, and its magnitude is determined by the overall strength of the interparticle network [148].

One of the theoretical expressions which directly relates to the solid fraction to the yield stress, proposed by Poslinski, that has been used in studies with fine ceramic feedstocks [82, 151] is

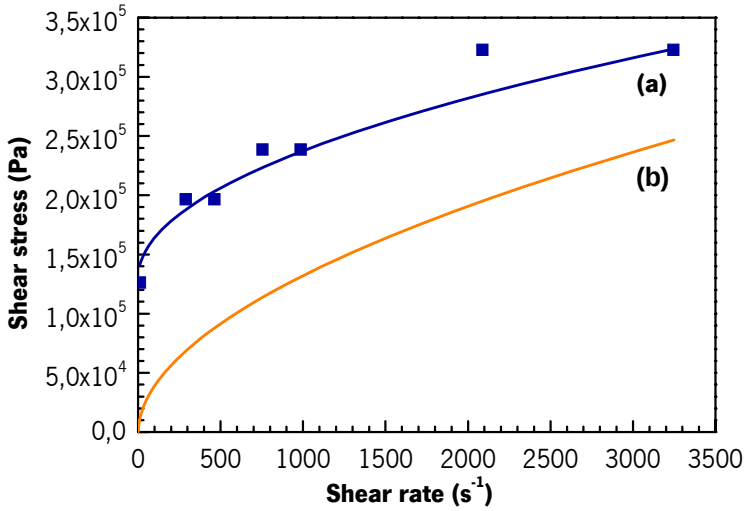

Figure 2.17 Shear stress vs. shear rate plot; (a) pseudoplastic feedstock exhibiting a yield stress, 55 vol% zirconia with wax binder at 58.5 °C [151], and (b) a schematic curve for a normal pseudoplastic behaviour.

$$\tau_y = \frac{N\,A}{8\,\pi\,d^3}\left(1-\frac{\phi}{\phi_m}\right)^{-4} + \frac{3\,N\,\varepsilon\,k_D\,\psi_0^{\,2}}{4\,\pi\,d} \qquad (2.3)$$

where τ_y is the yield stress (Pa), N is the particle coordination number, the total number of nearest neighbours of each particle, A the Hamaker's constant (J), a measure of van der Waals forces, d the particle size (m), ψ_o the surface potential of the particles (V), ϕ the solids volume fraction, ϕ_m the maximum solids volume fraction, ε the electric permittivity of the carrier fluid ($C^2\ J^{-1}\ m^{-1}$) and k_D the reciprocal Debye thickness of the electrostatic thickness interaction layer (m^{-1}). The first term in the right-hand side of this equation involves the van der Waals-London attraction force between particles associated with the fourth-power of solid concentration and the second term is a result of electrostatic interparticle potential. Equation (2.3) describes the dependence of the yield stress with the properties of powder, binder and feedstock formulation. It indicates that the magnitude of the yield stress increases with the increasing volume fraction of powder, decreasing size of the particles and increasing interparticle surface potential.

In most CIM applications, the powders employed are relatively fine, e.g. in sub-micrometer scale, and the fractions are high as usual, e.g. 50 - 60 % by volume, such that particle interaction forces

become significant and a yield stress is required to cause the suspension to flow [148, 158], even when the powder is loaded in a low-viscosity carrier fluid.

In practice, deviations from theoretical expectation of the yield behaviour are frequent, due to factors such as irregularity in particle geometry, degree of particle dispersion/agglomeration, etc. that are excluded in most theoretical assumptions. These factors complicate the yield behaviour analysis in such a way that empirical expressions have been developed in order to obtain a more precise behaviour of the viscoelastic suspensions. Liu and Tseng [151] have demonstrated that the yield stress of zirconia-wax suspensions can be related linearly to flow resistance parameter $\phi/(A-\phi)$ by an empirical equation,

$$\tau_y = C_1 \frac{\phi}{A-\phi} - C_2 \qquad (2.4)$$

where C_1 and C_2 are constants which are experimentally determined for a specific suspension system. The actual physical meaning of the constants is not well understood. This equation provides some understanding of the yield behaviour, but is limited to a narrow range of material properties and processing conditions and does not further understanding of the behaviour of highly-concentrated suspensions. This is just an example of the difficulties in model yield stress behaviour in PIM formulations.

The three most common models used to developed to describe the flow behaviour of a fluid exhibiting yield stress are as follows [3, 82, 148, 151, 155, 156]:

The Bingham Model $\tau = \tau_y + \eta_0 \dot{\gamma} \qquad \tau \geq \tau_y \qquad (2.5)$

The Herschel-Bulkley Model $\tau = \tau_y + k_0 \dot{\gamma}^n \qquad \tau \geq \tau_y \qquad (2.6)$

The Casson Model $\tau^{1/2} = \tau_y^{1/2} + (c\,\dot{\gamma})^{1/2} \qquad \tau \geq \tau_y \qquad (2.7)$

where η_0, k_0 and c are constant parameters that can be determined experimentally. For PIM suspensions equations (2.6) and (2.7) describe best the shear stress dependence on shear rate, because they translate the non linearity between the two variables and the shear thinning behaviour of such fluids.

Effect of temperature

It has been well documented in literature that viscosity of feedstocks decreases with increasing temperature [55, 149, 152, 155]. Figure 2.16 (a) shows the viscosity of two feedstocks at various temperatures. It can be observed that, at a given shear rate, the viscosity decreases with temperature.

The effects of temperature on feedstock rheology have not been simple to interpret as of a single component binder. One has found complicated temperature dependence of binder viscosity caused by different melting points of the various components of the binder. This may be caused by some components of the binder remain semi-solid while others are in liquid form [3]. Moreover, the effect of temperature is magnified by the difference of the thermal expansion of powder and binder. Thermal expansion of the binder is generally higher than that of the powders. Consequently, the effective solid volume fraction of the feedstock decrease with an increase of the temperature, causing the viscosity to decrease even further. Therefore, the decrease of the viscosity by an increase of the temperature is typically higher in the feedstock than in pure binder [1].

At temperature far above the melting point of a given binder, the temperature effect on viscosity follows the Arrhenius equation

$$\eta = k_T \exp\left(\frac{E_a}{R\,T}\right) \tag{2.8}$$

where η is the viscosity at a constant shear rate (Pa.s), k_T is a contant (Pa.s), E_a is the activation energy (J mol^{-1}), R is the gas constant (8,314 J mol^{-1} K^{-1}) and T is the absolute temperature (K). The activation energy is a measure of the viscosity sensitivity to temperature. A high E_a indicates high sensitivity to temperature, i.e., a high increase of viscosity with a temperature increase.

If the viscosity is very sensitive to the temperature variation, this causes undue stress concentration in the moulded part, resulting in cracking and distortion. In addition, a strong temperature dependence of viscosity dictates smaller pressure transmission to the cavity, thereby promoting the possibility of the formation of shrinkage related defects. High sensitivity of viscosity to temperature requires more accurate temperature control during injection moulding. Therefore, it has been stated that low activation energy is a requirement for a good PIM feedstock [33, 149].

Liu and Tseng showed that yield stress is dependent on temperature. In zirconia-wax suspensions the increase of temperature causes a reduction in the yield stress. This has been verified as a result of the change in attractive interparticle force due to an increased interparticle distance when the matrix melt is thermally expanded [151].

Effect of solids fraction

Solid volume fraction is the volume occupied by the solid particles as a fraction of the entire volume of the powder-binder mixture. The viscosity of a feedstock increases as more powder is mixed into the binder.

The effect of solid volume fraction can be partially summarized and illustrated according to Figure 2.18. If a small volume fraction of particles is suspended in a Newtonian liquid whose flow behaviour is given by curve a, the viscosity of the suspension is uniformly raised to curve b. On further addition of particles, the viscosity continue to increase but becomes shear thinning, although Newtonian flow could still be possible at low shear rates (curve c). If the suspending medium is non-Newtonian, the flow behaviour could follow curve c and addition of particles simply shifts the curve upwards to that of curve d. Further addition of particles, whether in

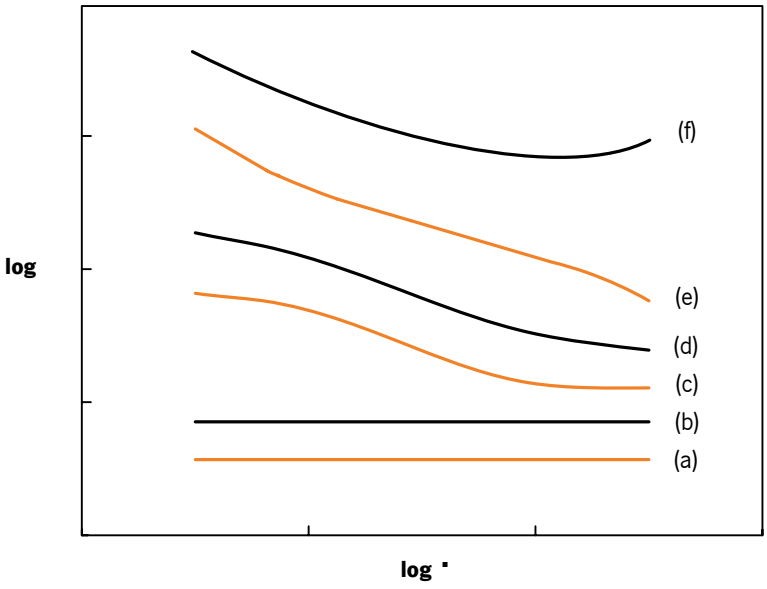

Figure 2.18 Qualitative representation of the influence of increasing solid volume fraction on feedstock viscosity [3].

Newtonian or non-Newtonian suspending medium, the appearance of an apparent yield stress occurs as shown in curve e. The slope of such a curve at low shear rates is found to have to value of -1. Finally, at solid volume fractions close to the critical value, shear thickening would occur, as shown in curve f [3].

2.3.2. Homogeneity

Feedstock homogeneity is one of the important properties to produce high quality injection moulded parts. Defects apparent after sintering have been traced to various errors introduced in the earlier processing step. The mixing step is critical to form feedstock with sufficient homogeneity for uniform cavity filling to deliver close density and dimensional control. Experiments with several powder materials have determined that formation of a homogeneous feedstock mixture requires a considerable effort [83]. In order to prevent the agglomeration of powder or binder polymeric constituents, several research works are focused in the optimisation of the solids concentration, understanding of the effects of surfactants and the comparison of various mixing instruments [1, 71, 159].

One concern assessing homogeneity is with the size scale over which segregation exists. Consequently, the point-to-point sample variance is a first measure of heterogeneity. It is desire that for every segment to have an equal concentration of powder and for this powder to have the same particle size distribution. Other concern is the scale of scrutiny. The scale of scrutiny relates to the sample size used to assess homogeneity. Too large sample misses segregation, while too small sample has too few particles to be meaningful. Somewhere it is suggested that samples sizes of 0.1 cm^3 are probably best [1].

Table 2.12 shows the methods in use for the evaluation of the homogeneity of PIM feedstocks. Small variations in the feedstock composition, in a small scale analysis, will lead to viscosity dispersion. For this purpose, capillary rheometry is commonly suggested, once has shown to be the most accurate and sensitive method for the homogeneity assessment. It was also demonstrated that the minimum viscosity for a particular mixture occurs with the most homogeneous feedstock [83]. The evaluation of feedstock homogeneity by this method is carried

Table 2.12 Methods for assessment of the homogeneity of feedstocks.

Method	Description	Property measured	Source
Capillary rheometry	Monitoring of the pressure drop/ viscosity of a feedstock trough the capillary along the time at a fixed temperature and flow rate. Pressure drop/ viscosity fluctuation is a measure of the heterogeneity of the mixture.	Viscosity or capillary pressure drop	[6, 33, 71]
Mixing torque rheometry	Monitoring the mixing torque along the time. The heterogeneity level of the mixture is given by the noise level of the steady-state curve or by the impossibility to reach a steady-state.	Mixing torque	[159-162]
Density	Measurement of density of an amount of feedstock samples by gas picnometry or Arquimedes method. The density variation is a measure of the feedstock heterogeneity.	Density	[1, 160, 161]
Binder burnout	Feedstock samples are submitted to high temperature in order to degrade the binder. The weight loss corresponds to the binder content of the samples. The weight loss variation among the samples is a measure of the feedstock heterogeneity.	Feedstock binder content	[71, 160, 163]
Morphology observation	Observation of morphology of a feedstock by SEM allows the visualisation of the degree of powder dispersion of a feedstock mixture. This method has been used to make qualitative analysis of the homogeneity.	-	[162-165]

at a determined shear rate, varying from study to study. Some examples of shear rates are 3.543 s^{-1} [33], 294.5 s^{-1} [58], 1180 s^{-1} [6] or 1504.7 s^{-1} [71].

However, Khakbiz et al. showed that the viscosity variation can be dependent on the shear rate [149]. At low shear rate, viscosity variation is higher. As a result of small shear stresses, the particles tend to agglomerate in clusters and feedstock may exhibit small regions with different particle concentration causing variation in the viscosity at microscopic level. Nevertheless, at

higher shear rate, the breakage of agglomerates is more feasible. The transition point, beyond that the fluctuation of feedstock viscosity with the shear rate was nearly constant was found to be ca. 750 s^{-1}.

Mixing torque method is a common method in laboratory because it can be performed during mixing of a feedstock sample with a mixing torque rheometer. By monitoring the torque of mixing, after reaching a steady state it can be possible to evaluate the suspensions homogeneity by the signal variation along the time.

Density method is the quickest method for the determination of feedstock homogeneity, thus is far used in the industry. Once the powder, binder and mixing procedure are selected, feedstock density becomes fixed and provides an easy method. Variation in composition in a batch of feedstock granulate is identified by the variation of density. More, any deviation between the theoretical and actual densities indicates improper formulation. This precaution is necessary since density is a measure of solids fraction, which responsible for dimensional accuracy in the manufactured components [1].

Binder burnout method is a simple method for the determination of the binder content dispersion in a feedstock. Binder loss experiments must be performed in an adequate atmosphere which does not react with the powder particles. The standard deviation between samples from each experiment is usually calculated to determine the level of homogeneity.

2.3.3. Thermal properties

Along the PIM process, the feedstock is repeatedly subjected to elevated temperatures. So, it is important to understand the thermal properties of feedstock of optimal processing parameters and aiding the development of simulation packages for the process. This section highlights some important thermal properties which include expansion coefficient, thermal conductivity, melting points and thermal decomposition behaviour.

Melting and crystallisation temperatures

Melting and crystallisation occurs in many stages of the PIM: compounding, moulding and sintering (only melting). If binder is removed by thermal degradation, so in this debinding process the binder is melted too. These temperatures, or temperatures ranges, must to be known as a base for the definition of the process conditions. The effect of the powder in feedstock does not change significantly melting and crystallisation temperatures of the binder, so it is frequently to assess only to the binder characteristics.

Differential scanning calorimetry (DSC) is used for investigating such characteristics. Figure 2.19 shows a DSC output for a binder sample containing EVA/beeswax of weight ratio 40/60. Binders, as multicomponent polymeric blends, show multi melting peaks, as observed. The first peak (on the 1eft) represented the melting or crystallisation of the beeswax in the binder while the second peak (on the right) represented that of the EVA copolymer. The area under the peak, indicated by ΔH, would represent the energy consumed or involved during the melting or crystallisation process.

The melting and crystallisation behaviour of a binder blend is affected by the degree of interaction between the constituents and the morphology of the resulting blend. A study of these behaviour would aid in the understanding the interactions between the components in the binder. The

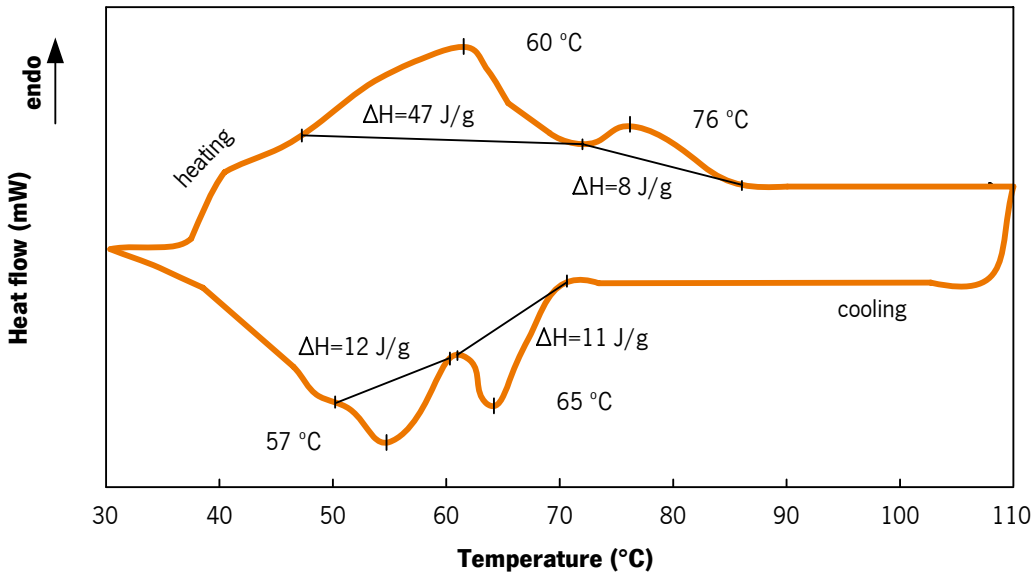

Figure 2.19 DSC curve of a binder containing 40/60 weight ratio of EVA/beeswax [3].

compatibility and interaction between the binder components is important for preventing binder separation and ensuring stable homogeneity [3].

Thermal decomposition behaviour

The study of the thermal decomposition of the binder, as a content of the feedstock, is important in order to provide information to establish optimised processing conditions. It is useful for the determination of the upper limit of processing temperatures and, in the case of use thermal debinding, to know the thermal decomposition profile with the temperature.

The thermogravimetric analysis (TGA) is usually used for this study. The samples are heated at a programmed heating rate, in a proper environment depending on the powder chemistry to avoid powder reaction. Thermal degradation profile generally depends on the binder components characteristics. A thermal debinding binder intend to have component having separated thermal degradation ranges. Phased thermal degradation of a binder provides a easier control of binder removal, so a subsequent binder component will degrade after its precedent component have already be removed from the part [1].

Figure 2.20 shows an example of a TGA curve of a PIM feedstock. The feedstock is formed by copper powder with a paraffin wax – polyethylene – stearic acid binder [166]. The powder

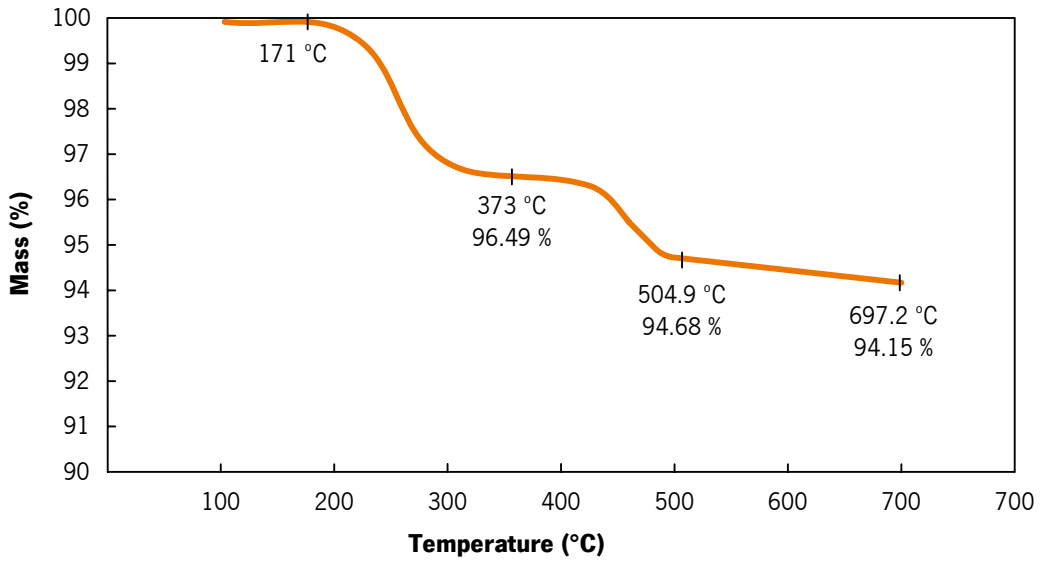

Figure 2.20 TGA curve of a feedstock of copper (95 wt.% / 66.2 vol.%) and wax-polyethylene binder [166].

fraction was 66.2 vol.%, corresponding to 95 wt.%. The curve exhibits two stages decomposition so that paraffin wax and polyethylene are degrading from approximately 170 to 350 °C and from 350 to 500 °C, respectively. Stearic acid degradation is diluted in the first stage. The thermal debinding cycle would be programmed in order to control the binder degradation and gaseous products flow out the parts, usually by establishing temperatures plateaus or very low heating rate in the range where the degradation rate is high. As the binder degradation starts at 171 °C, the processing temperatures such as the mixing and injection moulding temperatures must be lower in order that binder degradation does not occur.

Residual stresses and thermal expansion

During injection moulding process, pressure is applied to ensure that the melt feedstock completely fills the mould cavity. When the mould is completely filled, the part is cooled in the mould under pressure. This pressure is only removed at the end of the moulding cycle. Residual thermal stress is always present in conventional thermoplastic injection moulding due to molecule orientation that is "frozen in" during rapid cooling of the moulded part. This residual stress could cause shape distortion and warpage after moulding [58].

In PIM, it is believed to be one of the main causes of the cracking that presents itself during binder removal [34, 167-169]. For example, Tseng have concluded that relaxation of the residual stress occurs when ceramic injection mouldings are subjected to elevated temperatures, leading to deformation of the mouldings. It was presumably due to the rearrangement of the moulded microstructure as the temperature of the moulding was raised during debinding [64]. Zhang et al. further indicated that interactions between non-spherical particles (which tend to orient themselves along the direction of the moulding pressure) and polymeric binder vehicles may also induce residual stresses in the CIM process. Distortion results again when mouldings are subjected to high temperatures [170].

Due to the high difference in thermal expansion coefficients of the powder and the binder, the internal stress in the PIM moulded parts has an additional component. This stress can be estimated by the expression [3]:

$$\sigma = E_m \, \Delta T \left(\alpha_m - \alpha_f \right) \qquad (2.9)$$

where σ is the stress (Pa), E_m is the elastic modulus of the matrix (binder) (Pa), ΔT is the temperature change (K), α_m and α_f are the thermal expansion coefficients (K^{-1}) of the matrix (binder) and the filler (powder), respectively.

Upon cooling from processing temperature, the thermal contraction of the binder is usually higher than that of the powder, thus the net effect is a compressive stress acting on the powder particles. The particles are under a squeezing force. Even if the adhesion between the binder and the particle is poor, there might not be any relative motion across the interface due to the large compressive stresses and resulting friction. However, in regions where the particles are in contact, especially at high powder fraction, the thermal shrinkage of the binder can lead to local regions of tensile rather than compressive stress. In such cases, poor adhesion would allow lost of bonding at the interface and results in a void or pore.

The rule of mixture can be used to estimate the effective thermal expansion coefficient of a feedstock [3]:

$$\alpha = \alpha_{\mathrm{f}}\ \phi + \alpha_{\mathrm{m}}\ (1-\phi) \tag{2.10}$$

However, because of the high difference in the thermal expansion of the powder and binder, the solid volume fraction would change in the event of a change in temperature. The change in powder fraction can be calculated using the following expression

$$\phi_0 = 1+\left(\frac{1-\phi_1}{\phi_1}\right)\cdot\left(\frac{1+\alpha_{\mathrm{m}}\left(\mathrm{T}_0-\mathrm{T}_1\right)}{1+\alpha_{\mathrm{f}}\left(\mathrm{T}_0-\mathrm{T}_1\right)}\right)^3 \tag{2.11}$$

where T_1 and T_0 are the temperatures of the final and initial conditions (e.g., T_1 is the room temperature and T_0 the processing temperature). This equation would allow estimating the actual solid volume fraction during processing with an initial solid volume fraction at room temperature.

Thermal conductivity

Due to the high thermal conductivity of the powders, the feedstock normally possesses higher conductivity than the pure binders. A high thermal conductivity of the feedstock ensures heat is transferred fast enough to the entire compact. This will ensure a smoother temperature gradient in the compact, minimizing thermal stress and hence minimizing shrinkage cracks. It also means

that cooling is fast enough for longer moulding cycles. However, the high conductivity also causes potential problems such as premature gate freezing, which is the reason why generally it is used higher injection flow rates than in plastic injection moulding. This issue transforms completely the moulding process conditions and tooling.

Figure 2.21 shows the evolution of the thermal conductivity of a 316L stainless steel feedstock (from BASF AG) with temperature, comparing to the binder and the powder values. It was hypothesized that the change of the thermal conductivity of the feedstock is related to two phenomena: change of the thermal conductivity of the components with the temperature and change of the distance between filler particles with temperature. It has verified that the first effect is more relevant than the second one [84].

A simple approach to estimate the effective thermal conductivity is to use the rule of mixture:

$$k = k_f \, \phi + k_m \left(1 - \phi\right) \tag{2.12}$$

where k_f and k_m are the thermal conductivity (W m^{-1} K^{-1}) of the powder particles and the binder matrix, respectively. According to this equation, the thermal conductivity of PIM feedstocks depends only on the volume content and the inherent properties of the constituents. But, this expression is only applicable if the particles are in contact with one another in the heat flow

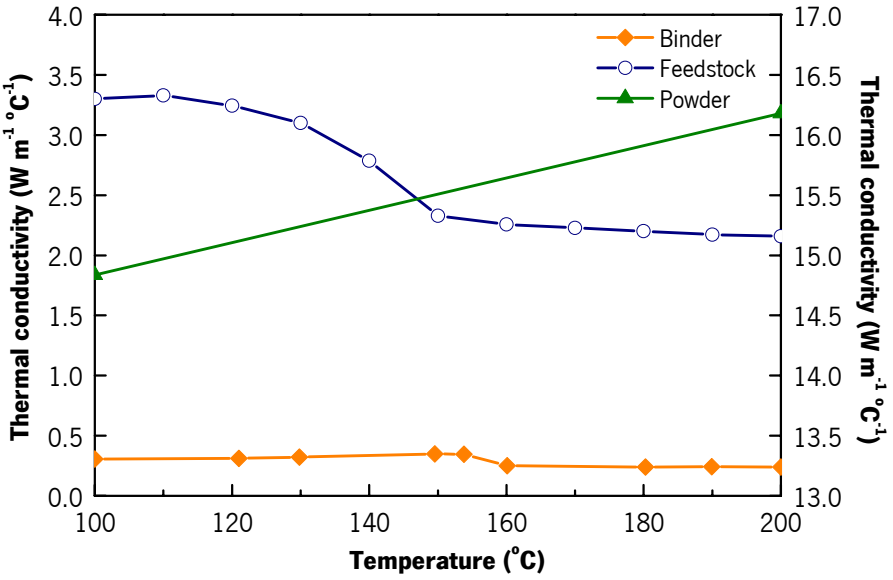

Figure 2.21 Thermal conductivity of a 316L stainless steel feedstock over the processing temperature range [84].

direction (similar to the long fibre composites) [3].

Alternative expressions in use [84, 171, 172] are the Maxwell and semi-theoretical Lewis & Nielsen models. Maxwell model is believed to describe well the thermal conductivity of a composite comprising high conductivity spheres in a low conductivity matrix. The conductivity of such a composite is given by

$$\frac{k}{k_m} = \frac{k_f + 2\,k_m + 2\,\phi\,(k_f - k_m)}{k_f + 2\,k_m - \phi\,(k_f - k_m)} \qquad (2.13)$$

The Lewis & Nielsen model includes the effect of the shape of the particles and the orientation or type of packing for a two-phase composite system. The thermal conductivity of a composite is described by the following formula:

$$\frac{k}{k_m} = \frac{1 + A\,B\,\phi}{1 - B\,C\,\phi} \qquad (2.14)$$

where $A = k_E - 1$ $B = \frac{(k_f/k_m) - 1}{(k_f/k_m) + A}$ $C = 1 + \frac{1 - \phi_m}{\phi_m^{\,2}}\phi$

k_E is the Einstein coefficient and ϕ_m the maximum packing volume fraction, related to the packing efficiency of the particles and hence is a function of the powder characteristics.

Kowalski et al. has compared the two models with experimental data of a 316L stainless steel feedstock with polyoxymethylene based binder at 60 % solids volume. The difference between the measured and the calculated values is large (15 – 85 %). None of the models fully take account the phase change in the processing temperature range (specific volume change) of the matrix material and the change of the thermal conductivity of the composite material which is related tõ this phenomenon. The most theoretical models were until now verified for much smaller filler concentrations (1 – 30 vol%). It was thus assumed that calculation of the thermal conductivity of the composite can only give reasonable results if a relatively thick layer of matrix material separates all filler particles from each other. In the case of high filled PIM feedstocks, the thickness of the binder layer among some powder particles is close to zero [84].

2.3.4. Mechanical properties

PIM feedstocks are normally fragile and brittle due to high powder fraction. An understanding of the mechanical properties of the feedstock is important to binder formulation. Poor mechanical properties caused difficulties in handling the moulded parts after moulding and in severe cases cracks after moulding. It was found that a higher green strength of moulding parts led to a much better sprues pulling behaviour, and this can be extended to the ejection behaviour of all moulded part [33].

The mechanical properties of particulate polymeric composites, where the particles are much stiffer than the matrix, are very dependent particle-particle and particle-matrix interaction. Factors such as critical solid volume fraction, degree of agglomeration and powder-matrix adhesion has been taken in account [3].

Investigations with feedstocks of 60 vol.% iron powder mixed with EVA, *Polybond* and polystyrene were performed in order to analyse three point bending mechanical behaviour (cited in [3]). It was reported that the strength of a feedstock does not increase by only increasing the strength of the binder. In addition, despite the binder containing EVA has lower strength, the feedstock containing EVA possess the highest yield strength, attributed to the higher matrix-powder adhesion for the EVA system due to the polar EVA molecules.

Figure 2.22 shows the strength of two binders, polyethylene and paraffin based, and those binders loaded with the same volume fraction of carbonyl iron powder. It can be observed that despite the strength of the pure polyethylene binder which is higher than that of paraffin binder, the strength of the feedstock of the first is lower than the latter. The feedstock with paraffin wax exhibits better adhesion to the powder and therefore, a greater increase in strength compared to the polyethylene binder. Binder strength is clearly not a indicator of feedstock strength. Instead, strong powder-binder adhesion contributes significantly to feedstock strength.

2.3.5. Morphology

The morphology of a feedstock can reveal useful information that can explain the results of the rheological, thermal and mechanical properties study. Scanning electron microscopy (SEM) will

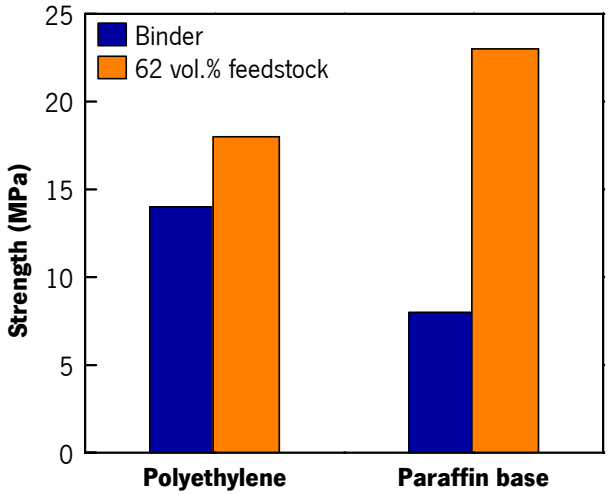

Figure 2.22 Strength of two binders and the corresponding feedstocks, with carbonyl iron powder [3].

be more appropriate for this purpose since the small powders normally used in PIM is hardly visible from optical microscopes.

Feedstock morphology analysis has been performed to evaluate the dispersion of powder particle among the binder and wetting of binder on the particles surface [162]. Agglomeration of the powder particle can be observed very frequently, normally due to the difficulty in dispersing the powders especially when the powder volume fraction is very high. Powder particles surfaces covered by a layer of binder is often understood as an indication that the adhesion between the powder and the binder matrix is good [3]. Figure 2.23 shows a SEM micrograph of a fractured surface of a metal powder feedstock, exhibiting a good powder dispersion and wetting.

Agglomeration is hard to prevent specially with very fine powders. A study with zirconia (0.25 μm of average particle size), mixed in a range of 45 to 60 vol.% with a wax based binder, show that controlled agglomeration cannot be disadvantageous or can be considered favourable for injection moulding process [93]. The presence of zirconia powder agglomerates causes the formation of interconnected particulate network and this structure retains the moulded compact free from volume change, i.e. shrinkage, after removing the binder. In spite of the presence of agglomerates, the moulded compacts illustrate a significant degree of homogeneity as revealed by their orientation-independent uniformity in shrinkage on sintering and it may be reflected as a result of the achievement of near-perfectly random distribution of the agglomerates throughout

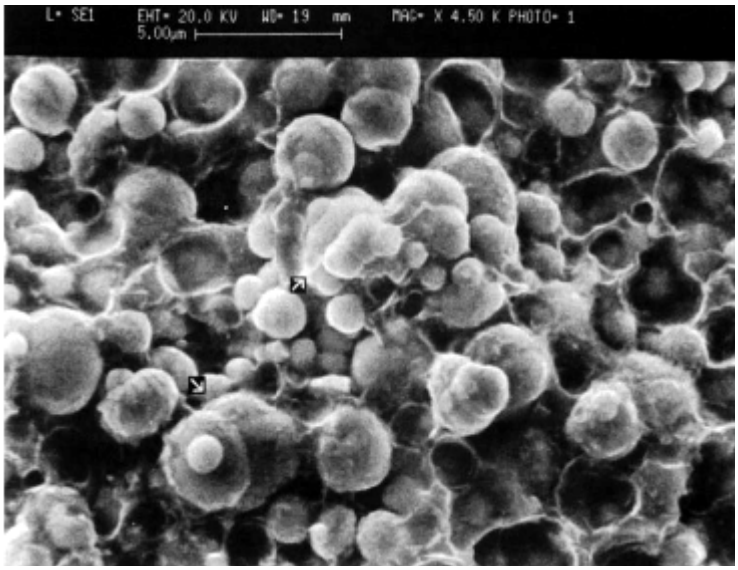

Figure 2.23 SEM micrograph of fractured surface of carbonyl iron powder, 58 vol.%, with EVA/beeswax binder (x4500) [3].

the moulded compacts. On the other hand, the presence of agglomerates causes poor particle packing efficiency. However, it was shown that particle packing tends to improve at higher solid fraction, e.g. above 50%. Moulded parts derived from these high solids suspensions, having a more homogeneous green microstructure are more susceptible to densify at lower temperatures than do the parts made from lower solid suspensions [74].

2.4. Design of binders and feedstocks

2.4.1. Binder formulation

As previously mentioned, the main role of the binder is essentially to be the carrier and allowing flow and packing of the powder in the mould cavity. Subsequently, the binder also assures the integrity of the green body before sintering.

The binder is the key component in PIM strongly influencing the mixing, moulding and debinding operations. It also affects the maximum powder fraction in the feedstock, the shape retention of the parts during debinding, the dimensional accuracy and other properties of the sintered parts. The development of binders has largely been empirical due to the lack of complete understanding of the underlying basic principles involved [3].

The binders in the PIM process must [1, 13]:

during mixing

- be capable of uniformly and efficiently covering the powder particles surface, creating a thin layer which should prevent the attraction force between them;

during injection moulding

- provide suitable plasticity and fluidity of feedstocks so that green parts without any defects are produced;
- provide enough strength on the green part to avoid any deformation or cracking during demoulding;

during debinding

- be effectively removed to obtain brown parts with good quality;
- provide enough strength on part to maintain the geometrical integrity against the diffusion processes;

during sintering

- not cause a deterioration in the properties of sintered parts, by contaminating the material by the remaining residue came with brown bodies.

Only a multicomponent mixture may satisfy simultaneously these requirements. The binder design methodology normally followed is based on three components (Figure 2.24):

- a base material that is easily removed in the debinding;
- a backbone polymer that provides strength to the green part and
- additives, predominantly a surfactant to link the binder and powder.

The base material is removed in the debinding step by an adequate technique and the other by thermal degradation during the sintering cycle [1]. These constituents are often present in roughly equal proportion, allowing their interconnection throughout the pore structure between the particles. Binder interconnectivity can be obtained with a minimum of 20 to 30 vol.% of each component. Table 2.13 presents some combinations of the main and the secondary constituents of binder systems for PIM.

2.4.2. Binder constituents

Although many binders are possible, on a production basis, thermoplastics are by far the most widely as major constituents. These include most of the common commercial polymers – polyethylene, polypropylene, polystyrene, poly(vinyl alcohol), polyacetal, poly(methyl methacrylate) and waxes. Typically, the two major constituents are high molecular and low molecular weight polymers that are partly miscible in each other due to differing molecular weights, chemical structures or melting temperatures, so that one component can be selectively

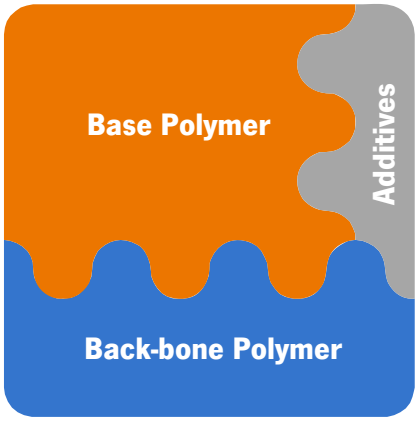

Figure 2.24 Typical functional structure of PIM binders.

Table 2.13 Examples of main and secondary constituents of binder systems for PIM [173].

Type of binder	Constituent *	
	Main	**Secondary**
Based on wax	paraffin wax	polyethylene
	microcrystalline wax	polystyrene
	natural wax	stearic acid
	liquid lubricants	butyl stearate
Based on polymers	polystyrene	stearic acid
	polyethylene	wax
	polyoxymethylene	patented additions
Thermosetting resins	epoxy resins	wax
		stearic acid
Gels	water	methyl cellulose
		agar
		glycerine

* the content of the main constituent is equal or more than 50%

removed by debinding.

Binders are usually composed of polymers, waxes, a plasticizer and other additives. Polymers provide the plasticity and mechanical strength of mixing mass. Waxes enhance the wettability and lubrication properties of the resulting materials. Lubricants are used to lower the viscosity of the feedstocks. Additives such as stearic acid or coupling agents will promote the interfacial reaction between binders and powders.

Base materials – major constituents

In the major constituents, beyond the polymer chemistry, molecular weight is a critical attribute. The melting temperature of a polymer depends on the molecular weight. Since the chain entanglement varies with the molecular weight, and chain branching, the tensile strength also increases. So, several variables determine the properties of a polymer, including the chain length, chain entanglement and side groups on the chain. Even in cases where the chemistry is fixed, the properties of a thermoplastic can be highly variable. Practice has preferred shorter molecules

to reduce residual stresses in moulding and to ensure isotropic powder packing and shrinkage. High molecular polymer has also been used, acting as a backbone material, in order to give mechanical strength to the green parts and offer the general rheological properties required [1].

Yang *et al.* studied the effect of the molecular weight of the major binder constituent, PEG, for the injection moulding of alumina [154]. Low molecular weight PEG's had low viscosity at 90°C and low yield stress, around zero, and because of this it was observed that they even could flow without force induced. The fluidity of such feedstocks was so high to prevent powder separation. Figure 2.25 shows that increasing the molecular weight of the major binder component viscosity increase too, however accompanying the decrease of PEG molecular weight, the fluid behaviour changed from pseudoplastic to dilatant behaviour, possibly explained by the dissociation occurring between the binder and the powder particles. Results indicated that the activation energy of feedstock decreased with increasing PEG molecular weight. Although the feedstock containing the highest molecular weight based polymer, PEG20K, had the lowest fluidity, it should have a stronger adhesion to powder that other low molecular weight PEG, giving a more flow stability and have a lower temperature dependence of viscosity in the temperature range just below nozzle temperature. So it needs a compromise solution to find the optimum molecular weight of the major binder component in order to achieve the best set of fluidity-temperature

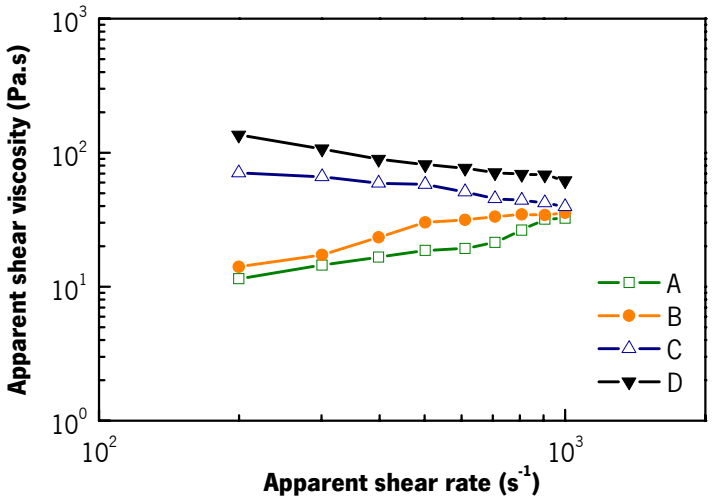

Figure 2.25 Viscosity as function of shear rate of various feedstocks with major binder components with different molecular weight: PEG 1K (A), PEG 1.5K (B), PEG 4K (C) and PEG20K (D) (alumina powder 55 vol.% with PEG:PE wax:SA weight ratio of 65:30:5) [153].

dependence-powder separation.

Song and Evans reached to same conclusion, that powder segregation can be controlled by choosing the right molecular weight binder components [72]. They verified that unstabilized ceramic injection moulding suspensions in low viscosity organic vehicle can undergo flocculation during the early stage of reheating to remove the binder, and any process that rearranges particles such that the pattern of contacts is irregular is a potential cause of defects. Particles can rapidly come into contact in a wax system if stabilizing repulsive interparticle forces are absent. Flocculation can be reduced by the use of a high molecular weight binder system which confers elastic stabilization and reduces mobility of particles or by the addition of appropriate and sufficient dispersant which adsorbs on particle surfaces and gives rise to interparticle repulsion.

The capability for the shape maintenance of during water extraction has observed to be dependent on the molecular weight. Park *et al.* studied the effect of the molecular weight of the major binder constituent, PEG, on a binder with PEG/CAB (cellulose acetate butyrate) for injection moulding of a water atomised 17-4PH stainless steel powder [34]. As the molecular weight of PEG was increased, binder failed to maintain the shape during extraction. This observation was related to the crystalline structure of PEG on the green parts, and its relationship with the molecular weight. They speculate that the size of crystal of PEG in the binder was related to the shape maintenance during the extraction; the bigger the crystal, the poorer the shape maintenance since a larger area is exposed to the solvent.

The effect of the molecular weight in thermal debinding was studied by Lee *et al.* [153]. Low molecular weight waxes and polymers which are decomposed by evaporation and chain depolymerisation left less carbon residue than polymers decomposed by random decomposition. The molecular weight was found to have a large effect on the residual carbon and showed a logarithmic linear increase with increase in residual carbon (Figure 2.26).

Waxes have been preferred as the low molecular weight constituents because of their small molecular size, thermoplastics character, low melting temperature, very low melt viscosity and good wetting [13]. Table 2.14 shows the typical properties of the waxes found in binder formulations. Beeswax is secreted by bees and is used to construct the combs in which bees store their honey. The wax is harvested by removing the honey and melting the comb in boiling water. Carnauba wax, a natural wax formed on brazilian palm leaves, because of its hardness is

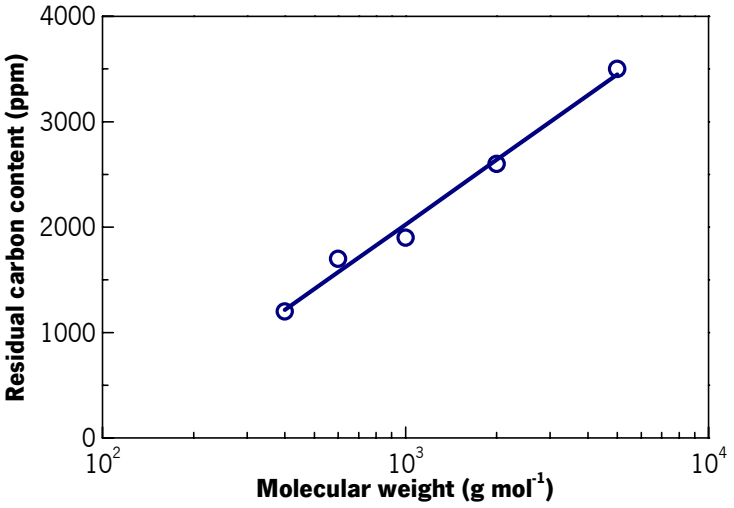

Figure 2.26 Residual carbon content as function of molecular weight of a polyolefin waxes [153].

another common ingredient in PIM binders. Waxes from mineral source are in use, such as montan, paraffin and microcrystalline waxes. Montan wax is derived by solvent extraction of lignite. The removal of some resins and asphalt of the primary montan wax by refining yields the whiteness of known wax. Paraffin wax, which is refined from petroleum, is macrocrystalline and brittle. Microcrystalline waxes, also refined from crude oil, are less crystalline than other waxes but have a stronger structure. Several wax-like short oligomers and polymers such as polyethylene or polypropylene waxes have also been used.

Hsu *et al.* studied the effect of wax molecular polarity on the injection moulding of a stainless powder and found that the polarity of waxes can be a reason for differences of behaviour in PIM

Table 2.14 Typical properties of waxes, from natural and mineral sources, used in PIM binders [174].

	Beeswax	**Carnauba wax**	**Paraffin wax**	**Microcrystalline wax**	**Refined montan wax**
Melting temperature (°C)	64	84	46 - 68	60 - 93	80
Molecular weight	-	-	350 - 420	600 – 800	-
Carbon atoms per molecule	16 - 31	-	20 - 36	30 - 75	-

feedstocks. Polar waxes mixtures, like Acrawax and Carbauna wax, appear to have higher viscosities and better pseudoplastic properties than non-polar mixtures. This is because of the hydrogen bonds formed between steel powders, resulting from the acid-base interactions. However, sintered parts from mixtures containing polar waxes exhibit lower tensile strength because of the poorer fluidity of these waxes and higher carbon contents in the brown parts [13].

Back-bone polymers – minor components

High and low density polyethylene (LDPE/HDPE), polypropylene (PP), polystyrene (PS), poly(methyl methacrylate) (PMMA) and co-ethylene-vinyl acetate are examples of common backbone polymers used in the design of thermoplastic binders. They were chosen mainly due to their simplicity, high availability, low cost and good properties [12, 19, 33, 153, 162].

Although they are a minor component comparing the base binder component, back-bone polymer can affect several features of the PIM process. The composition of the back-bone polymer (or a blend) can have a great influence in the feedstock rheology, injection moulding and debinding. It has been observed influence at the shear and temperature sensitivity in the feedstock flow, parts ejection behaviour and green strength and the rate of solvent extraction, and even the appearance of debinding defects caused by swelling effects [33]. Studies focused in the rheological behaviour, measured by the general rheological indexes, which takes in account the fluidity, the shear and the temperature sensitivity, suggest that better behaviour contributes for better mechanical properties. The best formulation also gave the best shrinkage homogeneity which suggests that good rheological properties are beneficial to the control of dimensional tolerance for MIM parts [153]. Back-bone polymer must be selected according to the debinding process. In solvent extraction debinding, polymer can fail to play it role of maintain the moulding shape while the base binder component is extracted. As the solvent diffuses into the moulded part, it causes the polymer molecules to swell. When the volume swell ratio is sufficiently large, the stress causes bubbles or cracks in the parts. Chemistry of the polymer is crucial to avoid the appearance of such defects [19]. Molecular weight of the minor components showed to affect the maximum powder fraction. The results found by Li *et al.* suggest that the maximum solids fraction increases with the decrease of the molecular weight [19]. In that particular case, for a paraffin wax-oil-polyethylene binder for the injection moulding of Fe-2Ni powder, when the

molecule weight of the PE is decreased, the maximum solids fraction is increased from 57 to 60 vol.%.

Omar *et al.* studied the effect of the back-bone polymer content in the binder formulation. The study, with a PMMA/PEG binder, showed that the back-bone polymer plays a several important roles in the composite binder system. Increasing its content increases the apparent viscosity of the binder system, stiffens the mouldings, increasing the strength of the mouldings and reduces the rate at which the PEG are leached (Figure 2.27). Increasing the PMMA content for a fixed metal powder content increases the density attained after sintering and the hardness of the specimens [12]. Thus it is clear that the back-bone polymer content needs to be carefully optimised.

Additives

Substances added in very minor concentration are called additive, but their function is very important to improve processing and parts quality. Lubricant, plasticizer and surfactant are the most used in binder systems. However, some material can have multifunction. Often, the surfactant also acts like a lubricant to help flowing and tool release. Some other additives are

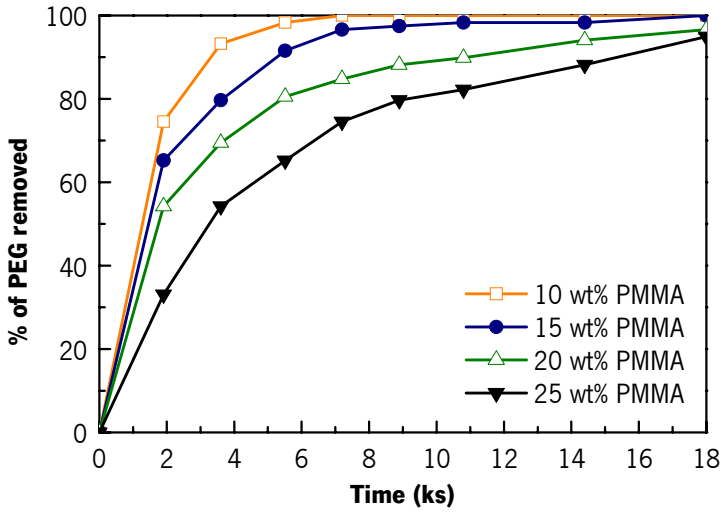

Figure 2.27 The percentage of a binder major component removed from moulded part by water debinding at various times for different back-bone polymer contents. Binder system: PEG/PMMA [12].

used in order to perform particularly modifications, such as to modify the feedstock rheology, to increase compatibilisation between binder components or to prevent binder or powder oxidation [1].

a) Lubricants

In PIM process, lubricants are used as processing aids, can be either internal or external. Internal lubricants can be used to improve throughput, while external lubricants may be used as for mould release, again improving productivity. Lubricants usually act by modifying the viscosity of the melt, by introducing different surface energies at the interface between phases. The viscosity of the binder must be low, since the desirable high solids fraction will give a substantial viscosity increase [1].

The efficiency of an internal lubricant represents its functional compatibility ort ability to compatibilise into the host polymer. An external lubricant or mould release agent relies on incompatibility, forcing it to the surface of the part during the moulding cycle. Certain materials can be used for both internal lubrication (at low addition) and for mould release (at higher level), aiming at a balance in compatibility and incompatibility. The key criteria for selecting lubricants are: compatibility/solubility with the host polymer; no adverse effect non properties; the rate of migration, easy addition and a suitable melting point.

Suitable materials for lubricants, also in use in plastics moulding, are metallic stearates, hydrocarbons, fatty acids and alcohols, esters, amides and polymeric additives [175].

b) Plasticizers

Plasticizers are stable, unreactive materials that are added to polymer to make them more flexible. In the mixture formed between a plasticizer and a polymer, molecules of the plasticizer are interspersed between molecules of the polymer, making the combined mass more flexible that the polymer alone. As for the internal lubricants, the key for the retention of the plasticizer in the mixture is to select a plasticizer that is compatible with the polymer. The conventional plasticizers, such as oleates and phthalates, are not compatible with polyethylenes. However, polyethylenes can be completely dissolved in hydrocarbon waxes or oils at temperatures above

their melting points, and the resultant blends can be processed by conventional thermoplastic techniques. Ethylene-vinyl acetate (EVA) copolymers, which are mutually soluble with polyethylenes, sometimes are used to enhance their plasticity. Plasticizers for polystyrenes, polypropylenes and acrylics include phthalates, adipates, laurates, stearates and oleates [2].

A study about the use of alternative plasticizers, dibutyl phthalate (DBP), organic alcohol glyceryl (OAG) and castor oil in the formulation of the binder for the injection moulding of zirconia had confirmed the effect of the plasticizers. They do not affect the rheological behaviour, but reduces the shear stress and thus the feedstock viscosity, thus acting like lubricant. The results demonstrate that plasticizer can affect the performance of debinding and sintering. Improper selection of the plasticizer can produce cracks in the moulded parts during thermal debinding. The zirconia sintered parts from feedstock with higher content of plasticizer exhibit higher flexural strength and fracture toughness [11].

c) Surfactants

Surfactants are additives that affect the performance of polymers during injection moulding by modifying the cohesive forces between the polymer and the filler. Usually, a low molecular weight component is used as a surface active agent, which consists of a functional group adhering to the powder surface and an oriented molecular chain extending into the binder to prevent aggregation of powder. It serves as a bridge between the binder and powder and creates the stabilization of the particles when they are broken apart by mechanical shearing during mixing. Enhanced adhesion of binder components onto the powder surface is primarily realized by hydrogen bonding between the powder surface and the surface active agent through a Lewis acid (electron acceptor)–base (electron donor reaction) [156, 176].

Surfactants reduce the viscosity of the mixture, improve the flow during moulding and ease the release of the moulded parts from the mould. The most relevant function of the surfactant is to uniformly distribute the binder components throughout the mix and to enhance the dispersion of the powder particles. The stable dispersion of the powder particles in a feedstock is essential to minimize the formation of agglomerates, which cause flow instability and inhomogeneous microstructures. In this way, surface active additives are also called dispersants.

Chan and Lin suited the effect of the addition of stearic acid, as surfactant, to an alumina feedstock [59]. Beyond the increase of feedstock fluidity, the use of the stearic acid was observed to alter the rheological behaviour from dilatant flow to pseudoplastic flow. The incorporation of the surfactant in the binder at a significant concentration substantially reduced the abrasion of the feedstock mixture against the machine components and minimized the separation of binder from the powder during injection moulding. In addition, the range of the binder pyrolysis temperature of the powder-binder mixtures was broadened as the concentration of stearic acid increased, which is very convenient for thermal debinding process. Song *et al.* demonstrated that the addition of appropriate and a sufficient dispersant, which adsorbs on particle surfaces, gives rise to interparticle repulsion and consequently can avoid particle flocculation during thermal debinding, which leads to large fissure in the parts [72].

The most used surfactants are fatty acids, like stearic acid or oleic acid, or their derivates, as zinc stearate. They proved to be very efficient because of their bi-functionality. Moreover, stearic acid has been recognized to be most successful both in oxide ceramics [11] or ferrous metals [8]. For the injection moulding of silicon nitride, the most advisable surfactants are silanes and titanates, as it has been verified their effect lowering the viscosity of feedstock and increasing of green strength [44, 45].

2.4.2.1. Blend compatibility in binders

Thermoplastic binders are mainly polymeric blends of different components. Typically, they are composed of at least two ingredients, polymers or waxes that would have affinity and miscibility to provide integrity to the binder blend [1]. The concept of blends are those mixtures of two molecularly or microscopically dispersed polymers.

Compatibility between constituents in the binder is essential to prepare a homogeneously mixed feedstock. The powder size employed in PIM is usually several micrometers, although fine submicrometer powder is also used for special cases. This implies that the binder components should have compatibility within the order of submicrometers [34]. The rate of binder separation was suggested to be dependent on the compatibility between binder components. Strong adhesion of binder to powder and good compatibility between binder components will reduce the

level of binder separation [7]. The chemical compatibility between major and minor binders has a significant effect on the debinding behaviour of the injection-moulded body with wax based binders. Even though it was not clear to which degree the incompatibility can be allowed in the mixture formulation, it might be a useful tool for a rapid debinding to utilize the limited incompatibility in binder formulation for injection moulding [10].

Miscibility refers to mixtures on the molecular level (nanometer range) that are in true thermodynamic equilibrium; that is, true thermodynamic solubility. Compatibility denotes the ability of mixtures to be blended to heterogeneous micro-composites that do not separate into macroscopic phases under experimental conditions. Blends of compatible polymers are not necessarily in thermodynamic equilibrium [177].

Homogeneous miscibility in polymer blends requires a negative free energy of mixing (ΔG_{mix}):

$$\Delta G_{mix} = \Delta H_{mix} - T \cdot \Delta S_{mix} \qquad (2.15)$$

where ΔH_{mix} is the heat of mixing (J kg^{-1}), ΔS_{mix} is the gain of entropy (J kg^{-1} K^{-1}) and T is the process temperature (K). If two high molecular weight polymers are blended, the gain in entropy, ΔS_{mix}, is negligible, and the free energy of mixing can only be negative if the heat of mixing, ΔH_{mix}, is negative. Therefore, the mixing must be exothermic, which requires specific interactions between the blend components. These interactions may range from strongly ionic to weak and nonbonding interactions, such as hydrogen bonding, ion-dipole, dipole-dipole and donor-acceptor interactions. Usually, only Van der Waals interactions occur, which explains why polymer miscibility is the exception rather than the rule [178].

The concept of the solubility parameters has been used for the estimation of polymer blending compatibility. This approach has been develop based on work on enthalpy of regular solution, turning possible to be applied strictly to non-specific molecular interaction, without forming associations or orientation, hence not of the hydrogen or polar type [179]. Miscibility parameters δ is can be determined from

$$\delta = \sqrt{\frac{\Delta E}{V}} \qquad (2.16)$$

where ΔE is activation energy for vaporization (J kg^{-1}), V is specific vapour volume of polymer (m^3 kg^{-1}). $\Delta E/V$ is the best criterion for measuring the function of the molecular chains, while δ is

used for measuring this function due to the difficulties in measuring the $\Delta E/V$ of the polymer. δ can be calculated by a group contribution method, considering the chemical structure of the repeating unit of the polymer, followed by use of the equation

$$\delta = \frac{\sum_i F_i}{\sum_i V_i} \qquad (2.17)$$

where F_i is the constant of attraction of the group i and V_i represents the molecular volume of the group i. F_i and V_i are obtained by experimental means and are usually tabulated in reference publications. Compatibility between two polymers is evaluated by the difference between their miscibility parameter, $\Delta\delta$. The lower is $\Delta\delta$ the higher is the compatibility between two polymers. It is considered that the compatibility is good when $\Delta\delta < 0.7$, while the miscibility is bad when $\Delta\delta > 1.0$ [11].

The biggest drawback of the solubility parameter approach is omission of the entropic and specific interactions effects. Furthermore, the fundamental dependencies do not take into account either the structural (isomeric), orientation, or the neighbouring group effects. However, since the contributions that are included in the solubility parameters are indeed detrimental to miscibility, minimizing values must but help the miscibility [179].

Several alternative experimental methods of assessment to the compatibility of polymer blends are used:

- Glass temperature - the most commonly used criterion for establishing the miscibility of the components of a polymer blend is the detection of a single glass transition temperature (T_g), usually at a point between the T_g's of the polymeric constituents [8, 162, 180];
- Transparency – polymer materials of which blend exhibits melt transparency are considered miscibles [34];
- Microstructure analysis – compatibility can be detected by X-ray diffraction analysis, shift of microstructure patterns indicates that chemical interaction exists among the blend constituents [19];

- Melting point depression - in blends where one component crystallizes there is a melting point depression resulted from specific interactions causing compatibility [180-182].

The most widely used technique for determining the magnitude of compatibility-inducing interactions in crystalline and compatible blends is melting point depression [180, 183]. The melting behaviour of a semicrystalline component in a miscible blend strongly depends on the blend composition. In several blends a depression of the melting point has been observed after addition of an amorphous polymer. Melting point depression, caused by morphological effects, is associated with changes in crystal thickness, perfection and geometry, as well as with different thermal histories of the samples. When a miscible diluent is added to a semicrystalline polymer, the equilibrium melting point of the crystallisable component can be depressed due to interaction between both components.

Melting point depression data are often used to determine the Flory-Huggins polymer-polymer interaction parameter, χ, that is a measure for the miscibility of the blend, i.e., χ is negative for a miscible blend. A lack of melting point depression means that χ is zero. Comparison of χ value is useful as lower χ means higher specific interactions, thus compatibility in polymer blend [184]. Nishi and Wang provided an analysis, from thermodynamic effects and the Flory-Huggins equation, which relates the melting point depression to the interaction parameter (χ) [181]:

$$\frac{1}{T_m^e} - \frac{1}{T_m^{e0}} = -\frac{R\, V_{m,A}}{\Delta H_f^0\, V_{m,B}} \chi\, \Phi_B^2 \qquad (2.18)$$

where T_m^e and T_m^{e0} are equilibrium melting temperatures (K) of the polymer blend and the pure polymer respectively, $V_{m,A}$ and $V_{m,B}$ are the molar volumes ($m^3.mol^{-1}$) of the repeating units of crystalline and amorphous polymers, respectively, ΔH_f^0 is the enthalpy of fusion of the perfect crystal (J mol^{-1}) and Φ is the volume fraction of the amorphous polymer χ is dependent on the heat of mixing but independent of combined entropy of mixing. Hence, melting temperature depression is only dependent on the degree of interaction between the polymers, provided the samples are crystallized and melted in the same manner [65].

To determine the interaction parameter, an accurate measurement of the equilibrium melting temperature is needed. However, for comparison purpose the non-equilibrium melting

temperature depression can be used to yield a qualitative, rather than a quantitative, estimation of the level of interaction between the components [3].

2.4.3. Powder fraction

PIM process has a great dependence of powder characteristics, such as size, particle size, shape and chemistry. Often, when a feedstock development is starting, these characteristics are already set because the required powder chemistry is obtained by a unique economic production method. Therefore, concerning to the powder, there is only one degree of freedom to play with – the powder concentration.

Powder concentration are commonly referred by solids fraction ϕ, which is the volumetric ratio of solids powder to the total volume of powder and binder,

$$\phi = \frac{w_p / \rho_p}{w_p / \rho_p + w_b / \rho_b} \tag{2.19}$$

where w_p and w_b are the weight fraction of powder and binder, respectively, and ρ_p and ρ_b are the densities of the powder and binder respectively. A value near 60 % is typical for PIM. Volumetric comparisons are useful when examining powders of different densities, but for manufacturing purposes feedstock formulation is by weight. For example, to obtain a 60 vol.% powder fraction where the binder and powder have densities of 1.0 and 7.9 g.cm^{-3}, it is required 92 wt.% of powder and 8 wt.% of binder. As the density of the solid material increases, there is a

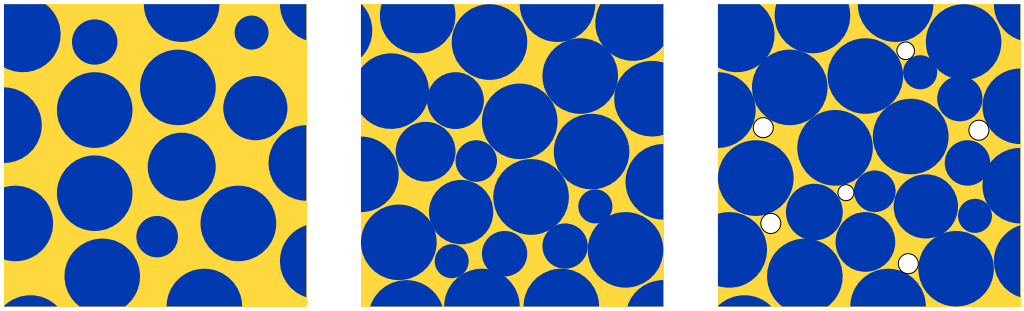

(a) Excess binder (b) Critical powder concentration (c) Excess powder

Figure 2.28 Three possible situations in a powder-binder mixture: (a) excess of binder, (b) critical powder concentration and (c) voids due to insufficient binder [1].

considerable reduction in the weight percent binder for a constant solids fraction.

PIM feedstock represents an equilibrated mixture of powder and binder. The proportion of powder to binder largely influences the success of subsequent processes. Three possible situations are sketched in Figure 2.28. Excess binder separates from the powder in moulding, leading to flashing (a thin layer of binder between the mould parts) or inhomogeneities in the moulded part. Most important, a large binder excess leads to component slumping during debinding, since the particles are not held in place as binder is removed. As the binder content decreased, a critical composition is encountered beyond which the viscosity is very high and voids form in the mixture. Most feedstocks are prepared with slightly less powder than the critical solids fraction. The critical solids fraction is the composition where the particles are packed as tightly as possible without external pressure and all space between the particles is filled with binder [1, 83]. Too little binder results in a high viscosity and trapped air pockets that make some difficulties in moulding. Internal voids or air pockets cause cracking during debinding [1].

Generally, a feedstock should contain the maximum powder fraction to minimize shrinkage during sintering, and at the same time, without sacrificing its ease of moulding. A feedstock with the optimal powder fraction will have good rheological properties for moulding, small distortion and good mechanical properties after debinding and sintering [185].

A binder concentration range is best for each powder. The amount of binder depends on the particle packing, since filling all of the void space between the particles is necessary to maintain a low viscosity. Therefore, factors like the particle size distribution and particle shape influence the optimal binder concentration. Additionally, depending on the powder surface chemistry and binder composition, an appropriate surfactant is required to bridge the gap between the powder and binder.

Solids fraction is a major factor that influences PIM parts shrinkage during sintering. When sintering, the existing voids left from the binder are eliminated and the parts shrink. A lower solids fraction determines higher part shrinkage and *vice-versa*. In conditions of full homogeneity of moulded parts and isotropic shrinkage, linear shrinkage R_L is related to solids fraction by

$$R_L = 1 - (\phi + P)^{1/3} \tag{2.20}$$

where P is the porosity of the sintered part. By this way the dimensions of PIM parts can be matched by adjusting the solids fraction.

The potential of tailoring the sintered part dimensions by changing of solids fraction is enormous, and can be applied for [28]:

- the correction of tooling errors;
- achievement of tighter manufacturing tolerances;
- the use a single moulding tool to fabricate parts of different sizes;
- matching the shrinkage of different materials;
- reduction in tooling investment for mass-produced consumer products, with short economic life and tool rework, by adapting the feedstock to the tool rather than the tool to the feedstock;
- the miniaturisation of metal and ceramic injection moulded components beyond the limits of conventional toolmaking.

2.4.4. Methods for the determination of the critical powder concentration

There is an optimal powder fraction which is just slightly below critical powder volume concentration (CPVC) (or critical powder fraction) for any given powder–binder system. Methods to determine the critical solids fraction include measuring of density, melt flow, mixing torque or viscosity versus composition.

Density versus composition experiments allow determination of the critical solids fraction [164, 186-188]. Figure 2.29 illustrates a typical curve of the mixture apparent density against solids fraction. The mixture density depends on the volume fraction of powder in the mixture. At high binder concentrations, the mixture density follows along the theoretical density line, calculated by

$$\rho_{\text{mix}} = \phi\, \rho_{\text{p}} + (1-\phi)\rho_{\text{b}} \qquad (2.21)$$

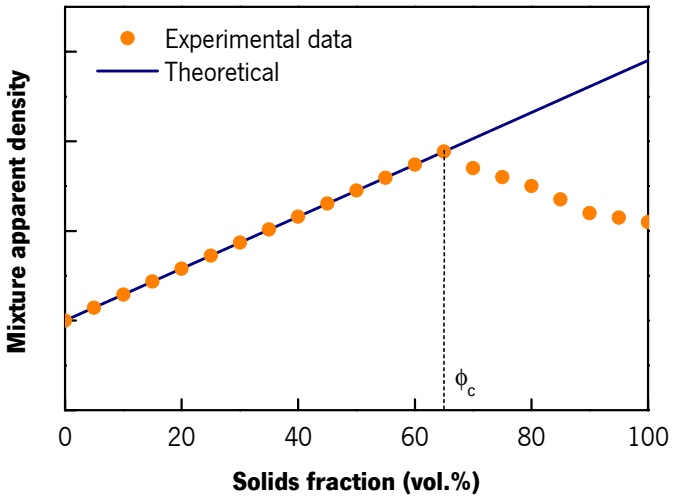

Figure 2.29 Representation of a fraction curve of mixture density versus solids fraction of a PIM feedstock.

At a certain composition, the mixture density breaks away from the theoretical line at the critical solids fraction; the particles are in their closest packing condition and just enough binder exists to fill the voids between the particles.

Rheology based method, consisting in the analysis of the dependence of the feedstock viscosity, have been applied. Viscosity of a PIM feedstock has a great dependence on the solids fraction. Increasing the solids fraction, it diminishes the mobile phase content and the mixture melt becomes difficult to flow and viscosity increases. As the solids fraction approaches to the critical value, the viscosity increases faster. The powder particles became closer together, increasing the friction to the point where the viscosity is unacceptably high as demonstrated in Figure 2.30. Attempting to enhance the critical solids fraction result, it has been used rheological models for highly loaded mixtures, whose the CPVC is a fitting parameter. Table 2.15 shows some proposed mathematical models attempting to describe the dependence of the mixture relative viscosity with solids fraction. This method has a great advantage of providing real viscosity data.

Although model fitting can be a powerful tool for the determination of the critical solids fraction, a precise evaluation of the quality of the fittings must be done, by using several models and calculating several statistical parameters [76]. As an example, a correlation coefficient (R_a) of 0.9953, appearing to represent a good fitting is actually a fitting exercise with 32 % of average

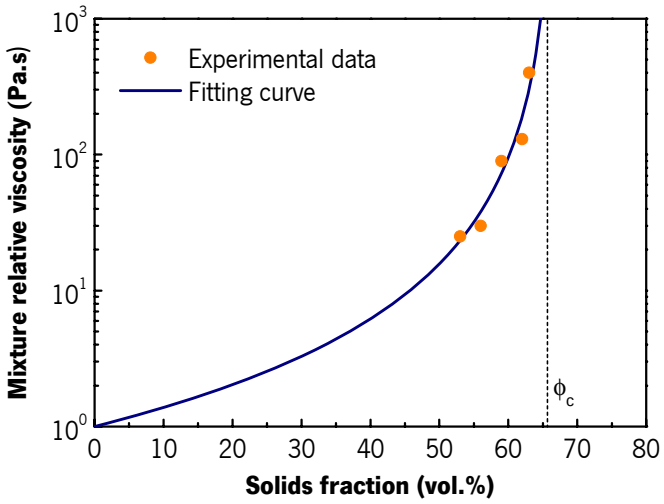

Figure 2.30 Representation of the elative feedstock viscosity ($\eta_r=\eta_m/\eta_b$) versus solids fraction. Line curve represents a model fitting for the estimation of critical solids fraction

Table 2.15 Mathematical models for the description of the effect of the solids fraction in the feedstock relative viscosity.

Mooney model	$\eta_r = \exp\left(\frac{2.5\,\phi}{1-\phi/\phi_c}\right)$	[76, 189]
Quemada model	$\eta_r = \left(1-\frac{\phi}{\phi_c}\right)^{-2}$	[76, 155, 190]
Chong et al. model	$\eta_r = \left(\frac{\phi_c - 0.25\,\phi}{\phi_c - \phi}\right)^{-2}$	[190]
Eilers model	$\eta_r = \left(1+\frac{1.25\,\phi\,\phi_c}{\phi_c - \phi}\right)^{2}$	[191]
Zhang and Evans model	$\eta_r = \left(\frac{\phi_c - C_1\,\phi}{\phi_c - \phi}\right)^{2}$	[192]
Maron and Pierce model	$\eta_r = \frac{C_2}{(1-\phi/\phi_c)^n}$	[1, 76]

relative error. The best model was found to have R_c = 0.9997 corresponding to 0.9 % of relative error [193].

Another way to determine the critical solids fraction is torque rheometry. It measures the mixing torque for mixtures of various solids fractions. In general, it is accepted that the CPVC is found when a high increase in mixing torque occurs and becomes erratic. There have been used two forms of proceeding, which can be called as:

- progressive powder additions method;
- mixing curves method.

The graph of the Figure 2.31 shows an example of the torque variations during mixing with progressive changes to the solids fraction, by consecutive additions of powder portions, in one run in the torque rheometer. Two features indicate the overcome of the critical solids fraction: higher overshoot in the torque and the emergence of an erratic value [1, 55, 58, 194]. This method is very familiar because its application takes the shortest time of all methods. Powder additions produce a higher percentage of mixer chamber volume, which affect both the torque value and fluctuation. Accordingly, it is needed an appreciable experience to correlate the data with the PIM technology optimisation to detect the profile changing only due to the CPVC.

The mixing curves method overcomes this disadvantage. It consist of making several mixing runs

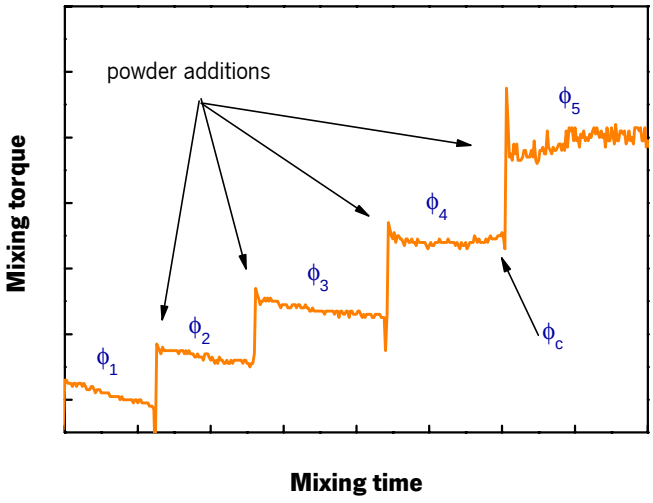

Figure 2.31 Mixing torque as function of the mixing time at several levels of solids fraction, by progressively adding the powder into the mixing chamber.

of several solids fraction and analysing the obtained profiles [162, 163]. Figure 2.32 has an example of four torque curves of mixture of different solids fraction. Torque increases with the increasing of solids content in the mixture. Beyond solids fraction of 63 vol.%, the curve reaches a steady with a noisy torque. Therefore, 63 vol.% is considered the critical solids fraction.

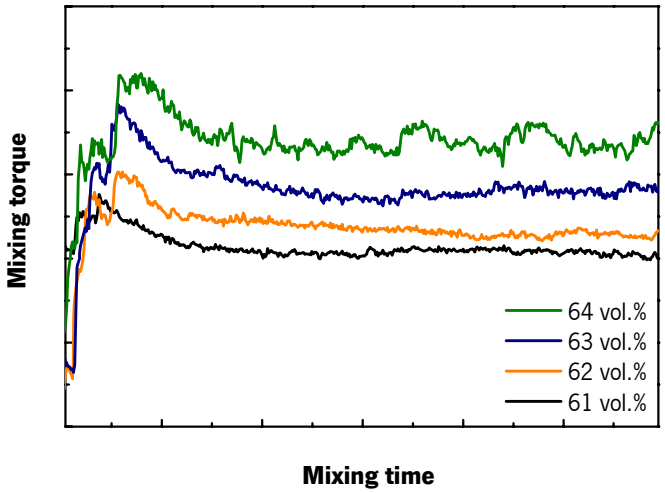

Figure 2.32 Torque versus mixing time profiles of several feedstock mixture of different solids fraction. ϕ = 63% is considered the critical solids fraction.

3. EXPERIMENTAL METHODS

The experimental part is structured in three parts (Figure 3.1). It begins by the characterisation of the powder and binders component materials. The second part involves compounding and characterization of binders and their feedstocks in order to evaluate their adequacy for powder injection moulding process. The third corresponds to the validation processing test using the selected binders, those predicted to have the best characteristics, in order to demonstrate their processability and capacity for the production of good quality sintered parts.

Procedure details and processing parameters are, in some cases, expressed in units which are not part of the International System of Units (SI), in order to keep this scientific work within the terms of common industrial practice.

3.1. Materials

3.1.1. Powder and binder components

The powder used for the experimental work was an AISI 316L stainless steel powder. This grade is typically used in applications that require good corrosion resistance, which with a carefully processing can meet the requirements of the more demanding applications [195].

The binders were based on polyethylene glycol (PEG), being the major binder constituent. Low density polyethylene (LDPE), elastomeric polyethylene (EPE), poly(methylmethacrylate) (PMMA) and poly(vinyl butyral) (PVB) were used as back-bone polymers. Two polyethylene waxes (PEW1 and PEW2) and an oxidized polyethylene wax (OPEW) were used as lubricants and stearic acid (SA) and oleic acid (OA) as surfactants.

Commercial details of the binder constituents are presented in Appendix A. As it is considered classified information, this print may not include that chapter.

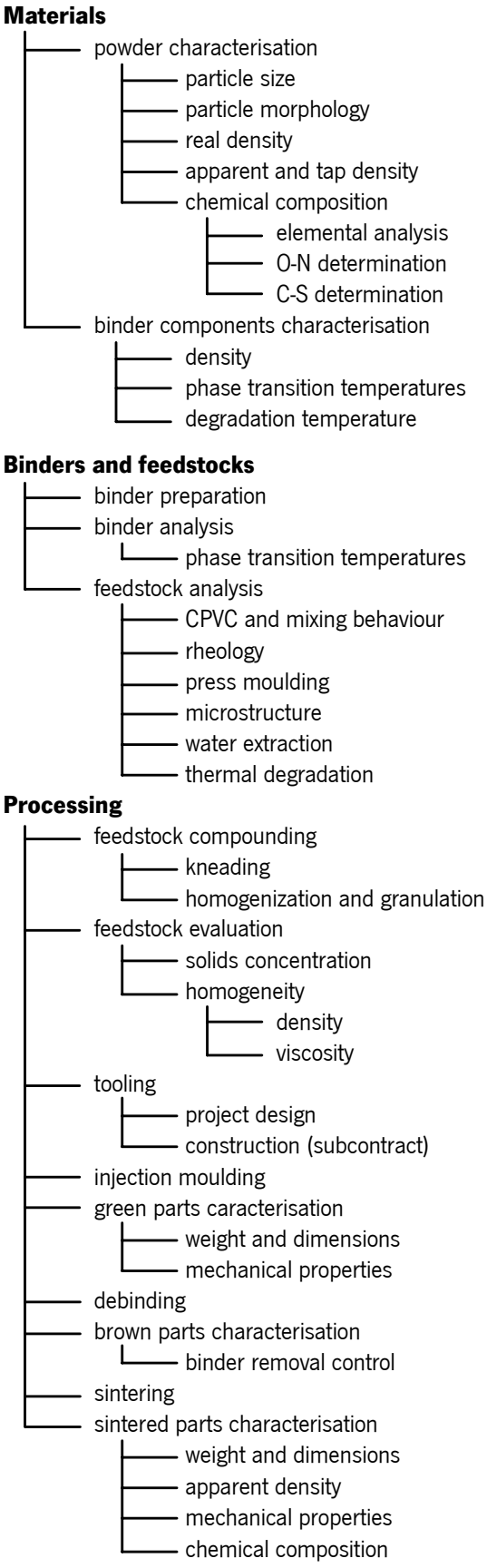

Figure 3.1 Summary scheme of the experimental program.

Metal powder

The most processed materials in PIM are stainless steels. Stainless steels are a wide range of alloys based on iron and chromium that give corrosion resistance in most common corrosive environments. In this group the most common are AISI 300 series (austenitic) that contain high nickel levels, 400 series (mostly ferritic or heat treatable into martensitic) that have low nickel content and precipitation hardened alloys (mostly heat treated into martensitic) such as 17-4 PH [1].

The AISI 316L powder, supplied by Sandvik Osprey, Ltd (UK), was produced by inert gas atomisation, as commonly applied with other alloys or readly oxidised materials. This production method yields mostly spherical powders unsuitable for conventional mechanical compaction, but highly suitable for processing by isostactic compression, spray forming and powder injection moulding [1]. Gas atomisation process is a very common method for fabrication of high performance metal powders, and it is regarded as the most economical method for the bulk production of alloy powders. In the case of special alloys, it is the method most widely used to obtain powders with very high purity and tightly controlled specifications. In this process a melt is disintegrated into droplets by the use of a high pressure gas. The resulting droplets solidify quickly in the protective atmosphere. By varying the amount of energy applied to the melt, its temperature, viscosity, and surface tension as well as by varying the quenching conditions, it is possible to vary the size, form, and structure of the particles over a very broad range [112].

Polyethylene glycol

Polyethylene glycols (PEGs), also called poly(oxyethylenes), are dihydric primary alcohols containing two hydroxyl (-OH) groups per molecule. The basic molecule of all ethylene glycols is ethylene oxide (EO), which is highly reactive. This compound readily opens its ring to form long-chain addition products, in which the group -CH_2CH_2O- is constantly repeated (Figure 3.2). EO and water form monoethylene glycol. Further addition of EO produces the series diethylene glycol, triethylene glycol, etc. The numerous members of this series are known as polyethylene glycols. PEG has in the crystalline state a fairly open helical structure as compared to poly(oxymethylene) (Figure 3.3); this structure is responsible for the low melting temperature of 69°C and its solubility in water [177].

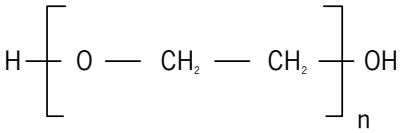

Figure 3.2 Chemical structure of PEG.

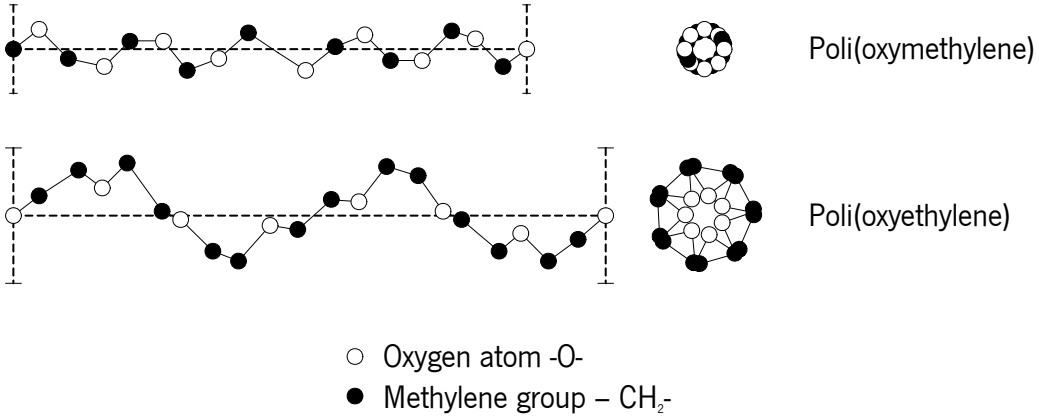

Figure 3.3 Helix conformation of chains in crystalline poly(oxymethylene) and poly(oxyethylene) [177].

The main characteristic of any PEG is the average molar mass, which can be established from the hydroxyl number, which in turn can always be determined analytically. The hydroxyl number (or OH number) and the molar mass are reciprocal, i.e. low molar PEGs have higher OH number and higher molar mass PEGs have lower OH number. Usually, commercial PEG grades are designated by a number that represents its average molar mass [27].

The combination of hygroscopicity, viscosity, lubricity, dissolving power and binding power inherent in the PEGs coupled with their solubility in water makes them ideally suitable for use in countless different applications. The applications list include textile and leather industry, rubber industry, manufacture of polyurethanes, ceramics industry, detergents and cleaners, lubricants and metalworking. Particularly, in pharmaceuticals, cosmetics and foodstuffs (packaging), the physiological safety of the PEGs is of crucial importance. When administered orally and cutaneously they are to be regarded as non-toxic. Furthermore, the vapour pressure of PEGs is so

low that inhalation of relevant amounts is impossible. Because of their good physiological tolerability the PEGs were first included in the US pharmacopoeia as long ago as 1950 [27].

Low density polethylene

LDPE is produced from ethylene under high pressure (82 to 276 MPa) and high temperature (130 to 330 °C) with a free radical initiator (such as peroxides and oxygen) and contains some long chain branches, which could be as long as chain backbones, and short chain branches. The latter disrupt chain packing and are principally responsible for lowering the melting temperature and the crystal density for hydrocarbon polymers [196]. The chemical structure of LDPE is shown in Figure 3.4.

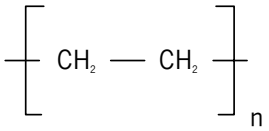

Figure 3.4 Chemical structure of LDPE.

Polyethylenes are semicrystalline polymers. Density, crystallinity and melting temperatures increase with decreasing branching. For LDPE, melting temperatures are ca. 115 °C. Special properties of interest include: optical clarity, flexibility, toughness, high impact strength, good heat seal, low brittleness temperature, good chemical resistance to aqueous solvents, and good electrical properties. LDPE may not be suitable for applications that require high stiffness and high tensile strength, low softening point, poor scratch resistance, poor gas and moisture permeability [177].

Thermal and mechanical properties of these semicrystalline polymers are strongly dependent on molecular weight, molecular weight distribution, branching content, and density. Controlled variations in these structural parameters result in a broad family of products with wide differences in thermal and mechanical properties. Most commonly LDPE grades are specially tailored for many processes, such as, blown film, moulding, and extrusion coating applications [197].

Major applications include blown film for bags and packaging; extrusion coatings for paper, metal, and glass; and injection moulding for can lids, toys, and pails. Other applications include blow moulding (squeeze bottles), rotomoulding and wire and cable coatings, carpet backing, and foam for packaging material. There is considerable use of blends of LDPE with high-density polyethylene (HDPE) and linear low-density polyethylene (LLDPE) in a wide variety of applications.

Metallocene polyethylene

Metallocene polyethylene (MPE) or metallocene linear low density polyethylene (mLLDPE) is a new type of linear low-density polyethylenes (LLDPE) based on the metallocene catalyst technology that has been introduced recently in the market. This new family of polyolefin copolymers has a significantly different chain microstructure than conventional LLDPE. The single site characteristics of metallocenes are known to produce essentially a random comonomer distribution and narrow composition distribution, with the chemical structure shown in Figure 3.5. The comonomers most frequently used commercially are butene, hexene, and octane [198].

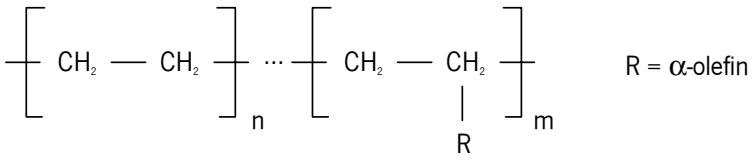

Figure 3.5 Chemical structure of MPE.

Flexibility, low extractability, high shock resistance, high toughness, exceptionally high dart-impact strength and puncture resistance, better clarity, good stress-crack resistance are some of the properties of special interest of MPEs.

Major applications include blown and cast packaging films, injection moulding goods, medical devices, automotive applications, wire and cable coatings, electrical cables, adhesives, and sealants. Other applications include blow moulding, pipe and conduit, rotomoulding, foams for sporting goods and houseware goods.

Poly(methyl methacrylate)

Poly(methyl methacrylate) (PMMA) is an amorphous-clear thermoplastic with excellent weatherability. Its high transparency of ca. 92 % combined with a fairly high Young's modulus (ca. 3200 MPa), moderate tensile strength at break (ca. 75 MPa), and reasonable thermal stability makes it the polymer of choice for outdoor signs, lamps, airplane windows (crosslinked polymers), dentures, etc. [199]. Chemical structure is shown in Figure 3.6.

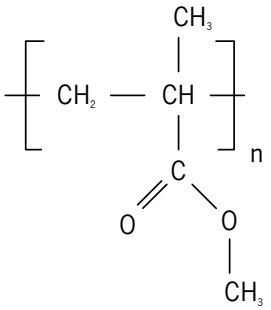

Figure 3.6 Chemical structure of PMMA.

Poly(vinyl butyral)

Poly(vinyl butyral) (PVB) is a member of the class of poly(vinyl acetal) resins. It is derived by condensing poly(vinyl alcohol) (PVA) with butyraldehyde in the presence of a strong acid. PVA reacts with the aldehyde, to form six-membered rings primarily between adjacent, intramolecular hydroxyl groups, leading to the structure shown in Figure 3.7 [200].

Properties to be noted are resistance to penetration by natural wood oils, film clarity, heat sealability, adhesion to a variety of surfaces, chemical and solvent resistance, physical toughness.

The significant use of poly(vinyl butyral) is in lamination of safety glass (automotive windshields). Others are structural adhesives, binders for rocket propellants, ceramics, in metallised brake linings, lithographic and offset printing plates, magnetic tapes, powder coatings; binder matrix in photoactive, elecrooptic and electronic devices and protective coatings for glass, metal, wood, and ceramics [201].

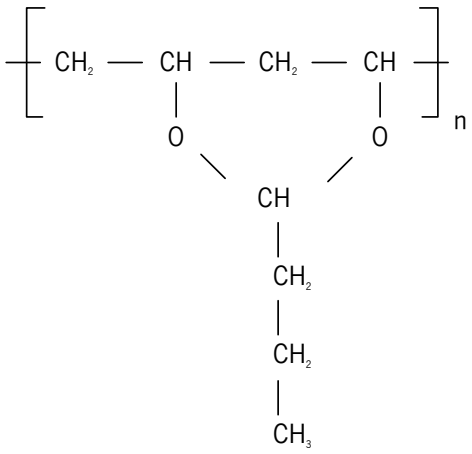

Figure 3.7 Chemical structure of PVB.

Polyethylene waxes

The mostly accepted definition of wax is: a technical collective designation for a series of natural or artificially produced materials that have the following characteristics: kneadable at 20 °C, firm to brittle hard, coarsely to finely crystalline, translucent to opaque, but not glassy, melts above 40 °C without breaking down, relatively low viscosity already just above the melting point, consistency and solubility heavily dependent on temperature, polishable under light pressure. If, in borderline cases, a substance fails to meet more than one of these characteristics, then it is not a wax within the meaning of this definition [202].

In general, waxes are classified as natural or artificial waxes. Natural waxes have an animal, vegetable or mineral origin. Artificial waxes are designated by waxes that are chemically modified (semisynthetic) or synthetic. The latter happen when they are built up on a short-chain, non-waxy molecule or by decomposition of a macro-molecular plastic.

Waxes used in this work are synthetic waxes. Polyethylene waxes (PEW) are non-polar, manufactured by low-pressure polymerization. This process is capable of producing both non-branched, hard higher density and lower density branched PEWs. Depending on their compatibility with plastics, polyethylene waxes are widely used as lubricants and as carrier

material for pigment concentrates or as a matting agent for paints. Their hardness makes them a preferred anti-abrasive agent in printing inks.

PEW1 is a high molecular weight and high density polyethylene wax, in such way that has a melt viscosity of about 25 Pa.s. PEW2 is a low density polyethylene wax, having a lower melt viscosity of about 650 mPa.s. Both waxes structures are sequences of methylene units, therefore these material are non-polar. Oxidized polyethylene wax (OPEW) is produced by oxidizing polyethylene wax. This results in a polar molecular chain.

Stearic and oleic acids

Stearic acid (IUPAC systematic name: octadecanoic acid) and oleic acid (9-octadecenoic acid) are fatty acids, i.e., carboxylic acids with a long unbranched aliphatic chain (tail) (Figure 3.8), which is either saturated or unsaturated. Saturated fatty acids, as stearic acid, do not contain any double bonds or other functional groups along the chain. The term "saturated" refers to hydrogen, because all carbons (apart from the carboxylic acid group) contain as many hydrogens as possible. On the other side, unsaturated fatty acids are of similar form, except that one or more alkenyl functional groups exist along the chain. This originates configurational isomers, in which the oleic acid is the cis-9-octadecenoic acid, as in illustrated in Figure 3.8. Most fatty acids in the trans configuration are not found in nature and are the result of human processing (e.g. hydrogenation) [203].

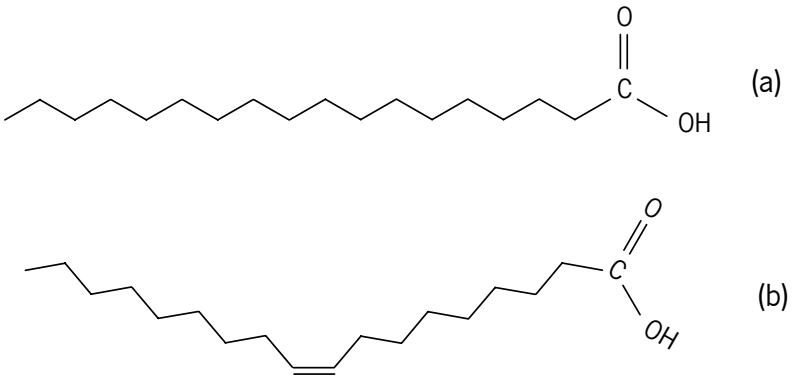

Figure 3.8 Chemical structure of stearic (a) and oleic (b) acids.

Industrially, fatty acids are produced by the hydrolysis or alcoholysis of the ester linkages in a fat of biological oil (both of which are triglycerides), with the removal of glycerol. The fatty acid or fatty esters produced by these methods may be transformed further through hydrogenation to convert unsaturated fatty acids into saturated fatty acids.

Both stearic and oleic acid have a long non-polar hydrocarbon chain and an ending polar acid group. This particular feature gives simultaneously two behaviours, one hydrophobic tail which has affinity to other neutral molecules and non-polar solvents, and one hydrophilic head capable of hydrogen bonding, enabling it to dissolve more readily in water than in oil or other hydrophobic solvents.

The unequal charge-behaviour characteristic is the base why fatty acids, mostly stearic acid, are most widely used materials industry of filled plastics. They are used to coat the filler particles, thereby creating a chemical bridge between the filler and the matrix. The polar group tend to anchor on the surface of the filler particle, in such a way that a layer of molecule covers interface. The tail is introduced in non-polar polymeric matrix. This mechanism increases wettability of polymeric matrix, reducing melt viscosity and making possible to raise fractions in compounds [175]. The mechanical strength of composites can be enhanced by coating the filler. They also facilitate processing and lower the water adsorption of the composites produced [204].

3.1.2. Powder properties

Particle size

The particle size distribution was determined by laser light scattering. This method is based on the principle of the light scattering when a beam of radiation is interrupted by the presence of a particle. For the particle size determination it was used a Coulter LS 230 analyser which uses the Fraunhofer and Lorentz-Mie theories for the mathematical modelling and the PIDS system (Polarization Intensity Differential Scattering), patented by Coulter, in such a way that it is able to measure in the size range of 0.04 μm to 2000 μm. Particles, while suspended in a slurry, are pumped in front of a laser beam. From the angle and intensity of the diffracted beams, the particle size distribution is calculated [195, 205].

A powder sample was previously dried in an oven at 105 °C for 2 hours and cooled in a desiccator at room temperature. It was prepared a low concentrated slurry with the powder and let it in ultrasounds for 5 minutes.

The characteristic parameters of the distribution are the mean value and the cumulative undersize D_{10}, D_{50} and D_{90}. Another measure of the size range is the distribution slope parameter S_w, defined as

$$S_W = \frac{2.56}{\log_{10}(D_{90}) - \log_{10}(D_{10})} \quad (3.1)$$

where the numerator represents the fact that 10 and 90 % are 2.56 standard deviation apart on a Gaussian distribution. The median particle size, D_{50}, and the distribution slope, S_w, provide important measures of a powder [1]. The latter is the slope of the log-normal cumulative distribution. Large values of S_w correspond to narrow particle size distribution and small values correspond to broad distribution. This parameter is similar to the coefficient of variation or standard variation.

The particle size distribution of the powder is shown in Figure 3.9. Table 3.1 presents the distribution parameters.

Particle morphology

Particle morphology was analysed by scanning electron microscopy (SEM), which uses electrons rather than light to form an image, having many advantages to use instead of a light microscope. The combination of higher magnification, larger depth of focus, greater resolution, and ease of sample observation makes SEM one of the most heavily used instruments.

SEM images were obtained using a FEG-SEM Hitachi S4100 microscope. A powder sample was dispersed on a carbon adhesive tape sticked on the sample holder and analysis microscopy observation was performed operating at 25 kV. Figures 3.10 and 3.11 show two micrographs allowing to observe the morphology of the stainless steel particles.

Real density

The real density of the powder was determined by gas picnometry. Gas picnometry is a method for the determination of volume and density by measuring the pressure change of the gas, in this case helium, in a calibrated volume. It was used a Micromeritics AccuPyc 1330 pycnometer with a standard sample holder of 10 cm^3.

Before performing the analysis, the equipment was let stabilized for 2 hours, as well as the helium pressure, set at 0.15 MPa. In each measurement set, it was carried a blank test with the sample chamber empty in order to verify the accuracy state of the equipment. If not, calibration is performed. A powder sample was previously dried in a oven at 105 °C for 2 hours and cooled in a desiccator at room temperature. A known weight sample is loaded into the sample cup, filling at least two-thirds of chamber volume. The sample is loaded into the equipment chamber cell and the test is started [206]. The pycnometer determines the volume and, with the sample weight, calculates the density. Each measurement set is programmed for 10 repetitions, so that an average value is obtained. Measurement results are shown in Table 3.2.

Apparent and tap densities

The method for the determination of the apparent density and tap density was based on the measurement of the mass of a known volume of powder [207]. The test was carried out using the following procedure: drying of the sample in the oven at 105 °C for 2 hours and cooling in a desiccator at room temperature, passing the dried sample trough a 0.5 mm sieve and transferring it to a graduated 1000 cm^3 measuring cylinder, in such way that no air pockets were entrapped. The apparent density was calculated with the mass of the filled powder. Then, placing of the cylinder in a rubber-covered table and taping it manually in steps of approximately 1250 revolutions until the difference between two successive steps of taping is less than 2 cm^3. The tap density was calculated by the mass and the volume after tapping. Table 3.2 shows the results.

Elemental chemical composition

a) X-ray fluorescence (XRF) spectroscopy

The concentration of the elements Fe, Cr, Ni, Mn, Mo, Si and P was measured by The analysis X-ray spectroscopy. This method is based on the fact that chemical elements emit characteristic radiations when subjected to appropriate excitation. Fluorescence is the emission of characteristic (or fluorescent) X-rays from a material that has been excited by bombarding with high-energy X-rays or gamma rays. When a primary X-ray source interacts with a sample material, the X-ray can either be absorbed by the atom or scattered through the material. Absorbed X-rays displace inner shell electrons of the atoms, creating vacancies. These vacancies present an unstable condition for the atom. As the atom returns to its stable condition, electrons from the outer shells are transferred to the inner shells and in the process giving off a characteristic x-ray whose energy is the difference between the two binding energies of the corresponding shells. Since each element has electrons with more or less unique energy levels, the wavelength of light emitted is characteristic of the element. And the intensity of light emitted is proportional to the elements concentration [208].

A Phillips Analytical X-UNIQUE II WD-XRF (wavelength-dispersive) spectrometer was used. The sample was prepared by compaction of 8 g of the stainless steel powder in a 30 mm diameter die at 15 MPa. Analysis was repeated with two more powder samples and the average of the concentration results were was computed.

b) Oxygen and nitrogen determination by inert gas fusion

A Leco model TC-136 analyser was used. The principle of operation is based on fusion of a sample in a single-use high-purity graphite crucible, under a flowing helium atmosphere at a temperature sufficient to release oxygen and nitrogen present in the sample. The oxygen will react with the carbon from the crucible to form carbon monoxide (CO); nitrogen is released as molecular nitrogen (N_2). The gases concentration in the inert gas stream is determined downstream: oxygen is detected either as carbon dioxide (CO_2), CO or both, using infrared (IR) detection; nitrogen is determined using a thermal-conductivity (TC) cell [209].

Procedure was carried as following:

- Calibration: Instrument was verified with standard samples (weighed to the nearest 1 mg) with known oxygen and nitrogen concentrations. The objective is to compare de

standard concentrations with the instrument measurements. In presence of deviation in the accuracy, an adjustment is performed.

- Analysis: A powder sample of about 1 g, weighed to the nearest 1 mg, was transferred to the instrument sample loading device. A crucible was placed on the furnace pedestal and the pedestal was raised into position. The instrument is run and the fusion procedure in done automatically.

  Concentration is calculated with the instrument calibration curve, corresponding the detectors signal intensity with the O and N concentration. Measurement results must be inside the instrument calibration range. If not, the analysis is repeated using a decreased or increased sample amount if the result was above or lowers that interval, respectively.

Once the result was inside the calibration, the measurements were repeated and the average was taken.

c) Carbon and sulphur determination by high-temperature combustion

A Leco model CS-200 analyser was used. The sample is poured in a ceramic crucible and inserted into a high frequency (HF) induction heated furnace, capable of attaining 1370 to 1425 °C. In the combustion furnace, oxygen is used to flood the chamber. The combination of a heated environment and abundant oxygen causes the sample to combust. The carbon in the sample is oxidized to carbon dioxide (CO_2) while the sulphur is converted to sulphur dioxide (SO_2). The released gases pass through a series of traps, absorbers, and converters to remove interfering elements and ensure that the gases have the proper structure for detection. Detection of the resulting gases is most commonly provided by infrared detectors. The signal is processed electronically to provide a percentage of carbon or sulfur by specimen weight [209].

The calibration and analysis procedures were similar to early oxygen and nitrogen determination.

The elemental composition of the stainless steel powder is shown in Table 3.3.

Summary of powder properties

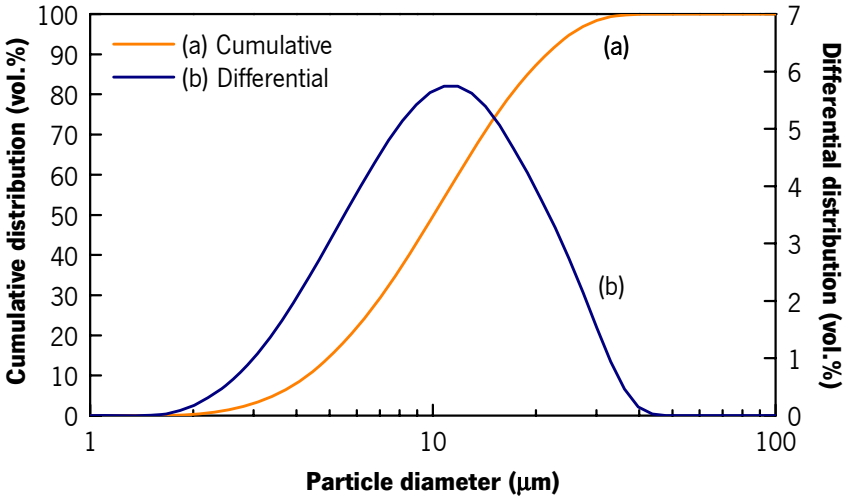

Figure 3.9 Particle size distribution of the 316L stainless steel powder.

Table 3.1 Particle size distribution parameters.

Parameter	Value
Mean	12.2 μm
D_{10}	4.7 μm
D_{50}	11.1 μm
D_{90}	23.6 μm
S_W	3.7

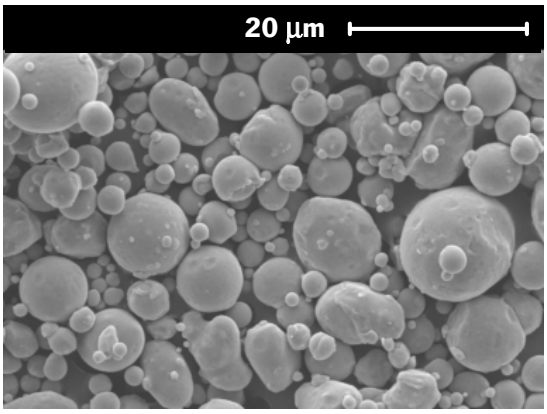

Figure 3.10 Micrograph of the powder (magnification: 2K x).

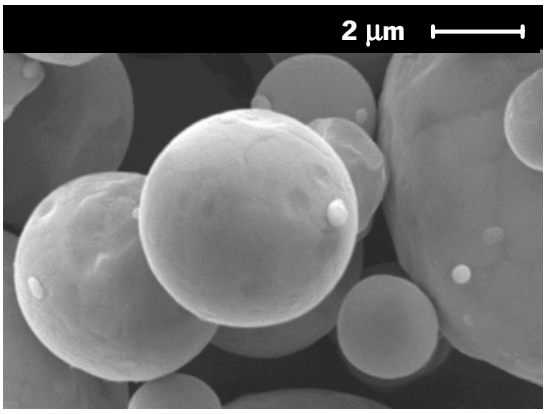

Figure 3.11 Micrograph of the powder (magnification:10K x).

Table 3.2 Densities of the powder.

Density	Value ($g.cm^{-3}$)	% of Real
Real	7.925	-
Apparent	3.3	42 %
Tap	4.5	57 %

Table 3.3 Elemental composition of powder

Element	Fe	Cr	Ni	Mn	Mo	Si	S	C	P	N	O
%(w/w)	68.6	16.7	10.1	1.30	2.62	0.40	0.011	0.02	0.02	0.097	0.124

German has resumed a list of properties of a powder which can be considered the ideal [1]. The particle size of the 316L stainless steel powder analysed is deviated to thickers comparing to the ideal size. Despite of this, D_{50} is closed to the range 4 – 8 μm and size distribution closed to the limits 0.5 and 20 μm. This thinner powder promotes the sintering process. A good packing capacity evidenced by tap density (over 50% of real) and a relative wide particle size distribution shown by S_w = 3.7 can anticipate the capacity to produce high solids fraction feedstocks from this powder. Powder particles have spherical shape which can drive to problems of shape retention during debinding and sintering caused by a lack of interparticle friction. In other way, feedstock melt flow is facilitated by introducing spheres.

Balancing the powder characteristics, it is shown the suitability of this 316L powder for PIM. However, some caution should be considered for the debinding and sintering process because of the high sphericity of the powder particles.

3.1.3. Binder components properties

Density

Density was determined by gas picnometry, adopting the same procedure applied to the determination of the real density of the metal powder, as previously explained.

Thermal properties

The thermal properties were determined by simultaneous thermal analysis (STA), performed in a Netzsch STA 449C Jupiter analyser. This thermal analyser is an equipment that works with two techniques of thermal analysis: differential scanning calorimetry (DSC) and thermogravimetry (TG).

Calorimetry is a technique for determining the quantity of heat that is either absorbed or released by a substance undergoing a physical or a chemical change. Such a change alters the internal energy of the substance, which at constant pressure, is known as enthalpy. Processes that increase enthalpy (endothermic) such as melting, evaporation or glass transition and those that lower it (exothermic), crystallisation, progressive curing and decomposition are analysed by calorimetry. Thermogravimetry (TG) measures the mass or change in mass of a sample as a function of temperature or time or both. Changes of mass occur during sublimation, evaporation, decomposition, and chemical reaction, magnetic or electrical transformations [210]. Both techniques are programmed with a thermal cycle, which can be defined by a combination of heating or cooling rate, temperature plateaus and an end temperature. Simultaneously, in a STA the heat flux and the mass variation are recorded along the cycle.

Table 3.4 presents two configurations of the equipment for the determination of the phase transition temperatures (melting, crystallisation and glass transition) and for the initial degradation temperature. In all samples analysis, correction curve was previously obtained running a test with the empty crucible, which was used for the respective sample analysis.

DSC tests were carried out under inert atmosphere, highly pure (99.999%) nitrogen in order to prevent reactions (oxidation) between the sample and the atmosphere. Two heating and cooling cycles were programmed because the first cycle reveals the thermal history of the material and the second one is used to determine the material characteristics. Since all materials were submitted to the same two cycles, those characteristics are comparable.

Melting and crystallisation processes were characterised by the melting and the crystallisation peak obtained in the DSC diagram, as it is illustrated in Figure 3.12. Peak temperature, or the temperature of the maximum peak,

was considered because it can assure higher reproducibility. Glass transition temperature was determined as the midpoint temperature, i.e. the arithmetical mean from the extrapolated onset and end temperatures of the glass transition, as exemplified in Table 3.13.

Initial degradation temperature was defined as the temperature at which a weight loss of 1% occurs, determined by TG as it is illustrated in Figure 3.14. In this case, the objective was to estimate the maximum processing temperature for the materials with non-inert environment, therefore the tests were performed in air.

Table 3.4 Experimental conditions of STA according to the properties analysed.

	Configuration 1	**Configuration 2**
Properties analysed	Phase transition temperatures /DSC	Degradation temperature /TG
Atmosphere	Dynamic Nitrogen 50 Ncm^3/min 0.15 MPa	Static Air
Thermal cycle	1. Heating at 3 °C/min to 160 °C 2. Cooling at 3 °C/min to 20 °C 3. Stage at 20 °C for 15 minutes 4. Heating at 3 °C/min to 160 °C 5. Cooling at 3 °C /min to 20 °C	1. Heating at 10 °C/min to 1000 °C

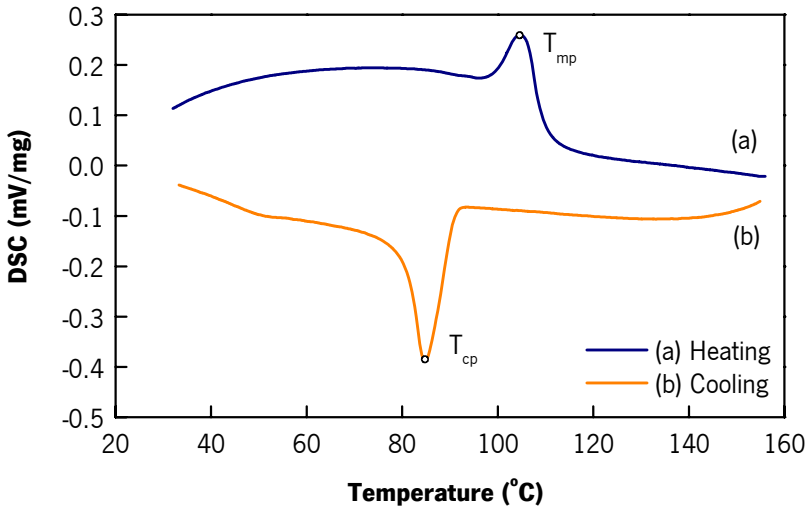

Figure 3.12 Definition of the melting peak temperature (T_{mp}) and the crystallisation peak temperature (T_{cp}) in a DSC diagram.

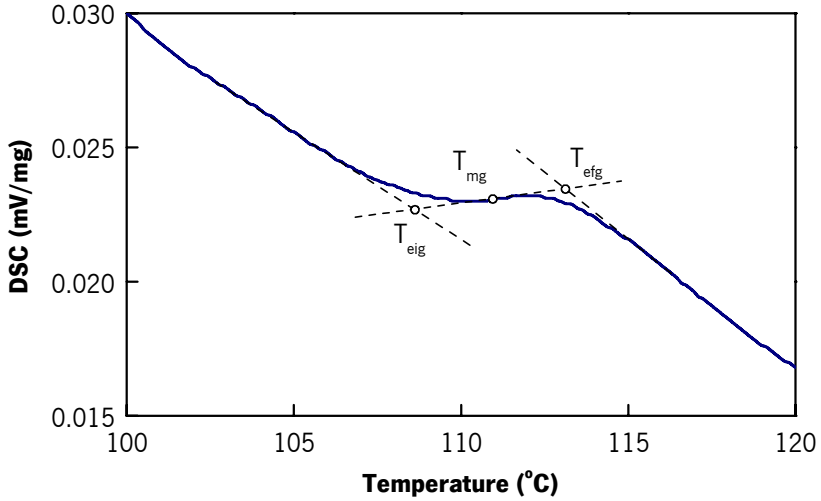

Figure 3.13 Determination of the midpoint glass transition temperature (T_{mg}) from a DSC curve, derived from the extrapolated onset temperature (T_{eig}) and the extrapolated end temperature (T_{efg}).

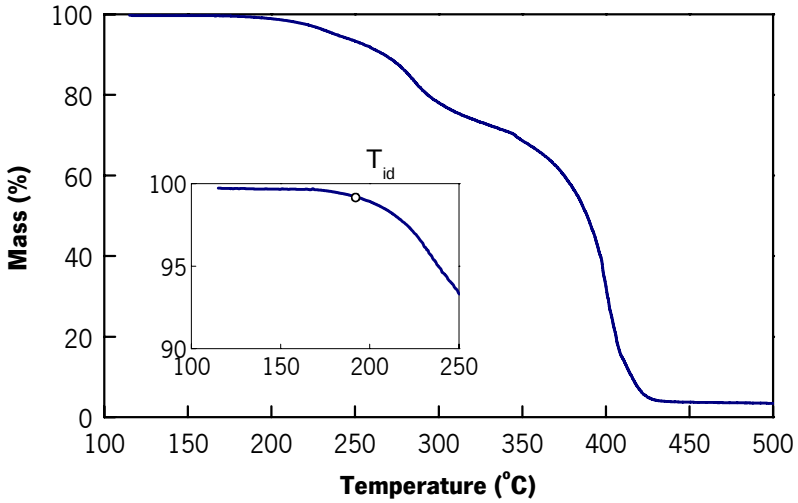

Figure 3.14 Example of the determination of the initial degradation temperature (T_{id}) from a TG curve, as the temperature at which a weight loss of 1 % occurs.

Summary of binder component properties

Table 3.5 presents the properties measured of the materials for binder composition and some complementary information, namely the chemical structure and the average molar mass. This latter is typical information obtained from the material producers.

Table 3.5 Properties of the polymers, waxes and additives.

Material	Chemical Structure	M (*) (g/mol)	ρ (g/cm³)	$T_{m,p}$ (°C)	$T_{c,p}$ (°C)	T_g (°C)	T_{id} (°C)
PEG	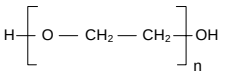	M_n = 7000-9000	1.222	68	40	n.d.	198
LDPE	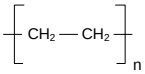	$M_w \approx 160\,000$ $M_n \approx 12\,000$	0.915	105	85	n.d.	265
MPE	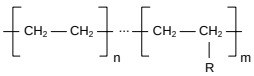	M_n = 20 000 – 25 000	0.901	97	77	n.d.	276
PMMA	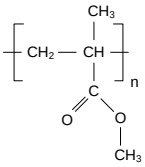	≈ 95 000	1.198	-	-	117	275
PVB	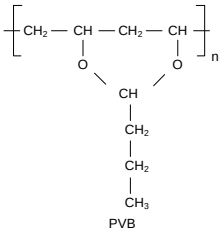	M_w = 57 000	1.140	-	-	150	273
PEW1	-$(CH_2CH_2)_n$-	≈ 9000	0.962	128	109	-	257
PEW2	-$(CH_2CH_2)_n$-	≈ 2000	0.918	114	100	-	257
OPEW	-CH_2- (O)		0.980	125	107	-	250
SA	$CH_3(CH_2)_{16}COOH$	284	0.845	69	-	-	212
OA	$CH_3(CH_2)_7CHCH(CH_2)_7COOH$	282	0.891	13	-	-	196

(*) Source: product data sheets and support literature from manufacturers.

3.2. Compounding and characterisation of binders and feedstocks

3.2.1. Binders preparation

Binder formulations were planned based on ten materials, whose compositions are shown in Table 3.6. The water soluble component, PEG had a constant concentration in all binders. LDPE, MPE, PMMA and PVB are back-bone polymers that were at 25 % by weight. In some binders they were reduced to 17.5 % and a lubricant at 7.5 % was added.

First twelve binders represent a 2 x 3 x 2 experimental plan, with 2 back-bone polymer (LDPE and MPE), 3 lubrication conditions (PEW1, PEW2 and none) and 2 surfactants (SA and OA). By using this plan, it was aimed to analyse the effect of the polyethylenes, the use of different waxes or no lubricant, and, the use of different surfactants. Binders L-13 and L-16 have amorphous back-bone polymers, in contrast to L-05 and L-11. L-15 shall give information about the possibility of use a polyethylene wax instead of polymers. L-14 makes possible to study the effect

Table 3.6 Binder compositions plan.

Binder	PEG	LDPE	MPE	PMMA	PVB	PEW1	PEW2	OPEW	SA	OA
L-01	70	17.5				7.5			5	
L-02	70	17.5				7.5				5
L-03	70	17.5					7.5		5	
L-04	70	17.5					7.5			5
L-05	70	25							5	
L-06	70	25								5
L-07	70		17.5			7.5			5	
L-08	70		17.5			7.5				5
L-09	70		17.5				7.5		5	
L-10	70		17.5				7.5			5
L-11	70		25						5	
L-12	70		25							5
L-13	70			25					5	
L-14	70							25	5	
L-15	70						25		5	
L-16	70				25				5	

of the polarity of OPEW in contrast to the non-polarity of the remaining waxes and polyethylenes.

Binders were prepared by stirring with a laboratory apparatus as illustrated in Figure 3.15. The binder constituents were loaded into a 250 cm^3 glass cup, heated by a hot plate. Melt was stirred by a vertical axis impeller with four paddles. Temperature was set in a controller with a Pt100 thermoresistor and the hot plate.

Table 3.7 shows the mixing conditions for the binder preparation. The temperature controller was not tuned, in this way an oscillation of about ± 5 °C occurred; this was considered not critical for this process. The mixture appearance was followed and the mixing time was set when no more changes during a period of 15 minutes were observed. Almost melts appeared to be a dispersion of tiny bubbles in a liquid medium, this latter suspected to be an enriched PEG phase, since it was the major fraction constituent of the formulations. Photography was tried but those heterogeneous melt blends were not perceptible. Binders L-13 and L-16, formulated with

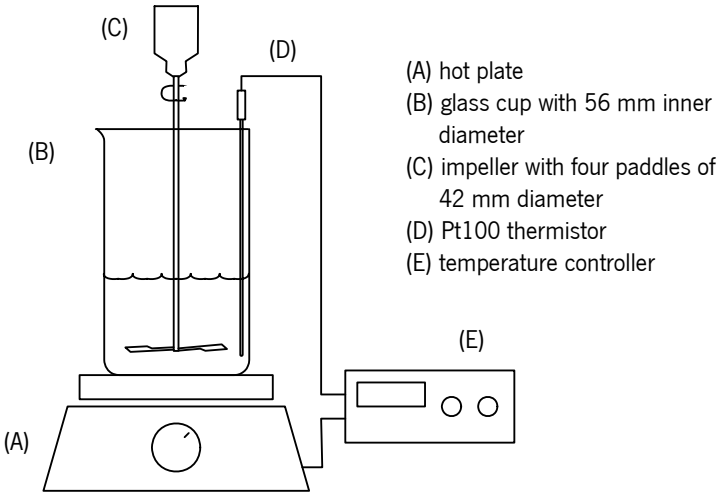

Figure 3.15 Apparatus for the preparation of the binder formulations.

Table 3.7 Binder mixing conditions.

Set-point temperature	155 °C
Mixer rotation speed	800 min^{-1}
Mixing time	30 min. or 8 hours *

* mixing time for formulations L-13 and L-16 was 8 hours.

amorphous polymer, needed much more time to be mixed (8 hours). At the end, a homogeneous melt was obtained presenting a yellowed colour, probably due to oxidation, and transparency.

3.2.2. Calorimetric analysis

Compatibility of binder components was determined by the analysis of the melting points depression, comparing the binder mixture to the pure components. Melting points were determined by the same technique used for the pure components, i.e., by DSC in Netzsch STA 449C Jupiter analyser.

The analysis was performed with the binder samples prepared with the procedure described on section 3.2.1. Samples were fragmented and, in order to make reproducible samples, the oversized particles were removed by sieving at 1 mm. Thermal cycle was the same as to the pure materials characterisation: heating at 3 °C/min to 160 °C and cooling to 20°C; pause for 15 min. and repeat the heating and cooling profile; dynamic atmosphere of 50 Ncm^3/min nitrogen 99.999 % pure. Correction curve was obtained by running a test with the empty crucible, which was used for the sample analysis.

3.2.3. Mixing torque rheometry

Critical solids fraction was determined by torque rheometry. This technique has been widely used for this purpose, although exists some variation in the procedures and data analysis [46, 55, 58, 162, 163, 211-215]. It was applied the method of the analysis of the mixing torque curves of separate formulations. With this method, the critical solids fraction is the value of the concentration from which it is more difficult to reach the steady state or is produced a noisy torque curve. At this point and at higher fractions, the homogeneity of the mixture is lost, the binder quantity is insufficient to promote the flow and the feedstock loses moldability.

A Brabender Plastograph EC rheometer was used. The working principle is based on the drag force imposed by the mixture when is running a mixing process in a chamber equipped with rotors. A dynamometer is coupled in the rotors axis and the torque is measured continuously and recorded along the time. Plastographs are electronic torque rheometers mostly used for testing

the quality and processability of thermoplastics, thermosets, elastomers, ceramic moulding materials, filters, pigments and other plastic materials [216]. Plastograph EC was setup with a mixing chamber of ca. 55 cm^3 and two counter-rotating W-shaped blades rotating at different speeds (3:2 ratio).

In the first use of the day, set-point temperature was set and let homogenise within the steel walls for 30 minutes. Test began by calibration the dynamometer with the blades running in the empty chamber. After, test was started and materials were introduced inside. First, it was introduced the binder and let the chamber temperature reach at least 10 °C below the set-point temperature. Then, powder was added stepwise in order to soften the temperature profile. The torque was recorded continuously as a function of time using the computerized data acquisition system. Runs were carried at the operation conditions shown in Table 3.8.

Mixing batches of different solids fractions were carried out in an iterative method. The first run was with ϕ = 65%, then following mixing iterations were done by increasing the fraction. In each mixing batch, the torque profile was evaluated in order to find out the fraction value at which it was visible a transition from a stable mixing torque to a non homogeneous and unstable profile. CPVC was defined by the maximum solids fraction which provided a mixing stability.

3.2.4. Cappilary rheometry

Cappilary rheometers are the most used devices to study PIM feedstock rheology, since it provides shear rates in the range of injection moulding. Melt is sheared at different rates along a moulding cycle, typically a range 10^2 to 10^5 s^{-1} [1]. Low shears are experienced in barrel, runners and in the cavity larger channels and high shears are encountered in the nozzle, mould gates and cavity thinner channels.

Table 3.8 Torque rheometry conditions.

Set-point temperature	155 °C
Blades speed	150:100 min^{-1}
Mixture volume	38.5 cm^3
Mixing time	20 min.

In a capillary rheometer (shown in Figure 3.16) the melt is forced through a capillary tube by the movement of a piston activated by a superimposed pressure. The melt is extruded at either a constant stress or constant strain, usually the last one. The shear stress can be quantified by a force balance over the volume of the fluid cylinder in the capillary, having a maximum value near the wall and null in the centre. Wall shear stress, τ (Pa.s), is expressed as:

$$\tau = \frac{r\,\Delta P}{2\,L} \tag{3.2}$$

where ΔP is the pressure drop in the capillary (Pa) determined with a transducer in the entrance of the capillary, r is the radius of the capillary (m) and L its length (m). The wall apparent shear rate is calculated by the following equation:

$$\dot{\gamma}_{ap} = \frac{4\,Q}{\pi\,r^3} \tag{3.3}$$

where $\dot{\gamma}_{ap}$ is the apparent shear rate (s^{-1}) and Q is the flow rate ($m^3.s^{-1}$).

Because the piston moves at a constant speed, the crosshead speed is a direct measure of the shear rate. The apparent viscosity thus can be calculated as the ratio of the shear stress to the

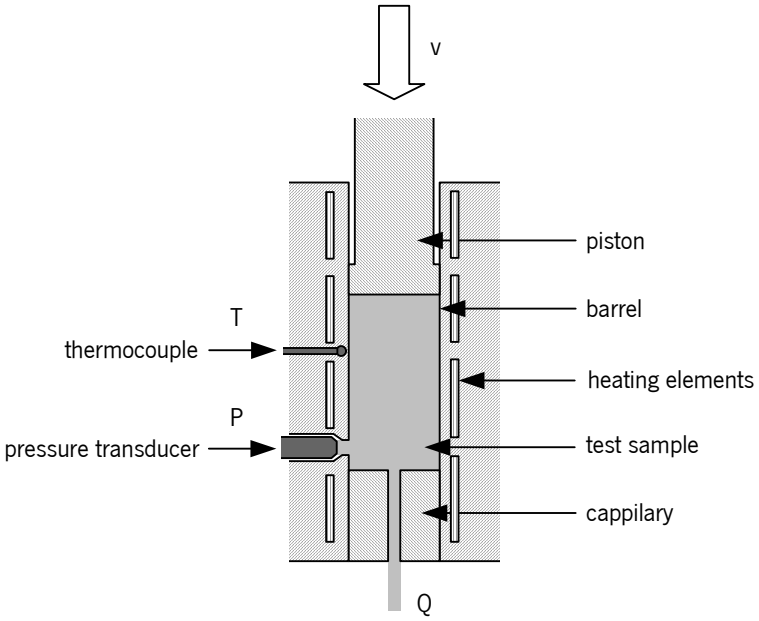

Figure 3.16 Schematic diagram of a capillary rheometer.

shear rate:

$$\eta_{ap} = \frac{\tau}{\dot{\gamma}_{ap}} = \frac{r^4 \Delta P}{8 L R^2 v} \quad (3.4)$$

where η_{ap} is the apparent viscosity (Pa.s), R is the barrel radius (m) and v is the piston speed (m.s^{-1}). The above expression is based on Newtonian flow behaviour. For shear-thinning fluid that follows the power-law behaviour, it must be applied the Rabinowitsch correction to calculate the shear rate at the capillary wall:

$$\dot{\gamma} = \frac{3n+1}{4n} \dot{\gamma}_{ap} \quad (3.5)$$

where $\dot{\gamma}$ is the shear rate (s^{-1}) and n is the index of the power-law expressions (Eqs. 2.1 e 2.2). The determination of a flow curve, shear stress vs. shear rate, thus needs the measurement of the pressure drop in the capillary for different piston speeds. Therefore, with a capillary rheometer one can measure the pressure drop between the beginning of the entrance and the exit of the capillary, i.e., the relative pressure measured by a pressure transducer, with different piston speed, directly related to the shear rate in the capillary, at a constant set temperature.

In capillary rheometers, since the pressure measurement is done upstream the capillary, there is a pressure drop due to entrance effects. So, the pressure drop along the capillary is lower than the measured. Bagley correction is done to determine the pressure drop due to the energy loss in the entrance. Experimental efforts are multiplied, as an example, by three to get data with three different L/D capillaries, in order to apply this correction. Therefore, usually one uses high L/D capillary in order to reduce the relative significance of the entrance pressure drop comparatively to the pressure loss along the capillary. For this purpose, in this work it was used a capillary with L/D=30, which has been the minimum recommended to eliminate the need for correction [217].

A Thermo-Haake Rheoflixer HT rheometer was used. This device has temperature PID control loops, which provides a temperature stability of ± 0.5 °C, measured by two thermocouples. Capillaries were manufactured in hard metal to minimise wear using high filled compounds.

Feedstocks were prepared from binders, previously blended according to the procedure described on section 3.2.1, and 316L stainless powder with solids fraction of 66 vol.% (

Table 3.9 Feedstock mixtures coding.

Feedstock code	Binder code	ϕ (vol.%)	Feedstock code	Binder code	ϕ (vol.%)
F-01-66	L-01	66	F-09-66	L-09	66
F-02-66	L-02	66	F-10-66	L-10	66
F-03-66	L-03	66	F-13-66	L-13	66
F-04-66	L-04	66	F-15-66	L-15	66
F-07-66	L-07	66	F-16-66	L-16	66
F-08-66	L-08	66			

Table 3.10 Operation conditions for feedstock mixing and rheometry.

Mixing		Rheometry	
Temperature	140 °C	Temperature	155 °C
Blades speed	105:70 min^{-1}	Melting time	5 min.
Time	20 min.	Capillary L/D	30/1 mm
		Shear rates	500, 1000, 2000 5000, 10 000 s^{-1}

Table **3.9**), using the Plastograph mixer with the operation conditions shown in Table 3.10. Rheometry tests were executed under the conditions shown in the same table. Two filled barrels were used to complete a five flow rates run. Each test was three replicated and the flow curve was calculated from the average viscosity in each point.

Shear stress vs. apparent shear rate data was obtained from the rheometer PC software. The parameter *n* was determined from a linear fitting based on the logarithm of the equation 3.6, substituted by equation 3.5, obtaining the following expression:

$$\log(\tau) = \log\left[k_0\left(\frac{3n+1}{4n}\right)\right] + n\log(\dot{\gamma}_{ap}) \qquad (3.6)$$

Therefore, *n* is the slope of the plot of log(τ) vs. log($\dot{\gamma}_{ap}$).

3.2.5. Preparation of moulded parts

Disc-shaped moulded samples were prepared using a Moore heated-plates press, in a process illustrated in Figure 3.17. Extruded materials resulted from the capillary rheometry test were granulated and used in this experiment. Mould was composed by three brass pieces: a die plate of 2 mm thick with a hole of 30 mm diameter; a lower plate which holds the die and an upper plate that cover the die. The mould was loaded with granulated feedstock. After the press plates stabilised at 155 °C, the mould was putted in the press. It was heated by conduction from the heated plates for 3 minutes. Then, press was closed and 20 N force was applied. This force was defined to assure a complete mould closing. After 3 minutes, the press was cooled and parts extracted. This task turned out to be a problem since just a few samples were extracted without breaking on the edges. In order to standardise the dimensions, the samples were cut into a parallelepiped form with dimensions of about 13 x 13 x 2 mm.

3.2.6. Scanning electron microscopy

The microstructure of the powder-binder mixtures were observed by scanning electron microscopy (SEM).

Samples of about 3 x 3 x 2 mm were obtained by fracture of the press moulded specimens; the fracture surface with 3 x 2 mm was considered for SEM observation. They were settled on an aluminium sample holder using a carbon suspension adhesive. Since there is a non-conductive phase (binder), the conductivity of samples was improved by coating with a thin layer of carbon

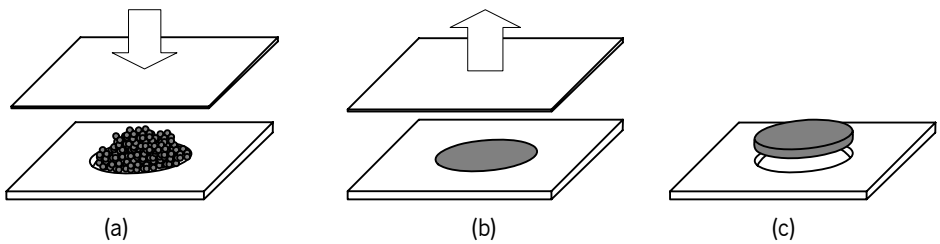

Figure 3.17 Schematic description of the steps of hot press moulding process: (a) granulate loading and pressing, (b) mould opening and (c) part extraction.

in an Emitech K950 evaporator. SEM images were obtained using a FEG-SEM Hitachi S4100 microscope operating at 25 kV.

3.2.7. Water extraction

The objective was to determine the weight loss of moulded parts along the water extraction process. The aim was to compare the extraction rate of moulded parts produced from different binder formulations, so, for such comparison, it was considered credible to use press moulded parts instead of injection moulded parts, since it has lower effort and consumes less material.

Press moulded parallelepipeds were grouped in batches, according to the scheme presented in Table 3.11, in order to perform the extraction process in a reasonable low concentration of material in the bathes. The objective was to minimize the concentration of the soluble binder component in solution to avoid effects on the mass transfer kinetics. Maximum concentration was recorded of 8.9 g of parts per cubic decimetre of water in the first batch. Three batches were carried under the conditions shown in Table 3.12. At starting time, all parts were immersed, standing on a stainless steel grid. Then, when the planned immersion time was reach, parts were taken from the water.

Table 3.11 Composition of the batches for water extraction; four parts, corresponding to different immersion time, of each feedstock.

Part no.	Immersion time	Batch 1	Batch 2	Batch 3
1	0.5 h	F-01-66	F-07-66	F-13-66
2	1 h	F-02-66	F-08-66	F-15-66
3	3 h	F-03-66	F-09-66	F-16-66
4	6 h	F-04-66	F-10-66	

Table 3.12 Water extraction conditions.

Solvent	Demineralised water
Temperature	50 °C
Volume of solvent	3.5 dm^3

After extraction, parts were dried in an oven at 50 °C along the night, about 16 hours. The mass weighing before and after extraction was executed to determine the removal of binder for different immersion periods in each feedstock.

3.2.8. Thermogravimetry

Thermal debinding of water-brown parts produced with the feedstock formulated from the binders in study was predicted by thermogravimetric analyses. This technique gives the amount of weight changes along a programmed temperature cycle. Therefore, one can obtain the weight loss of a water extracted part due to thermal degradation of the remaining binder and analyse the profile of degradation reaction along a temperature scan.

Samples were taken from the water debound parts with an immersion time of 6 hours, by sectioning of the central volume, according to the Figure 3.18. A Netzsch STA 449C Jupiter analyser was used for the TGA analysis. Weight calibration was performed in each test run with an empty crucible. This crucible was loaded with the parallelepiped sample and test started. The experiments were carried out under a dynamic atmosphere of argon 42 $Ncm^3.min^{-1}$, to prevent oxidation of powder particles, at a rate of 10 °$C.min^{-1}$ to 800 °C. In calibration and samples testing, heating chamber was purged three times, with vacuum and gas admission cycles, in order to remove the air inside and avoid oxidation by oxygen adsorbed on walls. TGA was linked to a PC with data acquisition software, which supplied net weight loss curve over the temperature ramp.

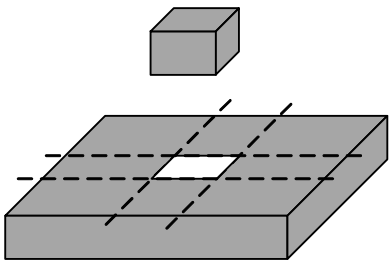

Figure 3.18 Cutting scheme for the preparation of TG samples (3 x3 x 2 mm), from the water debound parts (13 x 13 x 2 mm).

3.3. Process tools, conditions and procedures

3.3.1. Compounding

Compounding compositions are shown in Table 3.13. For comparison of the process and final parts properties, feedstock preparation was carried out with the solids concentration and the compounding conditions constant. An exception was the binder mixing time, as PMMA and PVB needed a longer time to make a homogeneous binder blend.

Compounding was performed in three steps:

- binder preparation in a high speed stirrer,
- feedstock mixing in a batch kneader and
- feedstock homogenisation and granulation.

Binders were prepared in the same stirring apparatus used in section 3.2.1. But now, a 500 cm^3 glass cup was used, providing a mixing capacity of about 350 g. With such amount of melt and an adequate distance of the impeller from the bottom, a high mixer speed was possible to set since the vortex at the surface was not enough to introduce air bubbles into the blend. Table 3.14 shows the mixing conditions. Afterwards, the melting binder was poured out into a stainless steel tray and let cool down at room temperature.

The first stage of feedstock production was done in a Coperion kneading machine type LUK 8,0 K2. This kneader has a 12 dm^3 bowl with two "Z"-shaped blades which rotates at different speeds in opposite directions. In order to heat and cool the compound, the bowl has a jacket

Table 3.13 Composition of the processed feedstocks.

Feedstock	FS-03-66	FS-09-66	FS-13-66	FS-16-66
Binder	L-03	L-09	L-13	L-16
Binder composition (wt.%)	PEG:70 LDPE: 17.5 PEW2: 7.5 SA: 5	PEG: 70 MPE: 17.5 PEW2: 7.5 SA: 5	PEG: 70 PMMA: 25 SA: 5	PEG: 70 PVB: 25 SA: 5
Solids fraction (vol.%)	66	66	66	66

Table 3.14 Binder mixing conditions.

Set-point temperature	155 °C
Mixer rotation speed	2000 min^{-1}
Mixing time	L-03 and L-09: 1 h L-13 and L-16: 8 h

connected to external temperature controller, providing the circulation of thermal oil in the closed-circuit. The real temperature is measured directly inside the bowl with a thermocouple.

The mixing conditions are shown in Table 3.15. Bowl mixer was heated previously until reach the set-point. Pre-formulate binder was added and let to melt. Afterwards, after reaching the set-point again, the powder adding process was started. The powder was added in four equal portions. This intended to avoid drastic temperature drops, preventing the binder crystallisation. After the last portion added, the feedstock was kneaded for 1 hour. Blades speed was set on the maximum and a vacuum pump was working permanently to avoid air entrapment inside the feedstock mass. Feedstocks were cooled inside the mixer, with slow blade rotation, until a fine granulation was formed, ready to feed in the following stage.

Homogenisation and granulation was carried out in a Bellaform type BSW 135 shear roll compounder. This machine is composed of contra-rotating horizontal rolls with axial and shaped grooves. The different rotation speed and the grooves creates an intensive shear zone between

Table 3.15 Process parameters of feedstock compounding equipments.

Z-blade kneader	
Temperature	140 °C
Blades rotation speed	100 : 55 min^{-1}
Mixing time	1 h
Chamber relative pressure	-0.5 bar
Shear roll compounder	
Rolls temperature	50 to 90 °C
Rolls rotation speed	20 : 30 min^{-1}

the rolls, which gap is usually 0.5 mm. Each of both rolls has two temperature zones. This equipment is a continuous kneader, having a granulation system at the end of the rolls. Process conditions are presented in Table 3.15.

3.3.2. Feedstock evaluation

Verification of solids concentration

Solids concentration of the mixed feedstocks was evaluated by TG. It was used the Netzsch STA 449C Jupiter analyser. Weight calibration was performed in each test run with an empty crucible. The crucible was loaded with a feedstock pellet (ca. 240 mg) and test started. The experiments were carried under a dynamic atmosphere of argon 42 $Ncm^3.min^{-1}$, to prevent oxidation of powder particles, at a rate of 10 °C.min^{-1} to 800 °C. In calibration and samples testing, heating chamber was purged three times, with vacuum and gas admission cycles, to remove the air inside and avoid oxidation by oxygen adsorbed on walls.

At the end temperature, all the binder is thermally degraded and all reaction products escaped throw the gas flow. The solids concentration was designated as the percentage of remaining mass at 780 °C.

Assessment of the homogeneity

Homogeneity was evaluated by two methods: density and rheometry. These methods are complementary since they allow to determine the homogeneity in different scrutiny sizes. In the density method, it is evaluated the dispersion of the feedstock density in several random feedstock samples. In rheometry, it is analysed the viscosity fluctuation of a feedstock sample.

Six samples were randomly taken from a feedstock batch. The size of each sample was the necessary amount to fill the picnometer cell, about 25 grams of feedstock. Samples stayed for 24 hours in an exicator in order to remove potential moisture. Then, density was measured by helium picnometry, according to procedure described in section 3.1.1. Statistical analysis was made with the density data.

Reometry tests were performed with an amount of 120 grams of feedstock randomly taken from a production batch. This test is a common capillary rheology test programmed with only one shear rate, which occurs during a long time, the necessary to empty the barrel. During this time, the pressure drop in the capillary is recorded. As it is an indirect measure of the viscosity, the pressure fluctuation is equivalent to the variation of the viscosity of the sample. The test run at temperature 155 °C, shear rate 1000 s^{-1}, using a capillary of 30 mm length and 1 mm diameter. Pressure curve was obtained and a steady-state segment of 3 minutes long was considered for the statistical analysis.

3.3.3. Tooling

Cavity

One of the testing geometries was a tensile specimen for mechanical studies of powder injection moulding materials. Cavity design and dimensions for making tensile test specimens of sintered metal materials (excluding hard metals) are specified in the international standard ISO 2740 [218]. It includes the specifications for pressing and sintering, metal injection moulding and sintering and machining of sintered and powder forges materials. Tool cavity for MIM tensile test specimens type B was chosen (Figure 3.19). It has been proposed by the European workgroup EuroMIM Network, which was integrated in the European Powder Metallurgy Association [219]. The design is particularly considered for the powder injection moulding process, namely the round shapes to facilitate a stable flow and the absence of pins (producing fastening holes) to avoid weld lines.

The second testing geometry was a flexure mechanical bar. It was not found a standard of PIM bars. The most approaching standard designs were considered not to be adequate, since it is required thickness of sintered part of ca. 6 mm, i.e. a green thickness of ca. 7 mm which is not common in PIM and it will be needed extra experimental efforts for the debinding of such thick part. Therefore, the dimensions were decided based on common use in other published studies (Figure 3.20).

The tensile specimen cavity was obtained by two symmetric halves, by machining of two inserts mounted in both mould plates. Then, the parting-line is located in the symmetry plane of the part.

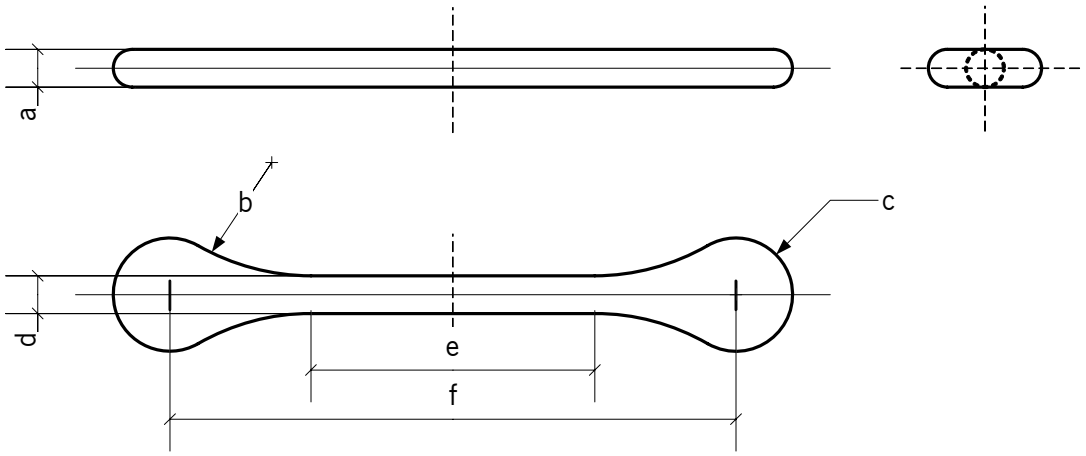

Dimension	Size (mm)	Tolerance (mm)	
a	5	- 0.02	+ 0.02
b	R30	- 0.1	+ 0.1
c	R7.5	- 0.1	+ 0.1
d	5	- 0.02	+ 0.02
e	37.6	0	+ 0.4
f	75	0	+ 0.5

Figure 3.19 Cavity drawing for moulding of tensile test specimens [218].

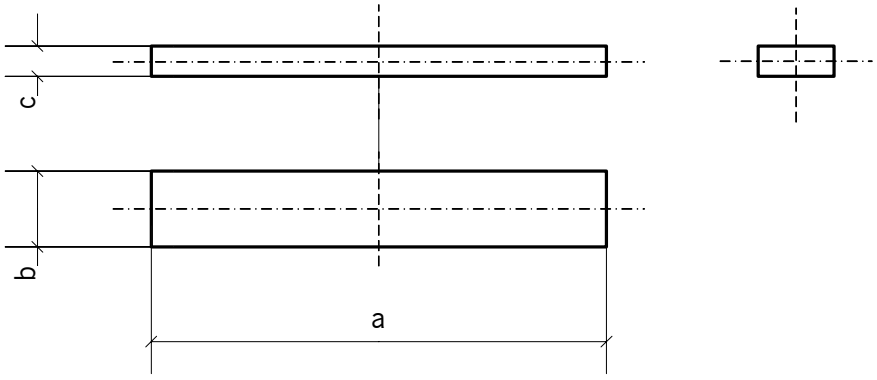

Dimension	Size (mm)	Tolerance (mm)	
a	60	- 0.2	+ 0.2
b	10	- 0.2	+ 0.2
c	4	- 0.2	+ 0.2

Figure 3.20 Mould cavity for the production of flexure test specimens.

The bar cavity was obtained by machining only the insert in the ejection plate, resulting a parting-line in a surface of the geometry (Figure 3.21). In latter, a tap angle of 2° in the four cavity side walls was introduced to facilitate parts ejection.

Ejection system and venting

Mechanical ejection of moulding was adopted, using 6 mm diameter ejection pins. Air evacuation out the cavity was aimed with venting channels machined in the ejection side with 5 mm wide and 0.1 mm deep, as detailed in drawings (c) and (d) of Figure 3.21.

Cavity feeding and gating

A tronco-conical sprue with a 2.5° taper was used to transport the melt to the runner system. A small cylinder, located opposite to the sprue having a negative ejection angle was designed to pulls the sprue and keeps the compact in the extraction plate when the tool opens for ejection.

A large section runner is desirable, which makes possible to increase flow rate without increase shear in order to avoid premature melt solidification. Typically, circular runners are adopted with a diameter in the 3 to 6 mm range [1]. In spite of a circular cross section is the most common and desirable shape for the runner, a lower expensive design was adopted. The runner had a half circle cross section with a radius of 5 mm, which is equivalent to a hydraulic diameter of approximately 6 mm.

Gate design is a critical issue in this shaping technology. It was placed in lateral position close to an end of the cavities, to avoid jetting, which is frequently in PIM [2, 73, 92, 220] (Figure 3.21). Geometry and size must minimize the mostly probable feedstock phase separation due to high shear rates experience in this narrow channel. Following the runner geometry, the gates had semi-circle section geometry with a relatively high radius – 1.5 mm.

Mould temperature control

Temperature control was performed by water channels inside the cavity inserts in both mould plated. The channels have 8 mm diameter and were designed according to Figure 3.21 (c) and (d). Water was pumped in close-circuit by an external temperature controller.

Mould material

Cavity material was an AISI H13 steel (DIN 1.2344). This material has a deep hardening response with very low distortion, high crack resistance, medium machining ease and medium wear resistance. It is recommended for powder injection moulding, especially for larger structures, intricate cavities, requiring high toughness and low wear [1]. A suitable wear resistance was achieved by heat treatment to 54 HRC.

Moulding surfaces (cavities, runners and sprue) were thin polished with diamond, following a common practice in PIM. This is a fundamental procedure to overcome the high mould surface adherence feedstocks. Polishing also avoids wear of these abrasive moulding materials.

The picture of the Figure 3.22 shows a view of the mould used in this work.

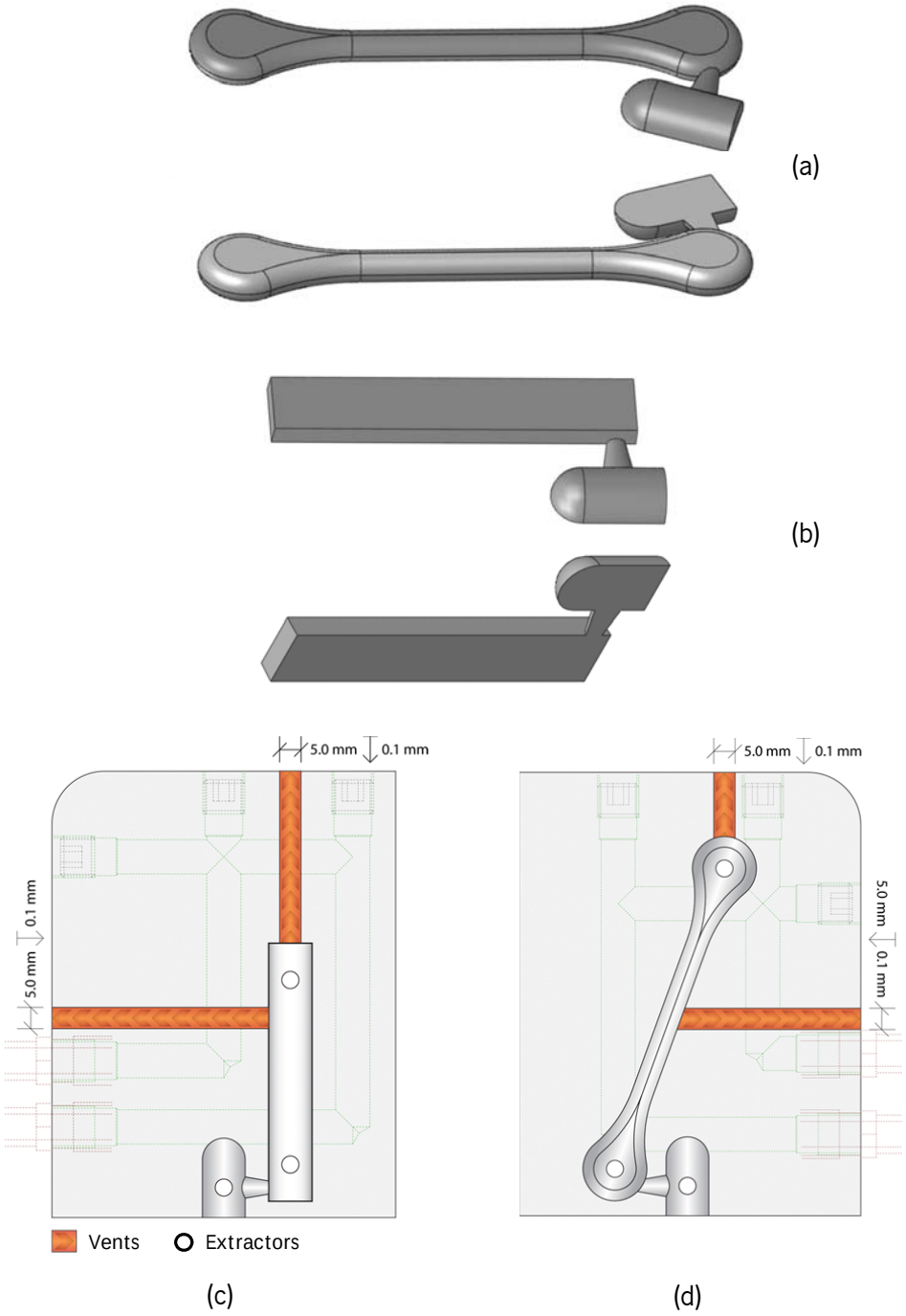

Figure 3.21 3D views of mouldings and gating areas, (a) tensile specimen and (b) flexure specimen, and drawings of the respective top-view inserts, mounted in ejection mould side.

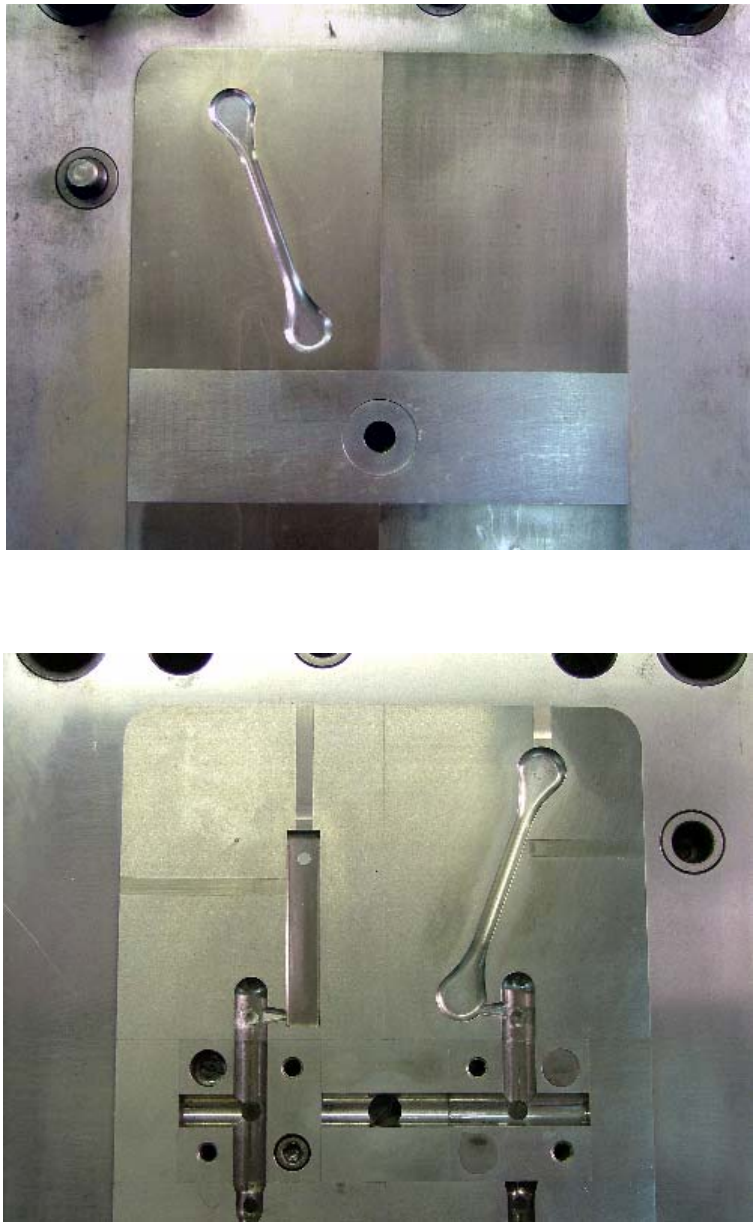

Figure 3.22 Pictures of the two-plates mould: (a) injection and (b) ejection plates.

3.3.4. Injection moulding

Injection moulding was processed in a Arburg Allrounder 270S 500-150 machine. This equipment has a clamping force of 500 kN and a maximum injection volume of 78 cm^3. It is special designed for PIM by using special treated materials in the parts that contact with the molten feedstock, namely the inner surface of the heated cylinder, the screw and the nozzle parts. The screw design is specific for powders moulding, including a lower compression rate.

ISO standard MIM tensile specimen and flexure bars were injection moulded. Feedstocks were moulded at the same conditions (Table 3.16), not only because they had a similar composition but also to compare the behaviour of different formulations at the same process conditions. A melt flow rate profile was designed as recommended for PIM [86]. Flow rate has to be high in order to avoid premature cooling of material in the mould, but not in an excessive range when enters in the parts cavity to avoid powder-binder separation in those thin sections and to permit venting. Therefore, the flow rate was relatively high in the beginning of the shot and became low at the end (Figure 3.23).

Packing pressure was established at approximately 90 % of the switchover pressure, as recommended [86]. Packing time was established by the weighing method: injection cycles using several packing times were carried out; a plot of parts weight against packing time was computed. Packing time was set as the minimum packing time necessary to fully pack the

Table 3.16 Injection moulding process conditions.

Parameter	Value
Nozzle temperature	120 °C
Mould temperature	27 °C
Maximum injection pressure	70 MPa
Average flow rate	29.2 $cm^3.s^{-1}$
Injection volume	11.5 cm^3
Injection time	0.42 s
Packing pressure	70 to 60 MPa
Cooling time	90 s

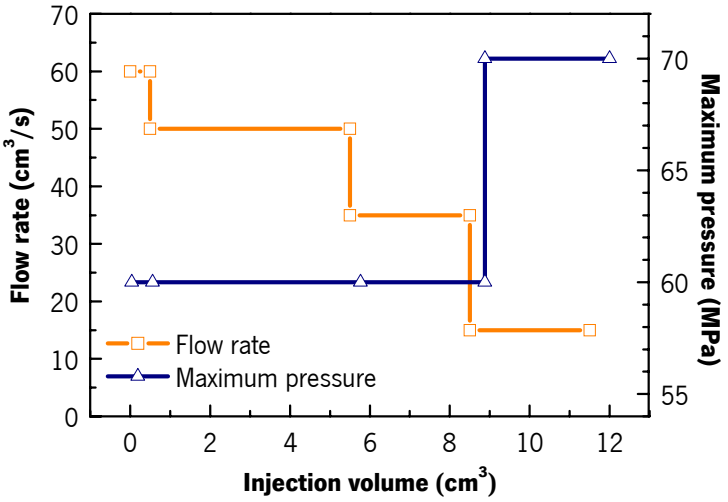

Figure 3.23 Flow rate and maximum pressure of the injection phase of moulding cycle.

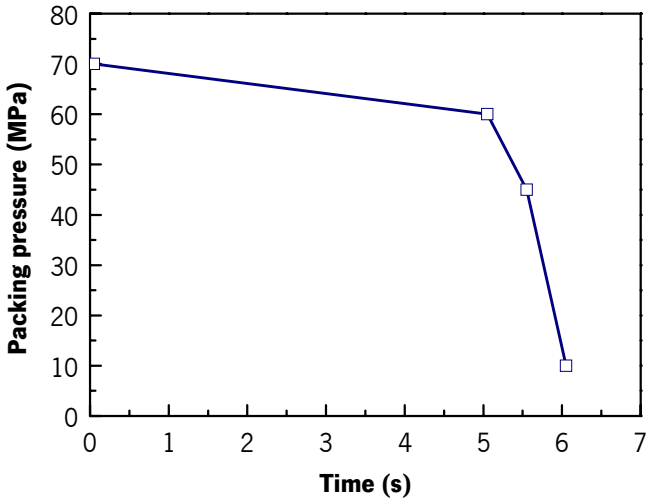

Figure 3.24 Packing pressure profile.

material into the cavity. Figure 3.24 shows the packing pressure profile designed for the injection moulding tests.

In each injection cycle, parts weight was monitored. In the first 10 to 15 cycles, the weight increased and then stayed constant. At this time, it was assumed that the machine was running in stationary conditions. 30 cycles were run; the ten last parts were kept for the study.

3.3.5. Characterisation of the green parts

Weight and dimensions

Moulded parts were weighed in an analytical balance with a resolution of 0.0001 g. Measurements were done with a calliper with a resolution of 0.01 mm in the dimensions shown in Figure 3.25.

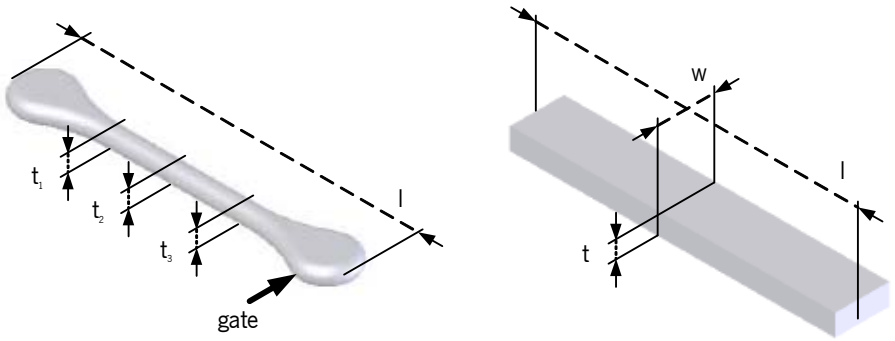

Figure 3.25 Measuring dimensions of the moulded parts.

Flexural strength

Flexural properties were determined with a Lloyd Instrument LK30 universal testing machine, in a three-point loading system, by testing the bar geometry parts. The span of specimen between supports was 40 mm and cross-head speed was 1 $mm.min^{-1}$.

The stress caused by bending is calculated by the following expression [221]:

$$\sigma = \frac{3\,F\,L}{2\,b\,d^2} \qquad (3.7)$$

where σ is the stress (Pa), F is the load or force (N), L is the span of specimen between supports (m), b is the width (m) and d is the thickness (m). If the load corresponds to the value at which failure occurs, then σ corresponds to the flexural strength.

The strain due to bending (compression at the side contacted by the loading head and tensile at the opposite face) is estimated by [221]:

$$e = \frac{6\,D\,d}{L^2} \tag{3.8}$$

where e is the strain (dimensionless) and D is the deflection at the centre of the beam (m).

The flexural modulus (E_B), which is also a modulus of elasticity, is determined by calculating the slope of the linear portion of the stress-strain curve during the bending test in GPa. The formula used to calculate the flexural modulus from the recorded load and deflection is [221]:

$$E_B = \frac{F\,L^3}{4\,b\,d^3\,D} \tag{3.9}$$

3.3.6. Debinding and sintering

Debinding

Either batches of tensile specimens and bars were debinded by water extraction in a thermostatic bath J.P.Selecta Precisdig with a capacity of 20 dm^3. The bath was filled with deionised water and previously heated to the set-point temperature. Table 3.17 shows the experiments map in terms of water temperature and immersion time.

- Tensile specimens: Primarily, four experiments at 50 °C were performed. In the presence of some parts defects of feedstock FS-13-66 and FS-16-66, experiments at lower temperature were carried.
- Flexure bars: Bars of FS-03-66 and FS-09-66 were extracted at 35 °C during 15 hours.

Parts were dried at 50 °C in an air flowing oven. PEG removal was determined by weighing.

Table 3.17 Operating conditions of the water debinding experiments.

		FS-03-66	FS-09-66	FS-13-66	FS-16-66
Temperature	25 °C			X	X
	35 °C			X	X
	50 °C	X	X	X	X
Immersion time		15 hours			

Sintering

Tensile specimens (debinding at 50 °C) and bars were sintered in a graphite vacuum furnace - Vacuum Industries Series 3710 Model 121236-150. Table 3.18 and Figure 3.26 show the program and the temperature profile of the sintering cycle. This cycle was design in two consecutive parts:

- a section of thermal debinding of the remaining binder having three plateaus: the two first ones correspond to the stages of high rate of polymers degradation, according to the thermogravimetry analysis previously made, so that high controlled binder burnout must be attained. The last plateau at 650 °C was intended to be the last degradation step, where all remaining residue of organic compounds were burned out of the parts.
- a sintering stage at 1360 °C, considered a typical sintering temperature of 316L stainless steel [12, 50, 106, 222]. Cooling was ruled by natural conditions. Parts were supported in 99.8 % pure alumina covered boxes produced by in-house slipcasting.

3.3.7. Characterisation of the sintered parts

Weight and dimensions

Sintered tensile specimens were weighed in an analytical balance with a resolution of 0.0001 g. Measurements were done with a calliper with a resolution of 0.01 mm in the dimensions shown in Figure 3.25.

Apparent density

Apparent density was determined by the Arquimedes principle in an analytical balance with a resolution of 0.0001 g and the density measurement accessories. Dust and powder residues from the sintering process were cleaned out from the surface of the parts with a brush. Procedure method consists in to weight a part (dry weight) and to weight it immersed in distilled water (immersed weight). The apparent density is calculated by

Table 3.18 Temperature-time coordinates of the sintering program.

Stage	Initial temperature (°C)	Final temperature (°C)	Heating rate (°C min^{-1})	Stage time (min.)	Cumulative time (min.)
1	20	225	2.5	82	82
2	225	225	-	120	202
3	225	350	2.5	50	252
4	350	350	-	120	372
5	350	650	2.5	120	492
6	650	650	-	60	552
7	650	800	2.5	60	612
8	800	1360	5	112	724
9	1360	1360	-	120	844

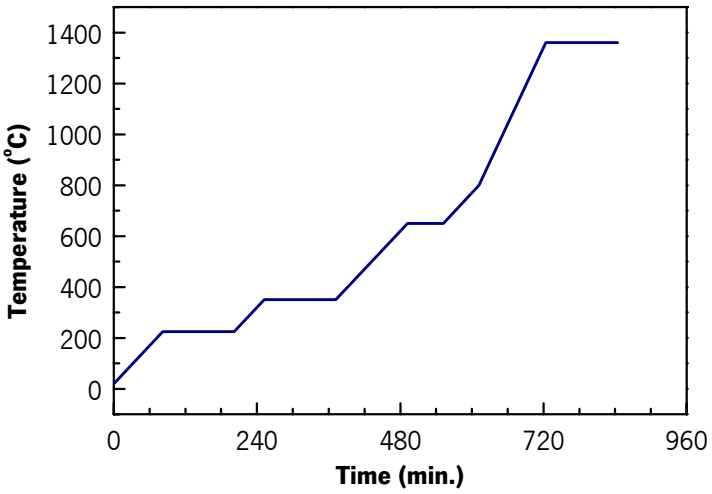

Figure 3.26 Thermal cycle profile of the sintering process.

$$\rho_a = \frac{m_d}{m_d - m_i}\rho_{H_2O} \tag{3.10}$$

where ρ_a is the apparent density, m_d is the dry weight, m_i is the immersed weight and ρ_{H2O} is the water density at the temperature measured during the experiment.

Mechanical properties

Tensile specimens were tested in a Dartec servo-hydraulic mechanical testing machine with a 10 kN loading cell. Diameter of the middle test section of specimens was previously measured with a calliper for the calculation of the tensile stress.

Testing conditions was set according to EN 10 002 standard [223]. Speed of a testing run was set in two configurations:

- For the determination of the yield strength, within the elastic region, the rate of stressing was fixed in 10 MPa.s^{-1}, not exceeding the straining rate of 0.0025 s^{-1}. An extensometer was coupled to the specimen to monitor the elongation;
- In the plastic region, the straining rate was programmed as 0,0076 s^{-1}. Percentage elongation, based in the machine heads displacement, was considered a reasonable measurement as it was dealing with a high ductile material.

Force and displacement data was acquired and the mechanical property results calculated by a computer.

The stress caused by tensile is calculated by the following expression [224]:

$$\sigma = \frac{4\,F}{\pi\,d^2} \tag{3.11}$$

where σ is the stress (Pa), F is the load or force (N) and d is the diameter of the test section of the specimen (m). If the load corresponds to the value at which failure occurs, then σ is called strength at break. If it corresponds to the maximum load the specimen sustains during the test, then it is called the ultimate tensile strength (UTS). The UTS may or may not equate to the strength at break. This all depends on what type of material you are testing.

The strain e (dimensionless) is calculated by:

$$e = \frac{L - L_0}{L_0} \tag{3.12}$$

where L_0 is the initial length (m) and L is the instant length (m), measured by an extensometer.

The tensile modulus (also designated by elasticity modulus or Young's modulus) is the ratio of stress to elastic strain in tension, i.e. in the region where the material follows the Hooke's law:

$$E_T = \frac{\sigma}{e} \qquad (3.13)$$

Yield strength is defined as the stress applied to the material at which plastic deformation starts to occur while the material is loaded. In this work, the off-set method was applied, at 0.2% strain, as described in Figure 3.27.

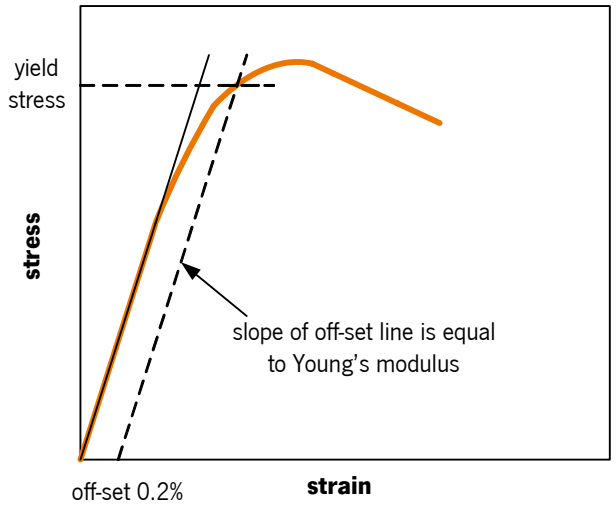

Figure 3.27 Determination of the yield stress by the off-set method.

Elemental chemical composition

Elemental composition of the sintered parts was determined by the same methods used for the powder:

- X-Ray fluorescence spectroscopy for elements Fe, Cr, Ni, Mn, Mo, Si and P;
- Inert gas fusion method for O and N;
- High-temperature combustion method for C and S.

Samples were obtained by cutting a piece of a tensile specimen. To eliminate surface oxidation layer effects, the sample surface was ground. Then, it was cleaned with ethanol and dried at 100 °C for 1 hour. Procedure was similar to powder analysis (Section 3.1.2).

4. RESULTS AND DISCUSSION

4.1. Binders and feedstocks characteristics

4.1.1. Compatibility of binder components

Binder components compatibility was analysed by melting point depression (mpd) method, i.e. by the analysis of melting temperatures of the pure component and the binder mixtures.

When preparing the binders, the melt appearance gave some indications about the mixture microstructure. Almost all the melt mixtures were biphasic, having a dispersed phase of LDPE or MPE. Droplets were perceptible at naked eye, but not in photography record. These were considered stable emulsions, as no coalescence was observed during the few minutes of draining and cooling. On the other hand, binders having PMMA and PVB were continuous phase mixtures.

Binders L-11 and L-12 were not successfully prepared because two continuous phases were formed when the total amount of the components were added. This fact could indicate that, in those conditions, low compatibility of components turns impossible to obtain a one-phase mixture or a two-phase dispersion. Binders L-05 and L-06 were difficult to be prepared. First trial resulted in the segregation of LDPE during the addition of this component. Special procedures, such as very low addition rate of LDPE into the PEG melt and the maximum agitation speed almost the time, were taken to obtain the dispersions.

Melting peak temperatures of the binders and its components were obtained from the DSC diagrams, as shown by the example of Figure 4.1, where one can observe the melting temperatures deviations. In order to enable a combined evaluation of compatibility, a new type of proper graph based on information of this test is shown in Figure 4.2.

It was found that in all binders there is at least one component which melting point decreases. PEG melting temperature decreases in all binder formulations, as well as polyethylene waxes. Thus, it is observed components compatibility in all binder systems. This fact can be explained by the analysis of the contributors for free energy of mixtures, seen in Eq. 2.15. A reason why the

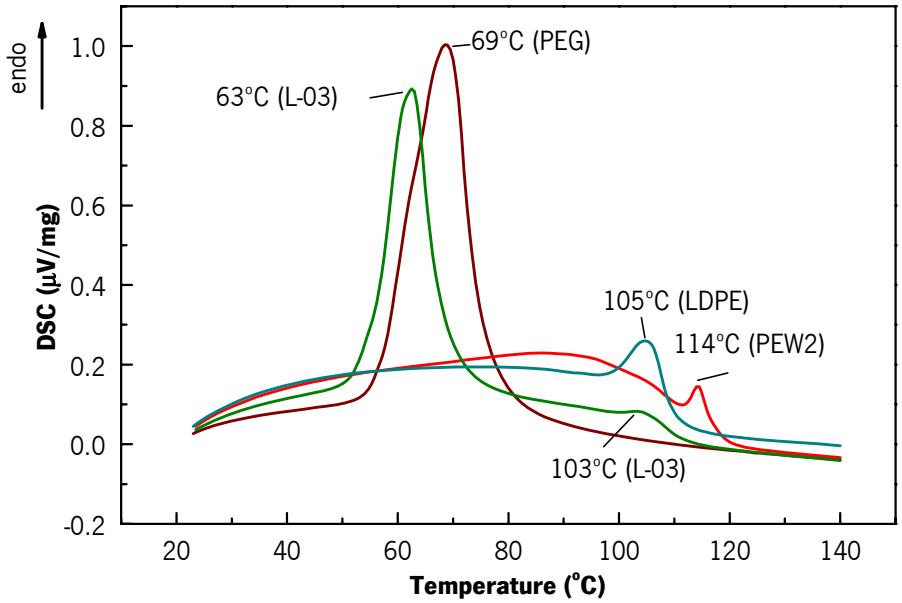

Figure 4.1 DSC curves of the binder L-03 and the pure components (PEG, LDPE and PEW2).

polymers are usually immiscible is the high molecular weight which is the cause for the not increasing of the entropy in mixture. In these binders, the major part of the components are low molecular weight materials (PEG, waxes and fatty acids) promoting the molecular chains interdiffusion.

Some components showed different mpd magnitude when present in different mixtures. PEG, PEW1 and PEW2 have higher mpd in binders with LDPE than with MPE. Under the Nishi and Wang model (Eq. 2.18), the magnitude of the mpd is proportional to the interaction parameter χ, and so to the compatibility. The effect of LDPE is conclusive by comparing the binary mixtures L-05 (PEG/LDPE) and L-15 (PEG/PEW2), here the mpd of PEG is higher in the binder with the polyethylene. Therefore, the magnitude of PEG mpd in L-03 (PEG/PEW2/LDPE) can be mainly due to LDPE. On the other hand, MPE does not show compatibility tendency as it shows no melting temperature variation (in binders L-07 to L-10). So, the use of MPE instead of LDPE lowers the PEG and PEWs compatibility.

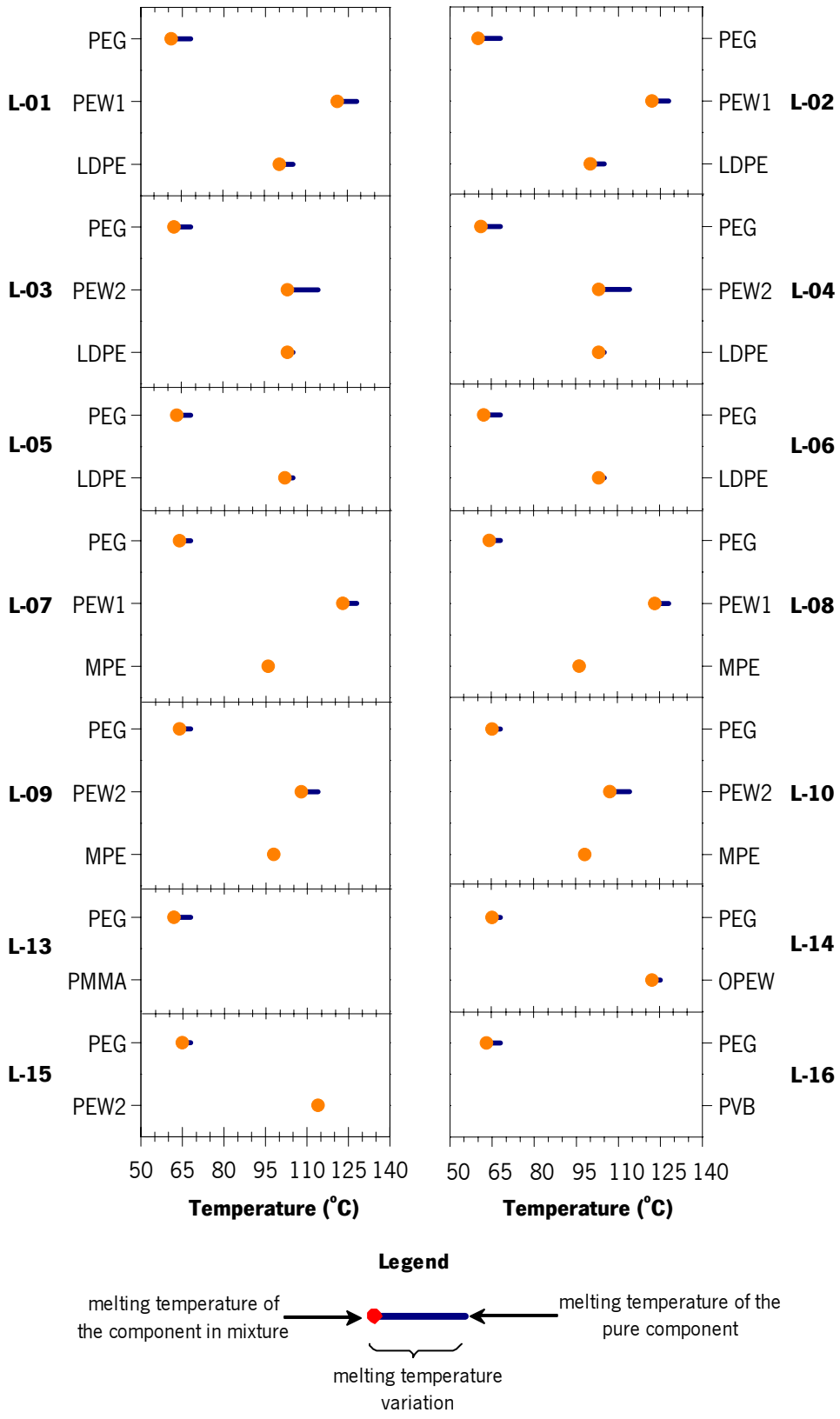

Figure 4.2 Melting temperature variation from the pure components to binder mixtures.

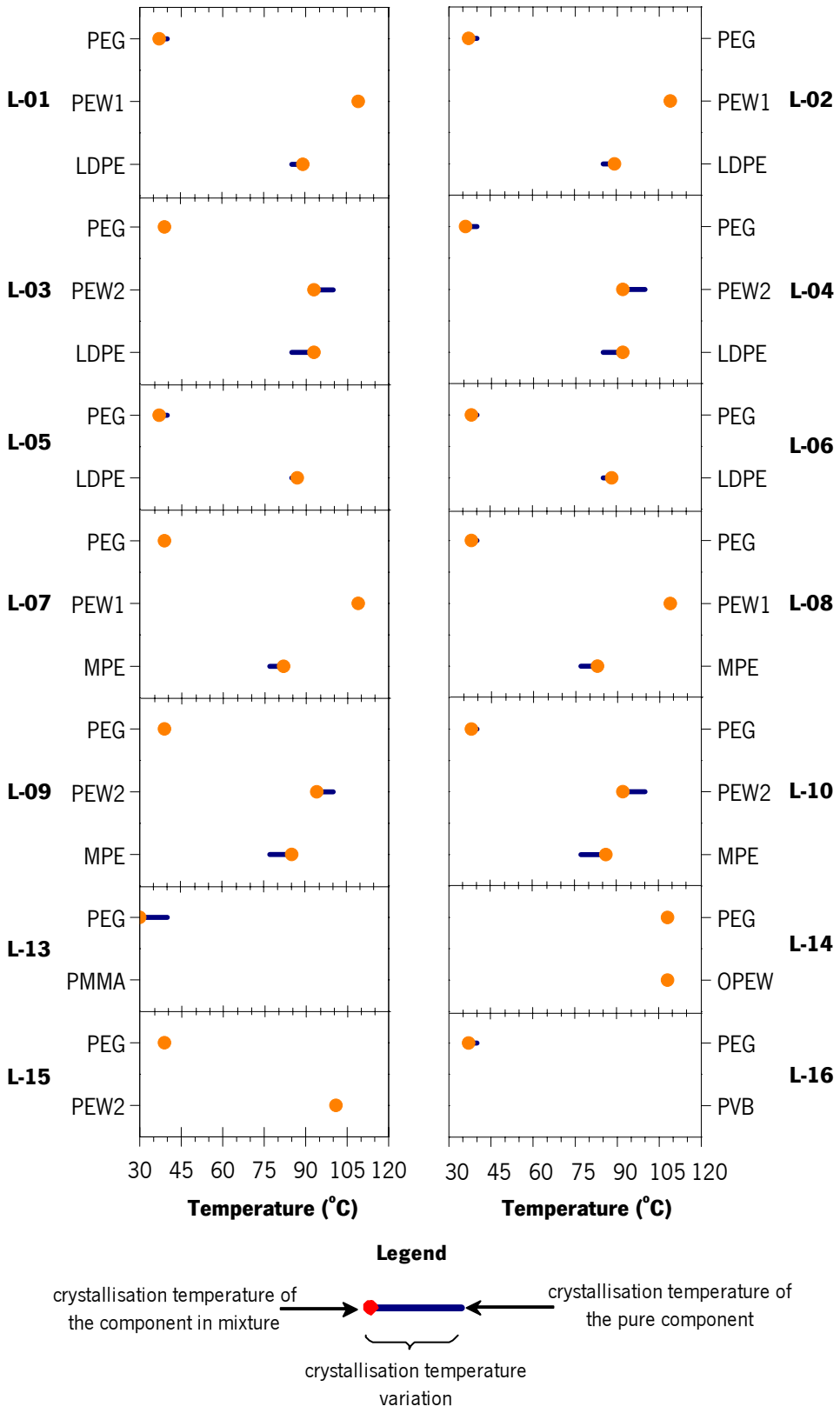

Figure 4.3 Crystallisation temperature variation from the pure components to binder mixtures.

The effect of the surfactant is not evident, since no relevant mpd differences were found between binders which composition had stearic acid or oleic acid.

Figure 4.3 shows the crystallisation temperature (T_c) variation of the components from pure to binder mixtures states. The T_c of PEW2 and LDPE or MPE are displaced in an approaching direction. As an example, observing the binder L-03 plot, when the mixture is cooled down, PEW2 crystallised later (T_c decreases) and LDPE crystallised earlier (T_c increases), so it seems that both components affects the crystallisation process of each other. This phenomenon can be related with the interdiffused polymeric chains in melting state which can affect the crystallites formation. Thus, this fact can suggest that these two pairs of components would have interacted in the melting state, showing compatibility. Binders L-05 and L-06 are blank composition, showing that in the absence of waxes the displacement of the T_c of LDPE is lower than with the waxes. In the same way, binder L-15 plot shows no modification of the T_c of PEG and PEW2.

Binders with PEW1 show an increase of T_c of LDPE and MPE, but not a T_c decrease of the wax. In this case, there would be an effect of the wax in the polymer but the effect of the polymer in the wax was not relevant or null. Therefore, the compatibility in PEW1 system is lower than in PEW2 systems. This can be explained by the effect of the molecular in the free energy of mixing. PEW1 and PEW2 have a molar mass of ca. 9000 and 2000 g/mol, respectively. Mixture with lower molar mass has higher entropy contributing to the decrease of the free energy, and so to a higher compatibility.

4.1.2. Mixing behaviour and critical solid fraction

Critical powder volume concentration of the mixtures of the binders and the stainless steel powder was determined by torque rheometry. Figure 4.4 shows the torque profile of mixtures with binder L-03 as an example of results obtained by this method. When the binder and powder are poured into the pre-heated rheometer bowl, the torque curve has a sharp peak. Binder begins to wet the powder particle providing lubrication to the particles motion decreasing the torque value. The torque value reaches a steady state when powder and binder are homogeneously mixed. With a solids concentration below the critical value, in the steady-state zone, torque presents low fluctuation (curve 67 vol.%). As the solids concentration approaches the critical

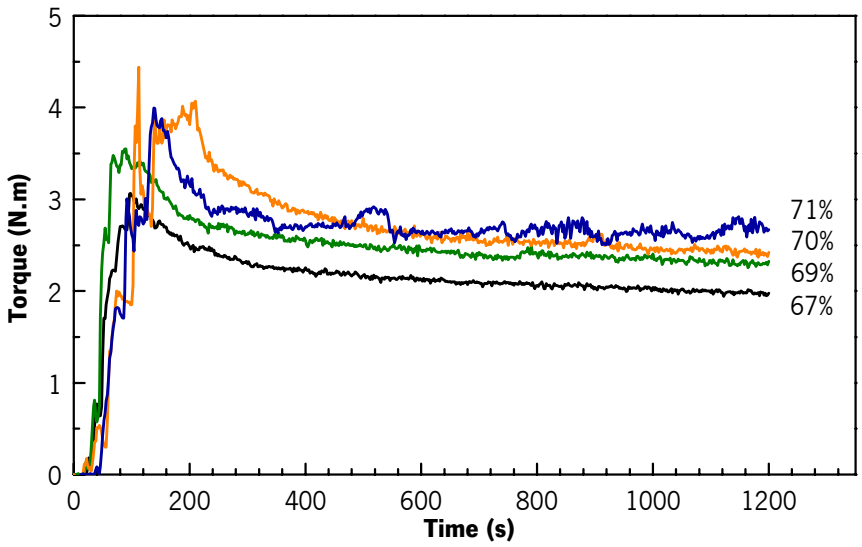

Figure 4.4 Torque curves for mixtures composed with binder L-03 at 155 °C, with several solids fractions.

value, the fluctuation is increased (curves 69 and 70 vol.%). In the case of high and erratic torque fluctuation, it is considered that the CPVC has been exceeded [162, 163]. However, not all the tested binder systems exhibited the same behaviour in order to apply this torque instability criterion.

Figure 4.5 shows the torque curve of mixtures with binder L-05. After passing through the peak zone, the torque begins to decrease towards to the steady state. Then, in case of mixtures with 65 and 67 vol.%, the curve departs from the plateau showing a torque slope, i.e. they begin to thick. This fact can be due to binder phase segregation, possibly related to the high propensity of segregation observed during the binder preparation procedures. Binder L-06, which is composed also by PEG, LDPE and a surfactant additive, as binder L-05, showed similar thickening behaviour. Such behaviour must be avoided in a PIM binder system to prevent flow anomalies of feedstock and subsequent processing problems. Binder L-05 and L-06 did not show adequate mixing characteristics when compounding highly concentrated feedstock, with solids fraction such as 65 vol.%, and so they were considered not acceptable for PIM technology and were eliminated from this study.

Binder L-14, composed by OPEW, showed also a single behaviour (Figure 4.6). Torque values had a tremendous increasing along time, for the two solids fraction tested – 63 % and 65 vol.%,

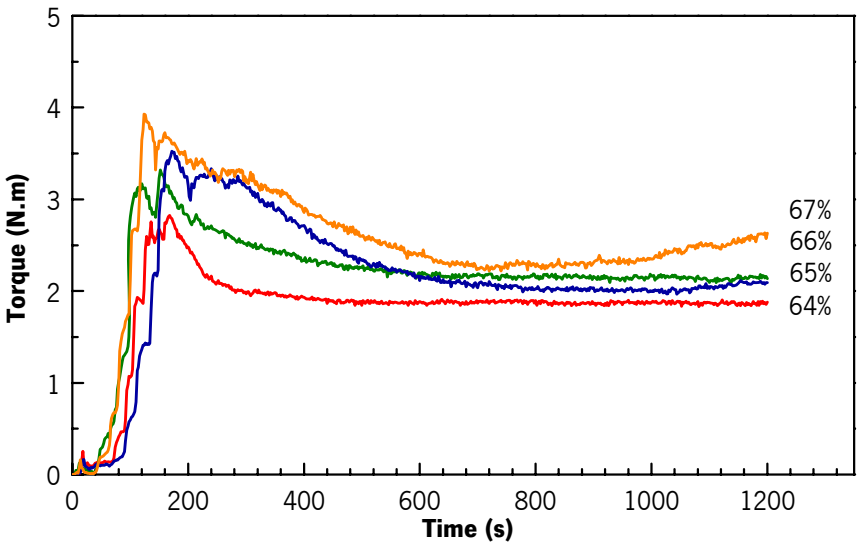

Figure 4.5 Torque curves for mixtures composed with binder L-05 at 155 °C, with several solids fractions.

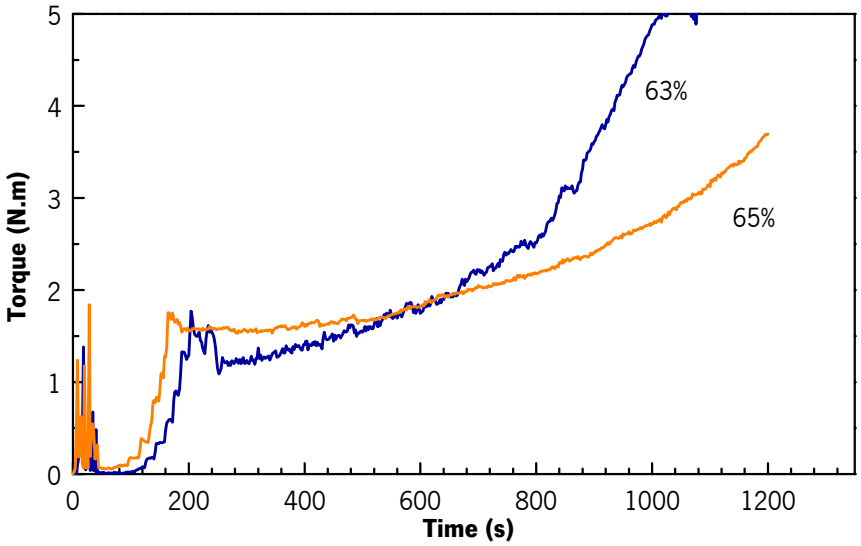

Figure 4.6 Torque curves for mixtures composed with binder L-14 at 155 °C, with several solids fractions.

without seeing any sign of torque stabilisation. As in general the oxygenated polymers are more susceptible to thermal oxide degradation, this was considered an explanation for those results. Comparing to the other binder mixtures, the premature thermal degradation in those mixing condition led the binder L-14 to be withdrawn.

Figures 4.7 and 4.8 show the plots of average mixing torque and fluctuation (measured by the standard deviation) calculated in steady-state, in the last 5 minutes of mixing, of the mixes of

different solids fraction of all binders. These are tools to help the analysis of the mixing rheometry aiming the determination of the CPVC. As expected, torque fluctuation is low in the mixtures with lower solids fractions, and then suddenly it increases after overcoming the critical fraction.

Most binders showed a common trend of the torque curve. They increase when fraction goes up and begin to decrease at or immediately after the critical fraction. This fall can be explained by slip behaviour of mixture on the bowl surface or paddles. This suggests that powder fraction at

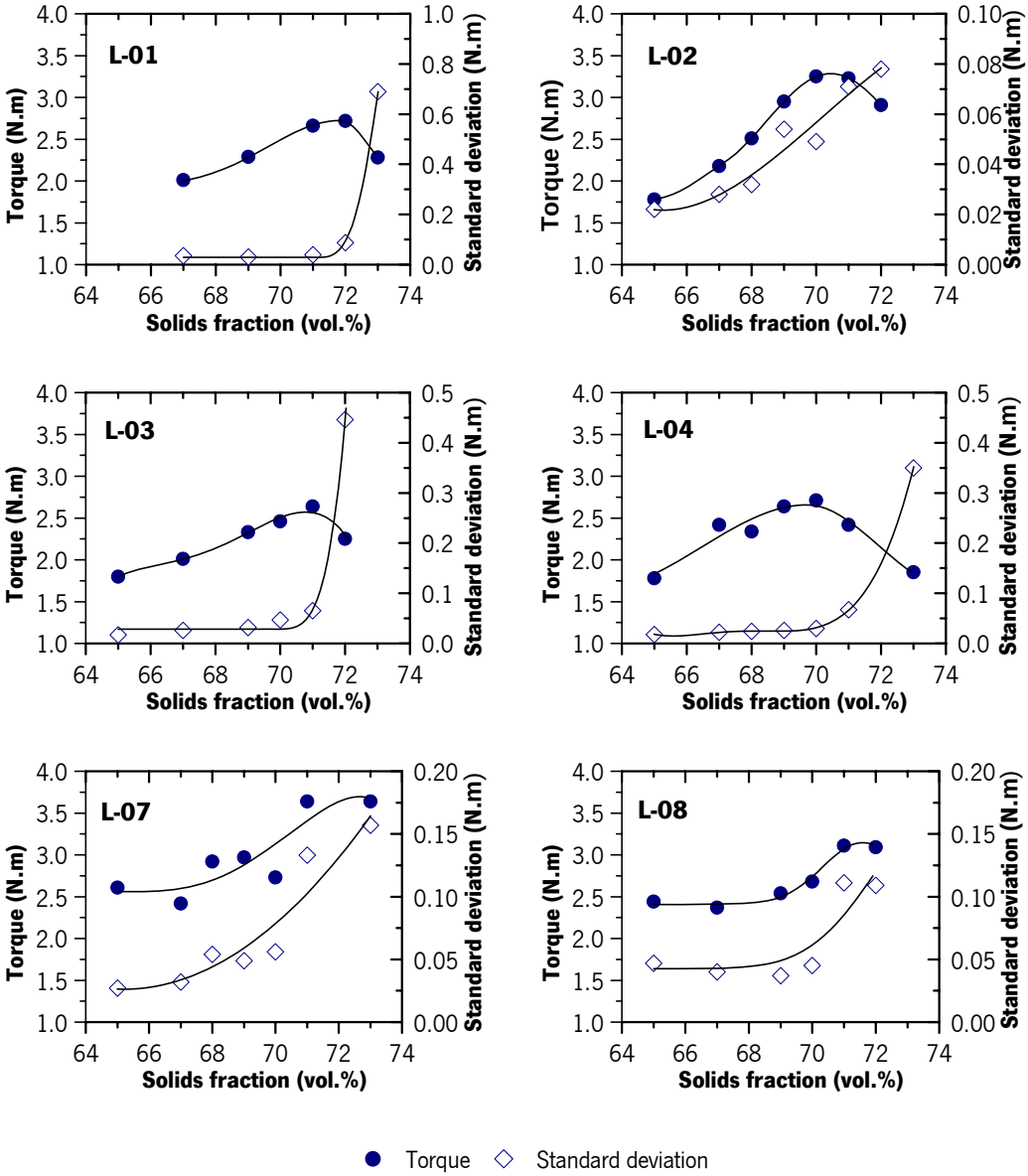

Figure 4.7 Torque and fluctuation in function of solids fraction of feedstock with binders L-01, L-02, L-03, L-04, L-07 and L-08.

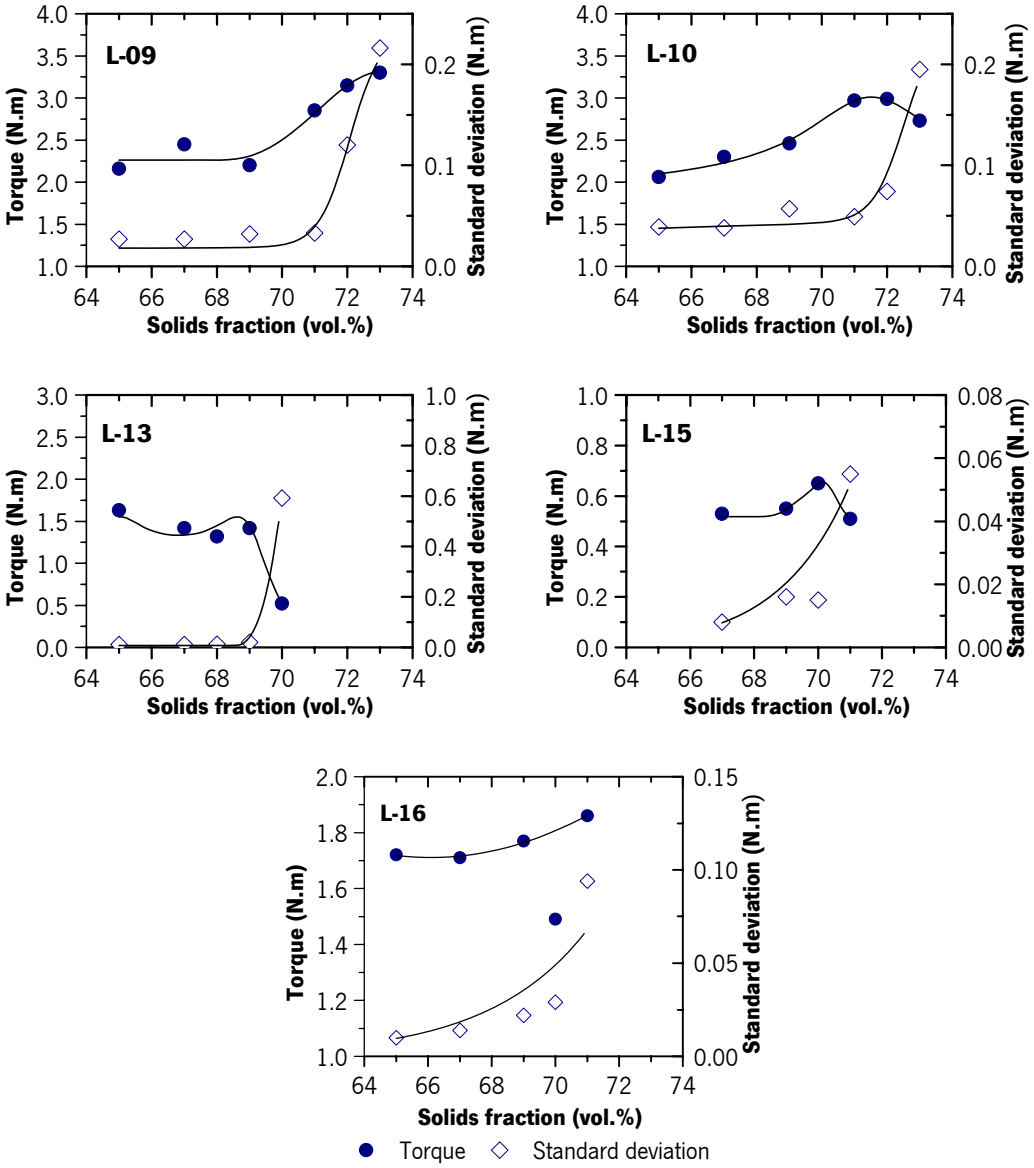

Figure 4.8 Torque and fluctuation in function of solids fraction of feedstock with binders L-09, L-10, L-13, L-15, and L-16.

the critical or higher value is responsible for that slipping. Considering that the torque is mostly due to the plasticity of the binder positioned between the moving solid materials, slipping can be due to relative motion of two powder particles or of particles and metallic surface of the bowl. Slipping may be explained by the lack of binder between the powder particles and between the particles and the paddles. Slip phenomenon has been reported in other studies as a result of increasing solids fractions [150].

Table 4.1 Critical solids fractions.

Binder	ϕ_c (vol.%)	Binder	ϕ_c (vol.%)
L-01	71	L-08	70
L-02	70	L-09	71
L-03	70	L-10	71
L-04	70	L-13	69
L-05	T.T.	L-14	T.T.
L-06	T.T.	L-15	70
L-07	70	L-16	70

* T.T.: Time thickening behaviour

Based on the standard deviation curves, CPVCs of the stainless steel powder with the different binder were determined (Table 4.1). CPVC do not vary by more than 2 vol.%, between 69 and 71 vol.%, confirming that CPVC is mostly influenced by the powder characteristics rather than the binder composition [1]. Considering these CPVC values and following recommendations indicating that optimum feedstock solids fraction are often 2 to 5 vol.% below the critical fraction [1], it was considered 66 vol.% as a proper value for the concentration of the following feedstock experimental tests.

4.1.3. Rheology of feedstocks

Rheological properties were determined by capillary rheometry. Figure 4.9 shows the viscosity curves at 155 °C of mixtures with 66 vol.% of stainless steel powder. Shear rate was corrected by Rabinowitch approaching. All feedstocks have shear-thinning behaviour in the analysed range, ca. 500 to 10,000 s^{-1}, which is a necessary condition for a well succeeded injection moulding process.

Viscosity of feedstock mixtures is expected as a compromise between the viscosities of the components. For polymers, the higher the molecular weight, the greater the chains entanglement and lower chain mobility, thus the greater the melt viscosity. Feedstocks can be grouped by the viscosity range, which can be related to the characteristics of the polymeric materials. The

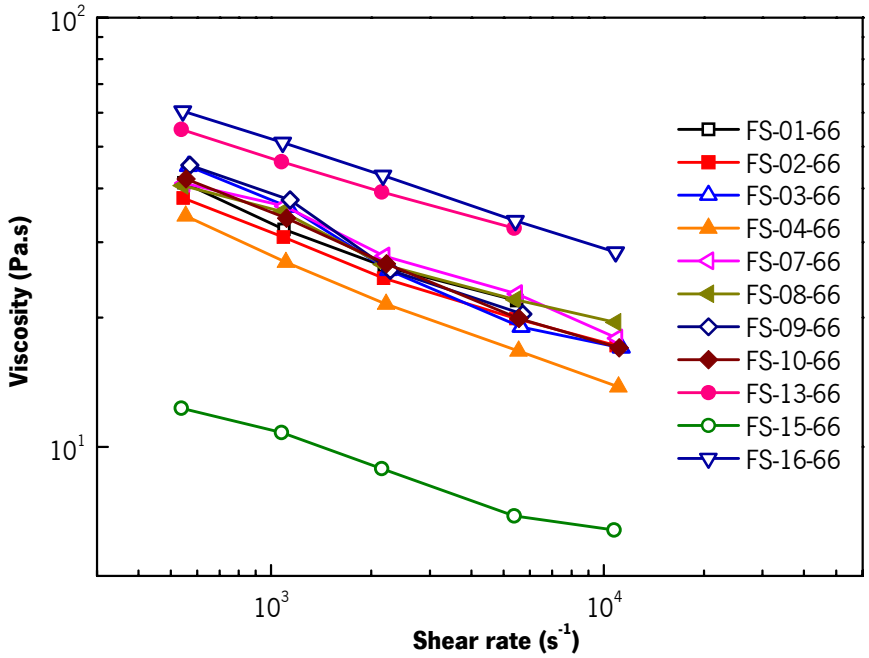

Figure 4.9 Apparent viscosity of 66 % solids fraction feedstocks as function of shear rate at 155 °C.

mixture prepared with L-15 is the less viscous because it has no high molecular weight polymer in its composition. Formulations with LDPE or MPE and waxes have intermediate viscosity, and those with PMMA and PVB have higher viscosity. In sum, the effect of the amount of wax is notorious in the viscosity of the feedstocks.

Table **4.2** shows the parameters n and k_o and the correlation coefficient R, obtained by fitting the power-law model to the data of Figure 4.9. A good correlation was obtained with coefficients between 0.989 and 1.000, validating the applicability of the model to the tested materials.

The similarity of the feedstocks composition, in powder and PEG amounts, is reflected in the small variation of n among the formulations (between 0.64 and 0.77). However, having a detail look, in the plot in Figure 4.10, there can be found some relationships between the binder formulations and n values. Binders with PEW2 provide feedstocks with lower n than those with PEW1 or no lubricant, which means that viscosity is faster to decrease with an increasing shear rate, i.e. those mixtures have higher shear sensitivity. Shear-thinning is explained by the chain orientation of polymers in the flow direction under higher shear rates. Waxes are generally used as internal lubricants, which act by reducing friction between polymer molecules. PEW2 seems to be more effective in reducing friction and thus increasing the mobility of polymer (LDPE or MPE)

Table 4.2 Fitting parameters of the power-law model.

Feedstock	k_0 (Pa.s^n)	n	R
FS-01-66	239	0.73	0.991
FS-02-66	211	0.73	0.996
FS-03-66	418	0.66	0.990
FS-04-66	245	0.70	0.998
FS-07-66	264	0.72	0.995
FS-08-66	214	0.75	0.991
FS-09-66	496	0.64	0.989
FS-10-66	320	0.69	0.998
FS-13-66	245	0.77	0.999
FS-15-66	56	0.77	0.993
FS-16-66	320	0.75	1.000

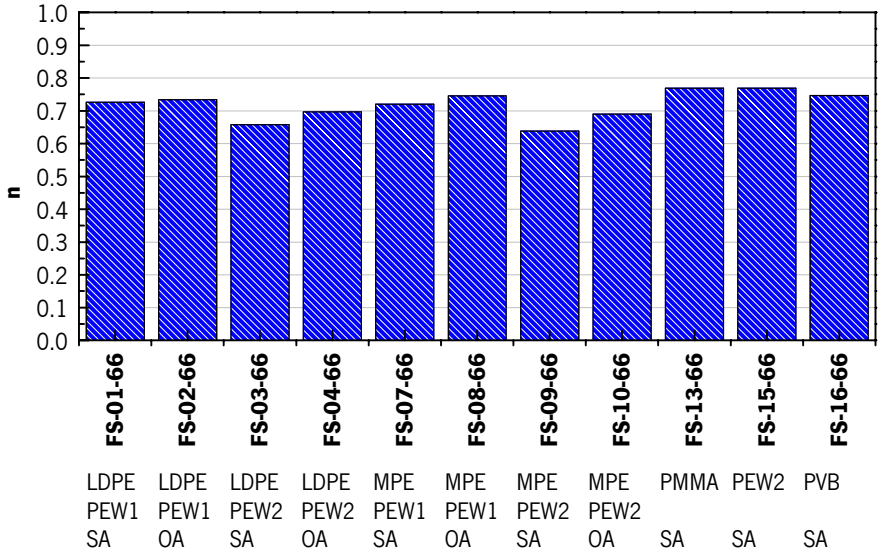

Figure 4.10 Power-law model indexes.

promoting the chain orientation under higher shear rate. This can be due to the lower molecular weight because smaller molecules are much easily diffused in the long chains of polymer. This results is verified to be consistent with the previously stated higher compatibility of PEW2 binders.

Formulations with stearic acid show also lower *n* than those with oleic acid. The effect of LDPE or MPE is not appreciable. High shear sensitivity, represented by lower *n*, is preferable for injection moulding as it makes easier the flow inside lower cross section channels, therefore allowing smaller features in PIM parts.

4.1.4. Microstructure of feedstocks

Microstructure of pressed feedstock was observed by scanning electron microscopy. The respective micrographs of the fracture sections are shown in Figures 4.11 and 4.12. With all binder systems, particles are well soaked in the binder matrix and some binder ligaments are visible, binding the particles, on the surface of the fracture. Therefore, it suggests that all binder systems have adequate wetting on the powder particle.

In some feedstocks polymer filaments were found. These are thought to be some high molecular weight polymer which is not dispersed in the PEG-riched binder matrix. As mixtures of polymers are deformed during flow, complex morphologies can develop [225]. Polymer may be drawn into filaments, and probably these were formed in the previous processes (mixing or capillary rheometry). Moreover there is a larger amount of those filaments in feedstocks made from binders with metallocene polyethylene (FS-07-66, -08-, -09- and -10-), which was previously verified to be less compatible with PEG. In the part produced with a binder with miscible components, as binder L-16, no back-bone polymer features were observed.

4.1.5. Water extraction behaviour

The progression of the water extraction of PEG in pressed parts is represented in Figure 4.13. PEG removal curves present two kinetic regimes. Up to about 3.6 ks (1 h) of immersion, the extraction speed is higher with extraction amounts reaching 40 % to 75 %. As soon as the PEG is dissolved in the part surface the water starts to penetrate in the porous formed. Then PEG

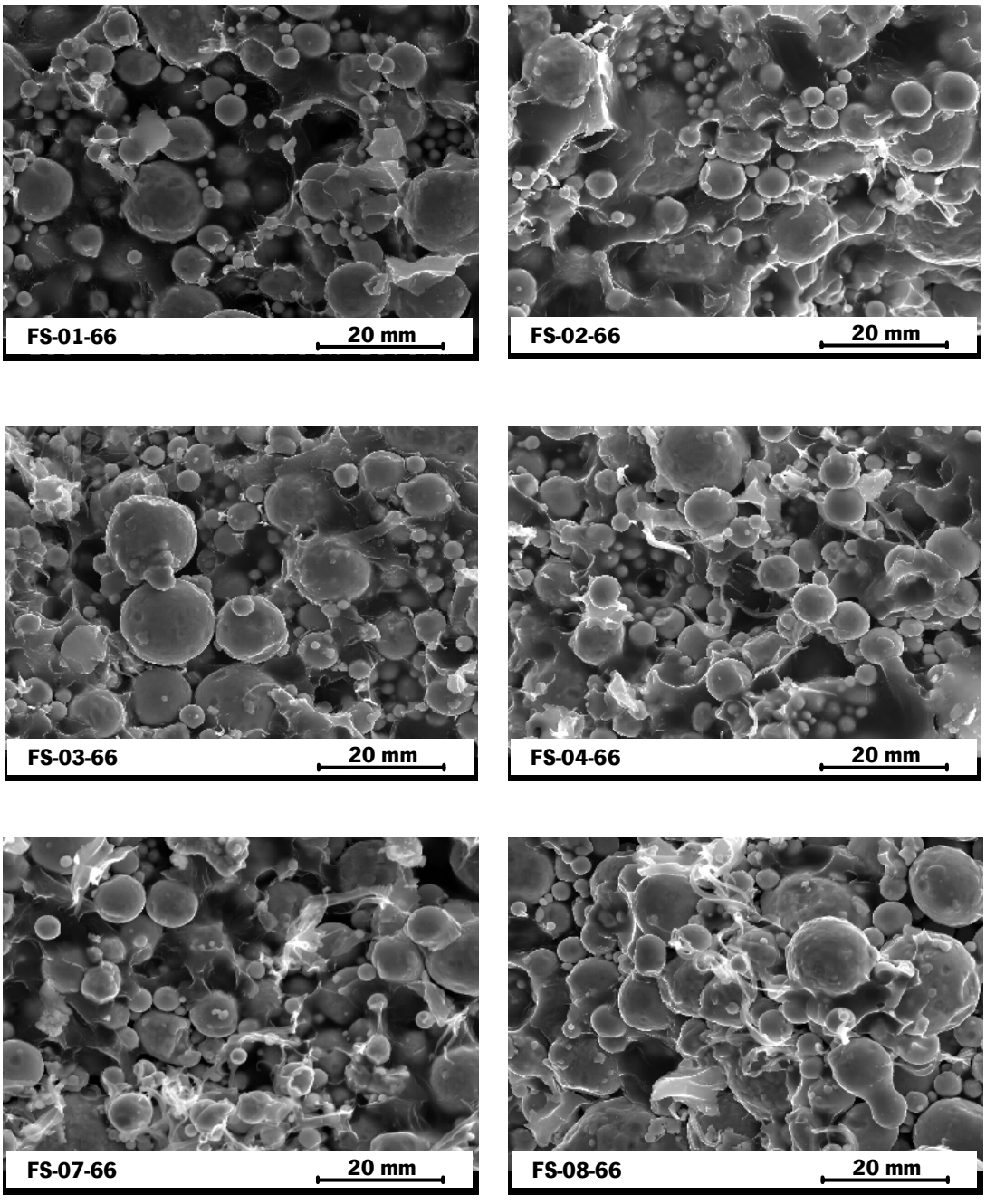

Figure 4.11 SEM micrographs of fracture sections of the pressed feedstocks.

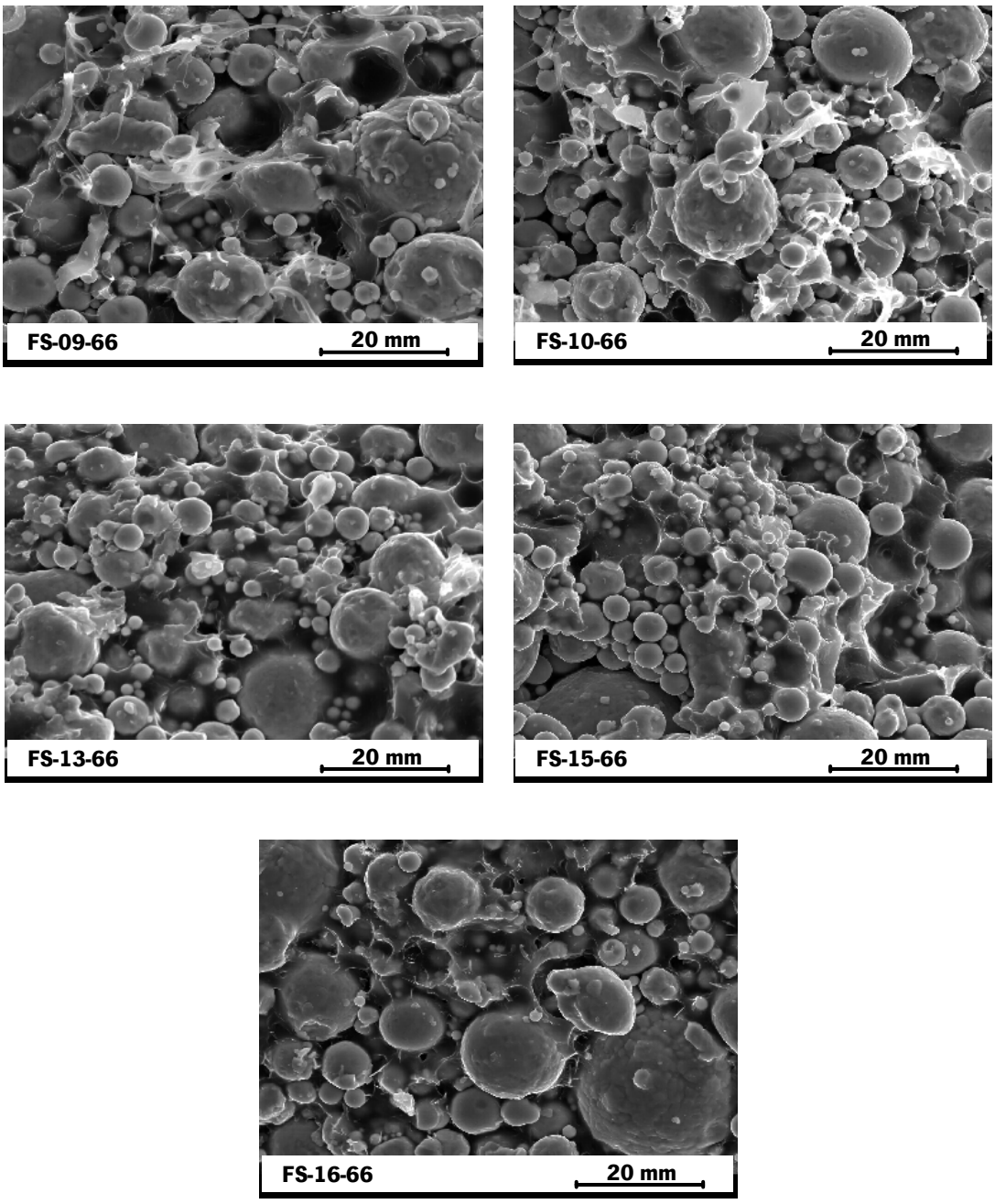

Figure 4.12 SEM micrographs of fracture sections of the pressed feedstocks.

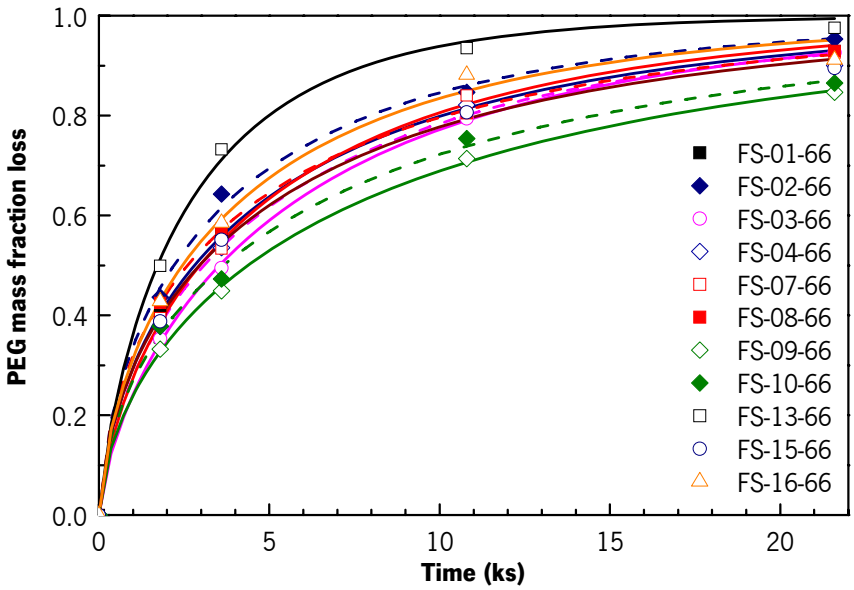

Figure 4.13 PEG removal from press moulded parts by water extraction as function of immersion time.

dissolution will occur inwards and solute diffusion will occur in the tortuous pathway which is continuously formed within the particles. At the first times, path is short so PEG diffusion is less significant compared to PEG dissolution. Therefore, the latter is considered the restrictive mechanism. After that, the water is progressive introduced inside the parts and the solute diffusion became most restrictive, as the tortuous path is increasing [23, 25, 26]. After approximately the first hour, the extraction is slowed down and the restrictive mechanism is replaced by the diffusion. After the debinding and drying, all parts were free of external defects.

Figure 4.14 shows the extraction fraction after 21.6 ks (6 h). The majority of the feedstocks reached the same extraction level – 90 to 95 %. Feedstocks produced with binders L-09 and L-10 showed lower removal, while FS-13-66 parts had the higher value.

Results show an influence of back-bone polymer and waxes in the LDPE and MPE based binder. It is observed that PEG removal is higher in binders with PEW1 than with PEW2, and it is also higher in binders with LDPE than with MPE. The use of PMMA results in a great increase in PEG extraction rate. PEG was nearly full extracted in PVB formulation after 6 hours. So, binders with different insoluble part show distinctive water debinding behaviour, which is in accordance with other studies [19, 33]. The effect of the use of different surfactants was not relevant.

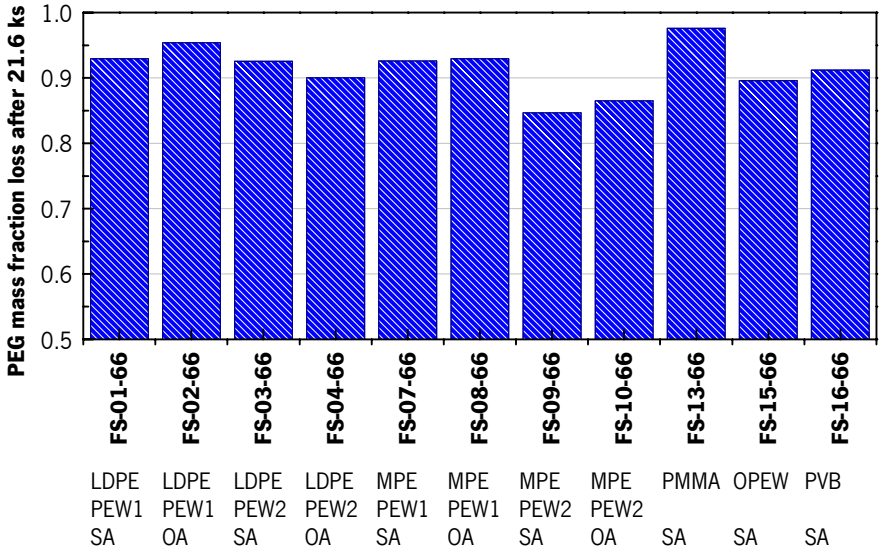

Figure 4.14 PEG removal after 21.6 ks (6 h) of immersion.

4.1.6. Thermal degradation behaviour

Thermal debinding consists basically in submitting the moulded parts to heat in order to crack the polymeric chains of the binder components. The resulting molecules are gaseous and can flow out of the bulk of the part. The gas generation inside the mouldings creates internal pressure which can cause part defects and distortions. Therefore, a heating cycle must be designed according to the binder thermal degradation.

Thermogravimetric curves of specimens obtained from the core of parts after water debinding are presented in Figure 4.15. All curves show a common reaction step at ca. 360 to 420 °C corresponding to the degradation of the remaining PEG. FS-16-66 loses PVB at lower temperatures, around 210 to 340 °C. PMMA, present in the FS-13-66, begins to be degraded slowly at 260 °C and overlays the PEG degradation. Curves of binders composed with polyethylene based material (low density, metallocene and waxes) have similar shapes. These materials begin decomposition around 420 °C.

Figure 4.16 shows TG curves of FS-07-66 (representing all ethylene based materials), FS-13-66 and FS-16-66 and the respective derivate curves. Temperature ranges and rate analysis are detailed in Table 4.3. FS-16-66 presents two problematic zones where the higher degradation

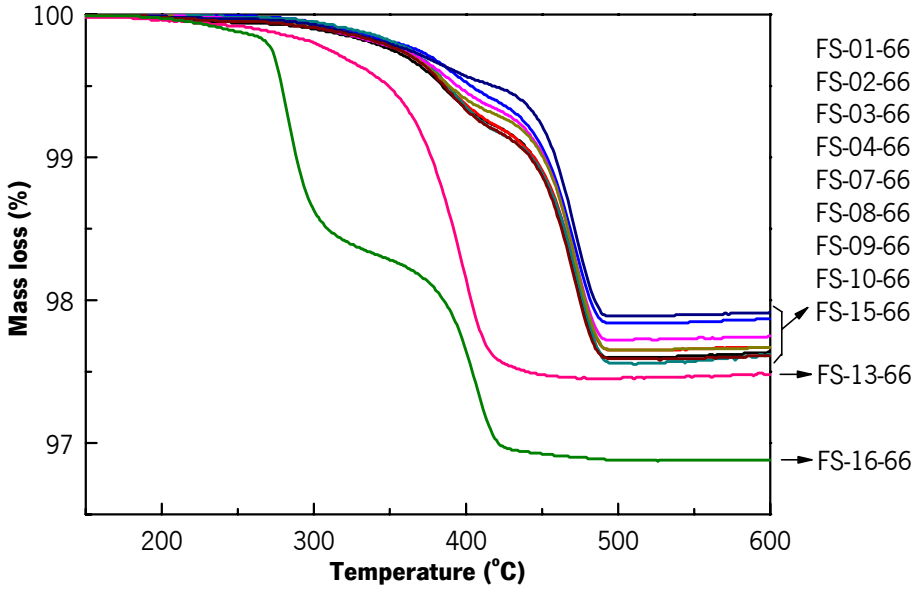

Figure 4.15 TG curves of water debinded parts.

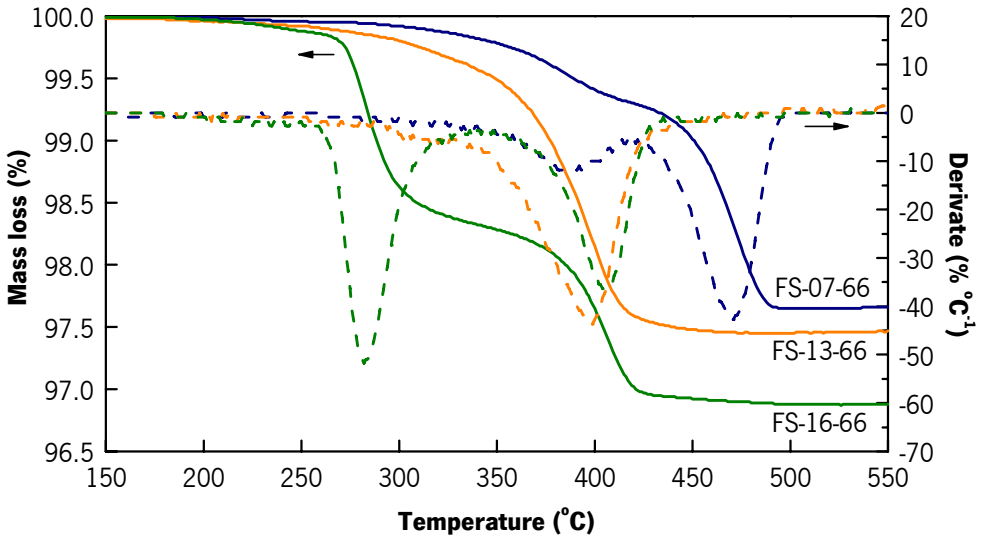

Figure 4.16 TG and derivate curves of water debinded parts produced with feedstocks FS-07-66, FS-13-66 and FS-16-66.

Table 4.3 Quantitative analysis of TG of water debound samples.

		FS-07-66	FS-13-66	FS-16-66
1st reaction	temperature interval (°C)	280-420	260-450	210-340
	average derivate (% °C^{-1})	-5.7	-12.0	-12.6
	minimum derivate (% °C^{-1})	-11.8	-43.6	-51.8
2nd reaction	temperature interval (°C)	420-495		340-455
	average derivate (% °C^{-1})	-21.2		-13.2
	minimum derivate (% °C^{-1})	-42.7		-36.4
All reactions	temperature interval (°C)	280-495	260-450	210-455
	average derivate (% °C^{-1})	-11.4	-12.0	-12.9

rates (average derivates -12.6 and -13.2 %.°C^{-1}) increase the probability for the occurrence of part defects. To overcome this problem, a long thermal cycle must be designed, with low heating rates and long plateaus. The degradation curve of FS-13-66 starts with a slow weight loss but becomes relatively fast after ca. 360 °C (average derivate -12.0 %.°C^{-1}). This degradation profile is more promising than the earlier since the initial slow removal increases the porosity and opens the path for the subsequent degradation products. This advantage is more pronounced in FS-07-66 for which the first reaction step is slower (average derivate -5.7 %.°C^{-1}). Therefore, these ethylene based binders create parts with less probability to have defects due to thermal degradation in the first step of the sintering process.

4.1.7. Partial conclusions

Binders were evaluated in terms of six important aspects in order to predict and evaluate their adequacy for powder injection moulding.

Preparation of binder mixtures was found to be hard with compositions without waxes, only possible with special experimental procedure. This was related to a lack of compatibility, assessed by the melting point depression method. At the end, binders L-11 and L-12 were not possible to be prepared in the defined conditions.

Compatibility between binder components was generally observed in all binders as there was always at least one component showing melting point depression. All binders contain low molecular weight components (PEG, waxes and fatty acids), which can promote the mixture entropy, lowering the free energy and promoting the molecular chain interdiffusion. Moreover, LDPE was demonstrated to be more effective providing compatibility with PEG and PEW's mixtures than MPE. Binders with PEW2 exhibited higher compatibility than with PEW1. No relevant effect of the chemical differences of stearic and oleic acids was detected. SEM observation of pressed feedstock revealed that lower compatible systems, with metallocene polyethylene, have formed heterogeneous features, in particular polymeric filaments.

Torque rheometry allowed to discriminate some binders which have produced feedstock mixtures demonstrating inadequate behaviour in mixing with 316L stainless steel. Binder L-05, L-06 and L-14 showed time thickening behaviour when compounded with highly concentrated feedstocks, being withdrawn. CPVC do not vary by more than 2 vol.%, between 69 and 71 vol.%, confirming that is mostly influenced by the powder characteristics rather the binder composition.

Binders were used to produce 66 vol.% stainless steel mixtures with shear-thinning behaviour, promising for injection moulding. Their viscosity demonstrated to be highly influenced by the amount of the wax content, acting as a lubricant. Shear sensitivity, analysed by the power-law model index, is enhanced with PEW2 rather than PEW1, and with SA than OA. Therefore, mixtures FS-03-66 and FS-09-66 was shown to be the most shear-sensible, considered the most appropriate for injection moulding.

An attempt to predict the water debinding performance of the different binder systems, led to experimental extraction tests in water at 50 °C of pressed feedstock and to evaluate the respective influence of back-bone polymers and waxes. Binders with PEW1 had higher PEG removal than with PEW2, and LDPE provided higher extraction than MPE. Water extraction showed to be the main advantage to use PMMA, creating the higher debinding rate. PMMA provides the easiest mixture to be debinded, reaching 98 % of PEG removal after 6 h.

Thermogravimetric analysis of the debinded parts determined that the ethylene based binders would have fewer propensities to cause defects related to binder thermal degradation. Binder L-13 would be the second choice and L-16 would need more efforts to avoid defects in the initial stage of the sintering.

It was not found a clearly favourite binder that stood out in all aspects, so a balance had to be done aiming global binder discrimination. An exercise was done by scoring the binders in each aspect. Microstructure of feedstock was not scored since it was a qualitative information. Binders were scored in a 1 to 5 range, where 1 was the least appropriate and 5 was the best appropriate. Binder score is graphically represented in Figure 4.17. L-03 is considered the most appropriate binder with the best score, followed by L-01, i.e. PEG/LDPE/PEW/SA was the best combination. PEW2 has dictated the best performance for L-03. This wax is also present in the best MPE based binders, L-09. Binder with PMMA, PVB and PEW2 alone are considered the least attractive for PIM. However, L-13 was top score in water debinding.

The selection of binder to be used in subsequent processing experiments was based not only on this benchmarking but also on the expectable behaviour of binder chemistry in processing. L-03 and L-09 was chosen, as the best binders with LDPE and MPE as back-bone polymers. Binders with amorphous back-bones, chemical distinct and tough polymers, PMMA and PVB, were also elected for processing experiments.

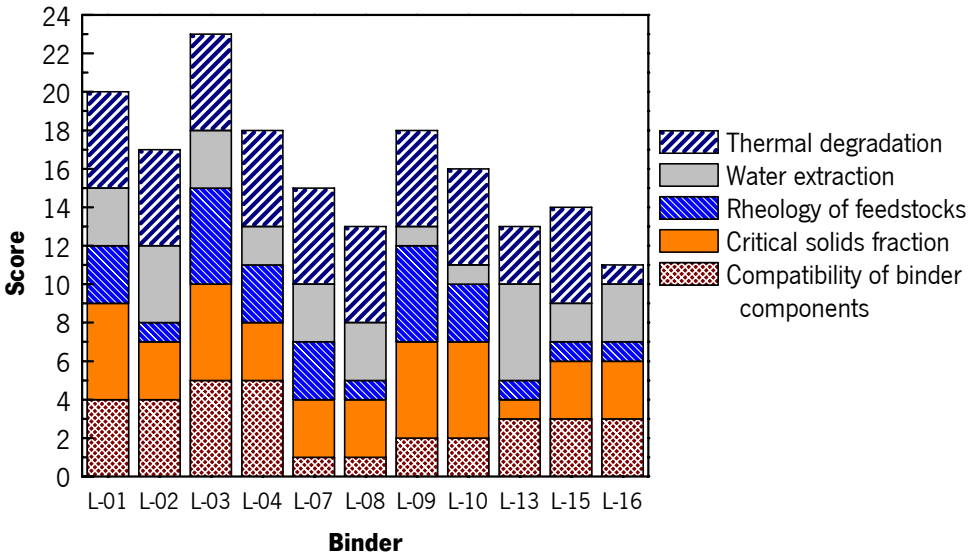

Figure 4.17 Scoring of the binders.

4.2. Process characteristics

4.2.1. Mixing

Solids fraction assessment

Solids fraction was assessed by thermogravimetric analysis. Table 4.4 shows a comparison between the formulation solids fraction and the measured value. TG values are slightly higher than formulation. This effect was associated to the mixing process, where binder is often thermally degraded due the long residence time in the equipment.

The solids fractions gaps, in 0.2 to 0.4 wt.% represent an increase rounded 1 vol.% in the solids fraction of the four feedstocks, which means that the fraction changed from the formulated value, 66 vol.%, to the real 67 vol.%.

Homogeneity

Homogeneity was assessed by two different methods: picnometry density and flow pressure stability. Table 4.5 presents the analytical characteristics of those methods. They are complementary since they analyse the homogeneity in different scrutiny sizes. Picnometry determines the density of 4 cm^3 samples and rheometry measures the pressure in every 0.024 cm^3 of feedstock melt passing trough the capillary (given by the shear rate of 1000 s^{-1} and the frequency of pressure acquisition of 5 s^{-1}). The size of total samples is approximately the same, so the results from these methods can be directly compared.

Table 4.4 Comparison of solids concentration between the formulation and the TG measurements.

Mixture	Formulation wt.%	Measured wt.%	Difference wt.%
FS-03-66	93.3	93.5	- 0.2
FS-09-66	93.3	93.6	- 0.3
FS-13-66	92.9	93.2	- 0.3
FS-16-66	93.0	93.4	- 0.4

Table 4.5 Comparison of methods for the assessment of feedstock homogeneity.

Method	Measured variable	Sample size	Number of samples	Analysed amount
Picnometry density	density	≈ 4 cm^3	6	≈ 24 cm^3
Flow pressure stability	pressure	0.024 cm^3	900	22 cm^3

Table 4.6 shows the homogeneity analysis in terms of standard deviation of the picnometric density. Feedstocks FS-03-66 and FS-09-66 registered lower density standard deviation and lower variation range than feedstock FS-13-66 and FS-16-66. Therefore, the first are considered more homogeneous than the latter.

In some cases, the average density is lower than the formulation value, which can be indicative of the presence of voids inside the mixtures. Porosity was calculated from the ratio of average and formulation densities. It increases as the density standard deviation is increased, and this relationship is approximately linear, as it is shown in Figure 4.18. This suggests the porosity can directly influences the homogeneity, and could be a major factor for some density dispersion. Therefore, powder dispersion can be assumed homogeneous. Then, a correct optimization of the mixing process could lead to a low air entrapment and thus lower standard deviation of density. Shear roll compounder could be the source of the air entrapment as it works in open air.

Table 4.6 Density analysis for feedstock homogeneity assessment.

		FS-03-66	FS-09-66	FS-13-66	FS-16-66
Formulation density ($g.cm^{-3}$)		5.62	5.62	5.65	5.65
Measured density ($g.cm^{-3}$)	Average	5.495	5.618	5.341	5.456
	Standard deviation	0.005	0.004	0.014	0.011
	Maximum, M	5.503	5.625	5.359	5.468
	Minimum, m	5.491	5.612	5.323	5.443
	Variation range, M-m	0.012	0.013	0.036	0.024
Calculated porosity		2.2 %	0.0 %	5.5 %	3.4 %

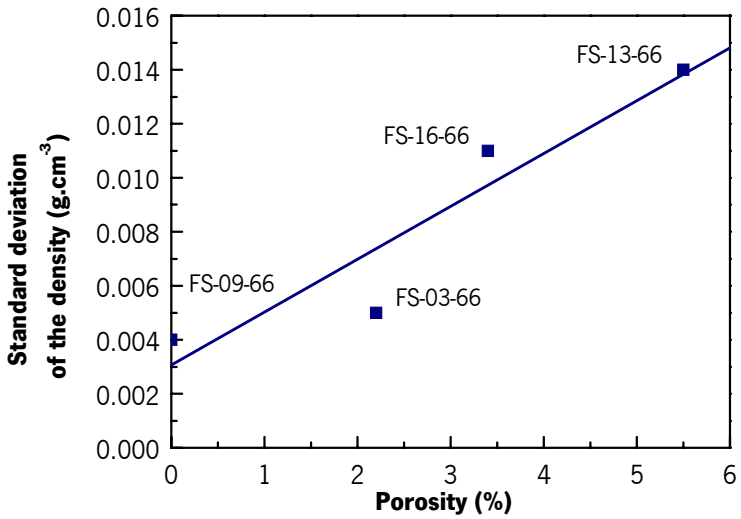

Figure 4.18 Standard deviation of the feedstocks density as function of the calculated porosity.

From the capillary pressure profiles, it was calculated the pressure mean value and the standard deviation, so that fluctuation was defined as two times the standard deviation, as illustrated in Figure 4.19. Figure 4.20 shows the pressure fluctuation, for the mixed feedstocks and a 316L stainless steel commercial feedstock – BASF Catamold 316LH. It is also plotted the maximum fluctuation admitted in the literature. Based in experience, Roetenberg considered that the

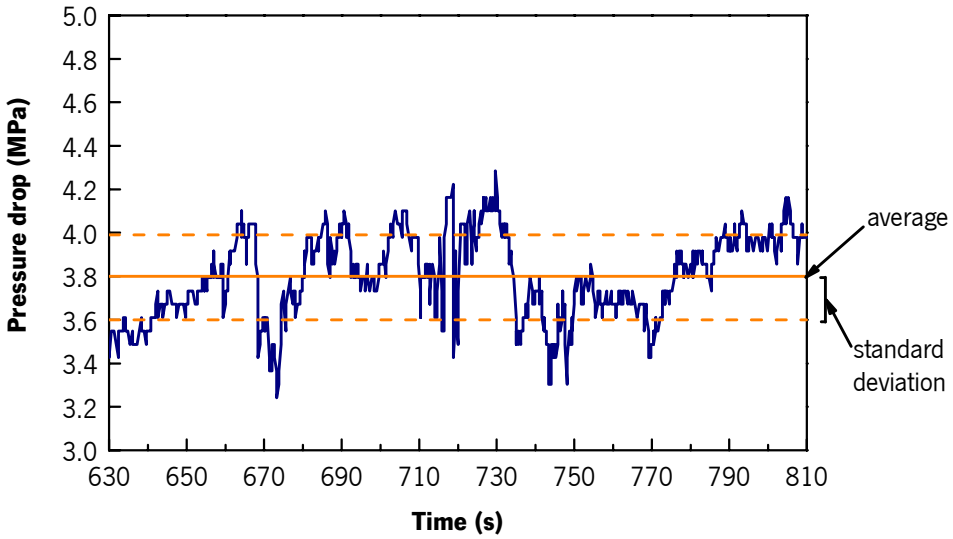

Figure 4.19 Pressure curve obtained from a capillary rheometer for the analysis of the feedstock homogeneity (example of a run with binder L-03).

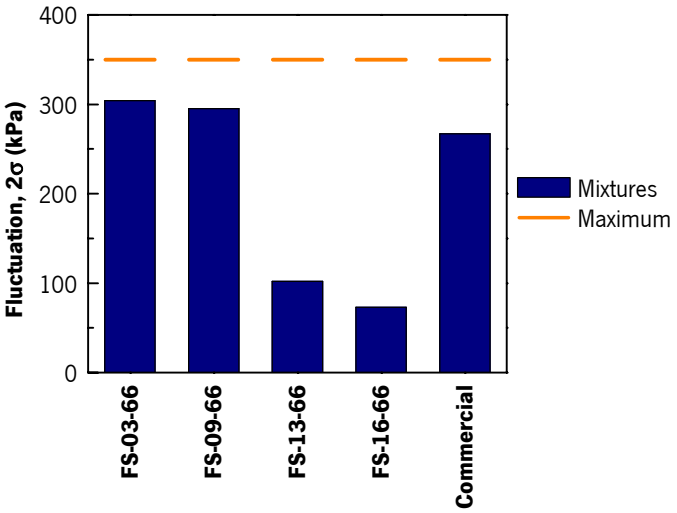

Figure 4.20 Pressure fluctuation of the prepared and the commercial feedstocks and comparison with the maximum admitted.

maximum pressure fluctuation for a homogeneous feedstock is 350 kPa [71]. It can be observed that all the analysed materials did not overcome the maximum value. Comparing to the commercial feedstock, all the prepared feedstock are at the level or lower of fluctuation. Therefore, they can be considered as reasonably homogenous for PIM process.

4.2.2. Injection moulding

Injection moulding process parameters were based on the properties of binders and feedstocks and optimised by trial and error method. Some adjustments were made in the process conditions

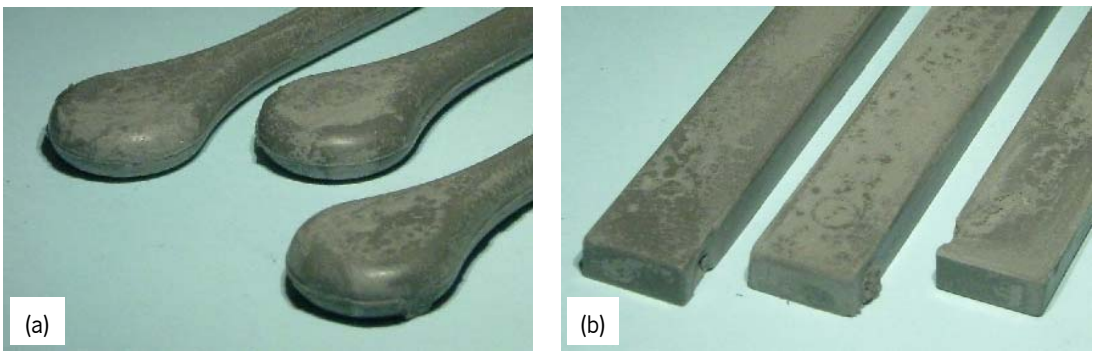

Figure 4.21 Surface conditions of inadequate injection moulded parts - (a) tensile specimens, (b) flexure specimens.

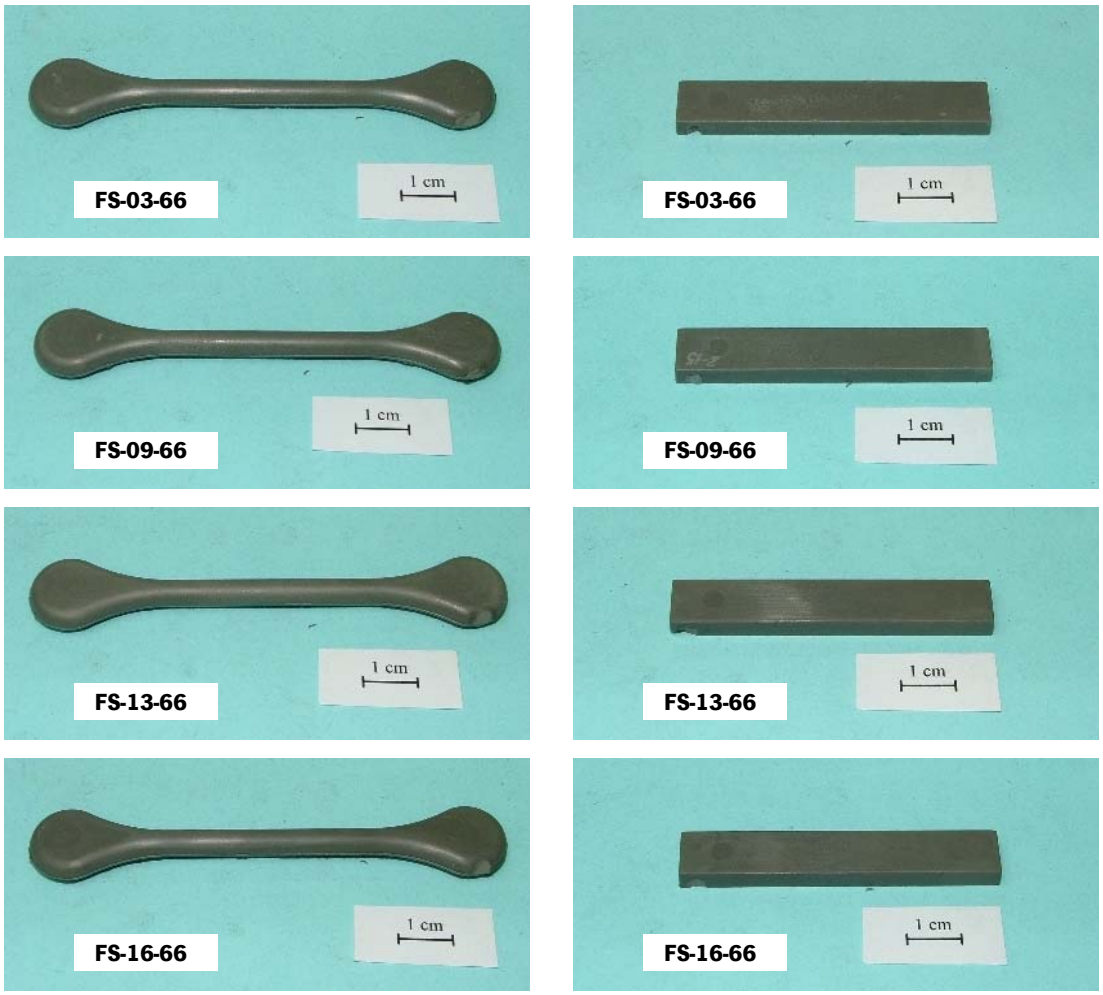

Figure 4.22 Green parts produced by the prepared feedstocks.

previously stated. The chosen set melt injection temperature (155 °C) led to non satisfactory moulded parts (Figure 4.21). Parts revealed poor surface finishing, possibly due to powder-binder separation or binder degradation, and surface peeling. Reducing injection temperature resulted in the diminishing of such defects. It was verified a relationship between part brakes during ejection and the packing pressure. The integrity of the ejected parts was achieved by increasing pressure, and then set in 70 MPa. The mould temperature should be below the crystallisation temperature of binders, 30 to 39 °C. Lower temperature will cool the part faster and will be able to result in a short injection cycle; but the installed water line was unable to supply refrigerated water to decrease the mould temperature less than 27°C. Therefore, 90 seconds were necessary to harden the moulded parts ready for ejection.

Figure 4.22 shows the moulded parts with the final machine operating conditions. Green parts were apparently correctly moulded, having complete cavity filling and smooth and uniform surface.

Weight, density and dimensions of moulded parts

Table 4.7 presents the statistics data of the green parts weight and Table 4.8 shows the apparent Arquimedes volume and density. Weight variability of moulded parts was used to inspect the stability of the process. Weight standard variation is considered relatively small in all parts because it represents no more than 0.27 % of the average. Therefore, the feedstocks are confirmed to be adequately homogeneous, giving a well stable injection moulding process. The variation of parts weight of feedstocks FS-03-66 and FS-09-66 are, in average, higher than those from feedstock FS-13-66 and FS-16-66. This evidences that the higher homogeneity of the latter, observed early by the pressure stability method, can be related to the lower parts weight

Table 4.7 Weight of the injection moulded parts.

Feedstock		FS-03-66	FS-09-66	FS-13-66	FS-16-66
Tensile	average (g)	16.9279	16.9651	17.3341	17.2007
	s.d. (g)	0.0192	0.0234	0.0097	0.0184
	% s.d./aver.	0.11%	0.14%	0.06%	0.11%
Flexure	average (g)	13.7586	13.7834	14.1181	13.8563
	s.d. (g)	0.0367	0.0157	0.0132	0.0101
	% s.d./aver.	0.27%	0.11%	0.09%	0.07%

Table 4.8 Apparent density and volume of the injection moulded parts.

Feedstock		FS-03-66	FS-09-66	FS-13-66	FS-16-66
Tensile	average ($g.cm^{-3}$)	5.51	5.52	5.56	5.55
	s.d. ($g.cm^{-3}$)	0.01	0.01	0.00	0.01
	volume (cm^3)	3.07	3.08	3.12	3.10
Flexure	average ($g.cm^{-3}$)	5.52	5.53	5.61	5.56
	s.d. ($g.cm^{-3}$)	0.01	0.01	0.01	0.01
	volume (cm^3)	2.49	2.49	2.52	2.49

variability. This suggests that a well mixed feedstock will yield a stable injection moulding process and a good part-to-part reproducibility.

Parts made with polyethylene polymers weight similarly, 16.9279 g and 16.9651 g. PMMA and PVB binders produce heavier parts, with 17.3341 g and 17.2007 g, respectively. Higher weight is due to bigger density and slightly bigger volume, as shown in Table 4.8. This means that there is a distinct Pressure-Volume-Temperature (PVT) behaviour of the feedstocks, originated by different binder formulation, especially between the two pairs of materials.

Apparent density of the green parts is between 5.51 and 5.61 $g.cm^{-3}$. Density is observed to vary with the moulded part. All feedstocks produced denser parts when moulded into the flexure specimen cavity than the tensile cavity. Thus, the green density is not only dependent to the feedstock composition but also to the injection moulding conditions. Other factor that could influence green density is the polymers densities in use: ρ(LDPE) = 0.92 $g.cm^{-3}$, ρ(MPE) = 0.90 $g.cm^{-3}$, ρ(PMMA) = 1.20 $g.cm^{-3}$, ρ(PVB) = 1.14 $g.cm^{-3}$. So, denser polymer will yield to denser green parts.

Table 4.9 presents the green parts dimensional statistics. Dimension precision is quite similar among the four tested feedstocks. Standard deviation is less than 0.04 mm and it is proportional to the average size, as following:

- size: 4-5 mm	s.d.: 0.00 - 0.01 mm	%.s.d/size: 0.1 - 0.3 %
- size: 10 - 60 mm	s.d.: 0.01 - 0.03 mm	%.s.d/size: 0.0 – 0.2 %
- size: 90 mm	s.d.. 0.02 - 0.04 mm	%.s.d/size: 0.0 %

Despite of standard deviation increase with the dimension size, the precision in %.s.d/average has an inverse behaviour. Precision range is between 0.0 % and 0.3 %.

Mechanical properties

Figure 4.23 shows examples of the stress curves resulting of the moulded bars and Table 4.10 resumes the mechanical flexure properties. Stress curves show a brittle behaviour, with a linear elastic region followed by a failure, which is a typical result for moulded PIM materials. This

Table 4.9 Dimensions of the injection moulded parts.

Feedstock			FS-03-66	FS-09-66	FS-13-66	FS-16-66
Tensile	Length	average (mm)	89.81	89.84	89.98	89.93
		s.d. (mm)	0.02	0.04	0.03	0.02
		% s.d./aver.	0.0%	0.0%	0.0%	0.0%
	Diameter	average (mm)	5.15	5.16	5.20	5.19
		s.d. (mm)	0.00	0.01	0.01	0.01
		% s.d./aver.	0.1%	0.2%	0.2%	0.1%
Flexure	Length	average (mm)	60.05	60.15	60.18	60.13
		s.d. (mm)	0.02	0.02	0.01	0.03
		% s.d./aver.	0.0%	0.0%	0.0%	0.0%
	Width	average (mm)	10.14	10.12	10.20	10.16
		s.d. (mm)	0.02	0.01	0.02	0.02
		% s.d./aver.	0.2%	0.1%	0.2%	0.2%
	Thickness	average (mm)	4.18	4.17	4.21	4.19
		s.d. (mm)	0.01	0.01	0.01	0.01
		% s.d./aver.	0.2%	0.1%	0.2%	0.3%

makes possible the machining of green parts useful to achieve some design features that could be hard or impossible to obtain in the moulding step or by operations after sintering [1].

Binder L-13 provides the strongest and toughest green parts, followed by L-16. Moulded materials of binder with LDPE/PEW2 and MPE/PEW2 have 28 to 35 % less strength. This lower performance can be explained by the lower strength of LDPE and MPE comparing to PMMA and PVB, which is also decreased with the addition of the wax.

Pictures of some tested parts and respective fractures sections are shown in Figure 4.24. If there is some weaker point in the bulk due to some anomaly in moulding process or feedstock heterogeneity, parts will fracture in that site even if it was less stressed than the maximum stressed point in the middle of the bar. In contrast, it can be observed that all parts failed in the middle section of the bars. Fracture sections do not show signs of heterogeneities, as voids or

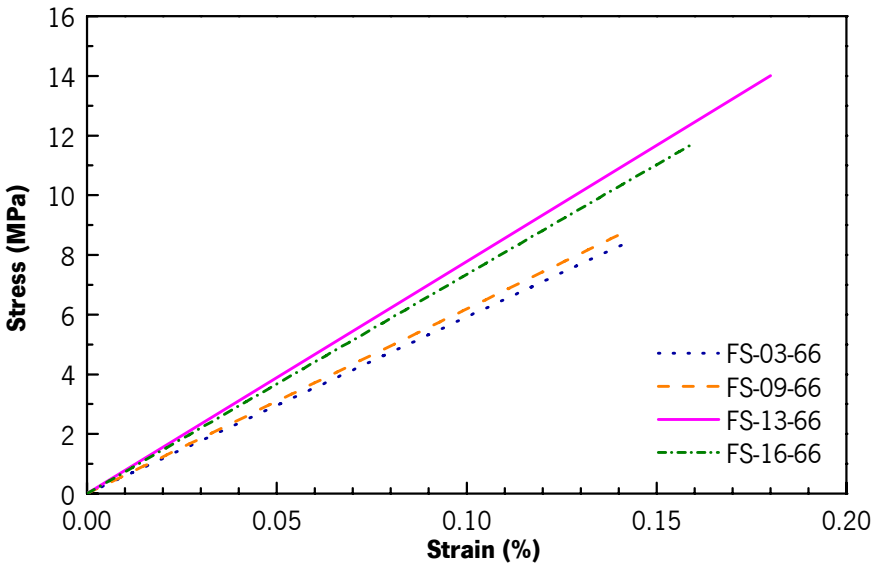

Figure 4.23 Stress curves of flexure test of the green parts.

Table 4.10 Mechanical flexure properties of the injection moulded parts.

	FS-03-66	FS-09-66	FS-13-66	FS-16-66
Strength (MPa)	8.53	8.49	13.38	11.84
Modulus (GPa)	6.04	6.18	7.64	7.36
Strain at break (%)	0.14	0.14	0.18	0.16

flaws. This suggests that the bars were appropriately moulded and homogeneous, evidencing once more a stable injection moulded process.

4.2.3. Debinding

Debinding of tensile specimens of FS-03-66 and FS-09-66 has removed binder without externally visible defects, reaching 93 % and 91% wt.% of PEG removal, respectively (Table 4.11).

However, debinding with binders L-13 and L-16 produced some defects. Cracks were observed in L-13 mouldings and softening and blistering in L-16 mouldings. Some experimental efforts (summarised in Table 4.12 and Figure 4.25) was done to eliminate these defects as following described:

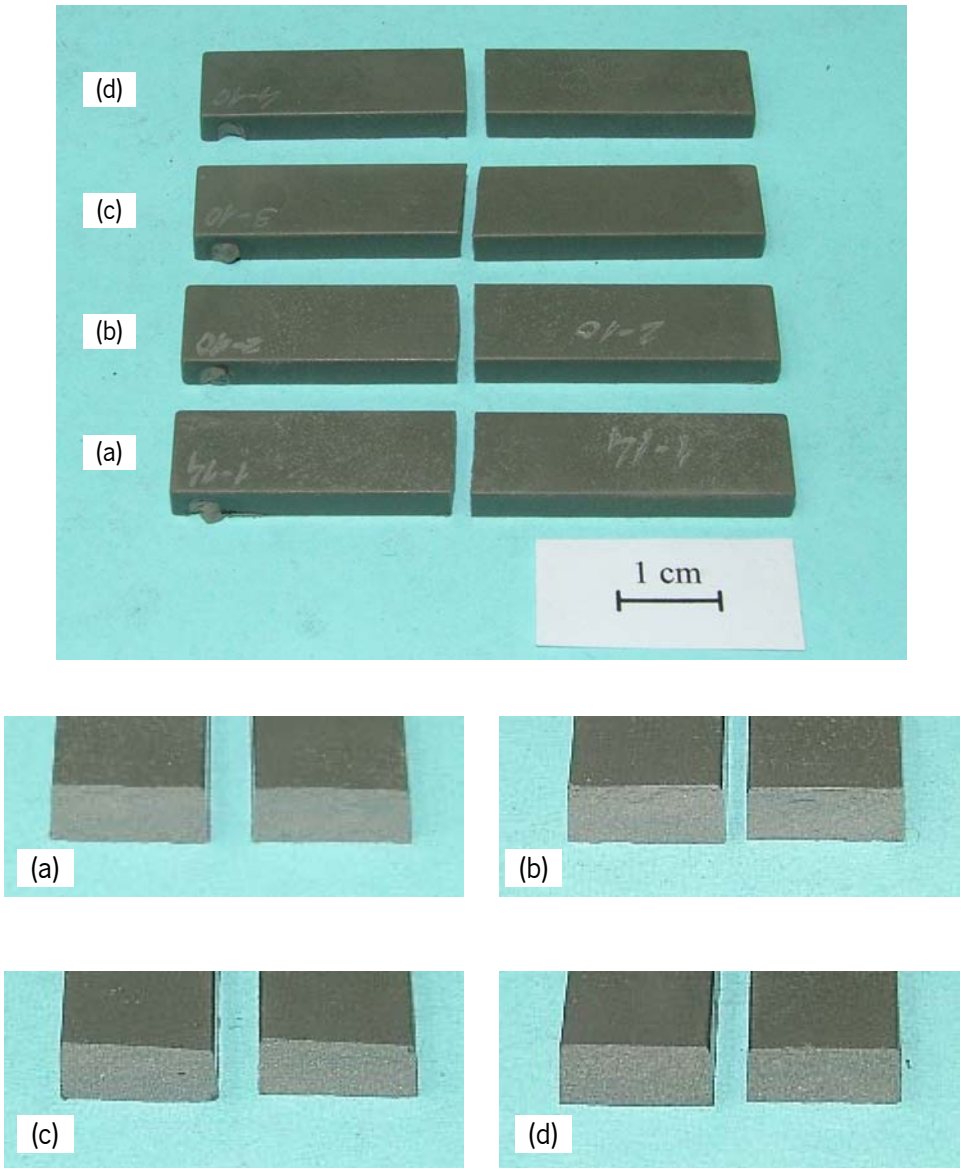

Figure 4.24 Fractured flexure specimens after testing from different feedstocks: (a) FS-03-66; (b) FS-09-66, (c) FS-13-66 and (d) FS-16-66-

- FS-13-66 parts:

At the initial stated conditions (run i), it was observed fissures on the surface in contact with the support. A test were performed with parts turned around to verify the effect of the face contacting the support (run i), suspecting that a moulded part has two different halves as an effect of thermal discrepancy in the two mould halves. This hypothesis was not verified. Inspecting the effect of the support, it was tried a wire mesh (run iii), attempting to increase

Table 4.11 Weight loss in water debinding at 50 °C of tensile moulded parts.

	FS-03-66	FS-09-66	FS-13-66	FS-16-66
Parts mass loss (wt.%)	4.4	4.2	4.5	4.4
Binder loss (wt.%)	66	64	62	64
PEG loss (wt.%)	93	91	89	91

the homogeneity of the binder extraction in part surface. The result was positive as the fissures disappeared.

It has been observed that moulded parts can show dimensional expansion when immersed in solvents as a response to the temperature changing and/or to binder swelling due to the solvent affinity [22, 226]. The reason for the fissures occurrence in PMMA mouldings rather than LDPE/PEW2 could be related to the higher affinity to water. PMMA has typical water absorption of 0.1 – 2 % [227], which is significantly higher comparing to LDPE under 0.02 % [227].

Despite of the reduction of the parts fissuring as they were more uniformly wet, on the wire mesh support, small cracks were still present resulting from a possible effect of moulding dimensional variation during immersion. Decreasing the water temperature in order to change process kinetics (run iv), changing parts position on support (run v) or suspending (run vi) were not succeeded strategies to avoid debinding defects on part with binder L-13.

- FS-13-66 parts:

None of the trials had success to prevent the blistering and softening. Picture (c) of the Figure 4.25 is indicative of the effect of the softening of the mouldings, causing sink marks due to the wire mesh support.

Binders L-13 and L-16 were quit since it was verified a propensity to the occurrence of debinding defects on the respective moulded parts.

FS-03-66 and FS-09-66 moulded flexure bars were debinded at 35 °C and 89 and 90 wt.% of PEG was removed.

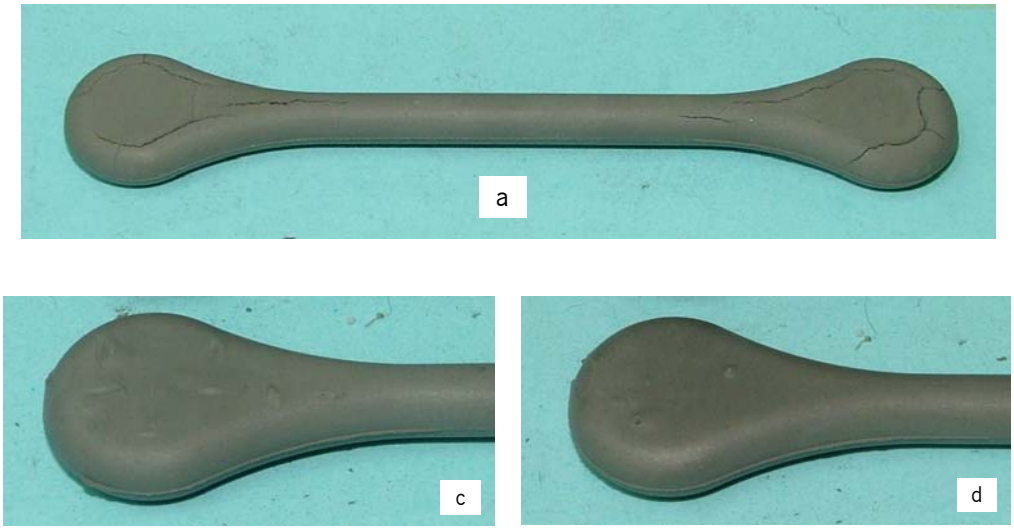

Figure 4.25 Defects detected on the debinded parts, referred on Table 4.12.

Table 4.12 Debinding trials of parts with binders L-13 and L-16.

Binder	Run	Water temp. (ºC)	Support	Face down	PEG weight loss (%)	Defects *
L-13	i	35	perforated sheet	Injection side	81	a
	ii	35	perforated sheet	Extraction side	81	a
	iii	35	wire mesh	Injection side	81	b
	iv	25	wire mesh	Injection side	77	b
	v	25	wire mesh	Extraction side	77	b
	vi	25	(Suspended)	-	78	b
L-16	i	35	perforated sheet	Injection side	88	c+d
	ii	35	perforated sheet	Extraction side	88	c+d
	iii	35	wire mesh	Injection side	90	c+d
	iv	25	wire mesh	Injection side	78	c+d
	v	25	wire mesh	Extraction side	78	c+d

* a: fissuring; b: cracking; c: softening; d: blistering

4.2.4. Sintering

Different results were obtained by sintering of the parts produced with binders L-03 and L-09, in terms of defects incidence (Figure 4.26). Tensile specimens of feedstock FS-03-66 presented two defects.

Blisters occurred in the centre of the heads of the tensile specimen (Figure 4.27 a), which

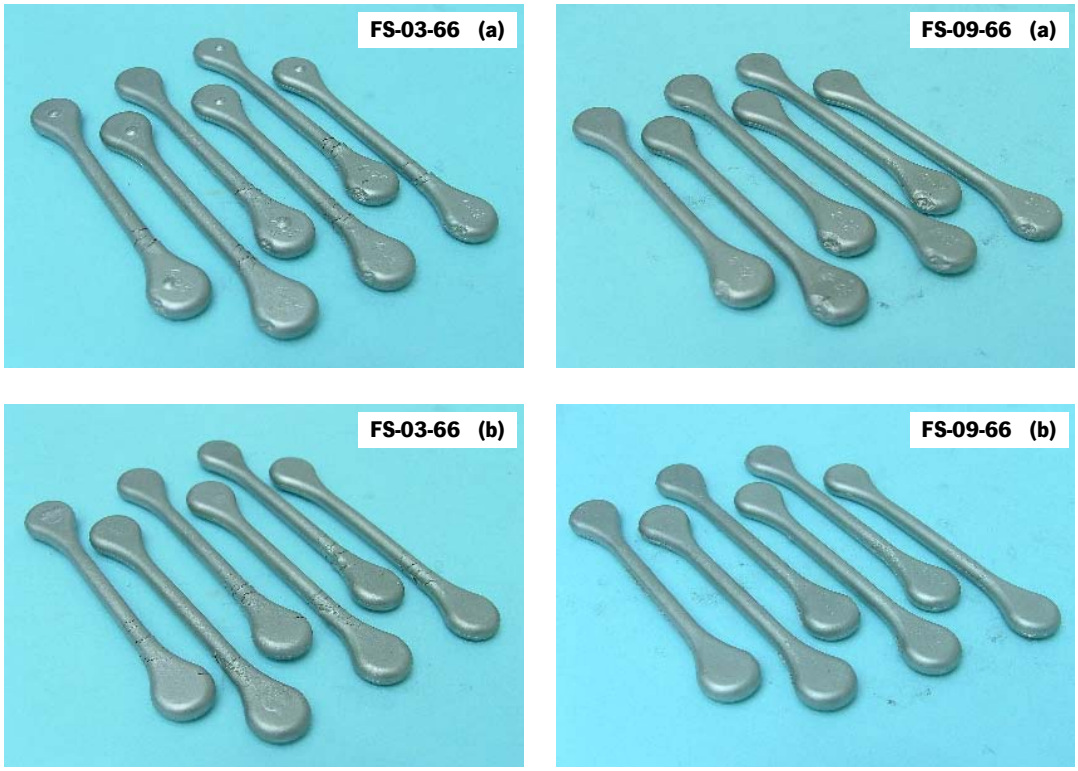

Figure 4.26 Sintered tensile specimens showing the upper side (a) and bottom side (b) relative to the sintering position.

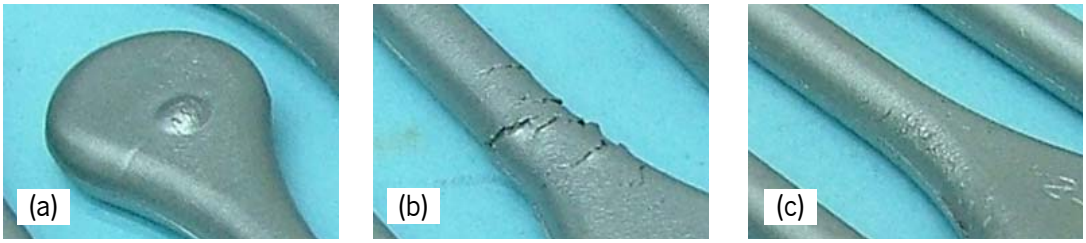

Figure 4.27 Detail of the defects observed on the surface of the sintered parts: blistering (a) and peeling (b) with feedstock FS-03-66 and non-smooth surface (c) with feedstock FS-09-66.

typically reveal an inadequacy between the thermal degradation process and the amount of binder in the parts. When the amount of binder is excessive or the degradation rate is relatively high, the degradation products generate pressure yielding to blistering. This problem can be solved by increasing of the PEG removal or so redesign the sintering cycle to relieve the binder degradation.

Peeling was formed in the testing zone of the specimen, particularly in the end near the injection gate (Figure 4.27 b). Parts of feedstock FS-09-66 also evidenced few defects. The only visible anomaly was the corrugated surface on the end of the test section near the gate (Figure 4.27 c). This defect was also visible in the sintered flexure bars of both feedstocks. Peeling and corrugated surface in all those parts are approximately at the same distance, close to the gate. The melt from which this defect appeared can be considered to be the first to enter the cavity, so an hypothesis rise that this problems can be related to phase-separation when melt feedstock is passing trough that narrow sectioned channel. Considering the injection flow rate profile (Figure 3.23) used, it is reasonable to suppose that the first melt was entering at 35 $cm^3.s^{-1}$, was exposed to excessive shear and thus phase separation. The remaining material, flowed at 15 $cm^3.s^{-1}$, was not affected. A solution would be to anticipate the final injection stage in order to fill the entire cavity at the lower rate. The reason for the different defects, peeling or corrugated surface, is not explained but it is speculated that they were the same problem at different magnitudes.

Weight, density and dimensional analysis of the sintered parts

Table 4.13 shows the statistics data of weight and density of the sintered parts. The parts are quite similar since they come from feedstock with the same solids fraction and green density. The variability of parts weight varies between 0.11 % and 0.19 %, which is close to the best for the PIM technology (best: 0.1 %, typical: 0.4 % [30]). Densities of 7.94 to 7.95 g/cm^3 were achieved, and are in the range encountered of PIM of 316L stainless steel, 7.6 to 8-0 g/cm^3 [30]. These values are close to the density of the powder, and considering the microstructure and the chemical composition of the material were not changed, the densification was near full.

Dimensional control data is presented in Table 4.14. The size variability, calculated by the ratio of standard variation and the average, is 0.1 to 0.3 % for FS-03-66 parts and 0.1 to 0.4 % for FS-09-66, which is typical for PIM. Common precision is a minimum of 0.03/0.05 %, typical of 0.3 % and a maximum of 2.0 % [30]. Observing the relationship of the standard deviation with the

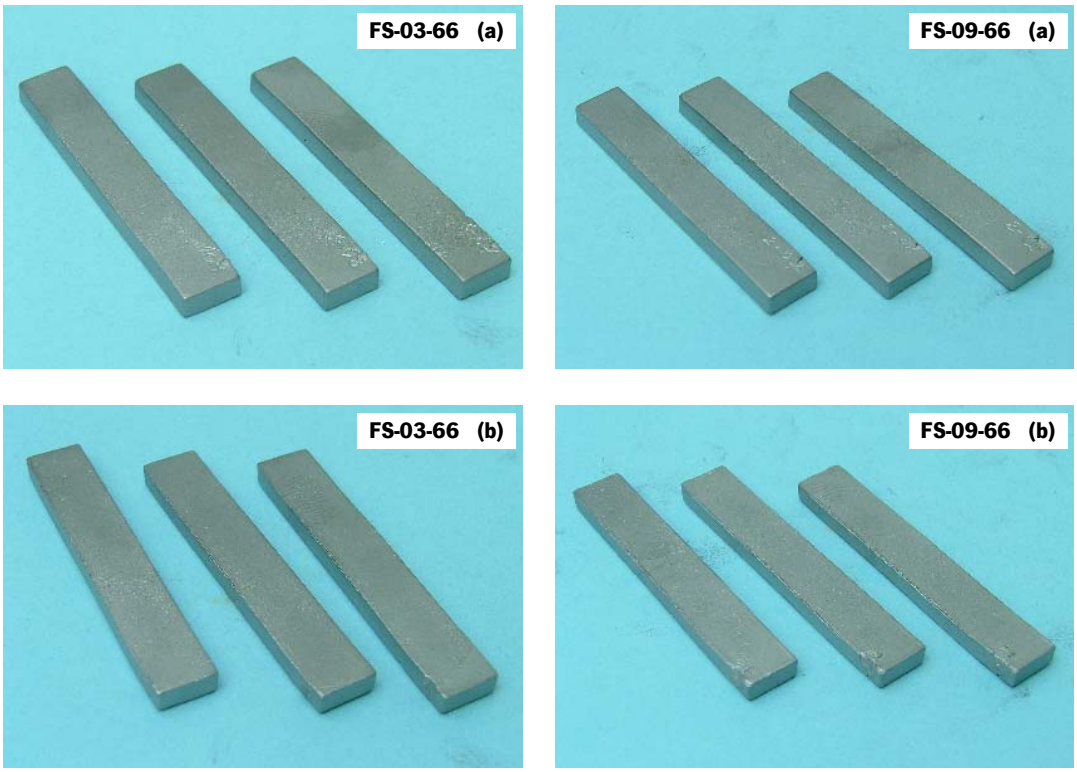

Figure 4.28 Sintered bars showing the upper side (a) and bottom side (b) relative to the sintering position.

Table 4.13 Physical properties of the sintered parts.

	FS-03-66			FS-09-66		
	average	s.d.	% s.d./aver.	average	s.d.	% s.d./aver.
Weight (g)						
Tensile specimen	15.6981	0.0168	0.11%	15.7418	0.0279	0.18%
Flexure specimen	12.7750	0.0192	0.15%	12.7890	0.0237	0.19%
Density (g/cm³)						
Tensile specimen	7.95	0.04	0.5%	7.94	0.01	0.1%
Flexure specimen	7.95	0.01	0.2%	7.96	0.02	0.3%

average of dimensions, in green and sintered parts (Figure 4.29), it is observed that the variation increase with the size. Moreover, the standard deviation increases after sintering, being more pronounced in the larger sizes. This is due to the shrinkage, resulting as another factor of dimensional inaccuracy. This effect seems to be proportional to the size of the dimension.

Figure 4.30 shows the shrinkage in the controlled dimensions, from green to sintered state. Nevertheless the solids fraction of a feedstock would be the major factor affecting the shrinkage, the results show that it is also influenced by the dimension and the geometry of the part.

Table 4.14 Dimensional control of the sintered parts

		FS-03-66			FS-09-66		
		average	s.d.	% s.d./aver.	average	s.d.	% s.d./aver.
Tensile specimen	l (mm)	77.81	0.12	0.2%	77.87	0.25	0.3%
	t_1 (mm)	4.43	0.01	0.2%	4.43	0.01	0.3%
	t_2 (mm)	4.43	0.01	0.2%	4.42	0.01	0.2%
	t_3 (mm)	4.47	0.02	0.5%	4.48	0.01	0.3%
Flexure specimen	l (mm)	51.92	0.05	0.1%	51.92	0.06	0.1%
	w (mm)	8.82	0.03	0.3%	8.86	0.04	0.4%
	t (mm)	3.61	0.01	0.3%	3.63	0.01	0.3%

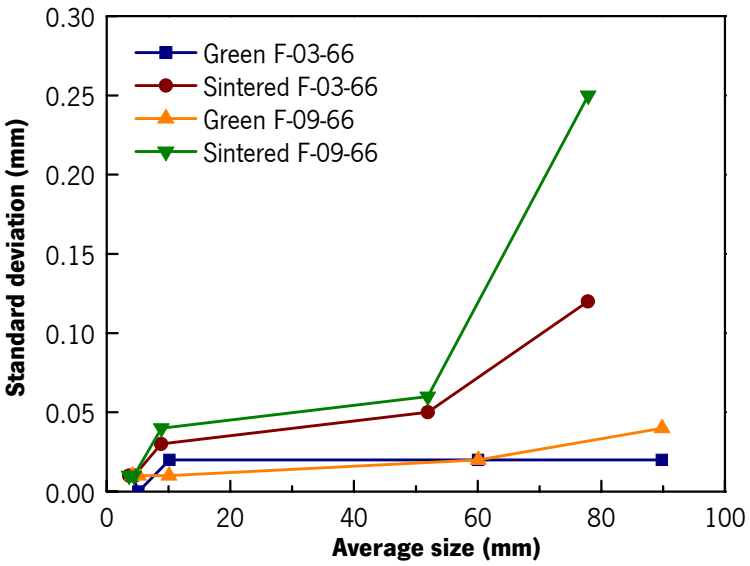

Figure 4.29 Standard deviation against the average size of green and sintered parts.

Back-bone polymers seem not to affect the shrinkage as the feedstocks produced similar results.

In the tensile specimen, length and thickness t_3 have shrunk ca. 13.3 %, however shrinkage has increased in thicknesses t_1 and t_2 to 14.0-14.4 %. Therefore, it is demonstrated that the present feedstocks, moulded in the tensile specimen cavity in those process conditions, have a

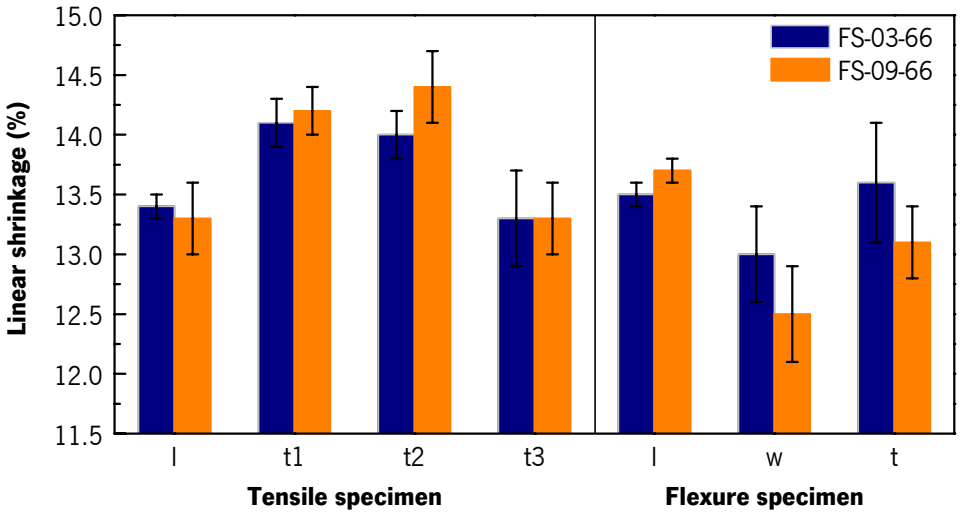

Figure 4.30 Linear shrinkage from green to sintered state.

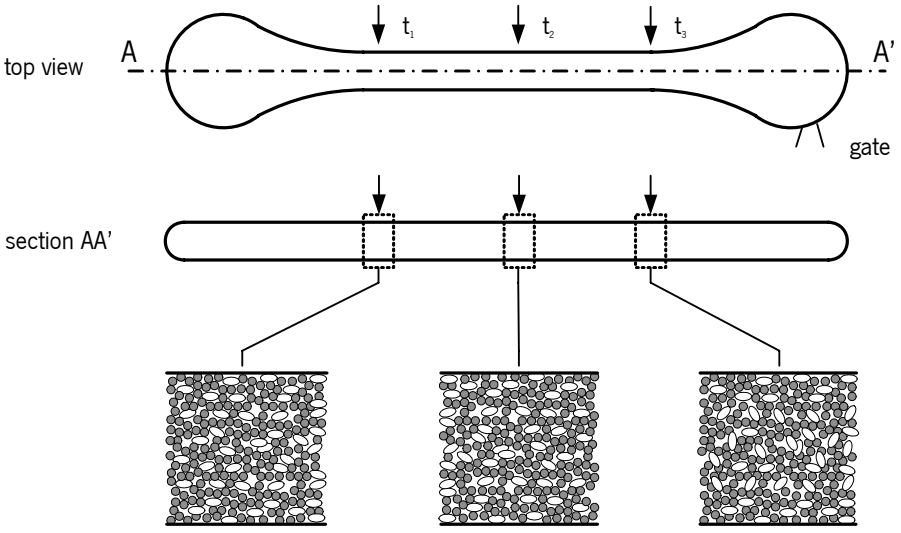

Figure 4.31 Model of the particle orientation in an injection moulded tensile part.

anisotropic shrinkage. This fact can be explained by the orientation of the non-spherical powder particles (previously observed by SEM) caused by the high sheared flow, as shown by the model in Figure 4.31**.** In thin section high shear stresses yield an alignment of non-spherical particles along the flow direction (sections t_1 and t_2). The particle alignment causes a difference in the linear powder concentration, higher in the longitudinal than in the transversal direction. Then shrinkage will be higher in the low concentrated direction, i.e. transversal. In section t_3, which shrinkage is at the level of the length, suggests that probably the shear stress was not enough to direct the particles.

Thickness t_3 is higher than t_1 and t_2 in sintered parts, differing by 0.04 mm. Therefore, it is demonstrated that anisotropy of shrinkage must be well known in order to design the mould with a very well dimensioned cavity, compensating the different material shrinkage in different dimensions.

Chemical composition

Changes in chemical composition of sintered parts comparing to the chemistry of the starting powder, shown in Table 4.15, was not relevant, in such a way that it is according to the standard

Table 4.15 Elemental composition of sintered parts, compared with the starting powder and the standard powder metallurgy material.

		Powder	FS-03-66	FS-09-66	Standard [48]
Chemical composition (wt.%)	**Cr**	16.7	16.9	16.6	16.0-18.0
	Ni	10.1	11.6	11.0	10.0-14.0
	Mn	1.30	0.60	0.84	0-2.0
	Mo	2.62	2.16	2.19	2.0-3.0
	Si	0.40	0.69	0.49	0-1.0
	S	0.011	0.006	0.006	0-0.03
	C	0.02	0.03	0.03	0-0.03
	P	0.02	0.05	0.05	0-0.045
	N	0.097	0.004	0.004	0-0.03
	O	0.124	0.007	0.012	–

composition range. The effect of the presence of graphite as construction material of the inner walls and the heating elements of the furnace is observed in the increase of carbon content. Nevertheless, the final carbon content 0.03 % is still acceptable.

Mechanical properties

As expected, FS-03-66 tensile specimens have fractured in the weakest point of the test section, where there was the peeling defect (Figure 4.33). However, the yield and the ultimate stress, 246 MPa and 545 MPa, are above the typical values according to the PIM standard, 172 MPa and 517 MPa, respectively (Figure 4.32 and Table 4.16). The fracture elongation, 21 %, did not reach the minimum required, 40 %.

FS-09-66 sintered specimens are outstanding comparing to the typical PIM standard, showing a typical high ductility - 58 % of fracture elongation. Beyond the minimum elemental contamination level, near-full density could be the reason for these results, and made possible to raise the mechanical properties to casted materials values.

Photos of the fracture section surface, taken with a stereomicroscope (Figure 4.33), reveals the differences of state of the material after stressing, which can be useful to attempt to the material condition after sintering. Peeling in FS-03-66 caused the reduction of the section area as there is a layer separated from the core material, which seems to be a reason for the lower mechanical properties comparing to FS-09-66. The latter shows a reduction of area typical of the ductile material. Visible defects were not found, explaining the good mechanical performance obtained.

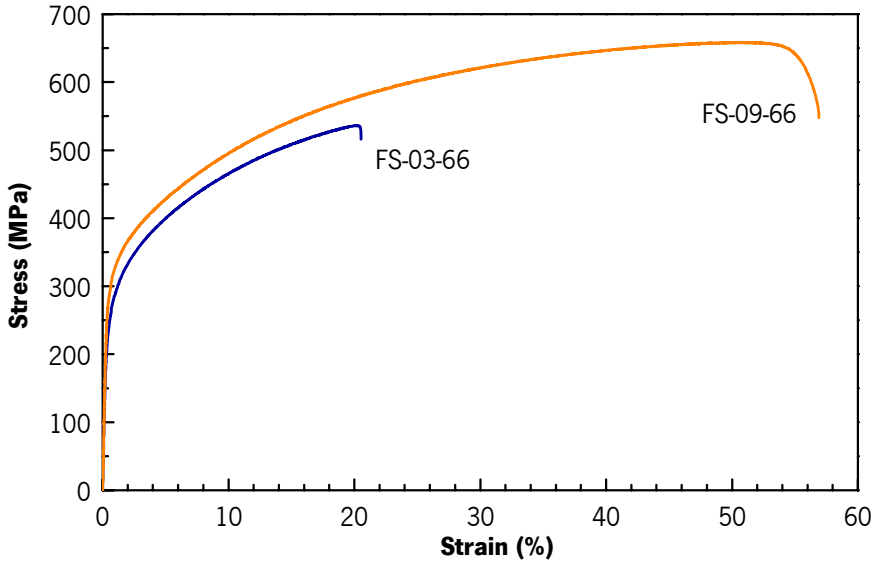

Figure 4.32 Tensile stress vs. strain of the sintered parts.

Table 4.16 Mechanical properties of the sintered parts.

	FS-03-66		**FS-09-66**		**PIM Standard** [228]		**Casted** [229]	[48]
	average	s.d	average	s.d.	min.	typical	min.	typical
Young's modulus (GPa)	166	1	185	1	-	193	-	-
Yield stress 0.2% (MPa)	246	22	264	32	138	172	205	353
Ultimate Tensile Stress (MPa)	545	13	647	29	448	517	485	693
Elongation at break (%)	21	2	58	1	40	50	30	50

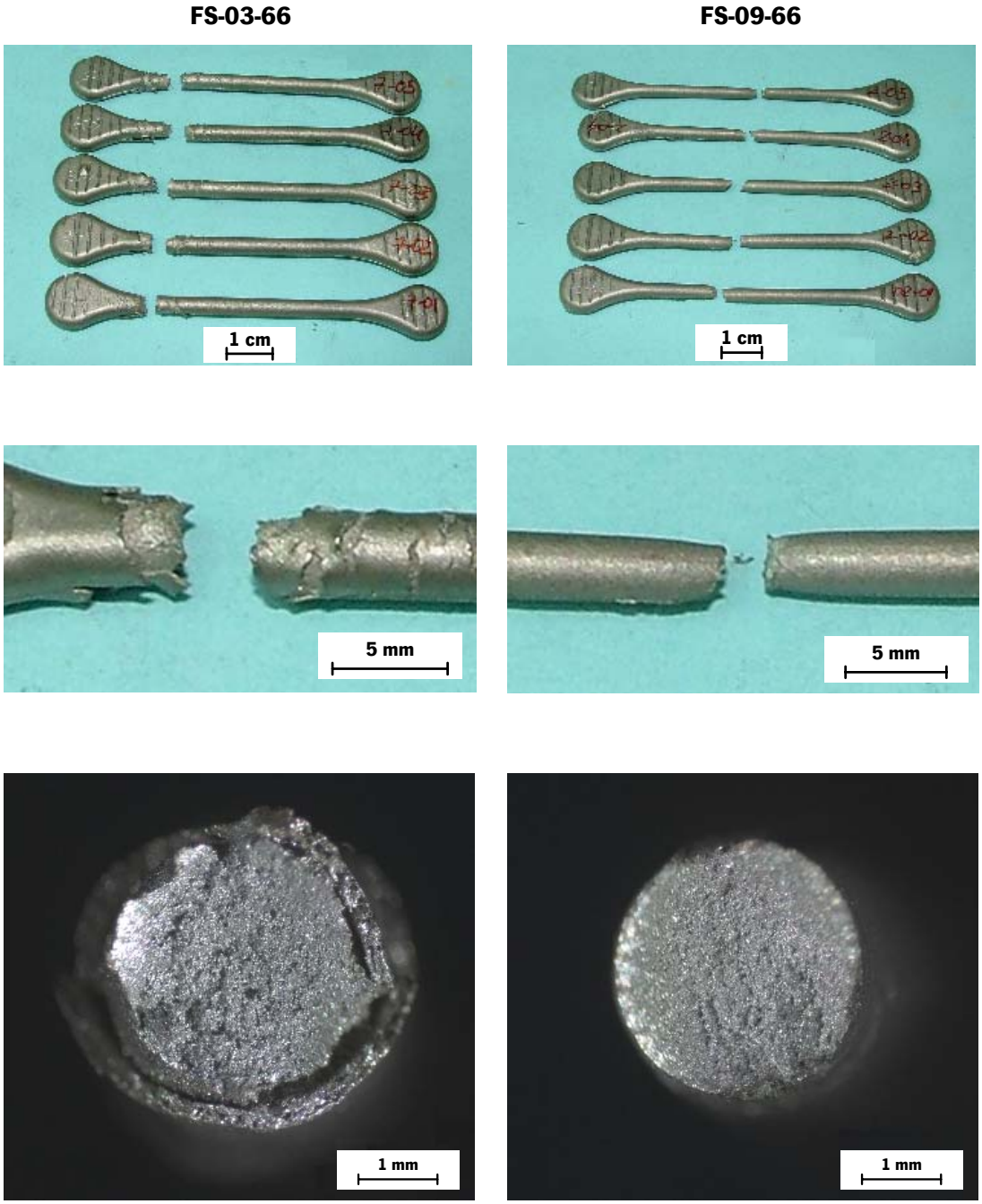

Figure 4.33 Pictures of tensile tested specimens.

4.2.5. Partial conclusions

Four binder compositions were tested in injection moulding process of stainless steel 316L powder. Common component were PEG, as the water soluble component, and stearic acid as surfactant. The formulations were different in the composition of the back-bone polymers having LDPE/PEW2 (L-03), MPE/PEW2 (L-09), PMMA (L-13) and PVB (L-16).

Mixing of the powder and binder resulted in a reasonable homogenous feedstock, according to the results obtained by the two homogeneity technique used: capillary flow pressure stability and picnometry density. Air entrapment was detected in mixtures with binders L-03, L-13 and L-16, which can be due to an inadequate process conditions in the shear roll mixer. The adequate homogeneity of the feedstock was related to the good stability injection moulding process, analysed by the variability of the part weight. Furthermore, it was concluded that the higher homogeneous mixtures, based on L-13 and L-16, provided a more stable moulding process. Homogeneity was also confirmed by the mechanical testing of moulded bars.

Feedstocks showed elastic mechanical behaviour. High solids content, as 66 vol.% present in the formulations, increases the flexure modulus of the injection moulded plastics. Present in a relatively low amount, by 9 to 10 vol.% in the four compounds, back-bone polymers has a great effect on the ultimate flexure stress and modulus of the moulded materials. Lower strength materials, LDPE/PEW2 and MPE/PW2, yield to around 30 % lower strength and about 19 % lower modulus than PMMA and PVB.

ISO standard tensile specimens were debinded in water at 50 °C for 15 hours, resulting in the removal of 93, 91, 89 and 91 % of the mass of PEG in parts produced from binders L-03, L-09, L-13 and L-16, respectively. Parts of binders L-03 and L-09 were free of external defects, however the others showed some defects which could not be avoided by the further trail and errors experiments. In view of such limitation in water debinding, binders L-13 and L-16 did not carry to the sintering.

Different results were obtained in terms of defects occurrence in the sintered parts. Tensile specimens produced with binder L-03 showed blisters in thick areas and peeling in a very particular zone. L-09 parts and bars of both materials showed minor corrugate surface defects. Peeling and corrugated surface was believed to have same source, due to phase separation in

the gate, but in different magnitudes. This difference was reflected on the results of the mechanical testing, being detrimental for the parts L-03. However, they had higher yield and ultimate stress (246 MPa and 545 MPa) than the minimum PIM standards (138 MPa and 448 MPa). L-09 parts presented higher mechanical properties comparing to PIM standard, similar to casted material. This satisfactory performance was attributed to the near-full density of the sintered material and to the preservation of the chemistry of the 316L stainless steel alloy.

Binders L-03 and L-09 produced similar parts in terms of weight variability, dimensional precision and linear shrinkage, thus different composition in back-bone polymers did not reveal to be a factor. Weight variability was remarkable low (from 0.11 % to 0.19 %), close to the best for PIM technology (0.1 %). Dimensional precision was achieved in 0.1 % to 0.4 % range, in both FS-03-66 and FS-09-66 feedstocks, in neighbouring the typical value of 0.3 %. Anisotropic shrinkage was detected, by the difference from ca. 13.3 % to 14.4 % in perpendicular dimensions, and it was correlated in the non-sphericity of a small part of the powder particles.

5. CONCLUSIONS

A common binder system is a multicomponent thermoplastic polymeric blend necessary for powder injection moulding. Despite of being a temporary actor in the process, it plays an important role since it has a major influence on success of all of the process stages. In order to develop structured knowledge in binder engineering, and thus being able influence in process, a new methodology was proposed and applied to characterise binders in some aspects considered relevant in all the process phases.

The work programme was basically divided in two parts. First, a set of binder formulations were characterised so that their behaviour in the process could be predicted and and their adequacy discriminated. Second, a group of these binders were studied in process by characterising the sub-processes and parts from compounding to sintering. This study was applied using a PIM standard powder of 316L stainless steel.

5.1. Influence of binder formulations on feedstock characteristics

A family of polyethylene glycol (PEG) based-binders, designed for water debinding was studied. Back-bone polymers were combinations of low density polyethylene (LDPE), metallocene polyethylene (MPE), poly(methyl methacrylate) (PMMA), poly(vinyl butyral) (PVB), two polyethylene waxes (PEW1 and PEW2) and an oxidized polyethylene wax (OPEW). Influence of surfactant was verified by using stearic or oleic acids. Characterisation methods and data analysis tools were developed and applied based on previously published knowledge and can be considered for further employment in future investigations. The melting point depression method was applied to the analysis of PIM binder polymeric components. An analysis method improvement was tried, aiming to standardise the method of critical powder volume concentration determination by mixing torque rheometry.

Compatibility of binder components was generally observed in all binder formulations as there was always, at least, one component showing melting point depression. Moreover, LDPE evidenced to be more effective providing compatibility with PEG and PEW's mixtures than MPE. Binders with PEW2 exhibited higher compatibility than with PEW1. No relevant effect of the chemical differences of stearic an oleic acid was detected. SEM observation of pressed feedstock revealed that lower compatible systems, with metallocene polyethylene, have formed heterogeneous features, in particular polymeric filaments.

Critical powder concentration was not considered to be reasonably scattered among the mixtures based on the studied binders, confirming that the powder characteristics would be the major factor influencing this parameter. Critical values were between 69 and 71 vol.%, thus feedstocks fraction of 66 vol.% was considered henceforth. The melt viscosity of feedstocks at 155 °C demonstrated to be highly influenced by the amount of the wax content, acting as a lubricant. Powder law indexes, between 0.64 and 0.77, did not vary notably. Yet, trends were discovered in shear sensitivity being enhanced with PEW2 rather than PEW1 and with SA than OA.

Debinding in water showed an influence of back-bone polymers and waxes. Binders with PEW1 had higher PEG removal than with PEW2, and LDPE provided higher extraction than MPE. Water extraction showed to be the main advantage to use PMMA, creating a higher debinding rate. PMMA provides the easiest mixture to be debinded, reaching 98 % of PEG removal in 2 mm thick pressed specimens after 6 h. Thermogravimetric analysis of those debinded parts determined that the polyethylenes based binders would have fewer propensities to cause defects related to binder thermal degradation in the initial stage of the sintering.

It was not found a clearly favourite binder which stood out in all aspects, so a balance needed to be done aiming global binder discrimination. A classification exercise was done by scoring the binders in each analysed aspect. Binder L-03 was considered the most appropriate binder with the best score, followed by L-01, i.e. PEG/LDPE/Wax/SA was the best combination. PEW2 has dictated the best performance for L-03. This wax is also present in the best MPE based binders, L-09. Binders with PMMA, PVB and PEW2 alone are considered the least attractive for PIM. However, PMMA binder was top score in water debinding.

5.2. Influence of binder on process characteristics

Four binder compositions were tested in injection moulding of stainless steel 316L powder: PEG/LDPE/PEW2/SA (L-03), PEG/MPE/PEW2/SA (L-09), PEG/PMMA/SA (L-13) and PEG/PVB/SA (L-16). Two complimentary methods for the assessment of the homogeneity of the mixtures of powder and binder were used. All binders resulted in a reasonable homogenous feedstock with 66 vol.% of solids. Air entrapment was detected in mixtures with binders L-03, L-13 and L-16, which could be due to an inadequate process conditions in the shear roll mixer. The adequate homogeneity of the feedstock was related to the good stability of the injection moulding process, analysed by the variability of the parts weight. Furthermore, it was concluded that the higher homogeneous mixtures, based on L-13 and L-16, provided a more stable moulding process. Homogeneity was also confirmed by the mechanical testing of moulded bars.

Moulded parts showed brittle behaviour. Present in a relatively low amount, by 9 to 10 vol.% in the four feedstocks, back-bone polymers had a great effect on the ultimate flexure stress and modulus of the moulded materials. Higher strength materials, PMMA and PVB, yield to about 35 % higher strength and 25 % higher modulus than LDPE/PEW2 and MPE/PW2.

ISO standard tensile specimens were debinded in water at 50 °C for 15 hours, resulting in the removal of 93, 91, 89 and 91 % of the PEG mass of parts produced with binders L-03, L-09, L-13 and L-16, respectively. Parts of binders L-03 and L-09 were free of external defects, however the others showed some. Fissuring and cracking was supposed to be related to the some water affinity of PMMA, based on the water absorption data, in comparison to LDPE, and to the possible swelling and anisotropic volume expansion. Debinding experiments in the first phase of the work were not effective to preview the occurrence of these defects. This divergence can be related to the geometry of the parts and moulding process. Previously, parts were pressed to a much smaller and thinner shape and then they were injection moulded to larger and thicker parts. It is well known the dependence of debinding defects on part size and on the process.

Binders L-03 and L-09 produced similar sintered parts in terms of weight variability, dimensional precision and linear shrinkage, thus different composition in back-bone polymers did not reveal to be an influencing factor. Weight variability was low (from 0.11 % to 0.19 %), close to the best for PIM technology (0.1 %). Dimensional precision was achieved in 0.1 % to 0.4 % range, in both L-03 and L-09 feedstocks, in neighbouring the typical value of 0.3 %. Anisotropic shrinkage was

detected, by the difference from ca. 13.3 % to 14.4 % in perpendicular dimensions, and it was correlated in the non-sphericity of a part of the powder particles.

Different results were obtained in terms of defects occurrence in the sintered tensile specimens. Parts produced with binder L-03 showed blistering and peeling in very particular zones. L-09 parts showed minor defects, with minimal effect on the quality of the part. The difference of the defects magnitude was reflected on the tensile properties, being detrimental for the parts L-03. However, these parts had higher yield and ultimate stress than the typical standards. L-09 parts presented higher mechanical properties comparing to PIM standard, similar to casted material. This satisfactory performance was related to the near-full density of the sintered material and to the preservation of the chemistry of the alloy.

This study was important to understand the influence of the binder composition in the powder injection moulding, in particular the effect of the back-bone polymers of a water soluble PEG-based binder. The influence of those components in a low content as 17.5 % w/w of binder was reflected in some aspects, as feedstock homogeneity, green strength, and defects incidence after debinding and sintering. In other hand, sintered parts density, weight, dimensions and chemistry were not evidently affected.

5.3. Suggestions for future work

The execution of this work has opened a range of possibilities to enrich knowledge around the binder design for powder injection moulding and to proceed for an improvement of the water soluble binder systems. This further work can be scientifically interesting and can be configured in the following items:

- To study the rheology of each individual binder components, binder formulations and feedstocks, in order to understanding the contribution of each binder component for the feedstock rheology, compare to literature models and develop new ones;
- To study the wet ability of the binder formulation as another discrimination factor in binder design. Defects observed in sintered parts could be related with phase separation during moulding. Wetting characterization can reveal the distinct interaction of different binders with powder;
- To study the effect of pre-coated powder, produced by adsorption of surfactants. Pre-coated powders has been considered to improve binder adhesion onto powder surface, having as an advantage the decreasing the binder-powder separation in the injection moulding process [60]. This suggestion intends to attempt suppress the peeling defect encountered in L-03 sintered parts by changing binder formulation instead of process conditions. Analysis must also be conducted to evaluate any effect in carbon or oxygen enrichment in sintered parts due to higher interaction of powder with binder.
- To use the methodology used and binder formulations with other powders with different characteristics, i.e. chemical, morphological, particle size. Work with other powders will provide validation of the methodology and, in case, to evaluate the influence of powder in the binder design. More, the development of a success binder system must be carried after the proof of being suitable for several powder materials, showing flexibility and economically interesting.

In the presence of reasonable good results in processing 316L stainless steel powder with the binder formulation L-09, a perspective of industrial environment application can be raised. Therefore, some work must be done around as in the following topics:

- To test the feedstock in the production of real application parts, usually with intricate geometries;
- To study the constancy of the feedstock by analysing the batch-to-batch reproducibility of the process and parts characteristics;
- To evaluate the recyclability of the feedstock.

6. REFERENCES

1. German, R.M. and A. Bose, *Injection Molding of Metals and Ceramics*. New Jersey: MPIF - Metal Powder Industries Federation (1997).
2. Mutsuddy, B.C. and R.G. Ford, *Ceramic Injection Molding*. New York, NY: Chapman & Hall (1995).
3. Foong, M.L. and K.C. Tam, *Application of Polymer Technology to Metal Injection Molding (MIM)*, in *Advanced Polymer Processing Operations*, N.P. Cheremisinoff, Editor. Noyes Publications: New Jersey (USA), 1998.
4. German, R.M., *PIM breaks the $1 bn barrier.* Metal Powder Report, 63(3): p. 8-10 (2008).
5. *Feedstocks: To buy, or not to buy?* 1999 [cited 27-03-2007]; Available from: http://www.immnet.com/article_printable.html?article=838.
6. Zauner, R., et al., *Variability of feedstock viscosity and its correlation with dimensional variability of green powder injection moulded components.* Powder Metallurgy, 47(1) (2004).
7. Rhee, B.O. and C.I. Chung. *Effects of the binder characteristics on binder separation in powder injection molding*. in *Powder Injection Molding Symposium*, 1992
8. Herranz, G., et al. *Effect of Binder Composition on Rheological Behaviour of M2-HSS Powder-Polymer mixtures for PIM Tech*. in *PM2TEC - Advances in Powder Matellurgy and Particulate Materilas 2002*, Orlando (USA), 2002
9. Lee, S.H., et al., *Effects of binder and thermal debinding parameters on residual carbon in injection moulding of Nd(Fe, Co)B powder.* Powder Metallurgy, 42(1): p. 41-44 (1999).
10. Kim, S.W., H.-W. Lee, and H. Song, *Effect of minor binder on capillary structure evolution during wicking.* Ceramics International, 25(7): p. 671-676 (1999).
11. Xie, Z.-p., et al., *The effect of organic vehicle on the injection molding of ultra-fine zirconia powders.* Materials & Design, 26(1): p. 79-82 (2005).
12. Omar, M.A., et al., *The influence of PMMA content on the properties of 316L stainless steel MIM compact.* Journal of Materials Processing Technology, 113(1-3): p. 477-481 (2001).
13. Hsu, K.C., C.C. Lin, and G.M. Lo, *Effect of wax composition on injection moulding of 304L stainless steel powder.* Powder Metallurgy, 37(4): p. 272-276 (1994).
14. Pompe, R. and J. Brandt, *Goceram's MEDPIMOULD technology offers cost-effective PIM production.* Metal Powder Report, 56(n°6), 01-06-2001: p. 14-17 (2001).

15. Bandyopadhyay, G. and K.W. French, *Injection molded ceramics: critical aspects of the binder removal process and component fabrication.* European Ceramic Society, 11: p. 23-34 (1993).

16. Wright, J.K., J.R.G. Evans, and M.J. Ediringhe, *Degradation of Plyolefin Blends Used for Ceramic Injection Molding.* J. Am. Ceram. Soc., 72(10): p. 1822-28 (1989).

17. Kim, S.W., et al., *Pore structure evolution during solvent extraction and wicking.* Ceramics International, 22(1): p. 7-14 (1996).

18. Schwartz, S., P. Quirmbach, and M. Kraus. *Solvent Debinding Technology for a Continuous 316L MIM-Production*. in *PM2TEC*, 2002

19. Li, S., et al., *A new type of binder for metal injection molding.* Journal of Materials Processing Technology, 137: p. 70-73 (2003).

20. Hwang, K.S., G.J. Shu, and H.J. Lee, *Solvent debinding behavior of powder injection molded components prepared from powders with different particle sizes.* Metallurgical and Materials Transactions a-Physical Metallurgy and Materials Science, 36A(1): p. 161-167 (2005).

21. Oliveira, R.V.B., et al., *Ceramic injection moulding: influence of specimen dimensions and temperature on solvente debinding kinetics.* Journal of Materials Processing Technology, 160: p. 213-220 (2005).

22. Lin, H.-K. and K.-S. Hwang, *In situ dimensional changes of powder injection-molded compacts during solvent debinding.* Acta Materialia, 46(12): p. 4303-4309 (1998).

23. Krauss, V.A., et al., *A model for PEG removal from alumina injection moulded parts by solvent debinding.* Journal of Materials Processing Technology, 182(1-3): p. 268-273 (2007).

24. Ozkan Gulsoy, H. and C. Karatas, *Development of poly(2-ethyl-2-oxaline) based water-soluble binder for injection molding of stainless steel powder.* Materials & Design, In Press, Corrected Proof (2006).

25. Eroglu, S. and H.I. Bakan, *Solvent debinding kinetics and sintered properties of injection moulded 316L stainless steel powder.* Powder Metallurgy, 48(4): p. 329-332 (2005).

26. Yang, W.-W., et al., *Solvent debinding mechanism for alumina injection molded compacts with water-soluble binders.* Ceramics International, 29: p. 745-756 (2003).

27. N.N., *Polyethylene glycols*. Burgkirchen (DE): Surfactants Division of Clariant GmbH (1998).

28. N.N., *The dawn of the MIM magicians.* Metal Powder Report, 58(9), 2003/9: p. 36-39 (2003).

29. Cornwall, R., *PIM 2001 airs industry's sucesses and challenges.* Metal Powder Report, 56(n°6), 01-06-2001: p. 10-13 (2001).

30. German, R.M., *Powder Injection Molding - Design and Applications*: Innovative Material Solutions, Inc. (2003).

31. Trunec, M. and J. Cihlar, *Thermal debinding of injection moulded ceramics.* J. Eur. Ceram. Soc., 17: p. 203-209 (1997).

32. Tsai, D.-S. and W.-W. Chen, *Solvent Debinding Kinetics of Alumina Green Bodies by Powder Injection Molding.* Ceramics International, 21: p. 257-264 (1995).

33. Cao, M.Y., J.W. O'Connor, and C.I. Chung. *A new water soluble solid polymer solution binder for powder injection molding*. in *Powder Injection Molding Symposium*, 1992

34. Park, M.S., J.K. Kim, and H.J.S. Sangho Ahn, *Water-soluble binder of cellulose acetate butyrate/poly(ethylene glycol) blend for powder injection molding.* Journal of Materials Science, 36: p. 5531-5536 (2001).

35. Krug, S., J.R.G. Evans, and J.H.H. ter Maat, *Reaction and Transport Kinetics for Depolymerization within a Porous Body.* AIChE Journal, 48(7): p. 1533-41 (2002).

36. *Starting a New Era in Catalytic Debinding of MIM Components.* CFI - Ceramic Forum International, (2006).

37. German, R.M., *Sintering Theory and Practice*: John wiley & Sons Inc. (1996).

38. *Kinetics - Metal Injection Moulding*. [cited 3-5-2004]; Available from: http://www.kinetics.com/application/.

39. *MIMECRISA*. [cited 03-05-2004]; Available from: www.ecrimesa.com/mimecrisa.

40. *Advanced Ceramitric - Products*. [cited 5-4-2004]; Available from: http://www.advancedcerametrics.com/pages/products/.

41. *AMT Electronics - Kovar Packaging, MIM Hinges, Latches & Counterweights Hard Disk Drives*. [cited; Available from: http://amt-mat.com/AMT-electronics.html.

42. Srinivasa Rao, A., *Effect of the surface active agents on the rheology of aqueous alumina slips.* Ceramics International, 14(1): p. 17-25 (1988).

43. Lenk, R. and A. Krivoshchepov, *Effect of Surface-Active Substances on the Rheological Properties of Silicon Carbide Suspensions in Paraffin.* Journal of the American Ceramic Society, 83(2): p. 273-276 (2000).

44. Xie, Z.P., J.L. Yang, and Y. Huang, *The effect of silane contents on fluidity and green strength for ceramic injection moulding.* Journal of Materials Science Letters, 16(15): p. 1286-1287 (1997).

45. Lindqvist, K., et al., *Organic Silanes and Titanates as Processing Additives for Injection Molding of Ceramics.* Journal of the American Ceramic Society, 72(1): p. 99-103 (1989).

46. GERMAN, R.M., *The Production of Stainless Steels by Injection Molding Water Atomized Prealloy Powders.* JOURNAL OF INJECTION MOLDING TECHNOLOGY, 1(3): p. 171-180 (1997).

47. Heaney, D.F., T.J. Mueller, and P.A. Davies, *Mechanical properties of metal injection moulded 316l stainless steel using both prealloy and master alloy techniques.* Powder Metallurgy, 47(4): p. 1-7 (2004).

48. N.N., *ASM Handbook - Vol.7 Powder Metal Technologies and Applications*: ASM International (1998).

49. Minuth, P.K., et al. *Mechanical and corrosion properties of MIM parts produced from blends of gas and water atomised powders*. in *PM2TEC'95*, 1995

50. Hartwig, D.T., et al. *MIM of 316L powders with large particles sizes*. in *PIM-97 - 1st European Symposium on Powder Injection Moulding*, 1997

51. *Thermat sets up for precision PIM.* Metal Powder Report, 51(6), 1996/6: p. 28-31 (1996).

52. Zauner, R., et al., *Variability of powder characteristics and their effect on dimensional variability of powder injection moulded components.* Powder Metallurgy, 47(2): p. 144-149 (2004).

53. Scott Weil, K., E. Nyberg, and K. Simmons, *A new binder for powder injection molding titanium and other reactive metals.* Journal of Materials Processing Technology, 176(1-3): p. 205-209 (2006).

54. Dobrzanski, L.A., et al., *Metal injection moulding of HS12-1-5-5 high-speed steel using a PW-HDPE based binder.* Journal of Materials Processing Technology, 175(1-3): p. 173-178 (2006).

55. Aggarwal, G., S.J. Park, and I. Smid, *Development of niobium powder injection molding: Part I. Feedstock and injection molding.* International Journal of Refractory Metals and Hard Materials, 24(3): p. 253-262 (2006).

56. Tseng, W.J., D.-M. Liu, and C.-K. Hsu, *Influence of stearic acid on suspension structure and green microstructure of injection-molded zirconia ceramics.* Ceramics International, 25(2): p. 191-195 (1999).

57. Baojun, Z., Q. Xuanhui, and T. Ying, *Powder injection molding of WC-8%Co tungsten cemented carbide.* International Journal of Refractory Metals and Hard Materials, 20(5-6): p. 389-394 (2002).

58. Suri, P., et al., *Effect of mixing on the rheology and particle characteristics of tungsten-based powder injection molding feedstock.* Materials Science and Engineering A, 356(1-2): p. 337-344 (2003).

59. Chan, T.-Y. and S.-T. Lin, *Effects of Stearic Acid on the Injection Molding of Alumina.* Journal of the American Ceramic Society, 78(10): p. 2746-2752 (1995).

60. Johansson, E., D.L. Nyborg, and J. Becker. *Interactions between surface active additives and 316L MIM powder*. in *PIM-97 - 1st European Symposium on Powder Injection Moulding*, 1997

61. Liu, D.-M., *Effect of Dispersants on the Rheological Behaviour of Zirconia-Wax Suspensions.* J. Am. Ceram. Soc., 82(5): p. 1162-1168 (1999).

62. Cheremisinoff, N.P., *Advanced Polymer Processing Operations*. New Jersey (USA): Noyes Publications (1998).

63. Trunec, M. and J. Cihlar, *Thermal removal of multicomponent binder from ceramic injection mouldings.* Journal of the European Ceramic Society, 22(13): p. 2231-2241 (2002).

64. Tseng, W.J., *Warping evolution of injection-molded ceramics.* Journal of Materials Processing Technology, 102(1-3): p. 14-18 (2000).

65. Bailey, D.F., *Moulding Ceramic Composition*, Patent No. US3285873

66. Michio Nakanishi, N. and K. Takuya Miho, *Composition and methos for producing a metallic sintered body*, Patent No. US4968739

67. Storm, R.S., *Ceramic composition suited to be injection molded and sintered*, Patent No. US4207226

68. Hiroshi Ono, I., et al., *Polyamide base binder for use in metal powder injection molding process*, Patent No. US5002998

69. Ohnsorg, R.W., *Composition and process for injection molding ceramic materials*, Patent No. US4144207

70. Wiech, R.E., *Manufacture of parts from particulate material*, Patent No. US4197118

71. Roetenberg, K.S., et al. *Optimization of the mixing process for powder injection molding*, 1992

72. Song, J.H. and J.R.G. Evans, *Flocculation after injection moulding in ceramic suspensions.* J. Mater. Res., 9(9): p. 2386-2397 (1994).

73. Dubus, M. and H. Burlet, *Rheological behaviour of a polymer ceramic blend.* Journal of the European Ceramic Society, 17(2-3): p. 191-196 (1997).

74. Liu, D.-M. and W.J. Tseng, *Influence of debinding rate, solid loading and binder formulation on the green microstructure and sintering behaviour of ceramic injection mouldings.* Ceramics International, 24(6): p. 471-481 (1998).

75. Zhu, B., X. Qu, and Y. Tao, *Mathematical model for condensed-solvent debinding process of PIM.* Journal of Materials Processing Technology, 142: p. 487-492 (2003).

76. Honek, T., B. Hausnerova, and P. Saha, *Relative viscosity models and their application to capillary flow data of highly filled hard-metal carbide powder compounds.* Polymer Composites, 26(1): p. 29-36 (2005).

77. Nyberg, E., et al., *Microstructure and mechanical properties of titanium components fabricated by a new powder injection molding technique.* Materials Science and Engineering: C, 25(3): p. 336-342 (2005).

78. Castro, L., et al., *Mechanical properties and pitting corrosion behaviour of 316L stainless steel parts obtained by a modified metal injection moulding process.* Journal of Materials Processing Technology, 143-144: p. 397-402 (2003).

79. Su, S.R., *Method of modifying thermal properties of polycarbosilane*, Patent No. US4939197

80. Fanelli, A.J. and R.D. Silvers, *Process for injection molding ceramic composition employing an agaroid gell-forming material to add green strength to a preform*, Patent No. US4734237

81. Hunt, K.N. and J.R.G. Evans, *The influence of mixing route on the properties of ceramic injection moulding blends.* British Ceramic Transactions Journal, 87: p. 17-21 (1988).

82. Tseng, W.J. and K.-H. Teng, *Effect of surfactant adsorption on aggregate structure and yield strength of zirconia-wax suspensions.* Journal of Materials Science, 36(1): p. 173-178 (2001).

83. German, R.M., *Homogeneity Effetcs on Feedstock Viscosity in Powder Injection Molding.* J. Am. Ceram. Soc., 77(1): p. 283-85 (1994).

84. Kowalski, L., J. Duszczyk, and L. Katgerman, *Thermal conductivity of metal powder-polymer feedstock for powder injection moulding.* Journal of Materials Science, 34(1): p. 1-5 (1999).

85. Rosato, D.V. and D.V. Rosato, *Injection Molding Handbook*. New York (USA): Van Nostrand Reinhold (1986).

86. Maetzig, M. and H. Walcher. *Strategies for Injection Moulding Metals and Ceramics*. in *PM2TEC - Powder Metallurgy and Particulate Materials 2002*, Orlando (USA), 2002

87. Fu, Y.Q., et al., *X-ray imaging of metal injection moulding parts.* Journal of Materials Science Letters, 16(22): p. 1873-1875 (1997).

88. Tseng, W.J. and D. Chiang, *Influence of molding variables on defect formation and mechanical strength of injection-molded ceramics.* Journal of Materials Processing Technology, 84(1-3): p. 229-235 (1998).

89. Krug, D.S., J.R.G. Evans, and J. ter Maat, *Aetiology of defects in large ceramic moldings.* J. Am. Ceram. Soc., 82(8): p. 2094-2100 (1999).

90. Wei, W.-C.J., R.-Y. Wu, and S.-J. Ho, *Effects of pressure parameters on alumina made by powder injection moulding.* Journal of the European Ceramic Society, 20(9): p. 1301-1310 (2000).

91. Barriere, T., B. Liu, and J.C. Gelin, *Determination of the optimal process parameters in metal injection molding from experiments and numerical modeling.* Journal of Materials Processing Technology, 143-144: p. 636-644 (2003).

92. Dvorak, P., T. Barriere, and J.C. Gelin, *Jetting in metal injection moulding of 316L stainless steel.* Powder Metallurgy, 48(3): p. 254-260 (2005).

93. Liu, D.-M. and W.J. Tseng, *Influence of solids loading on the green microstructure and sintering behaviour of ceramic injection mouldings.* Journal of Materials Science, 32(24): p. 6475-6481 (1997).

94. Greene, C.D. and D.F. Heaney, *The PVT effect on the final sintered dimensions of powder injection molded components.* Materials & Design, 28(1): p. 95-100 (2007).

95. Hopmann, C. and W. Michaeli. *Saving costs and time by means of gas-assisted powder injection molding*. in *ANTEC 1999*, 1999

96. Michaeli, W. and C. Hopmann, *New Perspectives for Ceramic Injection Molding with Gas Injection.* Advanced Engineering Materials, 2(12), 827-832 (2000).

97. Maetzig, M. and H. Walcher. *Assembly Moulding of MIM Materials*. in *PM2006*, Ghent (Belgium): EPMA, 2006

98. Heaney, D.F., P. Suri, and R.M. German, *Defect-free sintering of two material powder injection molded components Part I Experimental investigations.* Journal of Materials Science, 38(24): p. 4869-4874 (2003).

99. Heaney, D.F., P. Suri, and R.M. German, *Defect-free sintering of two material powder injection molded components Part II Model.* Journal of Materials Science, 38(24): p. 4869-4874 (2003).

100. Haupt, U. and H. Walcher. *Powder injection moulding - Concepts for presses and tooling*. in *PIM-97 - 1st European Symposium on Powder Injection Moulding*, 1997

101. *Arburg Practical Guide to Injection Moulding*, ed. V. Goodship. Shawbuty, UK: Rapra Technology Limited (2004).

102. Maniscalco, M., *Tools and runners designed for MIM.* IMM Magazine, December/1999: p. (1999).

103. Hu, S.C. and K.S. Hwang, *Dilatometric analysis of thermal debinding of injection moulded iron compacts.* Powder Metallurgy, 43(3): p. 239-244 (2000).

104. Lii, D.-F., et al., *The effects of atmosphere on the thermal debinding of injection moulded Si3N4 components.* Ceramics International, 24(2): p. 99-104 (1998).

105. Oliveira, A.A.M., et al., *Mass diffusion-controlled bubbling and optimum schedule of thermal degradation of polymeric binders in molded powders.* International Journal of Heat and Mass Transfer, 42(17): p. 3307-3329 (1999).

106. Omar, M.A., et al., *Rapid debinding of 316L stainless steel injection moulded component.* Journal of Materials Processing Technology, 140(1-3): p. 397-400 (2003).

107. Shengjie, Y., Y.C. Lam, and J.C. Chai, *Evolution of liquid-bond strength in powder injection moulding compact during thermal debinding: numerical simulation.* Modelling and Simulation in Materials Science Engineering, 12: p. 311-323 (2004).

108. Trunec, M. and J. Cihlar, *Effect of activated carbon bed on binder removal from ceramic injection moldings.* J. Am. Ceram. Soc., 84(3): p. 675-677 (2001).

109. Chartier, T., M. Ferrato, and J.-F. Baumard, *Influence of the Debinding Method on the Mechanical Properties of Plastic Formed Ceramics.* Journal of the European Ceramic Society, 15: p. 899-903 (1995).

110. Chartier, T., M. Ferrato, and J.F. Baumard, *Supercritical Debinding of Injection Molded Ceramics.* J. Am. Ceram. Soc., 78(7): p. 1787-92 (1995).

111. Santos, M.A., et al., *Plasma debinding and pre-sintering of injected parts.* Materials Research, 7(3): p. 505-511 (2004).

112. Schatt, W. and K.-P. Wieters, *Powder Metallurgy - Processing and Materials*. Shrewsbury (UK): EPMA - European Powder Metallurgy Association (1997).

113. Song, J.H. and J.R.G. Evans, *The injection moulding of fine and ultra-fine zirconia powders.* Ceramics International, 21(5): p. 325-333 (1995).

114. Petzoldt, D.F. and D.T. Hartwig. *Overview on binder and feedstock systems for PIM*. in *EURO PM2000 - 2nd European Symposium on Powder Injection Moulding*, 2000

115. Heaney, D.F., *Spoilt for choice - commercially available feedstocks for PIM.* Metal Powder Report, June 2002, 32-33 (2002).

116. *Advanced Metal Working MIM Feedstocks*. 2002 [cited 26-03-2007]; Available from: http://www.advancedmetalworking.com/page7.html.

117. *Planet Polymer Technologies*. [cited 7-01-2003]; Available from: http://www.planetpolymer.com/aquamim.htm

118. N.N., *ELUTEC feedstocks*. 7-6-2002 ed: Zschimmer & Schwarz GmbH & Co KG).

119. *Inmatec Technologies GmbH - Product Overview*. [cited 26-3-2007]; Available from: http://www.inmatec-gmbh.com/engl/overview_standard_feed.html.

120. N.N., *Standard Process Parameters for metasol-feedstock*. 10-04-2002 ed: Imeta GmbH (2002).

121. N.N., *Latitude Manufacturing Technologies - Process Guide for PowderFlo*: Latitude Manufacturing Technologies).

122. N.N., *Licomont EK 583 Application Note - Milling disk made of aluminium oxide*: Clariant GmbH).

123. Quirmbach, P. and S. Schwartz, *Elutec: Variable MIM-Feedstock Systems with Aqueous Debinding.* Ceramic Forum International, (81), E23-E24 (2004).

124. Yang, X. and R.J. Petcavich, *Powder and binder systems for use in metal and ceramic powder injection molding*, Patent No. US 6,008,281

125. *Planet Polymer Technologies, Inc. Announces Royalty Agreement with Ryer, Inc. and Six Month Period Ended June 30, 2004 Financial Results*. 2004 August 24, 2004 [cited; Available from: http://www.findarticles.com/p/articles/mi_m0EIN/is_2004_August_24/ai_n6166982.

126. *About Ryer Inc*. 2005 [cited; Available from: http://www.ryerinc.com/about.html.

127. Hesse, W. and K. Bittler, *Process for producing granular material and shaped parts from hard metal materials or cermet materials*, Patent No. US 5,860,055

128. Krueger, D.C., *Process for improving the debinding rate of ceramic and metal injection molded products*, Patent No. US 5,531,958

129. Blömacher, D.M., et al. *BASF's Catamold: a phenomenological description of the debinding process*. in *EURO PM2000 - 2nd European Symposium on Powder Injection Moulding*, 2000

130. N.N., *Licomont EK 583 Application Note - Porcelain Cup*: Clariant GmbH).

131. Bayer, M. and I. Nagl, *Molding composition for the production of inorganic sintered products*, Patent No. US5254613

132. Bayer, M., P. Pyka, and H. Wagner, *Process and molding compound for producing inorganic sintered products by injection molding*, Patent No. US5417756

133. Scheckenbach, H., A. Schleicher, and M. Bayer, *Molding material for processing sinterable polymers*, Patent No. US 6,005,037

134. *Tailor-made moulding compounds (Press Release)*. 2002 [cited 10-1-2002]; Available from: http://www.pigments.clariant.com/PA/internet.nsf/wwwMain/E0653680082B91ECC1.

135. Schwartz, S., et al., *Sugar binder for ceramic materials*, Patent No. GB 2 324 793 A

136. Quirmbach, P., S. Schwartz, and F. Magerl, *The Application of Injection Moulding Technology in Modern Tableware Prodution.* Ceramic Forum International, 3/2004, Marz 2004: p. (2004).

137. *Elutec - product Overviw*. [cited 26-10-2005]; Available from: http://www.zschimmer-schwarz.de/elutec%20webseite%20en/en/_pro...

138. *Where exotic plastics meet heavy metal*. 2001 [cited 28-3-2007]; Available from: http://www.polymertechnologies.com/editorial.html.

139. *Latitude Manufacturing Technologies Website*. [cited 9-1-2003]; Available from: http://www.latitudemanufacturing.com/.

140. Marsh, G.B., et al., *Injection molding of zirconia oxygen sensor thimbles by an aqueous process*, Patent No. US 5,087,595

141. Fanelli, A.J., et al., *Aqueous process for injection molding ceramic powders at high solids loadings*, Patent No. US 5,250,251

142. Fanelli, A.J., et al., *Gel strength enhancing additives for agaroid-based injection molding compositions*, Patent No. US 5,746,957

143. *Description of the Agar Based Aqueous Binder*. [cited 19-4-2001]; Available from: http://www.asplastics.com/powderflo/process/process02.html.

144. LaSalle, J.C. and M. Zedalis, *Net-shape processing using an aqueous-based MIM binder.* JOM, July-1999, 38-39 (1999).

145. Ballard, C., *Ceramic injection molding meets the demand for manufacturing complex shape.* Ceramic industry, March 1997, 01-03-1997: p. 42-44 (1997).

146. N.N., *Catamold Feedstock for Powder Injection Molding: Processing - Properties - Applications*. 29.09.1997 ed. Technical Information: Catamold, BASF AG: BASF AG (1997).

147. Covas, J.A. and J.M. Maia, *Reologia de polímeros*, in *Reologia e suas aplicações industriais*, A.G.d. Castro, J.A. Covas, and A.C. Diogo, Editors. Instituto Piaget: Lisboa. p. 9-46, 2001.

148. Gupta, R.K., *Particulate Suspensions*, in *Flow and Rheology in Polymer Composites Manufacturing*, S.G. Advani, Editor. Elsevier Science B.V.: Amsterdam, The Netherlands. p. 9-51, 1994.

149. Khakbiz, M., A. Simchi, and R. Bagheri, *Analysis of the rheological behavior and stability of 316L stainless steel-TiC powder injection molding feedstock.* Materials Science and Engineering: A, 407(1-2): p. 105-113 (2005).

150. Krauss, V.A., et al., *Rheological Properties of Alumina Injection Feedstocks.* Materials Research, 8(2): p. 187-189 (2005).

151. Liu, D.-M. and W.J. Tseng, *Yield behavior of zirconia-wax suspensions.* Material Science and Engineering, A254: p. 136-146 (1998).

152. Khakbiz, M., A. Simchi, and R. Bagheri, *Investigation of rheological behaviour of 316L stainless steelâ€“3 wt-%TiC powder injection moulding feedstock.* Powder Metallurgy, 48(2): p. 144-150 (2005).

153. Li, Y., B. Huang, and X. Qu, *Viscosity and melt rheology of metal injection moulding feedstocks.* Powder Metallurgy, 42(1): p. 86-90 (1999).

154. Yang, W.-W., K.-Y. Yang, and M.-H. Hon, *Effects of PEG molecular weights on rheological behavior of alumina injection molding feedstocks.* Materials Chemistry and Physics, 78(2): p. 416-424 (2002).

155. Karatas, C., et al., *Rheological properties of feedstocks prepared with steatite powder and polyethylene-based thermoplastic.* Journal of Materials Processing Technology, 152: p. 77-83 (2004).

156. Tseng, W.J., *Influence of surfactant on rheological behaviors of injection-molded alumina suspensions.* Material Science and Engineering, A289: p. 116-122 (2000).

157. Morais, J.L., A.G.d. Castro, and A.C. Diogo, *Noções básicas de reologia*, in *Reologia e suas aplicações industriais*, A.G.d. Castro, J.A. Covas, and A.C. Diogo, Editors. Instituto Piaget: Lisboa, 2001.

158. Edirisinghe, M.J., *The effect of processing additives on the properties of a ceramic-polymer formulation.* Ceramics International, 17(2): p. 89-96 (1991).

159. Loh, N.H., S.B. Tor, and K.A. Khor, *Production of metal matrix composite part by powder injection molding.* Journal of Materials Processing Technology, 108(3): p. 398-407 (2001).

160. Thian, E.S., et al., *Ti-6A1-4V/HA composite feedstock for injection molding.* Materials Letters, 56(4): p. 522-532 (2002).

161. Supati, R., et al., *Mixing and characterization of feedstock for powder injection molding.* Materials Letters, 46(2-3): p. 109-114 (2000).

162. Herranz, G., et al., *Development of new feedstock formulation based on high density polyethylene for MIM of M2 high speed steels.* Powder Metallurgy, 48(2): p. 134-138 (2005).

163. Liu, L., et al., *Mixing and characterisation of 316L stainless steel feedstock for micro powder injection molding.* Materials Characterization, 54: p. 230-238 (2005).

164. Rei, M., et al., *Low-pressure injection molding processing of a 316-L stainless steel feedstock.* Materials Letters, 52(4-5): p. 360-365 (2002).

165. Herranz, G., et al. *Influence Of The Debinding Process On The Microstructure Of Injected M2 High Speed Steel Feedstock*. in *Sintering'03 - An International Conference on the Science, Technology & Applications of Sintering*, 2003

166. Moballegh, L., J. Morshedian, and M. Esfandeh, *Copper injection molding using a thermoplastic binder based on paraffin wax.* Materials Letters, 59(22): p. 2832-2837 (2005).

167. Krug, S., J.R.G. Evans, and J.H.H. Ter Maat, *Solidification of large section ceramic injection mouldings under low hold pressures.* Journal of Materials Science, 37(13): p. 2835-2841 (2002).

168. Zu, Y.S. and S.T. Lin, *Optimizing the mechanical properties of injection molded W–4.9%Ni–2.1%Fe in debinding.* Journal of Materials Processing Technology, 71(2): p. 337-342 (1997).

169. Shaw, H.M. and M.J. Ediringhe, *Shrinkage and Particle Packing during Removal of Organic Vehicle from Ceramic Injection Mouldings.* Journal of the European Ceramic Society, 15: p. 109-116 (1995).

170. Zhang, T., S. Blackburn, and J. Bridgwater, *The orientation of binders and particles during ceramic injection moulding.* Journal of the European Ceramic Society, 17(1): p. 101-108 (1997).

171. Bilovol, V.V., et al., *Characterisation of 316L powder injection moulding feedstock for purpose of numerical simulation of PIM process.* Powder Metallurgy, 46(3): p. 236-240 (2003).

172. Bilovol, V.V., *Mould filling simulations during powder injection moulding*. 2003, Delft University of Technology: Delft, The Netherlands.

173. Kryachek, V.M., *Injection Moulding (Review).* Powder Metallurgy and Metal Ceramics, 43(7-8): p. 336-347 (2004).

174. Schwartz, S. and P. Quirmbach. *Water debinding technology for MIM production*. in *EURO PM2000 - 2nd European Symposium on Powder Injection Moulding*, 2000

175. Murphy, J., *Additives for Plastics Handbook*. 2nd ed., Oxford (UK): Elesevier Science Ltd. (2001).

176. Lin, S.T. and R.M. German, *Interaction between binder and powder in injection moulding of alumina.* Journal of Materials Science, 29(19): p. 5207-5212 (1994).

177. Elias, H.-G., *An Introduction to Plastics*. 2nd ed., Weinhem (DE): Wiley-VCH GmbH & Co. KGaA (2003).

178. Koning, C., et al., *Strategies for compatibilization of polymer blends.* Progress in Polymer Science, 23(4): p. 707-757 (1998).

179. Utracki, L.A., *Polymer Blends Handbook*. Dordrecht, The Netherlands: Kluwer Academic Publishers (2002).

180. Coleman, M.M. and P.C. Painter, *Hydrogen bonded polymer blends.* Progress in Polymer Science, 20(1): p. 1-59 (1995).

181. Nishi, T. and T.T. Wang, *Melting Point Depression and Kinetic Effects of Cooling on Crystallization in Poly(viny1idene fluoride)-Poly (methyl methacrylate) Mixtures.* Macromolecules, 8(6): p. 909-915 (1975).

182. He, Y., B. Zhu, and Y. Inoue, *Hydrogen bonds in polymer blends.* Progress in Polymer Science, 29(10): p. 1021-1051 (2004).

183. Rim, P.B. and J.P. Runt, *Melting Point Depression in Crystalline/ Compatible Polymer Blends.* Macromolecules, 17: p. 1520-1526 (1984).

184. Aubin, M. and R.E. Prud'homme, *Miscibility in Blends of Poly(viny1 chloride) and Polylactones.* Macromolecules, 13: p. 365-369 (1980).

185. Li, Y., L. Li, and K.A. Khalil, *Effect of powder loading on metal injection molding stainless steels.* Journal of Materials Processing Technology, 183(2-3): p. 432-439 (2007).

186. Qu, X., et al., *Rheologic behaviour and PIM processing of WC-TiC-Co powder feedstock.* Journal of University of Science and Technology Beijing, 11(4): p. 334-337 (2004).

187. Qu, X., et al., *Application of a wax-based binder in PIM of WC-TiC-Co cemented carbides.* International Journal of Refractory Metals and Hard Materials, 23(4-6): p. 273-277 (2005).

188. Shibo, G., et al., *Powder injection molding of Ti-6Al-4V alloy.* Journal of Materials Processing Technology, 173(3): p. 310-314 (2006).

189. Liu, F.-J. and K.-S. Chou, *Determining critical ceramic powder volume concentration from viscosity measurements.* Ceramics International, 26(2): p. 159-164 (2000).

190. Agote, I., et al., *Rheological study of waste porcelain feedstocks for injection moulding.* Journal of the European Ceramic Society, 21: p. 2843-2853 (2001).

191. Wright, J.K., et al., *Particle packing in ceramic injection molding.* J. Am. Ceram. Soc., 73(9): p. 2653-2658 (1990).

192. Zhang, T. and J.R.G. Evans, *Predicting the Viscosity of Ceramic Injection Moulding Suspensions.* Journal of the European Ceramic Society, 5: p. 165-172 (1989).

193. Jorge, H.R., A.M. Correia, and A.M. Cunha. *Rheometric Properties Based Model for an Improved Solid Contents CIM Feedstock*. in *ANTEC2005*, 2005

194. Johnson, J.L., et al., *Evaluation of copper powders for processing heat sinks by metal injection moulding.* Powder Metallurgy, 48(2): p. 123-128 (2005).

195. ASM_International, *ASM Handbook*. Vol. 7 - Powder Metal Technologies and Applications (1998).

196. Prasad, A., *Polyethylene, Low-density*, in *Polymer Data Handbook*. Oxford University Press. p. 518-528, 1999.

197. N.N., *Polyehtylene - Products and Properties (Brochure)*: Basell B.V (NL) (2005).

198. Prasad, A., *Polyethylene, metallocene linear low density*, in *Polymer Data Handbook*. Oxford University Press. p. 529-538, 1999.

199. Hsu, S.L., *Poly(methyl methacrylate)*, in *Polymer Data Handbook*. Oxford University Press. p. 655-657, 1999.

200. Sundararajan, P.R., *Poly(vinyl butyral)*, in *Polymer Data Handbook*. Oxford University Press. p. 910-924, 1999.

201. N.N., *Mowital - Polyvinyl butyral*. August 1997 ed., Frankfurt am Main (DE): Clariant GmbH (1997).

202. Malitschek, O., *Waxes by Clariant - Products, characteristics and applications*. May 2003/W 320 GB ed., Augsburg (DE): Clariant GmbH (2003).

203. N.N., *Fatty acid*. 2007, Wikipedia, the free encyclopedia http://en.wikipedia.org/wiki/Fatty_acid.

204. Ulutan, S. and M. Gilbert, *Mechanical properties of HDPE/magnesium hydroxide composites.* Journal of Materials Science, 35(9): p. 2115-2120 (2000).

205. Allen, T., *Particle Size Measurement*. 4th ed: Chapam and Hall (1990).

206. Micromeritics, *AccuPyc 1330 Pycnometer Operator's Manual*. 1989.

207. NF-EN-ISO787-11:1995, *Méthodes générales d'essai des pigments et matières de charge – Partie 11: Détermination du volume massique apparent et de la masse volumique apparente après tassement.* AFNOR - Association Française de Normalisation).

208. Tertian, R. and F. Claisse, *Principles of Quantitative X-Ray Fluorescence Analysis*. London (UK): Heyden & Son Ltd. (1982).

209. N.N., *ASM Handbook - Vol.10 Materials Characterization*. 9th ed: ASM International (1986).

210. Ehrenstein, G.W., G. Riedel, and P. Trawiel, *Thermal Analysis of Plastics*. Munich: Carl Hanser Verlag (2004).

211. Wu, R.-Y. and W.-C.J. Wei, *Kneading behaviour and homogeneity of zirconia feedstocks for micro-injection molding.* Journal of the European Ceramic Society, 24(14): p. 3653-3662 (2004).

212. Reddy, J.J., et al., *Loading of solids in a liquid medium: determination of CBVC by torque rheometer.* Journal of the European Ceramic Society, 16: p. 567-574 (1996).

213. Bigg, D.M. and R.G. Barry. *Rheological Analysis as a Tool to Predict Quality in Powder Injection Molding*. in *ANTEC1998*, 1998

214. Reddy, J.J., N. Ravi, and M. Vijayakumar, *A simple model for viscosity of powder injection moulding mixes with binder content above powder critical binder volume concentration.* Journal of the European Ceramic Society, 20: p. 2183-2190 (2000).

215. Barreiros, F.M. and M.T. Vieira, *PIM of non-conventional particles.* Ceramics International, 32(3): p. 297-302 (2006).

216. McCabe, C.C., *Rheological Measurements with the Brabender Plastograph.* Transactions of the Society of Rheology, IV: p. 335-346 (1960).

217. Castro, A.G.d., J.A. Covas, and A.C. Diogo, *Reologia e suas aplicações industriais*. Ciência e Técnica: Instituto Piaget (2001).

218. N.N., *ISO 2740:1999(E) - Sintered metal materials, excluding hardmetals - Tensile teste pieces* (1999).

219. N.N., *Metal Injection Moulding - A Manufacturing Process for Precision Engineering Components* EPMA - European Powder Metallurgy Association).

220. Ilinca, F., et al., *Metal injection molding: 3D modeling of nonisothermal filling.* Polymer Engineering & Science, 42(4): p. 760-770 (2002).

221. N.N., *ASTM D790 - Standard Test Methods for Flexural Properties of Unreinforced and Reinforced Plastics and Electrical Insulating Materials* (2003).

222. Ji, C.H., et al., *Sintering study of 316L satinless steel metal injection molding parts using Taguchi method: final density.* Material Science and Engineering, A311: p. 74-82 (2001).

223. N.N., *EN 10002 - 1 - Tensile testing of metallic materials. Method of test at ambient temperature* (2001).

224. Han, P., *Tensile Testing*: ASM International (1992).

225. Nielsen, L.E., *Polymer Rheology*. New York (USA): Marcel Dekker Inc. (1977).

226. Yang, W.-W. and M.-H. Hon, *In situ evaluation of dimensional variations during water extraction from alumina injection-moulded parts.* Journal of the European Ceramic Society, 20(7): p. 851-858 (2000).

227. Mark, J.E., *Polymer Data Handbook*. New York (USA): Oxford University press (1999).

228. MPIF, *Standard 35 - Materials Standards for Metal Injection Moulded Parts*, ed. MPIF: MPIF (2001).

229. ASTM, *ASTM A743/A743M-06 Standard Specification for Castings, Iron-Chromium, Iron-Chromium-Nickel, Corrosion Resistant, for General Application* (2006).

APPENDICES

Appendix A. Commercial information about binder materials

Acronym	Designation	Producer	Product Reference
PEG	Polyethylene glycol	Clariant	Polyglykol 8000 S
LDPE	Low density polethylene	Basell	Lupolen 1800S
MPE	Metallocene polyethylene	ExxonMobil	Exact 0210
PMMA	Poly(methyl methacrylate)	Degussa	Plexiglas 8N
PVB	Poly(vinyl butyral)	Clariant	Mowital B 30 H
PEW1	Polyethylene waxes	Clariant	Licowax PE 190
PEW2	Polyethylene waxes	Clariant	Licowax PE 520
OPEW	Oxidized polyethylene waxes	Clariant	Licowax PED191
SA	Stearic acid	Sigma-Aldrich	reagent grade 95%
OA	Oleic acid	Sigma-Aldrich	reagent grade 90%

Appendix B. List of communications

(1) Oral Communication

(with paper published in the conference proceedings)

Hélio Jorge, A. M. Sousa Correia, António M. Cunha, *Evaluation of powder injection moulding feedstocks using different test geometries,* PPS-20 Annual Meeting, Akron (OH), USA, 22nd of June, 2004

Two new formulations for PIM (powder injection molding) feedstocks were proposed and evaluated using a specially developed test mold. Both formulations have 60% (v/v) of alumina powder dispersed in a polymeric matrix. A low molecular weight polyethylene and a polyethylene glycol were selected for matrices. The new compounds were prepared using a two stage process involving a z-blade mixer and shear roll compounder. The evaluation procedure used a commercial feedstock as comparison and was based on two test geometries of the referred mold. The work was also supported by high pressure capillary rheometry, STA measurements and apparent density measurements by He picnometry.

The developed compounds show adequate processing parameters, with viscosity levels within the typical limits of PIM. Furthermore, the compounds are homogeneous and present a processibility comparable to commercially available products.

(2) Oral Communication

(with paper published in the conference proceedings)

Hélio Jorge, A. M. Sousa Correia, António M. Cunha, *Rheometric properties based model for an improved solid contents CIM feedstock*, ANTEC Conference 2005, Boston (MA), USA, 2nd of May, 2005

A new formulation for Ceramic Injection Molding (CIM), based on a high-grade alumina powder bound with a water debinding system, composed by a mixture of a low molecular weight polyethylene and a polyethylene glycol, has been developed.

The present paper reports the determination of the critical powder concentration of the developed feedstock by rheological model fitting. Semi-empirical models were discriminated in order to establish the optimum ceramic powder concentration window.

(3) Poster Communication

(with paper published in the conference proceedings)

Hélio Jorge, Luc Hennetier, A.M. Sousa Correia, António M. Cunha, *Tailoring solvent/thermal debinding 316L stainless steel feedstocks for PIM: An experimental approach*, Euro PM2005 Conference, Prague, Checz Repubublic, 2nd of October, 2005

Powder Injection Moulding is considered one of the most promising near net-shape forming technologies for metals, cermets and ceramics. Debinding is a crucial step for the technical and cost viability of this process and quality of the obtained products.

This paper presents a study on a two step debinding processed AISI 316L stainless steel feedstock based on a thermoplastic binder, compounded with polyethylene glycol as a water-soluble component. Using design pf experiments (DOE) based on Taguchi techniques together with analysis of variances (ANOVA) analysis, 2-step water/thermal debinding process experimental combinations were tested. Within the analysed limits, it was confirmed that the design of moulded parts has a great importance in water debinding performance since the part shape ratio (volume/surface area) was the main contributor for the binder removal and the porosity evolution. Solvent extraction time is significant, but it is shown that water temperature has lower effect.

(4) Poster Communication

(with paper published in the conference proceedings)

Hélio Jorge, António M. Cunha, *Development of a water-soluble binder for PIM: effect of the back-bone polymer and the surfactant*, Euro PM2007 Conference, Toulouse, France, 14th of October, 2007

Under the framework of preparing water debinding feedstocks for injection moulding of AISI 316L powder, the formulation for the insoluble part was developed and evaluated, using polyethylene glycol (PEG) as the base polymer. Four chemically different back-bone polymers and two surface active additives were tested in order to study their effect on the characteristics of the binders and feedstocks. All binder formulations showed components compatibility, yet binders of low density polyethylene and polyethylene wax showed higher interactions. Although there was not an appreciable difference in critical solids loading among the binders, metallocene polyethylene binder provided the highest value, 71 vol.%. The use of stearic acid showed to be preferable to oleic acid, as it produces shear-thinner feedstocks and a higher water debinding rate. Poly(vinyl butyral) and poly(methyl methacrylate) led to lower quality binders and feedstocks, but provided a faster PEG removal in water. Polyethylene based binders were presumed more adequate for a final burnout, promising a more controlled process in shorter time.

(5) Oral Communication

(paper accepted to be published in the conference proceedings)

Hélio Jorge, António M. Cunha, *Metal injection moulding using a water-soluble binder: effect of the back-bone polymer in the process*, Euro PM2008 Conference, Manheim, Germany, 29th September – 1st October 2008

Under the framework of developing water debinding feedstock for injection moulding of AISI 316L powder, the formulation of the binder was developed and evaluated using polyethylene glycol as the base polymer. This paper addresses the effect of the use of two binders with chemically different back-bone polymers on MIM process: a widely used low density polyethylene (LDPE) and an elastomeric metallocene polyethylene (MPE).

Feedstocks showed similar acceptable degree of homogeneity and yielded to a stable moulding and debinding steps. Sintered parts had similar characteristics - high density, low part weight variability, typical dimensional precision for MIM and shrinkage. However, sintering process has revealed some defects in LDPE-binder parts, attributed to phase separation during moulding, which were detrimental for the mechanical properties. In the other hand MPE was found to provide quality parts. A slight difference in binder chemistry has proved to be a key to produce quality MIM parts.